Analysis and Control of Saline Water Intrusion in Coastal Aquifers of Purba Midnapur District of West Bengal, India

Thesis Submitted by

PRABIR KUMAR MAITY

Index No.: 66/16/19/E

Doctor of Philosophy (Engineering)

School of Water Resources Engineering
Faculty Council of Engineering & Technology
Jadavpur University
Kolkata, India

2019

Dedicated to

My Parents

Late Santosh Kumar Maity
&
Late Snehalata Maity

JADAVPUR UNIVERSITY
KOLKATA – 700 032, INDIA

INDEX NO. **66/16$_{/19}$/E**

Title of Thesis

Analysis and Control of Saline Water Intrusion in Coastal Aquifers of Purba Midnapur District of West Bengal, India

Name, Designation & Institution of the Supervisors

Dr. Subhasish Das
Assistant Professor
School of Water Resources Engineering
Jadavpur University
Kolkata, 700 032

Dr. Rajib Das
Assistant Professor
School of Water Resources Engineering
Jadavpur University
Kolkata, 700 032

List of Journal Publications:

1) Maity, P.K., Das, S. and Das, R. (2017). "Methodology for Groundwater Extraction in the Coastal Aquifers of Purba Midnapur District of West Bengal in India under the Constraint of Saline Water Intrusion". *Asian Journal of Water, Environment Pollution*, Vol. 14, No. 2, pp. 1-12. DOI: 10.3233/AJW-170011. *WoS, Scopus and UGC indexed.*

2) Maity, P.K., Das, S. and Das, R. (2017). "Assessment of Groundwater Quality and Saline Water Intrusion in the Coastal Aquifers of Purba Midnapur District, West Bengal, India". *Indian Journal Environmental Protection*, Vol. 37, No. 1, pp, 31-40. *Scopus and UGC indexed.*

3) Maity, P.K., Das, S. and Das, R. (2018). "Remedial Measures for Saline Water Ingression in Coastal Aquifers of South West Bengal in India". *MOJ Ecology & Environmental Science*, Vol. 3, Issue 1, pp. 00061. DOI: 10.15406/mojes.2018.03.00061.

4) Maity, P.K., Das, S. and Das, R. (2018). "A geochemical investigation and control management of saline water intrusion in the coastal aquifer of Purba Midnapur district in West Bengal, India". *Journal of the Indian Chemical Society*, Vol. 95, Issue 3, pp. 205-210. *WoS, Scopus and UGC indexed.*

5) Chakraborty, S., Maity, P.K. and Das, S. (2019). "Investigation, simulation, identification and prediction of groundwater levels in coastal areas of Purba Midnapur, India using MODFLOW". *Environment, Development and Sustainability*, Springer Netherlands, published online. DOI: 10.1007/s10668-019-00344-1. *WoS, Scopus and UGC indexed.*

List of Presentations in National/International/Conferences/ Workshops:

1) Maity, P.K., Das, S. and Das, R. (2017). "A Geochemical Investigation and Control Management of Saline Water Intrusion in the Coastal Aquifer of Purba Midnapur District in West Bengal, India". *National Conference on Sustainable Advanced Technologies for Environmental Management* (SATEM-2017) organized by IIEST Shibpur, 28-30 June, 2017. [Full paper was published in *Journal of the Indian Chemical Society* as mentioned above]

2) Maity P.K., Das S. and Das R. (2018). "Geochemical Study and Remedial Measures of Seawater Ingression in the Southern Part of Purba Midnapur District in West Bengal, India". *1st International Conference on Emerging Trends on Engineering and Science* (ETES:2018) at Asansol, India, 23-24 March, 2018. *Scopus indexed.*

CERTIFICATE FROM THE SUPERVISORS

This is to certify that the thesis entitled "**Analysis and Control of Saline Water Intrusion in Coastal Aquifers of Purba Midnapur District of West Bengal, India**" submitted by **Shri Prabir Kumar Maity**, who got his name registered on **18th April, 2016** for the award of Ph.D. (Engineering) degree of Jadavpur University is absolutely based upon his own work under the supervision of **Dr. Subhasish Das**, Assistant Professor and **Dr. Rajib Das**, Assistant Professor of School of Water Resources Engineering, Jadavpur University and that neither his thesis nor any part of the thesis has been submitted for any degree or any other academic award anywhere before.

1. _____

THESIS ADVISOR

Dr. Subhasish Das

Assistant Professor
School of Water Resources Engineering
Jadavpur University

2. _____

THESIS ADVISOR

Dr. Rajib Das

Assistant Professor
School of Water Resources Engineering
Jadavpur University

ACKNOWLEDGEMENTS

The author wishes to express his heartfelt gratitude towards his thesis supervisors Dr. Subhasish Das and Dr. Rajib Das, Assistant Professors, School of Water Resources Engineering, Jadavpur University, for their valuable guidance and continuous encouragement in planning, wholehearted involvement, advice, support execution and presentation of this thesis.

The author expresses his deepest gratitude to Mr. Moloy Kayal, Assistant Engineer, Contai Division and Mr. Sukumar Barman, Assistant Engineer Digha Division, Public Health Eng. Dept. under Govt. of West Bengal, India for their permission to use their soil-investigation report & test results.

The laboratory work was carried out in the Hydraulics Laboratory of Department of Civil Engineering in Contai Polytechnic Institute under Govt. of West Bengal.

A special gratitude is due to Prof. Dr. Asis Mazumdar, Director, School of Water Resources Engineering, Jadavpur University & Former Dean, Faculty Council of Interdisciplinary Studies, Law and Management, Jadavpur University for his initiation, encouragement and providing moral support during tenure of my Ph.D. work. Heartfelt gratitude is expressed for his valuable suggestions at various stages of the work.

Thanks are also due to all the staff members of School of Water Resources Engineering, Jadavpur University, for their co-operation during the investigation.

Thanks are also due to Mr. Souvik Chakraborty, former M.E. student; Mr. Biprodip Mukherjee & Mr. Asim Kuila, Research Scholars of School of Water Resources Engineering, Jadavpur University, for their unconditional support and help during preparation of this thesis.

Last but not the least, the author would like to dedicate this thesis to his parents and other family members, without whose motivation and constant backup, the completion of this thesis might be a distant dream to the author.

Date:
Place: SWRE, Jadavpur University

PRABIR KUMAR MAITY
Ph.D. Scholar
School of Water Resources Engineering
Jadavpur University

Abstract

Saline water ingression into fresh groundwater aquifers happens in the region of coastal areas of whenever seawater displaces or mixes with fresh groundwater. This situation happens in coastal regions having hydraulic continuity with the sea. Seawater intrusion into freshwater coastal aquifers is likely to cause serious problems if only such aquifer is tapped for domestic water supply, irrigation or any other specific purposes. Salinity in coastal area is a widespread problem of Purba Midnapur district in West Bengal.

Amongst significant contributions in the relevant area of investigation, the work of Wang (1965), Bennett *et al.* (1968), Yeh (1968), Goswami (1968), Pinder and Cooper (1970), Fetter (1972), Mughal and Awan (1977), Dasgupta and Gaikwad (1987), Reilly and Goodman (1987), Fand *et al.* (1987), Schincariol and Schwartz (1990), Motz (1992), Kececioglu and Jiang (1994), Xue *et al.* (1995), Mahesha (2001), Barlow (2003), Raghu Babu *et al.* (2004), Chandra (2005), Chachadi (2005), Papadopoulou *et al.* (2005), Mohan and Pramada (2005), Gallardo and Marui (2007), Mahesha (2009),Werner and Simmons (2009), Olufemi *et al.* (2010), Bianchi *et al.* (2011), Sherif *et al.* (2012), Ayolabi *et al.* (2013), Das *et al.* (2014), Sahu (2014), Adedotun *et al.* (2015), Grundmann *et al.* (2016), Toste *et al.* (2017) and Alfarrah and Walraevens (2018) were found to be worthy of note.

This research is aimed towards conducting theoretical investigation, laboratory experimentation, simulation of groundwater level modelling by computing software and field investigation and control of saline water ingression into coastal aquifers with special emphasis on Purba Midnapur. Here the derivation of formula for permissible discharge of wells from shallow aquifers is done in general. The horizontal infiltration galleries called qanat coupled with vertical risers are presented as a viable solution to the problem of upconing below deep vertical wells. The vertical wells may not be feasible in several situations and qanat coupled with vertical risers can be effectively used in such cases.

An experimental study has also been conducted to determine the hydraulic conductivity of well-graded fine sand experimentally using a Falling-Head Permeameter and the variation of hydraulic conductivity of the sand sample with saline concentration and period of submergence has been studied. Further, an experimental study regarding variation of kinematic viscosity and density of sodium chloride solutions for the variation of saline concentration and temperature has been conducted. Based on these findings, the governing non-linear flow Forchheimer's equation has additionally been modified. The flow pattern of seepage due to saline water intrusion and freshwater recharge into granular porous medium has been conducted using standard model test. Three dimensional views of piezometric surface, pre-monsoon and post-monsoon depth to groundwater level and pre-monsoon piezometric surfaces contours had also been developed. For the year 2014 and 2015, the pre-monsoon piezometric surface contours show depressions near Ramnagar, Bhagbanpur, and Sutahata. In the predominant climatic situation in the zone, the pre-monsoon condition is undeniably critical as compare the post-monsoon condition. Consequently, assessment of the probable for salinisation is conducted considering the pre-monsoon position. It is very clear that the Ramnagar area which includes the tourist resort of Digha and the town of Contai, is highly prone to saline water intrusion as is the Sutahata area which includes the industrial town of Haldia.

The Visual MODFLOW 2000 has been utilized to analyze the groundwater level simulation for entire Purba Midnapur. The simulated data for the year 2012 based on the measured data of 2002 and the observed data of 2012 have been compared and a correlation coefficient is found out to signify data validity. Also simulated groundwater level data of 2019 to 2023 based on well discharge data of 2002, 2012 and combined data of 2002 and 2012 have been correlated for its justification. The groundwater flow occurs from south to north direction of Purba Midnapur, as the saline water intrusion from the Bay of Bengal takes place into the aquifers towards inland direction. In the real field situation saline water encroachments have affected the aquifers and it has covered up to 50 km of location from Kalindi (near seashore) to Nandakumar (inland) location. This chapter focuses on the prediction of future groundwater levels as a potential groundwater management scenario in the region concern.

During field investigation, the water samples were collected from different depths at selected locations of coastal West Bengal, India. To expedite the process, reasonable assistant is taken from the Public Health Engineering Directorate under Government of West Bengal. Collected samples were analysed at the laboratory of State Water Investigation Directorate under Government of West Bengal to investigation the chemical and hydro geological characterisation. Based on the field data, contours are plotted at the selected coastal zone for Chloride, Specific Conductivity, Iron content, Total Dissolved Solids, etc. These results are used to determine the probable path of saline water ingression. Owing to heterogeneity of the aquifer in the selected areas, the spatial irregularity in salinity is significant.

An innovative method of control of saltwater intrusion into the coastal aquifers has been recommended by the author. This new method comprises of withdrawal by qanat-well structures with reasonable compensation by rainwater harvesting by methods for recharge tank and recharge well. The salient features of the methodology are depicted by considering a design example adopted by the author in the Contai Polytechnic Institute Campus of the area of Purba Midnapur.

The plan of the study area in Purba Midnapur has been divided into six zones based on aquifers soil characteristics and status of piezometric surface which is recognized as aquifer improvement plan and imposing certain restriction of abstraction of groundwater by deep tube in the area concern, will help in recharging the aquifer, control the danger of saline water intrusion and enhancing the quality of groundwater. Other plan of solution to meet future freshwater demand in the area, using alternative freshwater sources has also been additionally been encouraged, the existing Subarnarekha river water are collected and distribution to the various purpose after proper treatment. Lastly, a series of important conclusions are drawn based on the specific research findings.

Keywords:

Coastal Environment, Coastal Structures, Water Sampling, Chemical Analysis, Case Studies, Geotechnical Investigation, Hydrogeology, Laboratory Experimentations, Mathematical Analysis, Quantitative Analysis, Simulation of Groundwater level Modelling, Management and Control of Seawater Intrusion, Porous Media Flow.

Table of Contents

List of Figures

List of Tables

CHAPTER - 1

(Introduction)

- Background
- Reasons of Contamination of Freshwater into Coastal Aquifers by Saline Water Intrusion
- Factors affecting Saline Water Intrusion into Coastal Aquifers
- Basic Components for Management of Saline Water Intrusion
- Saline Water Intrusion – International Status
- Saline Water Intrusion - Status in India
- Coastal Salinity and Factors affecting on it
- Physical Characteristics of Purba Midnapur District
- Present Status of Saline Water Intrusion in Coastal Aquifers of Study Area
- References

1.1 Background

Water is a precious resource which is already scarce and the large parts of our planet are already under serious threat. Although astronomers call our planet as 'water planet', very little of that resource is actually available directly for human consumption. This circumstance is deteriorating as the worldwide populace develops and the rate of environmental change and airborne contamination quickens. The continuation of the existing trend signifies desertification, epidemic, diseases and, increasing conflict on ownership of the earth's dwindling water supply. In coastal zones in particular, withdrawal of groundwater for various human usages like agricultural, municipal and industrial applications are severely hampered by the saline water ingression in response to freshwater extraction. Sometimes, this may introduce serious adverse consequences. Examples of salt water encroachment are numerous in coastal areas, and even occasionally present in few inshore aquifers as well.

1.2 Reasons of Contamination of Freshwater into Coastal Aquifers by Saline Water Intrusion

The reasons, by which freshwater aquifers are contaminated by saline water intrusion, are listed below:

- Saline water intrusion increases due to extraction of freshwater by pumping.
- Inappropriate water utilizes, unintended shrimp culture, inadequate administration frameworks, insufficient or defectively maintained infrastructure and feeble water administration frameworks at neighbourhood.
- Over extraction of groundwater from coastal aquifers leads lateral or horizontal intrusion and consequently saline water from the coast to move towards the inshore direction.
- Vertical advancement or upconing of saline water can happen close to a discharge well when water advances toward the well tip and saline water in the more profound aquifers ascends.
- Cross-aquifer defilement can be caused by wells that are available to different aquifers or have casings that have been corroded or broken (Prinos *et al.,* 2002).
- Environmental change expectations incorporate the ascent of ocean levels by a normal of 2 feet (0.61 m) throughout the following 100 years (Somerville *et al.*, 2007). The ascent of ocean levels pushes ocean water advance inland, debilitating the freshwater aquifers.

1.3 Factors affecting Saline Water Intrusion into Coastal Aquifers

The following factors which affect saline water intrusion are listed below:

- Category of aquifer and its geometry and geography.
- Agricultural and irrigation implementation.

- Intensities and frequencies of precipitation.
- Total rate of groundwater extraction contrasted to recharge rates.
- Existence of freshwater seepage trenches that need salinity control structures.
- Separation of stresses, for example, wells and ditches, from the source(s) of saline water ingression.
- Long-term changes in ocean level started by the tidal movements.
- Regular and yearly varieties in groundwater recharge and evapotranspiration rates
- Geologic stratum formation and the heterogeneity of aquifers including the presence of confining units which can intercept the saline water encroachment.

1.4 Basic Components for Management of Saline Water Intrusion

The following four basic components for control and management of saline water intrusion are listed below:

- Measurement: Engineering knowledge and basic understanding of the hydrogeological properties, geologic setting, site characterisations and geomorphic changes of the area under consideration.

- Monitoring: Using of monitoring wells to provide a reasonable sufficient screen length for monitoring the changes in the saline water interface.

- Modelling: Adequate modelling to provide long-term prediction and behaviour of the interface as against the changes in the population, water usage and rainfall of the area concerned.

- Modification: Modifying the planning, the way of water usage, the pumping and the control runoff or consider re-injection of wastewater to maintain the freshwater head to prevent the further encroachment of the saline water.

The management of saltwater intrusion has been described by means of a flowchart depicted in the Figure 1.1.

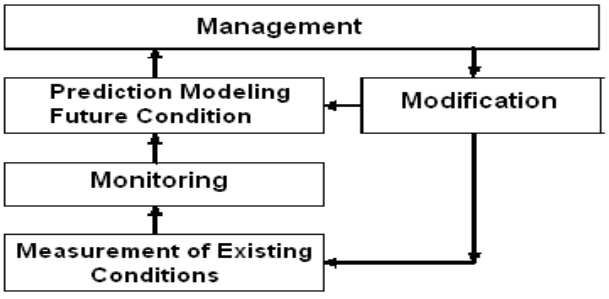

Fig. 1.1: Flow diagram for management of saline water intrusion.

1.5 Saline Water Intrusion - International Status

The changeability of hydro-geologic settings, wellsprings of saline water, history of groundwater withdrawals and freshwater seepage along the Atlantic coast, United States of America have derived in different modes of saline water ingression across the region. The same have been documented throughout the Atlantic coastal, USA zone for more than 100 years (Barlow, 2003), initiating both the lateral intrusion and the upconing.

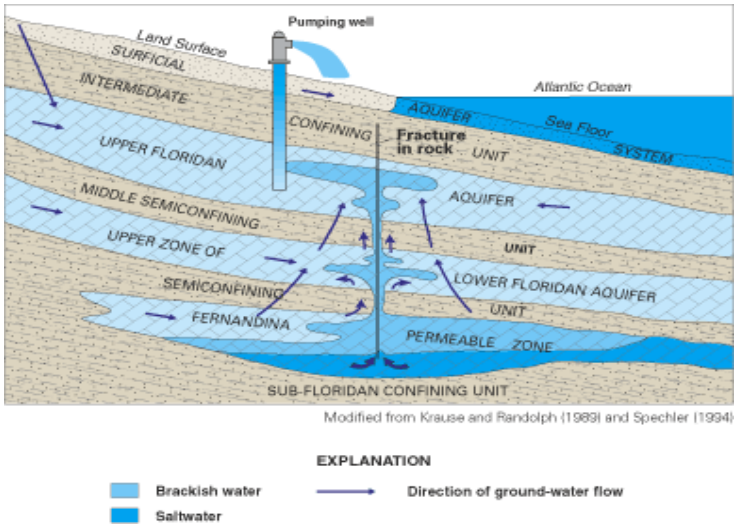

Fig. 1.2: Saline water in the Fernandina permeable zone (after Barlow, 2003).

The problem has derived in a complex process of saline contamination by upward migration of saltwater from the deepest zone of the aquifer system (called the Fernandina permeable zone) to overlying freshwater zones along structural anomalies in the geologic framework of the aquifer system providing preferential conduits for groundwater flow [Figure 1.2].

Bangladesh is the eighth most populous country in the world. About 50% land of Bangladesh is hardly 3 m above the mean sea level and 30% land is under tidal bore. As reported by Rahman and Bhattacharya (2006), the saline water intrusion is the main problem in the south-western zone, having a temporal phenomenon, being minimum during the monsoon (June-October) by push back of the river discharge at the salinity front in estuarine and floodplains, and intrusion in the inland during November- February due to the reduction of freshwater flows. A maximum salinity level occurs during March-April. In the south-western coast of Bay of Bengal, a total of about 1.0 Mha croplands are adversely affected by salinity in the winter months. The salinity in groundwater table of Bangladesh is described in Figure 1.3.

Similarly adverse effects of saltwater intrusion in coastal area of various parts of the World like Greek islands, Japan and different coastal areas of India which have been reported and described by various researchers (e.g. Papadopoulou *et al.*, 2005; Gallardo and Marui, 2007; Goswami, 1968; Mohan and Pramada, 2005). The detailed descriptions of these contributions are given in the Chapter 2.

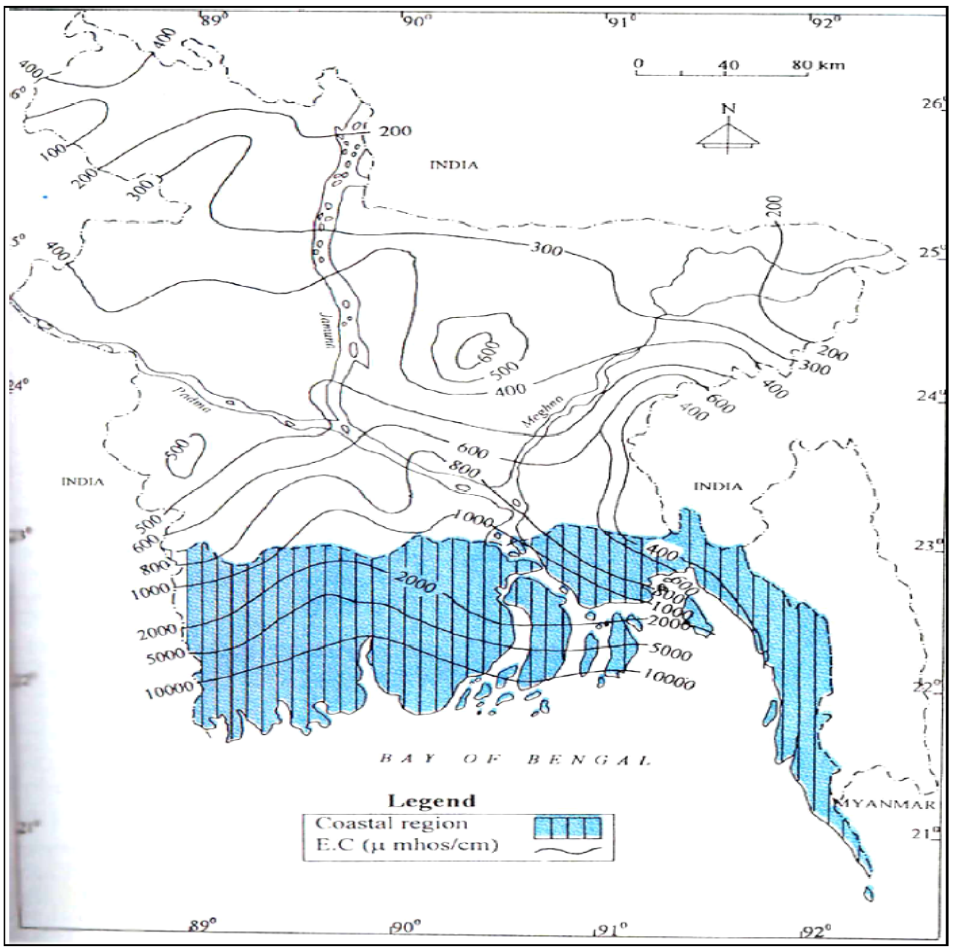

Fig. 1.3: Salinity in groundwater of Bangladesh (after Rahman and Bhattacharya, 2005).

1.6 Saline Water Intrusion – Status in India

The nation of India has a fundamentally long seaside belt of 5700 km. The east coast, likewise named particularly as 'Coromandel' coast, is reached out from the province of West Bengal to Kanyakumari, Tamil Nadu. The west coast then again, which is named as 'Konkan' coast, is extended from Kanyakumari to the province of Gujarat. It was observed that the saline water ingression in the east coast is serious in contrast with the west coast apart from the province of Gujarat and a restricted part of the territory of Maharashtra. The coastal salinity of groundwater in India is described briefly in Figure 1.4.

1.7 Coastal Salinity and Factors affecting on it

The mechanisms of geo-formation, soil-salinity conditions of any place are the direct and indirect effects of the local climate. And these phenomena also have indirect influences on climate. All these factors are interdependent and interrelated. Meteorological details are nothing but the conceptual description about the average rainfall, wind speed,

temperature and evapo-transpiration of an area whereas coastal morphology is the description of geography, geology, hydrogeology and aquifer system. River basin with other formation of land such as mud flats, lagoons bays etc and ecological phenomenon comes in some special cases such as coastal salinity.

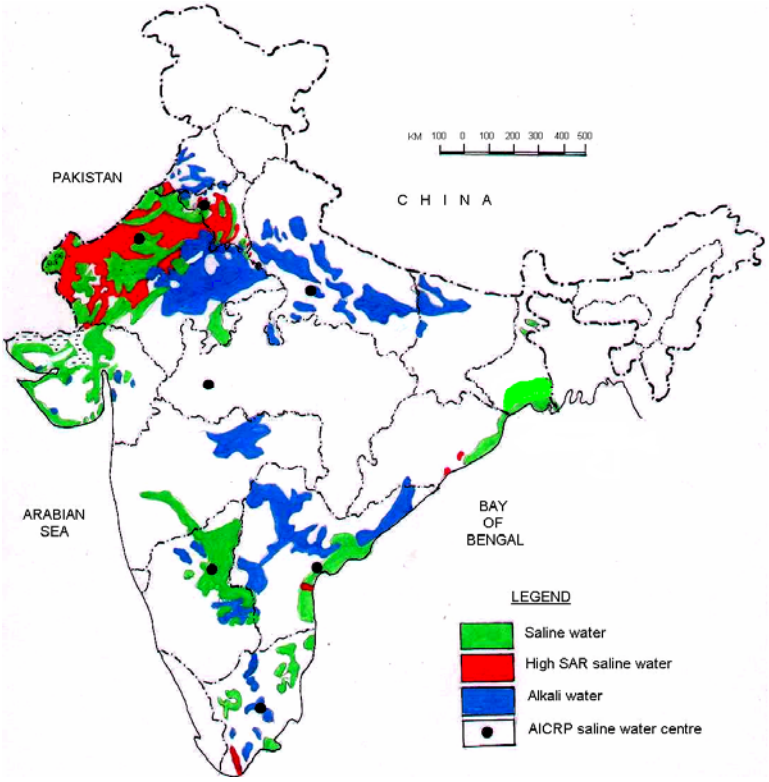

Fig. 1.4: The coastal salinity of groundwater in India.

1.7.1 Meteorology (Atmospheric Feature)

1.7.1.1 Coastal Plain of West Bengal

The coastal plain of West Bengal comprises of 16 blocks in Purba Midnapur district, five blocks in North 24-Paraganas, 32 Blocks in South 24-Paraganas and seven in Howrah district. Climatic Condition in coastal areas of West Bengal does not vary much from the average Indian climatic condition.

Annual rainfall in coastal areas of West Bengal is estimated approximately 1803 mm; variability coefficient of rainfall is 13. Temperature varies from a minimum of 13^{o}C in winter (especially during December-January) to a maximum of 35^{o}C in summer with an average temperature of 26^{o}C. Relative Humidity varies from 68% (minimum) in winter to 89% in rainy season (specifically at the month of August). All these meteorological factors affect on the evapotranspiration of this particular area.

1.7.1.2 Coastal Plain of Orissa (Utkal)

Climatic condition in Orissa coast also does not vary much from the average Indian condition. Annual rainfall in Orissa Coast is estimated approximately 1700 mm; variability coefficient of rainfall is 11. Temperature varies from a minimum of 14^{o}C in winter to a maximum of 36^{o}C in summer. Relative humidity varies from 63% (minimum) in winter to 85% in rainy season. All these meteorological factors affect on the evapotranspiration of this particular area and also evaporation of fresh and saline water may result in salt deposition in this region.

1.7.1.3 Coastal Plain of Andhra

Annual rainfall in Andhra coastal plain is estimated approximately 986 mm, which is much lower in comparison to West Bengal and Utkal coastal plain; but variability coefficient of rainfall is 16 (higher than other two regions). Temperature varies from a minimum of 19^{o}C in winter to a maximum of 34^{o}C in summer. Relative humidity varies from 64% (minimum) in winter to 80% in rainy season. All these meteorological factors affect on the evapotranspiration of this particular area. In the month of May-June, the wind speed is highest with a net loss in water productivity, which may affect adversely to the tidal effect. Therefore, from meteorological point of view this coastal region possesses adverse scenario to the salinity problem. Aquifer system and geo-hydrology in addition to meteorological characteristics are discussed considering landform of the area.

1.7.1.4 Coastal Plain of Tamil Nadu

Annual rainfall in Tamil Nadu coastal plain is estimated approximately 1217 mm, which is higher than Andhra plain; and variability coefficient of rainfall is 14 mm. Temperature varies from a minimum of 21^{o}C in winter to a maximum of 37^{o}C in summer especially in the month of June. Relative humidity varies from 58% (minimum) in winter to 79% in rainy season.

All these meteorological factors affect on the evapo-transpiration of this particular area. Meteorological characteristic in Tamil Nadu coastal plain is similar to the Andhra Pradesh (AP) plain. In this plain, potential productivity from rainfall is positive in the month of October and November only but with a larger quantity with compared to AP plain. Here also the rainfall and wind speed characters are favourable towards adverse effect against tidal and salinity problem. The geology and aquifer system is another consideration to analyse the final effect of salinity and its mechanism.

1.7.2 Geomorphology and Landform (Surface Feature)

In order to develop a rough background about the geomorphologic feature, first of all few coastal landforms and constructional features are described briefly. And there after, those features are described in context of Indian coastal zone. To have a clear understanding for the transitional zones from marine floor to mainland extend, a decent continuity from continental self to coastal zone is tried to capture. This is done to capture

by describing the nature and forms of three components such as continental self, shore and coastal zone and their extensions in a sequence with Indian coast.

1.7.2.1 Continental Shelf of West Bengal

In whole east coast, the continental shelf is narrow beyond shore; most of the places it is found within an average range of 20 km to 35 km. In some places such as northern Orissa, it is as wide as 30 km to 40 km. Continental extension is very thin towards east of Bengal coast and becomes wider towards west of it. It is having varying width from 10 km to 33 km and a steep slope though the slope changes as it goes deeper into the sea.

Shore Zone: Shore zone is the zone affected by tides. Here tidal height ranges from 4 m to 6m. Also there is low land of around 10 m extending up to a width of few kilometres including a convex curve of 400 km long along the Bay of Bengal. It is a low land of dead level plain of Ganga delta. The shore zone is consisting of peat of a depth around 10 m and then pebbles of different grade.

Coastal Zone: The coastal front from Hooghly to Midnapur is having a varied width of around 40 km to 50 km from shore zone. That place lies in the low land of Ganga delta. In east behind the mangrove of Sundarban, the predominant feature is the numbers of distributaries separated by marshy land aligned from north to south. In westward, at the south of Midnapur and part of Balasore, that monotonous feature is broken by the existence of sand dunes [Figure 1.5]. The main characteristic of this coastal area is the over moist marshy and muddy low land with number of distributaries and creeks stretching as of north to south. Alluvium deposition of a very high depth can be noticed in this zone.

Nature of Horizontal Continuity: Therefore, it can be noticed that the sea water level touches the land in an alluvium edge. And the "I"-shaped continental self has a steep slope in this region. Marine action of sea floor towards surface must have lesser significance and the transition zone between sea and land is having a depositional or constructional feature rather than erosion by sea.

1.7.2.2 Continental Shelf of Orissa

Utkal coast is prolonged from Subarnarekha River to Rushikulya River near Berhampore in Orissa. The continental plate at the northern zone is wider (nearly 30 km) and become narrower in the southern part with a steep slope towards sea.

Shore Zone: Shore and coastal zone of Utkal plain can be broadly divided in three predominant zones depending on its physiographic. First is from Subarnarekha to Mahanadi, second predominant feature is Mahanadi delta and third is the southern part of Mahanadi delta. Width of shore zone also varies along its length from north to south,

followed by the topography. The most common width of foreshore zone is around 800 m to 1200 m. And backshore width varies from 200 m to 400 m.

The shore zone mainly consists of beach, which is demarcated from coastal zone by ridges and berms of varying height of 6 m to 20 m. This ridge height is gradually dimensioning from south-west to north-east approximately from Mahanadi towards Hooghly. Sandy beaches and shore zone is quite wide at the southern part of Mahanadi near Puri town as approximately 4.5 km, may be due to extensive deposition by Mahanadi. Further south, near Cuttack and far south from there, the shore zone becomes narrower with a crystalline and laterite front line near the transition zone of shore and coast.

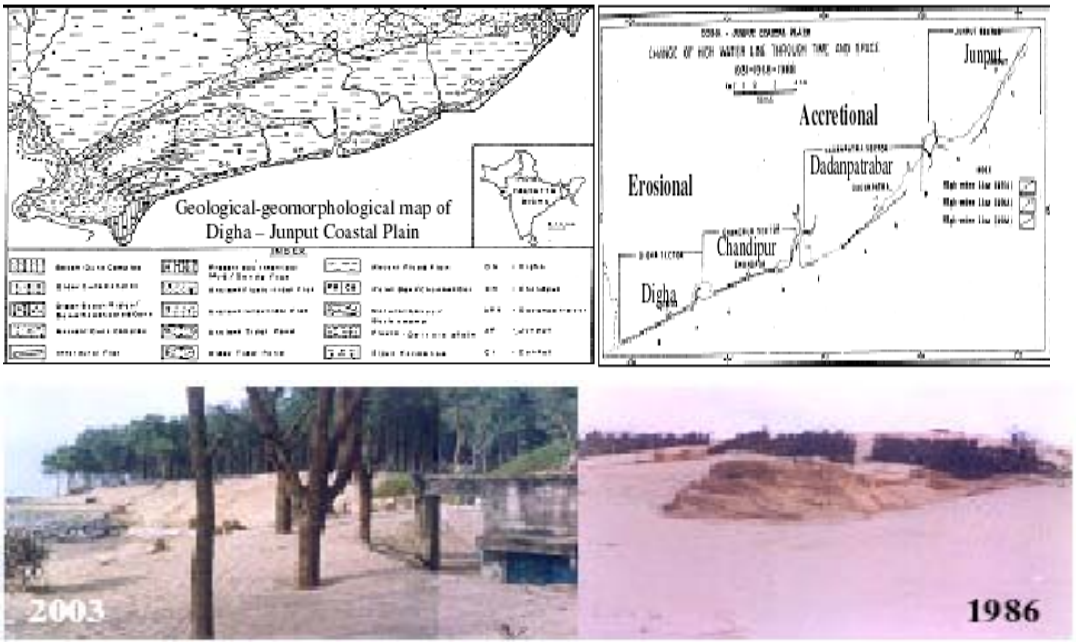

Fig. 1.5: The geological-geomorphological map of Digha-Junput coastal plain.

Then the Mahanadi delta, plain topography with curved mangrove formation can be found along coast. In comparison with Ganga delta, Mahanadi delta is less moist, sandier with less grained deposition and narrower with lesser thick deposition. Towards inland laterite hills can be found near Cuttack. Further south-west, the main feature is the Chilka Lake. It is 60 km long from north-east to south-west direction with a varying width of 7 km to 20 km from west to east.

The north-east of the lake consists of low marshy land while in the north and north-west, rocky hilly region appears. Therefore, the inner age of the coast near the lake touches the Rambha hills and at some places shore zone directly meets with the hills and coast disappears in this southernmost region [Figure 1.6].

Nature of Horizontal Continuity: Incorporating the above scenarios, it can be noticed that in this location also the marine action is constructional. And in northernmost region as well as Mahanadi delta and north-east of Chilka Lake, sea water level touches the

alluvium at shore zone, whereas in southern part at some places sea water level touches the hard rock directly instead of alluvium.

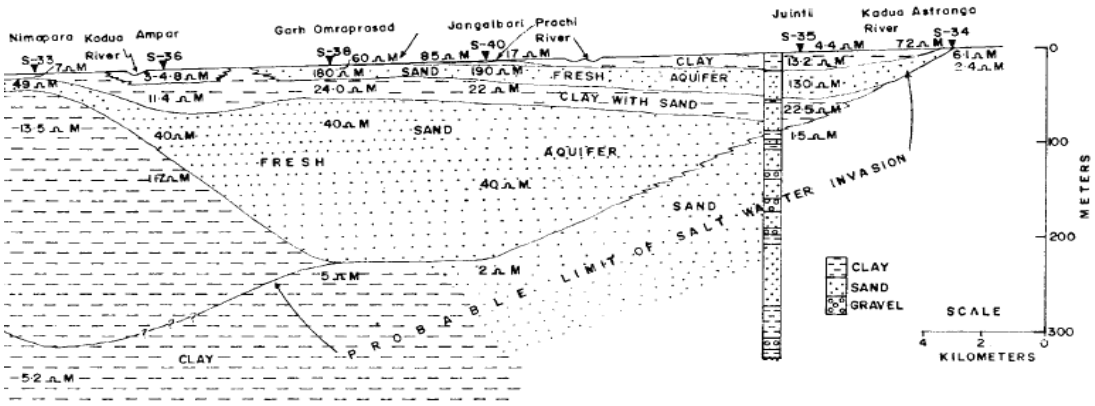

Fig. 1.6: Geoelectrical sections in Mahanadi Delta (after Das, 2007).

1.7.2.3 Continental Shelf of Andhra Pradesh

The continental shelf is having a steep slope of around 1 in 100 in seaward and comparatively less steep towards land where it is wide around 20 km.

Shore Zone: Andhra coastal region is extended from Rushikulya to Pulicat Lake. The shore zone of this region is very much irregular and varying in nature; at many places coast and shore merges with each other by the hilly front. In the northern region such as Vizag, the 50 m contour can be found at a distance of 2 km from shore zone. Knolls of 200 m height can be found discretely along the shore. In the delta, zone of Godavary and Krishna the shore zone are wider. In delta zones the shore comprises of sandy dunes and alluvium.

Coastal Zone: The coastal zone in the northern part of this region is narrow & discrete and some time merges with shore zone. The discrete knolls become continuous behind the coastal zones. In deltas like Godavary and Krishna, the deltas or coastal zone are extended up to 150 km and 90 km respectively from shore zone but with a comparatively thinner layer of deposition. The continuous knolls appear to the delta head of those streams. A number of distributaries and few seawater lakes are the main features of this zone. Godavary and Krishna delta is having medium amount of moist, marshy and medium-grained sediment in comparison with Ganga and Mahanadi delta [Figure 1.7].

Nature of Horizontal Continuity: In this coastal region, in the northern zone at most of the places water line touches the land in hard rock interface, whereas in Krishna and Godavary delta the water land interface is in alluvium.

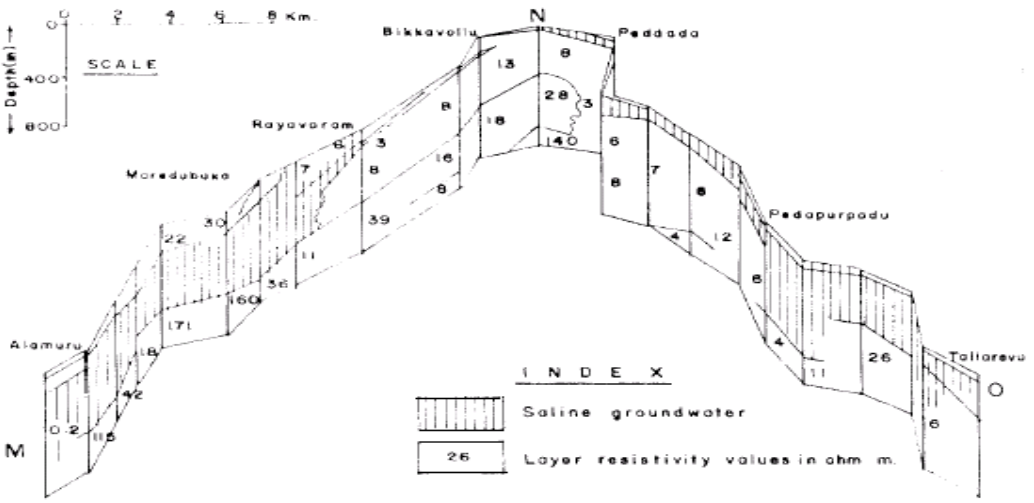

Fig. 1.7: Geoelectrical section of E. Godavari delta (after Das, 2007).

1.7.2.4 Continental Shelf of Tamil Nadu

Continental shelf-width and slope is approximately same with the average of whole eastern shore zone. The steep slope varies from 3 m to maximum 180 m with an approximate width of 60 km.

Shore Zone: Northernmost part of this region bounded within south of Krishna delta to Caleroon is having a total shore width ranging from 200 m to 400 m, while the foreshore zone is approximately 200 m wide. The main feature of this region is the presence of sand dune having an average height of 8 m to 13 m situated at its south. At north to Point of Calimere, the foreshore zone is 400m wide while backshore zone is about 300 m. Further south of Point Calimere the foreshore zone is only 100 m broad and backshore zone is ranging between 200 m to 400 m. Most important feature of this shore zone is the existence of a number of sand ridges between shoreline and lagoons, which are 1.5 km inlands from shore. Those ridges are nearly 18 km long, 200 m wide with a height of approximately 10 m. Further south between Point Calimere and Cape Comerin, again four types of physical differences are predominant. In Palk Strait area, foreshore zone is 50-200m wide while backshore is 1.5 km. In Gulf of Manner, between Dhanushkadi and Tutikorin, backshore zone is 200 m to 2 km wide with a height of 3 m to 6 m. The main feature of this region differing from other part of east coast is the presence of coral reef and oyster banks. It is a sandy beach with rocky shore and having a curved alignment of shore outliner along the Gulf of Manner. In the more southern side, between Tutikorin and Mannapad, a narrower beach of an average height of 20 m can be noticed. Calcareous sand hills of 30 m height and a long stretch of 30 km can be observed here. Further west, a backshore zone of 200 m to 600 m is presented. Near Cape Comerin, sandy beach disappears and rocky front appears to the shore zone; west of it again beach can be noticed.

Coastal Zone: The coastal plain at south of Krishna basin consists of low plain land with an average height of 10 m to 1.5 km in some places. In the coastal zone, sand dunes are there and behind them, a swamp can be noticed up to a distance of 6 km – 8 km from shore. At the southern part near Pondicherry at a distance of 3 km to 5 km from shoreline, rocky hills are another predominant feature of coastal zone. Further south at Cauvery delta, 50 m contours can be found at a distance of 125 km from shoreline. Here sandy dunes overlying on alluvium is the main landforms. In this region number of lagoons and lakes can be noticed around 1.5 km inland from shore zone. Proceeding more southwards, alluvium of thinner layer extended up to 3 km to 5 km can be observed, sandy hills often extended from shore to landwards up to a stretch of 4 km to 6 km inland. Sandy alluvium (of sea origin) merges with reddish alluvium, which is completely different from sea floor deposition. Near by Cape Camerin, 50 m contours can be found at a distance of 2 km from shoreline [Figure 1.8].

Nature of Horizontal Continuity: The incorporating all aspects it can be observed that the coastal shore feature in this region is having very much varied characteristics. Some places in between Krishna and Cauvery and at Gulf of Manner, rocky front interfaces the seawater, whereas at places like Cauvery Basin, comparatively thick alluvium touches the sea level. The region at southernmost part is a transition zone between east and west coast, having a very narrow area consisting of hard base rock.

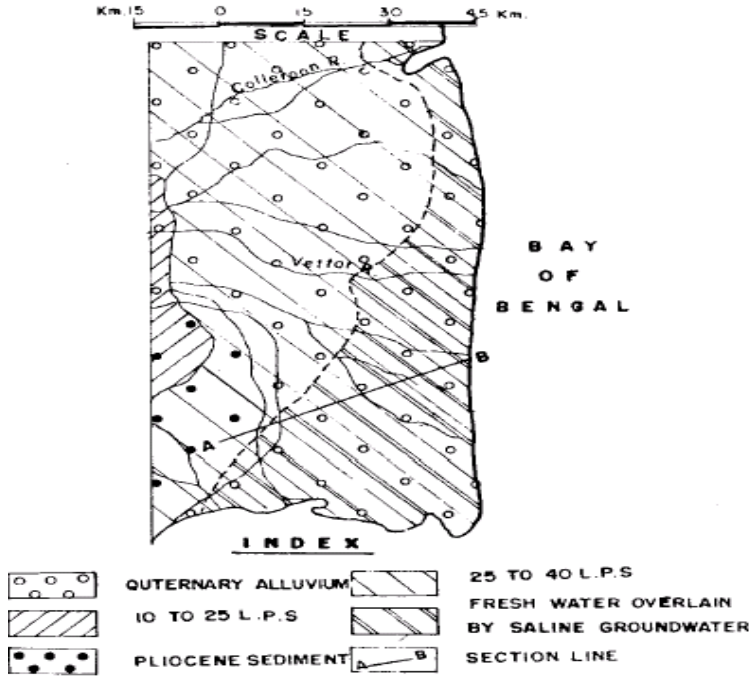

Fig. 1.8: Hydrogeology sections in Cauvery delta (after Das, 2007).

1.8 Physical Characteristics of Purba Midnapur District

1.8.1 Geology

The Purba Midnapur district is situated south-eastern part of West Bengal. The landscape feature is slowly changing with alluvium deposit of Gangetic delta. The lateritic rocks territory is marginally raised from the abutting alluvial plain. The gravelly structure is found in the majority of the territories. The lateritic rock and laterite covering regions are described by dry, burnt and stony soil which isn't reasonable for crop farming. The upper laterite frequently enrooted by conglomeratic and stones of quartz or someplace it rests upon grayish white and reddish clayey soil, delicate lathery and felspathic rocks. The earth underneath down the lateritic rock is marginally soaked with iron. Most unusual exceptional element of geography of the district is the long and immense lateritic sheet found into the plunge of abutting Gangetic plain and furthermore the plunge of western upland. There is a long narrow and elongated strip of saline and alkali soils of Aridisols group, stretching from Digha to the east of the Haldi River. In Tamluk, Sahid Matangini, Panskura-I & II, Nandigram-I, Ramnagar-I & II, Nandigram-I, Sutahata, Haldia, Ramnagar-I & II, Egra-I, Contai-I & Deshpran blocks are covered with sandy loam soil by more than 10% of their area. In Moyna, Bhagwanpur-I, Egra-II and Deshpran blocks less than 10% soils are sandy loam (Sahu, 2014).

1.8.2 Physiography

On the essential of the qualities of the district, the whole Midnapur region (Purba and Paschim) has extensively been partitioned into two common divisions – the western upland including undulating lateritic Rarh plain and the eastern Gangetic alluvial plain alongside southern sea tract. It is accepted that a metalled street going from Raniganj to Cuttack through unified Midnapur area that slice over the region north to south is the rough limit line of these two regular divisions. Physiographically, the region has been sub-divided into three macro-regions and five micro-regions. The macro-regions are:

a) The Western Upland.
b) The Rarh.
c) The Plain (Deltaic and Coastal).

The micro-regions lies within these macro-regions are:

i) Medinipur upland
ii) Silai plain
iii) Lower Kasai plain
iv) Contai plain
v) Digha coastal plain.

Among the above five micro-regions, The lower Kasai plain, Contai plain and Digha coastal plain falls in the Purba Midnapur physiographical regions [Figure 1.9].

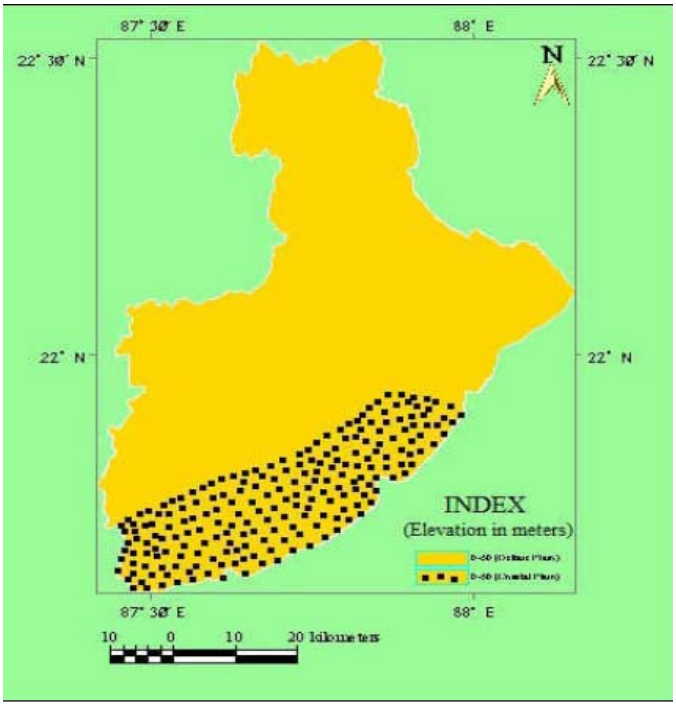

Fig. 1.9: Physiography map of Purba Midnapur district.

1.8.2.1 Lower Kasai plain

Kasai is the principle stream in this area. The district reaches out finished both the side of the Kasai River. Being the biggest plain zone of unified Midnapur area, the upper eastern part is knowledgeable about the deltaic nature while the lower northern part encountering the tidal impacts; ebb tide and stream current is very much dynamic in this area. It is a since quite a down zone regarded as low laying tract of alluvium. This is shaped because of the incorporation of the deltas of Kasai and Silai in the north-west part which is triangular in nature. The rate of alluvial assembling is high with respect to the waterway bed of Kasai is completely lost her navigability. A few blocks like Binpur, Jhargram, Salboni, Midnapur, Kharagpur, Keshpur, Ghatal, Daspur, Panskura, Moyna, Debra, Bhagwanpur, Pingla, Nandigram, Tamluk, Sutahata and Haldia have their offer of terrains in this physiographic unit.

1.8.2.2 Contai plain

Contai plain is to be found in the inner and southern piece of the district. The area is very much agriculturally in nature. The eastern part is for the most part level alluvial plain while the western part is delicately undulating. The extents fluctuate from 5 to 46 meters. Rasulpur, Keleghai, Kapaleswari are among the primary streams of this area. The region reaches out between Debra, Pingla, Moyna, Sabang, Khejuri, Contai, Pataspur, Egra, Dantan, Nayagram, Mohanpur etc. blocks.

1.8.2.3 Digha Coastal Plain

It is a littoral tract of Bay of Bengal. The region is characterized by sandy soil and is exposed to southerly strong wind. Embankment, sand dunes and the several coastal features have been found in the region. The coastal plain extends from mouth of Rasulpur River to the mouth of River Subarnarekha. The sandy tract has its own attributes of vegetation which is verdant and it is especially phenomenal. The blocks incorporated into seashore plain are Ramnagar-I and II, Kanthi– I and II. The general surface of the area is pretty much level with an extremely moderate angle towards the Bay, banks made for security from high tide waves and the sand ridges are the main exemption. At Digha appropriate the shoreline is marginally extensive and enlarges eastbound to a width of ever a kilometre. The sand dunes are the most exceptional morphological component of the tract. This dune belt runs relatively parallel to the present shore line; however the width and elevation change from place to place. These rises for the most part rise upto 12 meters; however the height diminishes towards the east. The between dune tract is level and by and large dry. The dunes may move their area affected by solid summer winds. The reliable breeze wind at constant rate amid the midyear storm is one of the main variables of their source and they are transverse in type. The character of the dunes changes with expanding separation from ocean. They are steadier and more under vegetation cover towards north. The area is partitioned by a tidal creek streaming southward between the rural area of Mukandapur and Shankarpur in the seaside part of the region. A little stream begins in the area west of tidal creek and flows in a meandering course coastward to meet the tidal creek. The creek and in addition the tributary of the creek said above is hold by dikes to shield the settlements and agriculture fields from intermittent floods. There are a couple of conduits to empty the water from the banks. The land in the middle of the bunds and that between the bund and the southern dunes the central and south central parts of the region are particularly low-lying and are liable to occasional flooding. The territory alongside border territories are secured with Quaternary (Pleistocene) sediments having a place with Eclocene age upto 10 km north of Digha. Inside the 10 km wide seaside plain, there are a few sandy ridges with dominant depression of which three lines of edges alongside sorrow, parallel to the ridges, are in the prompt region of Digha Township.

1.8.3 Climate

The area is experienced by a great variation in climatic characteristics. The atmosphere is particularly tropical and practicing monsoonal attributes with varieties in small scale locales. The atmosphere of the northern and western piece of the region is being portrayed by arid climate having violent dry warmth in summer, a short winter season and respectably precipitation. The climate of eastern and southern part is different in nature; characterized by hot and humid climatic condition. The seasons are however well marked for the entire area.

- Summer season – (March to May)
- South west monsoon season – (June to September)

- Post-monsoon season – (October to November)
- Winter season – (December to February)

The normal yearly precipitation happens in the territory is 1525.5 mm which is especially changeable in nature from place to place. A large portion of it happens amid monsoonal period. No less than 74.0 percent of the aggregate yearly precipitation happens in monsoonal period. The normal yearly scope of temperature fluctuates from 25.5^0C to 38.6^0C in Purba Midnapur given in Figure 1.10 and monthly rainfall and temperature in the district of purba midnapur in 2011 is given in Table 1.1.

Table 1.1: Monthly rainfall and temperature in Purba Midnapur in 2011.

Month	Rainfall (mm)		Temperature (°C)				
	Average	Actual	Maximum	Minimum	Mean	Mean Maximum	Mean Minimum
January	17	3	29	8	18.5	25	13
February	14	10	32	13	22.5	28	17
March	32	13	36	14	25	31	22
April	41	76	34	19	26.5	32	25
May	108	112	35	22	28.5	33	26
June	286	309	35	25	30	32	27
July	320	272	35	24	29.5	32	27
August	325	384	35	25	30	31	26
September	333	335	34	25	29.5	31	26
October	200	24	34	18	26	33	24
November	16	-	33	17	25	30	19
December	5	-	30	10	20	30	10
Total	1697	1538					

Source: District Statistical Handbook of Purba Midnapur, 2010 and 2011 combined.

1.8.4 Hydrology

Groundwater is concerned with landforms geomorphology, soil characteristics, its drainage system, topography, land use/land cover characteristics, vegetation condition and also underlying geological characteristics like lithology or structure as shown in Figure 1.11. In Purba Midnapur district the whole regime is a part of alluvial plain except coastal sandy stretches. Regarding all measures of ground water possibility, the area practices a decent stipulation of ground water. Saline water intrusion and the expansion of saline aquifers have likewise discernible. In the district, the ground water level in pre-monsoon varies from 3 to 15 meter below and in post monsoon varies from 4 to 12 meters below. The hydro- geological map of Purba Midnapur district is given in Figure 1.12.

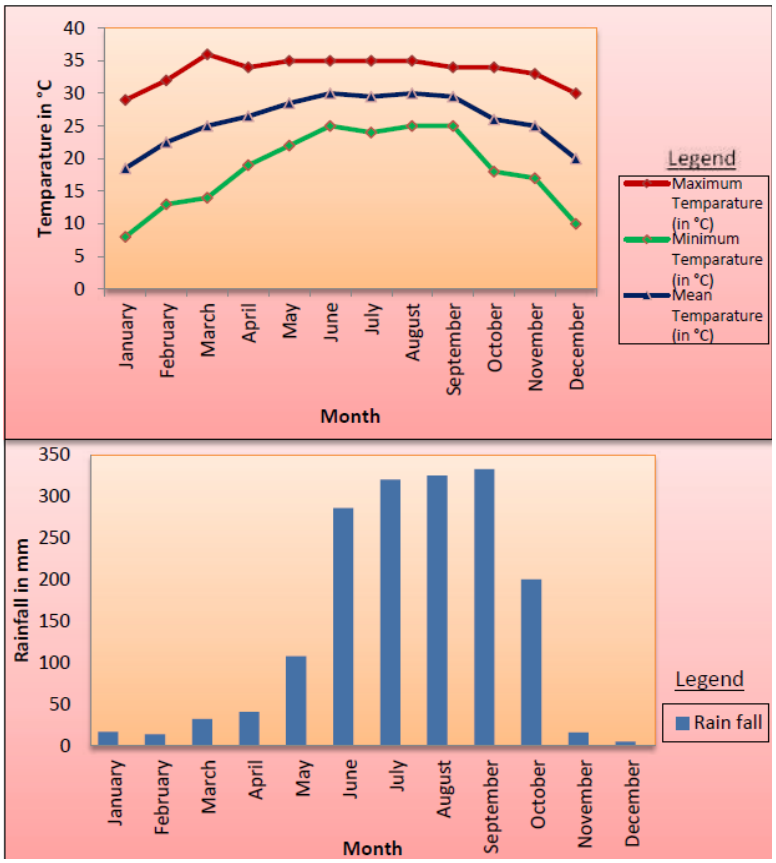

Fig. 1.10: Month-wise rainfall and temperature graph of Purba Midnapur.

1.8.5 Drainage and River system

- The Hooghly
- The Silai
- The Kasai
- The Keleghai
- The Rasulpur
- The Subarnarekha

1.8.5.1The Hooghly

The Hooghly River flows along the eastern boundary of the district Purba Midnapur from where the water of river Rupnarayan falls into it. The river flows to the Bay of Bengal. Hooghly River has several braided channel across its length. A line of sand hillocks are present on the bank of the river.

1.8.5.2 Silabati or Silai

The Silai River originates from Chhotonagpur plateau of Jharkhand and flowing through Bagri Paragana in Paschim Midnapur (via Puruliya and Bankura) and joined with

Darakeshwar and falls into the river Hooghly. The tributaries are Tamal, Parang, Kubai, Birai etc. The whole catchment zone covers upto a division of Garhbeta-I and II, Daspur-II and Keshpur block. Siltation and over the top storm cause every now and again surge circumstance in whole catchment region.

Fig. 1.11: Drainage and River system of Purba Midnapur.

1.8.5.3 The Kangsabati or Kasai

The Kangsabati or Kasai River is a noteworthy stream framework in the study area. It begins from Chhotonagpur plateau and streams in the locale Paschim Midnapur and conjoined with Keleghai and falls into the Haldi River close Mahishadal. The stream is navigable amid stormy season. Waterway Kumari in Bankura and Cossye from Kapastikri in Paschim Midnapur are the fundamental tributaries of Kasai River. The stream conveys a lot of residue causing silting up the channel.

1.8.5.4 The Keleghai

The stream starts from the western end of the region in Dudhkundi in Jhargram P.S. and courses through Sankrail, Keshiary, Narayangarh, Sabang, Moyna and Pataspur block and meets into Haldi River. Kapaleswari and new Cossye are the tributaries of Keleghai River.

1.8.5.5 The Rasulpur River

The waterway begins from the south-western part and continues east ward. Close Kalinagar, the stream joins into another waterway and named as Rasulpur River and streaming along south-east course till to meet into the Hooghly River.

1.8.5.6 The Subarnarekha

The waterway Subarnarekha is starting from Chhotonagpur plateau close Ranchi in Jharkhand and enters the region at the north west from Dhalbhum and going through Gopiballvpur-I and II, Sankrail, Keshiary, Dantan-I and furthermore in Balasore locale in Odisha lastly falls into the Bay of Bengal. Sandy bed is seen along its stream. Dulong is the tributary of the stream. Over the top release of water from the Chandil reservoir at some point causes flood in the catchment territory.

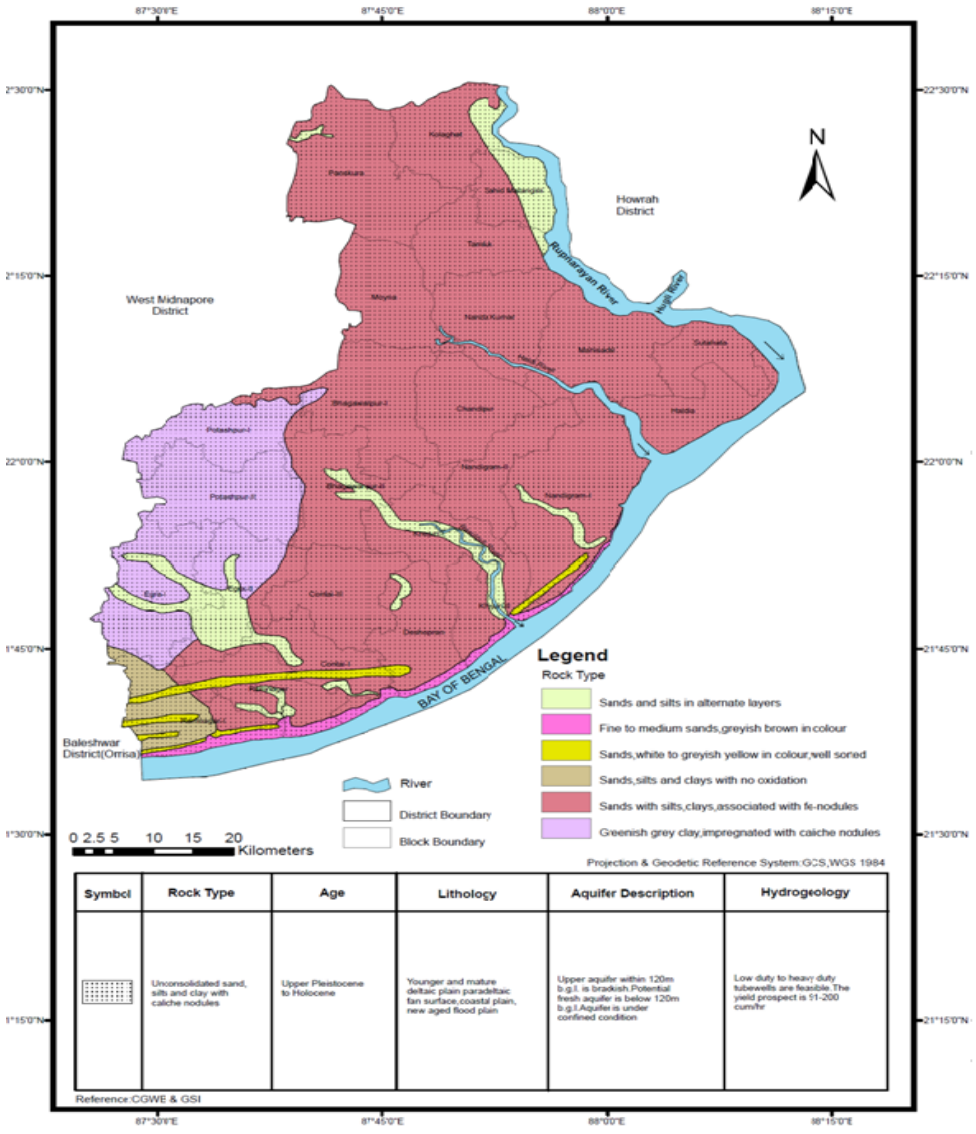

Fig. 1.12: Hydrogeology map of Purba Midnapur.

1.8.6 Landuse and Landcover:

The land-use pattern of the district Purba Midnapur is most varied in nature. Generally, a large open and well-cultivated plain is predominant land use of Purba Midnapur as given in Table 1.2.

Table 1.2: Landuse and Landcover data of Purba Midnapur.

2010-2011	Area ('1000 hectare)
Reporting area	396.59
Forest area	0.90
Area under non-agricultural use	102.24
Barren and unculturable land	0.69
Permanent pastures and other grazing land	0.18
Land under miscellaneous tree groves not included in net area sown	2.15
Culturable waste land	0.29
Fallow land other than current fallow	0.24
Current fallow	1.85
Net area sown	288.05

Source: District Statistical Handbook of Purba Midnapur, 2010 and 2011 combined.

1.8.7 Electrical Conductivity

Salt content of the soil samples is determined on the basis of electrical conductivity (EC). The higher the salt content, the lower is the productivity of soil. Map given in Figure 1.13 shows the spatial variability of electrical conductivity in soils of Purba Midnapur. It demonstrates that in most of the blocks electrical conductivity of soil lies below the tolerable limit. But electrical conductivity is critical for seed germination in part of Kolaghat, Sahid Matangini, Tamluk, Moyna, Nandakumar, Mahishadal, Sutahata, Haldia, Chandipur, Bhagwanpur I & II, Khejuri I & II Nandigram I & II, Part of Egra II, Contai I & III, Ramnagar I & II, Part of Khejuri I, and Deshapran blocks. In Haldia and in parts of Deshapran, Khejuri I, Nandigram I, Sahid Matangini blocks soil salinity has become critical for the growth of salt sensitive crops. Electrical conductivity of soils in part of Deshapran, Khejuri I and Haldia blocks are injurious to most crops (Sahu, 2014).

1.8.8 Agriculture

The Kanthi coastal area plain lying between the estuary of the Subarnarekha River and Hugli River is an upper east southwest shifting seaside zone portrayed by lines of shoreline edges and prevailing low-lying swales. The coast is a meso-tsunami ruled drift. The wave condition of the Kanthi coast is overwhelmed by wind driven waves originating from SE or SSE.

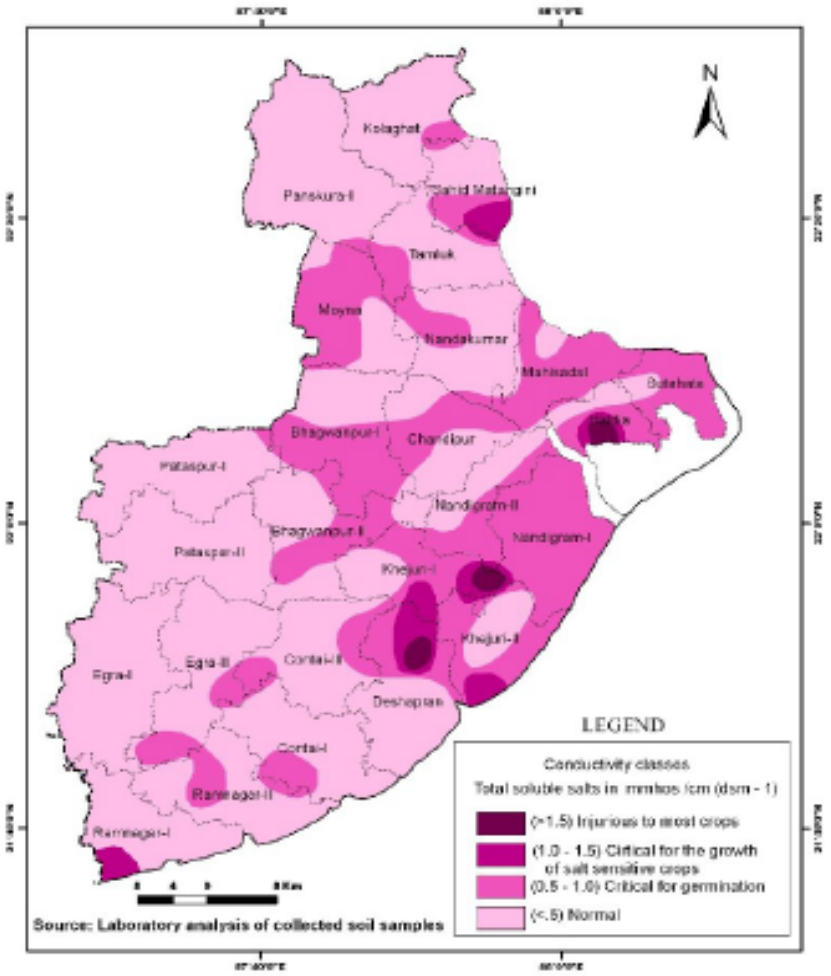

Fig. 1.13: Spatial variability of electrical conductivity (after Sahu, 2014).

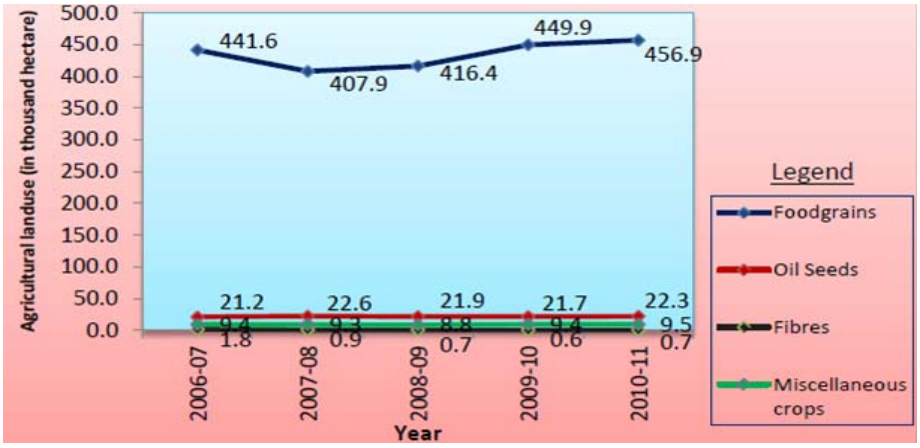

Fig. 1.14: Agricultural landuse of Purba Midnapur.

Wave stature in the untamed ocean is beneath 1 m which increments generously as the waves move over slanting close shore ocean floor (the bathymetric shapes are for the most part shore parallel) at a little point to the coast line. The Ganga (Hugli) delta in the

south 24 Pargana district is a tide overwhelmed delta. There is a major difference regarding agribusiness and water system in the areas Purba Midnapur. The economy of the regions depends on agribusiness and industry. So, the development of standards of living of the people depends solely on the advancement or development of agriculture and industry. Out of total cultivable area in the Purba Midnapur district, almost 80% of land area is used for rice production. Floriculture and horticulture are also a great concern in the districts. Horticulture is work on while floriculture is fine practiced in Panskura and Kolaghat area. Betel vine agriculture and cashew-nut agriculture are additionally practiced in the area. Indiscriminate use of chemical fertilizer, which leads to the loss of fertility of soil and excessive withdrawal of ground water which leads to the scarcity of ground water are the major hindrances for the advancement of agriculture. The major crops grown in this district are Paddy (Aus, Aman and Boro), Wheat, Potato, Oilseeds, Vegetables, Pulses, Jute, Betel vine, Mat stick, etc. Net cropped area of this district is about 304800 ha. The experience of drought and flood are common in this district and sometimes one is followed by another in a year. Normal rainfall of this district is 1683 mm and average rainfall is 1752 mm (12 years average). The agriculture landuse of Purba Midnapur district is given in Figure 1.14.

1.8.8.1 The different sources of irrigation

Irrigation is the most important factor for agriculture and its development. The different sources of irrigation in the district are mentioned below. In Purba Midnapur, a stable condition is prevailing from 2006-2007 to 2010-2011 (District Statistical Handbook: Purba and Paschim Midnapur, 2011). Area irrigated by different sources in the district of Purba Midnapur is given in Table 1.3.

Table 1.3: Area irrigated in Purba Midnapur.

Year	Area irrigated by (thousand hectare)									
	Govt. Canal	Tank	HDTW	MDTW	LDTW	STW	RLI	ODW	Others	Total
2006-2007	63.58	26.25	6.45	20.47	0.05	48.81	3.65	-	-	169.26
2007-2008	62.78	26.25	6.45	20.47	0.05	48.81	3.65	-	-	168.46
2008-2009	62.78	22.38	4.77	36.70	-	36.60	2.77	-	26.72	192.72
2009-2010	62.78	22.38	4.77	36.70	-	36.60	2.77	-	26.72	192.72
2010-2011	62.78	22.38	4.77	36.70	-	36.60	2.77	-	26.72	192.72

Note: HDTW- High Capacity Deep Tubewell; MDTW- Medium Capacity Deep Tubewell; LDTW- Low Capacity Deep Tubewell; STW- Shallow Tubewell; RLI- River Lift Irrigation; ODW- Open Dug Well.

1.9 Present Status of Saline Water Intrusion in Coastal Aquifers of Study Area

In coastal areas, extraction of groundwater for various human usages like agricultural, municipal and industrial applications are seriously hampered by the ingression of saline water in light of freshwater withdrawals. Sometimes, this may introduce serious adverse consequences. The reasons by which freshwater aquifers are polluted by saline water ingression are various. Some of them are: pumping of freshwater initiating lateral or horizontal intrusion and vertical intrusion with upconing, cross-aquifer contamination caused by wells open to multiple aquifers (Prinos *et al.*, 2002), climate change initiating rise in sea water level, thereby pushing back the freshwater zones (Treut *et al.*, 2007), etc. The variability of hydro-geological settings, sources of saline water, history of groundwater withdrawals and freshwater drainage along different coasts around the world has resulted in different modes of saline water intrusion across the region. The same has been documented throughout the Atlantic coastal, USA zone for more than 100 years initiating both the lateral intrusion and the upconing (Barlow, 2004). Similar adverse effects of saltwater intrusion in coastal area of Greek islands, Japan and Bangladesh have been reported and described by various researchers like Papadopoulou, (2005), Gallardo and Marui (2007), Rahman and Bhattacharya (2006).

The country of India has a significantly long coastal belt of about 5700 km. The east coast (Coromandel) is reached out from the province of West Bengal to Kanyakumari, Tamil Nadu. The west coast (Konkan), then again, is extended from Kanyakumari to the province of Gujarat. It was observed that the saline water ingression in the east coast is serious in contrast with the west coast aside from the territory of Gujarat and a restricted bit of the province of Maharashtra. All parts of the east coast of India do not have a similar defencelessness to saline water ingression. The east cost of India consists of diverse deltaic districts. For cases are the Ganga delta, the Mahanadi delta, the Godavari delta, the Krishna delta and the Cauvery delta. In these deltas, there is considerable recharge into the aquifer from the upstream. This balances to some degree saline water interruption. There are likewise puts on the east shore of India like Vishakhapattanam where the Eastern Ghats (which is a scope of slopes running parallel to the coastline) contacts the ocean. Here saline water ingression is of no significance. Saline water ingression is of awesome significance in areas having differing features, *viz*., the Purba Midnapur district of West Bengal which lies on the western edge of the Ganga delta. In this research, work is aimed towards conducting a thorough and in-depth field based study on extend and intensity of saline water intrusion in Purba Midnapur district, a coastal city of West Bengal, by means of subsurface characterizations, future groundwater level simulation and water quality analysis and to discuss about the control methodologies. Sub-division wise block map of Purba Midnapur is given in Figure 1.15.

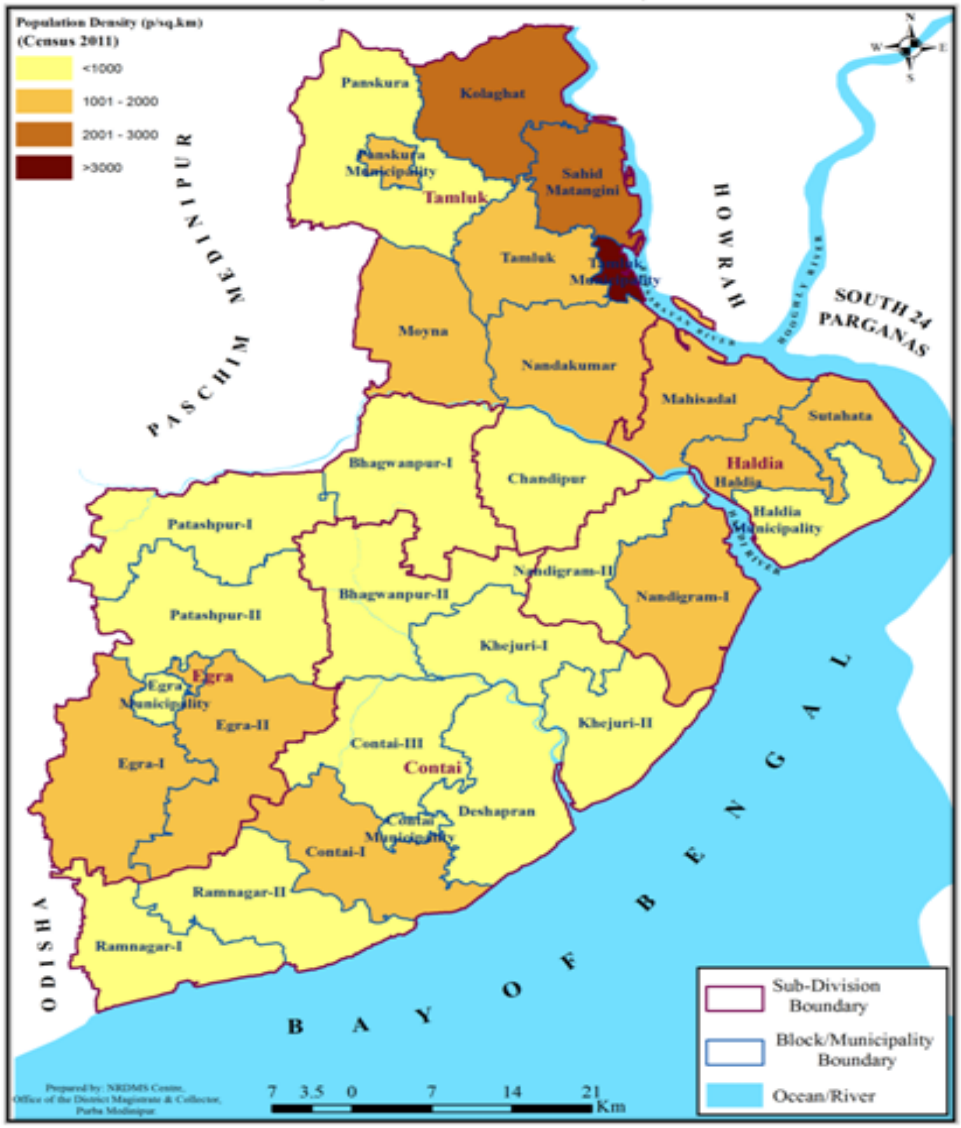

Fig. 1.15: Sub-division wise block map of Purba Midnapur.

1.10 References

Barlow, P.M. (2003). Ground Water in Freshwater-Saltwater Environments of the Atlantic Coast. Circular 1262, U.S. Geological Survey, Reston, Virginia, USA.

Das, S. (2007). Hydrogeological Features of Deltas and Estuarine Tracts of India. *National Seminar on Changing Geohydrological Scenario in hard rock terrains of India*, April, 29-30, 2007, pp. 69-105.

District Statistical Handbook: Purba and Paschim Midnapur (2011). Department of Planning, Statistics and Programme Monitoring, Government of West Bengal.

Gallardo, A.H. and Marui, A. (2007). Modeling the Dynamics of the Freshwater-Saltwater Interface in Response to Construction Activities at a Coastal Site. *International Journal of Environmental Science & Technology*, Vol. 4, Iss. 3, pp. 285-294.

Goswami, A.B. (1968). A Study of Salt Water Encroachment in the Coastal Aquifer at Digha, Midnapore District, West Bengal, India. *Bulletin, International Association of Scientific Hydrology*, Vol. 13, No. 3, pp. 77-87.

Mohan, S. and Pramada, S.K. (2005). Management of South Chennai Coastal Aquifer System-A Multi Objective Approach. *Jalvigyan Sameeksha*, Vol. 20, pp. 1-14.

Papadopoulou, M.P., Karatzas, G.P. and Koukadaki, M.A. (2005). Modeling the Saltwater Intrusion Phenomenon in Coastal Aquifers - A Case Study in the Industrial Zone of Herakleio in Crete. *Global Nest Journal*, Vol. 7, No. 2, pp. 197-203.

Prinos, S.T., Lietz, A.C. and Irvin, R.B. (2002). Design of a Real-Time Ground-Water Level Monitoring Network and Portrayal of Hydrologic Data in Southern Florida. *USGS Water-Resources Investigations Report* 01-4275.

Rahman, M.M. and Bhattacharya, A.K. (2006). Salinity Intrusion and Its Management Aspects in Bangladesh. *The Electronic Journal of the International Association for Environmental Hydrology*, Vol. 14, paper 14, pp. 1-8.

Sahu, A. (2014). Status of Soil in Purba Medinipur District, West Bengal– A Review. *Indian Journal of Geography & Environment*, Vol. 13, pp. 121-126.

Somerville, R., Treut, H.L., Cubasch, U., Ding, Y., Mauritzen, C., Mokssit, A., Peterson, T. and Prather, M. (2007). Historical Overview of Climate Change. In: Climate Change 2007: The Physical Science Basis. Contribution of Working Group I to the Fourth Assessment Report of the Intergovernmental Panel on Climate Change. Cambridge University Press, Cambridge, United Kingdom and New York, USA. pp. 93-128.

CHAPTER - 2

(Review of Literatures)

- Overview of Available Literatures
- Inferences from available Literatures
- References

2.1 Overview of Available Literatures

From the review of previous literatures, the major informant explored were the journals, conferences proceedings and other study materials. The survey of literatures has been completed on a worldwide premise with due emphasis given to Indian publications. The significant developments have been outlined under the accompanying general classifications, distinguished as: laboratory-based experimental, research facility based test works, theoretical contributions, computer software modelling and field-based investigations. The most significant developments by different scientist pertinent to the previously mentioned classes are examined in the following sections.

2.1.1. Theoretical Contributions

Muskat and Wyckoff (1935) provided the first physical explanation of water coning beneath an oil well. Although the problem was too difficult to make an exact theoretical solution; they demonstrated an approximate analytical solution. It was expected that the potential circulation in the flow region was same as if the second fluid was absent. The hypothesis does not rely on liquid involved so that their analysis may be taken in conditions of both saline water and freshwater.

Charmonman (1965) studied saline water ingression in freshwater aquifers problems in a two dimensional domain and the freshwater flow pattern in coastal zones a theoretical study has made. Solution was done applying Laplace's equation with known boundary conditions for steady freshwater in an unconfined aquifer, using potential plane. The exact solutions be differentiated with the rough result proposed by other researchers and were establish to be satisfactory for all practical purposes. The author also studied the usefulness of an artificial barrier for preventing saline water intruding inland and offered a numerical solution to the complex free surface problems.

Wang (1965) designed a partially penetrating well for extracting freshwater in an aquifer underlain by saline water. The reason behind this examination was to relate the well discharge to their spacing, penetration, and radius, thickness of aquifer and densities of the fluids and to estimate the maximum production of freshwater without entrainment of saline water. The author presumed that the critical discharge above which the saline water became unstable was obtained for a well penetration ratio between 30-40%. However, in her analysis, water level changed at depth at depth, on the interface itself. It was further supposed that the maximum discharge of freshwater would be achieved while the upconing had reached the beneath of the discharging well.

Li and Yeh (1968) determined a theoretical report on the distribution at the interface of miscible fluids move through a permeable media. The dispersion at the interface could be depicted by Fick's law with a speed dependent coefficient. Firstly, to expose the property of gravity and variation in density and viscosity for the stream in the zone of dispersion, a simple two dimensional steady state flow of two liquid in the horizontal direction was studied. It was assumed that in many cases, one of the fluids remains at rest over the other. These are given in Figure 2.1. The author accomplished that the zone of dispersion was wider when one of the liquid is at rest.

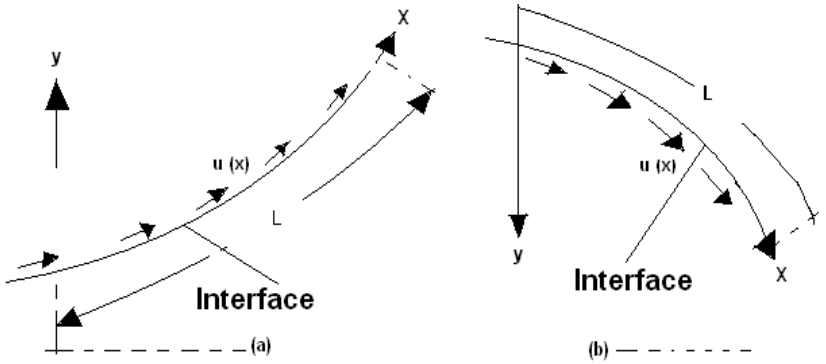

Fig. 2.1: Schematic diagram of (a) flow above a heavier liquid at rest, (b) flow beneath a lighter liquid at rest (after Li and Yeh, 1968).

Pinder and Cooper (1970) presented a transient solution to the saline water ingression issue using the method of characteristics. This problem was characterised by freshwater and saline water flowing in opposite directions at the bottom of the aquifer, resulting in dynamic equilibrium in the areas of low liquid velocities, and in addition the presence of a stagnation point at the base of the aquifer. Since the main dispersive mechanism in the lack of liquid movement is molecular dissemination, the utilization of a speed subordinate parameter of mechanical dispersion appeared to be essential.

Chandler and Mcwhorter (1975) studied the upconing of saline water in reaction of pumping from an overlying layer of freshwater by numerical integration of the governing differential equation, considering of non-linear limit conditions on the water table and the interface surface for unfaltering flow toward partly penetration pumping wells in both isotropic and anisotropic aquifers. They concluded the reality of an optimal well penetration into freshwater layer permitting maximum discharge exclusive of salt entrainment. The optimum penetration was watched to increase as the vertical permeability was reduced comparative to the horizontal permeability. The maximum well discharge obtained without saline water entrainment was watched to be greater for the aquifers with a reduced vertical permeability than for isotropic aquifers.

Segol *et al.* (1975) obtained a result of saline water ingression based upon a velocity dependent diffusion. They solved the fluid pressures and the two velocity components at the same time at each joint in the fine grid and obtained a constant velocity field. In this work, the creators expected that the propagation of the fluid pressure to be greatly faster respect to the solute transport.

Weiss (1982) developed three-dimensional simulations in which liquid density was indicated ahead of time as a component of position instead of ascertained because of solute motion after each time step. This approach is valuable in the study of a steady state flow system where the density distribution of fresh and saline water is known in advance from field observation. It is also used in non-equilibrium analysis where the density distribution does not change appreciable due to solute movement through the time of simulation.

Ranganna and Channabasappa (1983) provided theoretical study with experimental validation of flow through highly porous media using the nonlinear nature of non-Darcy equation. Both methodical and numerical solutions of that equation were determined by utilizing suitable limit conditions. The investigations were performed in a horizontal steady head permeameter on four kinds of hardened permeable foam of various densities with the objects of estimating the hydraulic conductivity and the nature of connection between the liquid and porous foam structure. A decent understanding between the hypothetical and investigational results was found. The creator additionally watched some deviation from the research findings of Ward (1964).

Rudraiah (1985) conducted done a hypothetical report on the steady laminar stream in a parallel plate channel limited by a permeable layer of limited thickness and above by a rigid impervious plate working with a uniform speed. The two cases, viz., the permeable mediums limited beneath by (i) a static liquid and (ii) a rigid impermeable stationary wall, were considered separately. The basic equations were determined by assuming steady, uniform, laminar, unidirectional flow of Newtonian, viscous and incompressible fluid driven by a uniform pressure gradient. The solutions were determined by applying suitable limit conditions. The author watched that the speed profile exhibited a boundary layer in the region of the permeable surface. The velocity profile was watched to increase the profundity of the permeable medium and decreases with the velocity factor. It was additionally discovered that the impact of the limited thickness of the permeable medium was significant only for large values of viscosity factor and small values of porous parameter.

Rudraiah *et al.* (1986) analysed the damping of inside gravity waves proliferating in using the Eargun-Darcy model. It was accepted that the turbulence can be parametrically spoken to by an eddy mixing coefficient. It was demonstrated that the damping-length and period-increment is, in general, dependant on the permeability parameter, the Prandtl number, the Rayleigh number, the depth of the permeable layer, and the eddy thermal diffusivities.

Gupta and Gaikwad (1987) built up a rearranged scientific model to foresee the balance position of upconned interface because of level well in unconfined seaside zones of limited thickness. The model depended on Dupuit presumption and Ghyben-Herzberg estimate with altered limit conditions along the shore line. The author derived formulations for a specified the quantity of freshwater discharge to the ocean, interface profile and length of interface. Under the common stream condition, the calculated interface profile by the model was observed to be in good conformity with the results of obtainable analytical solutions and by conducting experiments for different well locations and withdrawal rates. The comparison indicated that the projected model underestimated the interface depth underneath mean ocean level as a result of the simplified assumptions of horizontal flow and hydrostatic pressure distribution. But presumably the model provided an acceptable prediction. It should be noted that with low rate of withdrawal of water, the interface moves upward from its position in normal stream condition without any upconing effect along its length. The author found the presence of a significant extent of upconing depending on location of the well. The investigation of the authors is briefly described in the Figure 2.2.

Reilly and Goodman (1987) studied the difficulty of saline water upconing underneath a discharge well using a sharp-interface method and using a fluid-density based on solute transport method. It was observed that: (i) the well can discharge significant concentration of saline water when a stable cone exists underneath the well screen; (ii) A relatively straight relationship exists between the well discharge rate and the attention of the discharge at low pumping rates requires to keep up a steady cone; (iii) Although upconing is delicate to transverse dispersivity, though it is obtuse to longitudinal dispersivity.

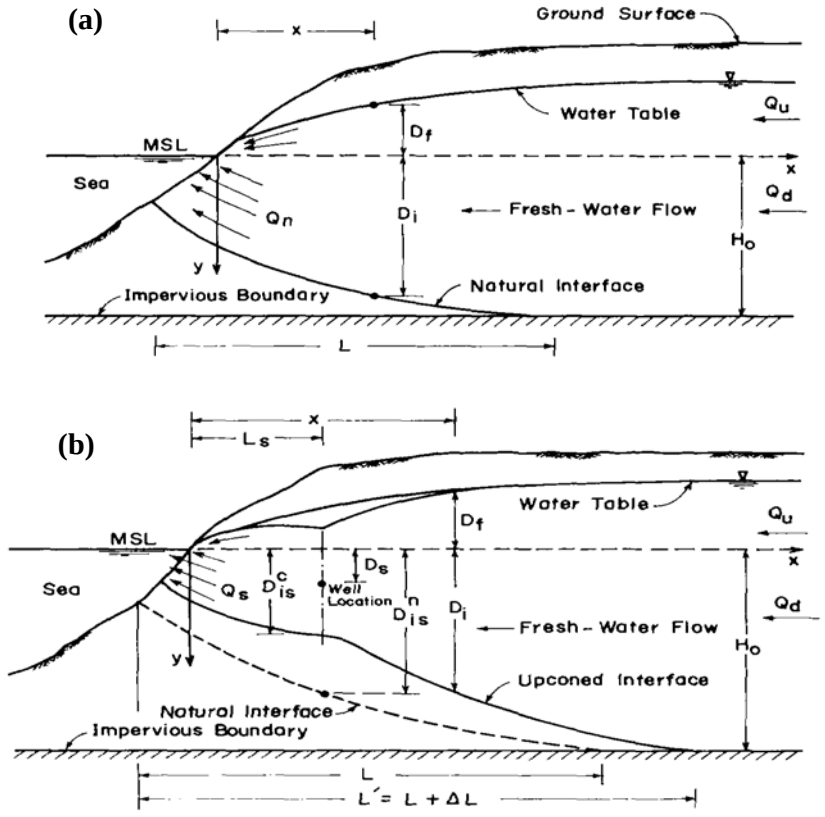

Fig. 2.2: Diagram illustration of the study of Gupta and Gaikwad (1987) for (a) natural flow condition and (b) upconing.

Motz (1992) developed an analytical model to investigate the upconing of saline water beneath a well pumping freshwater from an aquifer over-lain by a leaky confining bed. The drawdown was calculated along and then, the Ghyben-Herzberg connection was utilized to ascertain ascends in the interface. The interface rise and the critical pumping rate were resolved as far as aquifer and confining bed properties and the degree of penetration of the discharge well into the freshwater zone. In light of Muskat (1937) approach, it was accepted that the ascent of the interface is little and it goes about as a streamline or an impervious boundary. It was further assumed that no stream happens underneath the interface. The analytical model was utilized to estimate the critical pumping rate from well using site specific parameters. However, the significant

discharge rate was originated to be comparatively insensible to changes in values of well radius. The author suggested further advancement of numerical solutions for an aquifer overlain by a permeable confining bed using the sharp-interface and the density reliant solute transport approaches.

Xue *et al.* (1995) proposed a finite element technique to study the three dimensional miscible transport model for saline water ingression in a phreatic aquifer with a transition zone. This model considers numerous imperative factors, for example, the impact of variable thickness of liquid stream, precipitation in filtration, phreatic surface change on the procedure of saline water ingression, presence of enormous discharge pumping wells, and so forth. Proper conditions were utilized to depict the saline water ingression experiencing significant change zone for the stream of variable thickness liquid (mixture of seawater and freshwater) and also the transport of dissolved salt. The model was confirmed with the actual regional data of the investigating zone (China) with reasonable good agreement.

Millham and Howes (1995) provided a relationship of the various methods to estimate hydraulic conductivity (*K*) in a shallow coastal aquifer including tidal damping, tracer, slug, permeameter and grain size analysis. These methods were differentiating in together upland and the shore area of a sandy coastal aquifer.

Inoue and Nakayama (1998) conducted a numerical modelling of a non-Newtonian liquid move through a permeable medium utilizing a three dimensional cluster. The goal of this study was to find out the viscous and porous inertia effects on the pressure drop. The porous media was idealized as a gathering of cubes of infinite extent. The three-dimensional momentum equation was utilized alongside the continuity equation at a pore scale, in order to simulate a flow through an interminable number of impediments organized in dimensionless pressure gradient. It was summarised that the permeability for a gathering of cubes was nearly the same as that of the filled spheres of same diameter under the identical porosity.

Andrade *et al.* (1999) explored the source of the deviations from the established Darcy law by numerical simulation of the Navier Stocks conditions in two-dimensional uncombed permeable media. They connected the Forchheimer condition as a phenomenological model to relate the varieties of the contact factor for various porosities and stream conditions. At adequately high Reynolds numbers when the inertia becomes applicable, a change from linear to non-straight performance was watched. They found that such transition could be comprehended and statistically described as far as the extraordinary conveyance of kinetic energy in the framework.

Rudraiah (2001) did a hypothetical investigation for non-linear flow of stratified liquid through permeable media. Arrangement was acquired for the liquid in movement owing both the consistent density gradient and additionally piecewise density gradient. The uniform density gradient was found to start an absolutely even horizontal motion fulfilling the non-linear Forchheimer equation. The creator likewise watched that the vertical density gradient varies persistently in the space time allotment, with the even horizontal density gradient remaining unaltered. On account of a piecewise constant density gradient, a stream work definition was utilized and the arrangement were obtained utilizing time-arrangement examination.

Mahesha (2001) built up a one-dimensional finite element investigation [Figure 2.3] to anticipate the impact on ocean water ingression of freshwater recharge through a limited width strip parallel to the coast. The study investigated the impact of area, width, force and the time of recharge on ocean water-freshwater interface movement. The model was utilized to do parametric examinations thinking about a few speculative cases. Connections were set up between the interface movement and the recharge parameters relevant to wide ranging reasonable cases. From the studies significant reduction of saline water ingression appropriate to strip recharge was observed [Figure 2.4]. The ideal location for recharge was identified to achieve the maximum repulsion of intrusion.

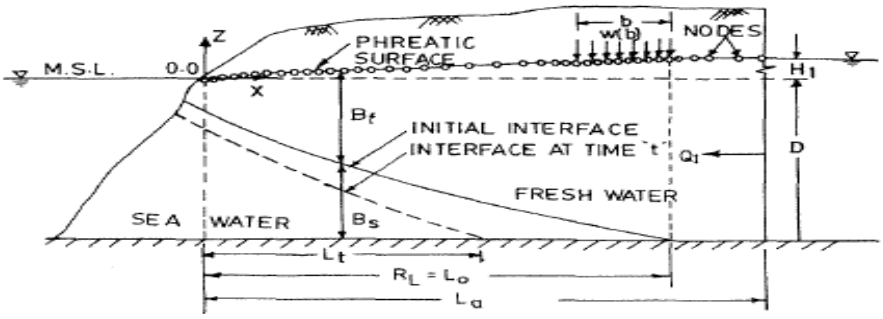

Fig. 2.3: The problem definition of Mahesha (2001).

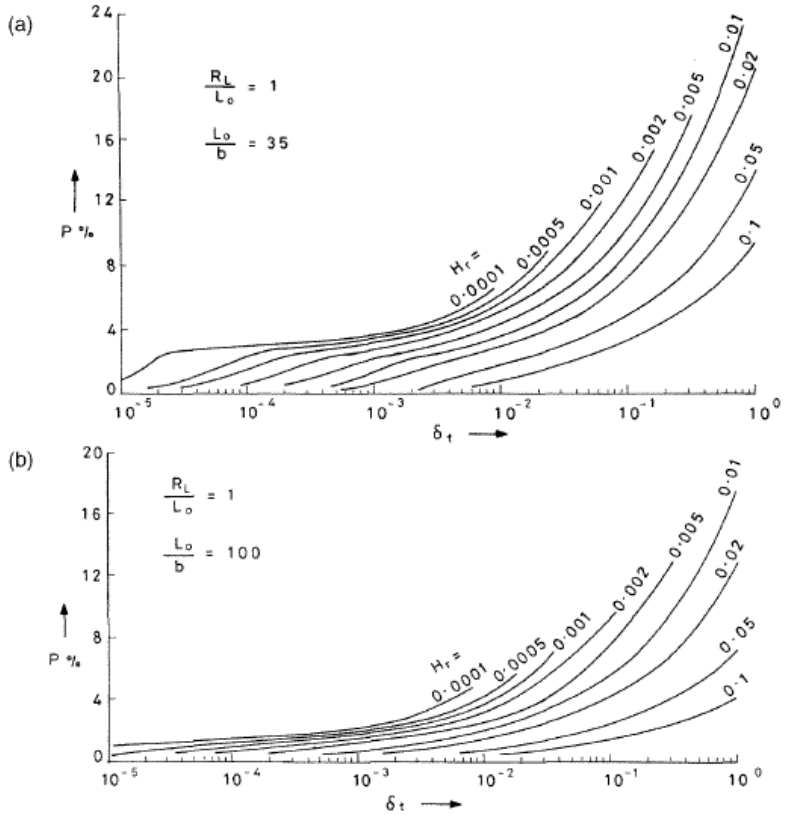

Fig. 2.4: Reduction of intrusion due to strip recharge. (a) $b = L_0/35$; (b) $b = L_0/100$ (Mahesha, 2001).

Chan and Govindaraju (2003) projected an innovative model for soil hydraulic properties in view of a stochastic conceptualization of permeable media. The model depended on irregular collection of soil particles represented by arbitrarily sized overlapping spheres. The spatial course of action of the spheres was expected to take after a homogeneous Poisson process. A stochastic examination was used to get expressions for soil water retention curves and relative hydraulic conductivity. The model provided a reasonable fit with the experiential curves for the water retention and the relative hydraulic conductivity.

Mohan and Pramada (2005) investigated a comprehensive study using numerical software for management of coastal aquifer strategy in Chennai, India [Figure 2.5]. The examination region of South Chennai aquifer was found to confront extreme risk by saline water ingression.

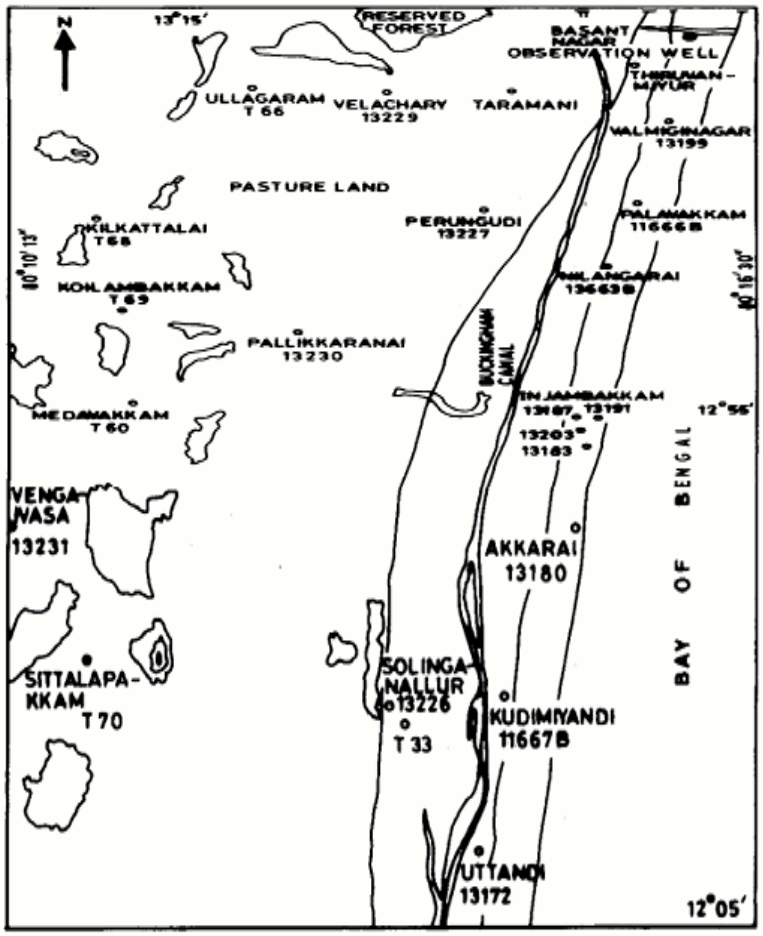

Fig. 2.5: Study area after Mohan (2005).

The parameter Cl/ HCO_3 +CO_3, was taken as the pointer of saline water ingression. The numerical model was designed using the ARGUS-ONE software with the SEAWAT computer code based disperses interface approach. The investigation was completed by partitioning the examination region utilizing the finite difference grid [Figure 2.6]. Comparisons of computed results with the available field data have shown good

agreement. While the model was approved for the time of 2003, forecasts were made up to the year 2010 [Figure 2.7].

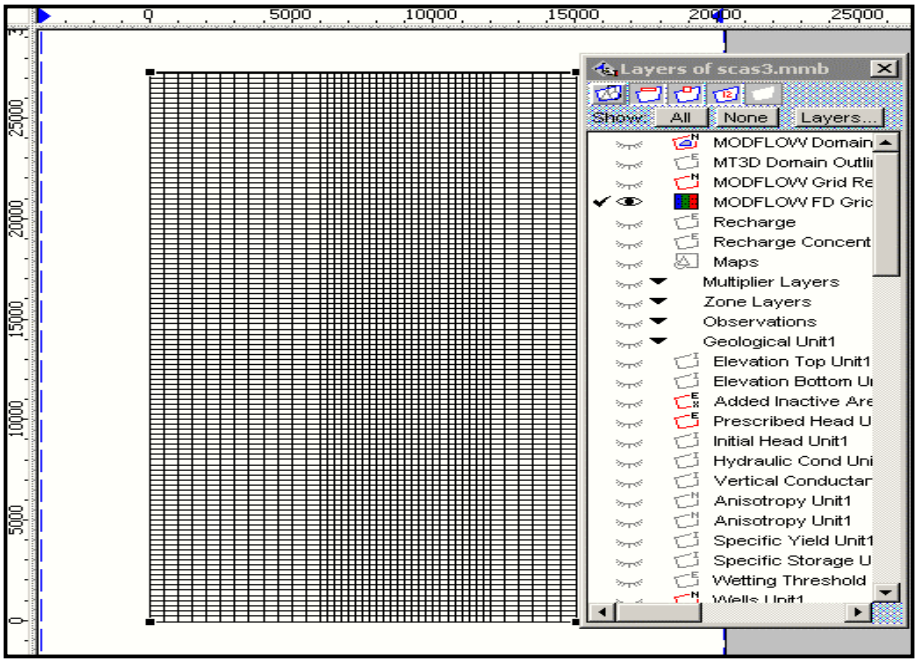

Fig. 2.6: Finite difference discretization of the study area (after Mohan, 2005).

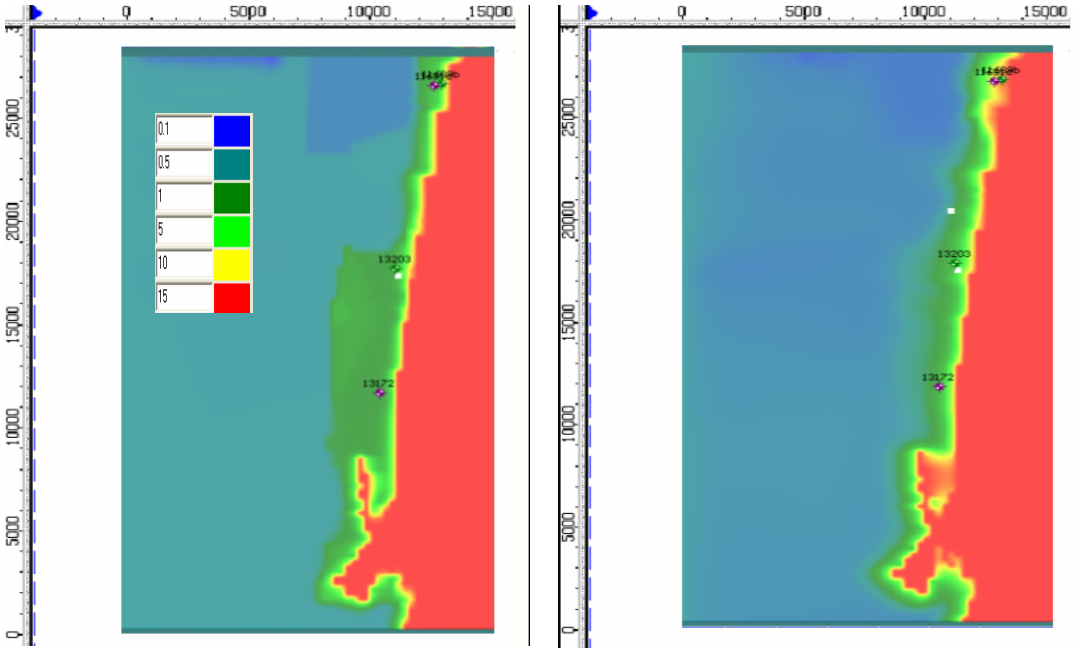

Fig. 2.7: Simulated $Cl/HCO_3 + CO_3$ ratio (a) left side January 1990, (b) right side. January 2010 (after Mohan, 2005).

The authors discussed the administration methodologies to control ocean water ingression when the event of defilement of the investigation zone. A maximization model was designed by maximization of pumping with minimization the desalination cost [Figure 2.8].

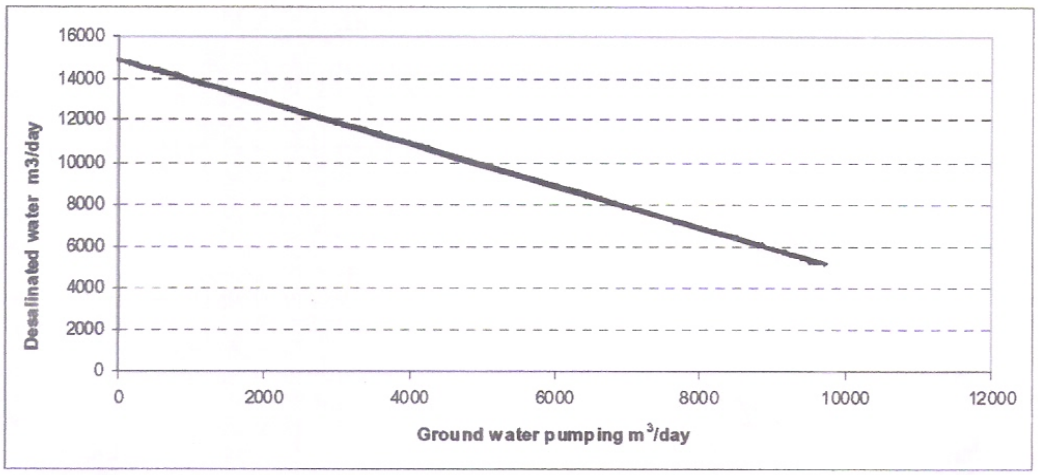

Fig. 2.8: The trade-off between total groundwater withdrawal and desalinated water (after Mohan, 2005).

Elhamid and Javadi (2008) proposed cost effective technique to control the saltwater ingression into the coastal aquifer based on Abstraction, Desalination and Recharge (ADR). The proposed procedure is appeared in Figure 2.9. A coupled transient density-dependent finite element model was produced to simulate fluid flow, solute transport and ocean water ingression. The optimum depths, locations and extraction / recharge rate were determined to decrease the total cost. It was watched that the proposed region framework performs altogether superior than separate use of abstraction and recharge well in terms of cost effectiveness and reduction of saline concentration in the aquifer.

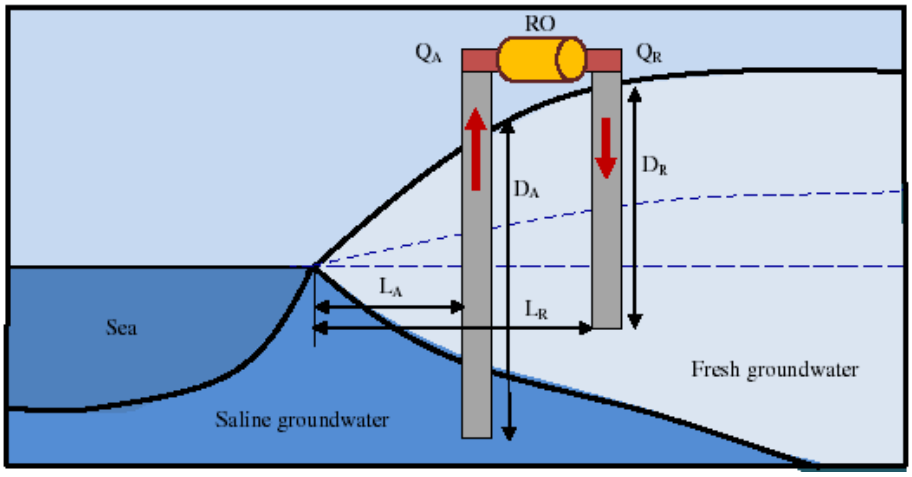

Fig. 2.9: Diagram of the ADR methodology (after Elhamid and Javadi, 2008).

Mahesha (2009) built up an applied model for safe withdrawal of new water from freshwater from coastal aquifers. A Galerkin finite-element model was applied considering a sharp interface. Investigation was finished presenting a semi pervious sub surface boundary to control the probable progression of the interface because of withdrawal of freshwater [Figure 2.10]. Utilizing numerical model, the creator examined the examples of the steady state interface profiles, the cone of depression, the upconing and the interface progression [Figure 2.11].

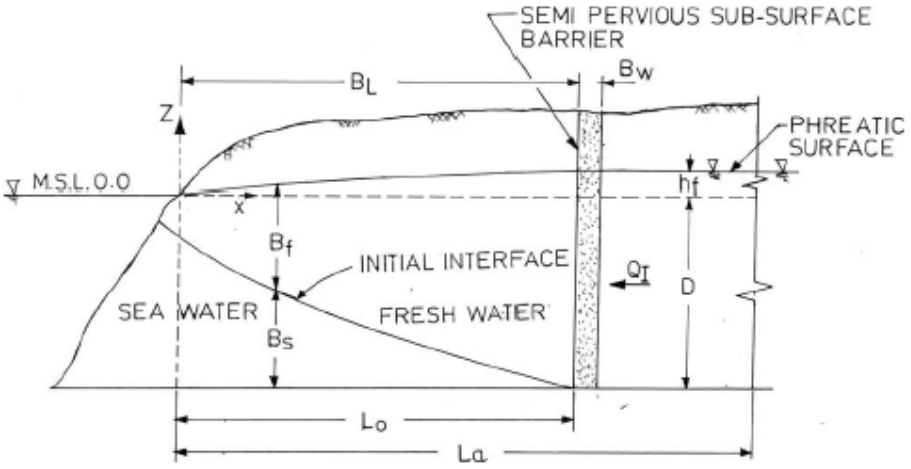

Fig. 2.10: The problem definition of Mahesha, 2009.

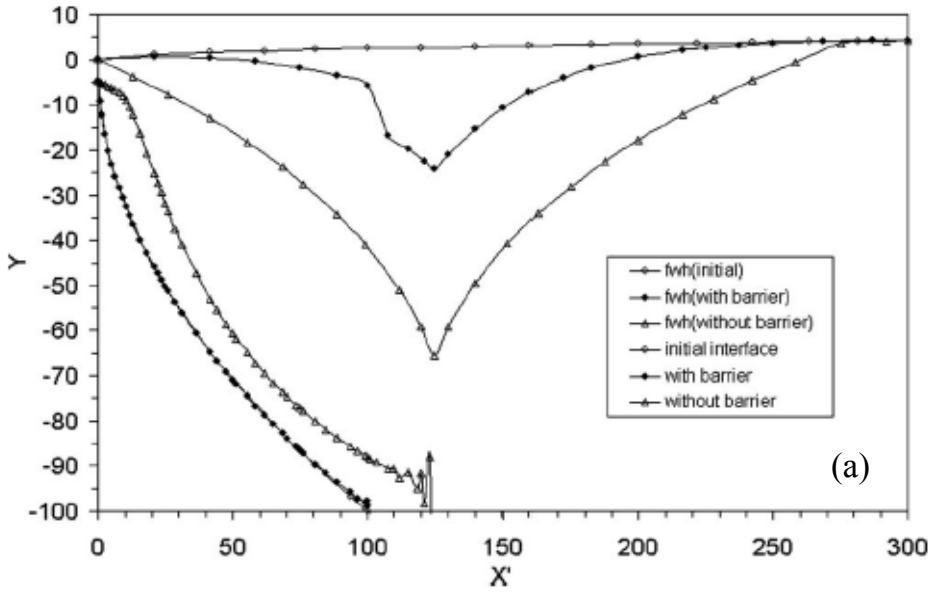

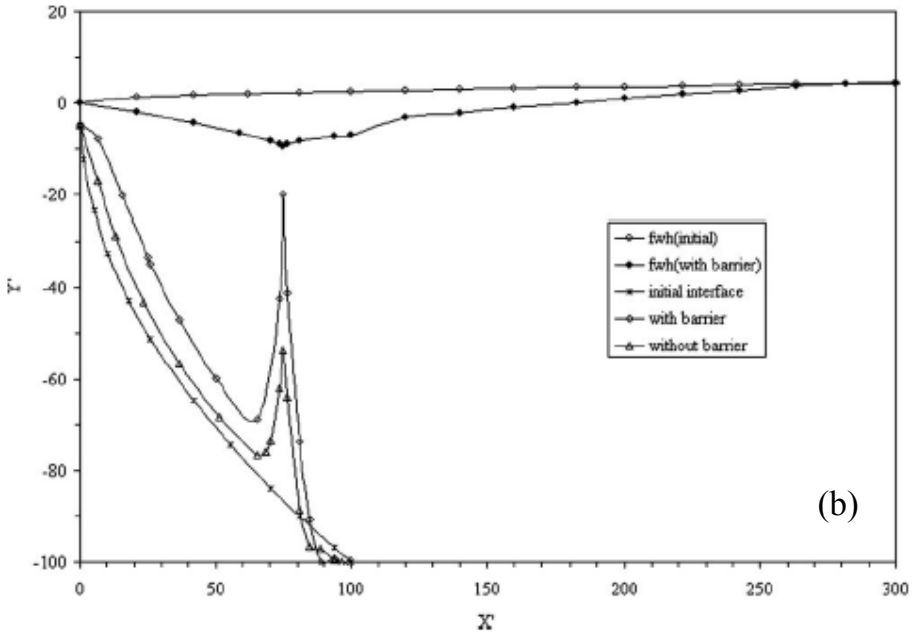

Fig. 2.11: Illustration for: (a) upconing, (b) interface extension (Mahesha, 2009).

2.1.2. Laboratory Based Experimental Works

Bennett *et al.* (1968) extended the study of Muskat and Wyckoff (1935) to the skimming well problem, using an analog model for a radial flow to determine the required head distributions in the freshwater aquifers. This model was made up of a network of electric resistances, capable of with an arrangement of switches, by methods for which the lower segment of the system of resistors could be balanced by trial and error to obtain a lower boundary. It would simulate the salt water and freshwater interface for a given set of conditions. The results provided an evaluation of skimming well operation following the achievement of a stable interface, under a selection conditions relating to original fresh and saline groundwater and well penetration. The outcomes were exhibited in dimensionless structures and can be connected to any situation provided the field parameters fall within the range covered by the dimensionless stipulations of the analysis. However, the approach uses the interface mechanics initiating an approximation to the actual behaviour of saline and fresh groundwater, as against a total miscibility of the fluids. As well, the equilibrium analysis provides no particulars on the transient period during which the saline water is adjusting to its new position or the time required for that adjustment. They concluded that well having 15% penetration would provide maximum freshwater discharge over a stable brine cone.

Mughal and Awan (1977) analysed the issue of upconing of the freshwater and saline water interface below a drain using the Hele-Shaw model. They considered the freshwater and saline water as immiscible liquids with sharp interface. They concluded the interface to rise very rapidly with a small increase in the normalized discharge in the beginning. The approach to this progressively became stable.

Fand *et al.* (1987) directed an exploratory examination for the resistance from the stream of liquids through straightforward and complex permeable media whose frameworks were made out of randomly packed spheres. In this specific situation, Simple' and 'complex' were introduced to permeable lattices having the same distinctive sphere diameters respectively. The goal of this examination was to get valuable connections to relate the pressure gradient the speed of liquids through permeable media. The test area was a stainless steel water burrow through which the water was either pumped or gravity-encouraged with a calibrated orifice oblate to gauge the stream rate [Figure 2.12]. An electrically warmed segment and a water cooled concentric tube warm exchanger were joined for temperature control. The pressure drop over the test area was estimated a differential pressure cell for low pressure contrasts and by methods of a series of manometers for higher pressure differences. Darcy stream happened for basic media for Reynolds number less than 2.3, and the Kozeny-Carman constant equal to 5.34 and the Forchheimer flow occurred for Reynolds number in the vicinity of 5 and 80, and Ergun constants in the vicinity of 182 and 5. For complex media, then again, the Darcy stream occurred for Reynolds number not surpassing 2.3 and the Kozeny-Carman constant equal to 5.3 and Forchheimer flow happened for Reynolds number in the vicinity of 5 and 80 and the Ergun constants are 182 and 1.92.

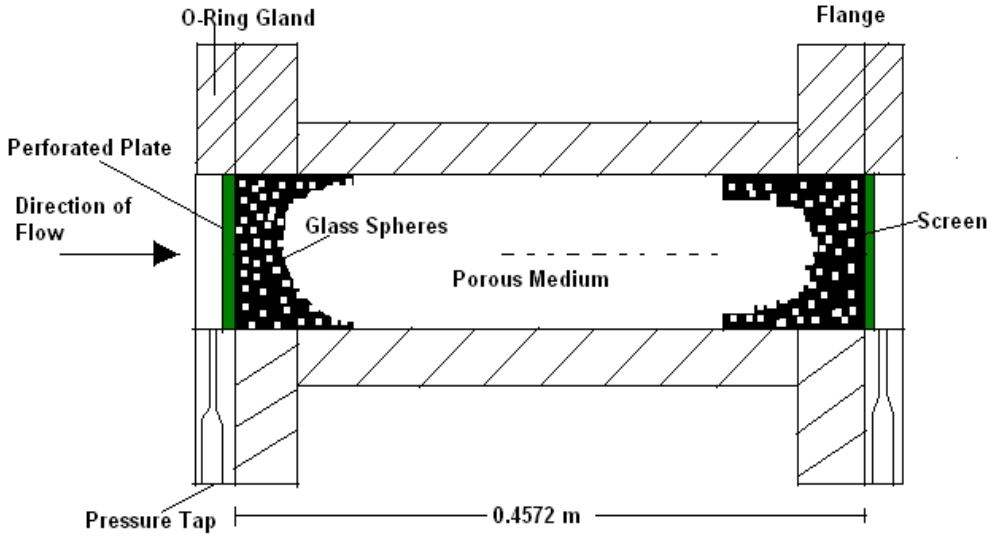

Fig. 2.12: Test section of water tunnel, after Fand *et al.* (1987).

Schincariol and Schwartz (1990) developed an exploratory examination to research the mixing of a variable thickness stream in a permeable media. They demonstrated the complexity of mass mixing when density deriving forces develops considering the occurrence of the high density water over the water of lower density which results in gravitational instability difference as low as 0.0008 g/cm^3 (1000 mg/l of NaCl) causes instabilities to develop in homogeneous media. They showed that the stability of the pressure in the flow field should be maintained across the assumed interface when treated as a boundary surface.

Kececioglu and Jiang (1994) led an exploratory examination for move through permeable media of packed spheres immersed with water. The target of this examination was to give experimental confirmation to deciding the outline criteria for flow in the course of a bed of arbitrarily packed spherical beads. The test set up comprised of a Plexiglas cylindrical tube loaded with consistently measured glass beads [Figure 2.13]. Water was either pumped or gravity fed via a loop instrumented with stream meters. The pressure differences were estimated by either pressure transducer or manometers. As watched Darcy's law has an extremely restricted appropriateness for Reynolds number under 0.12 (Pre-Darcy flow). Also, Forchheimer flow was applicable for a Reynolds number less than 2.3. The results also suggested that the pressure drop in Forchheimer equation could be modelled by an approximately non-dimensionalized Ergun's equation.

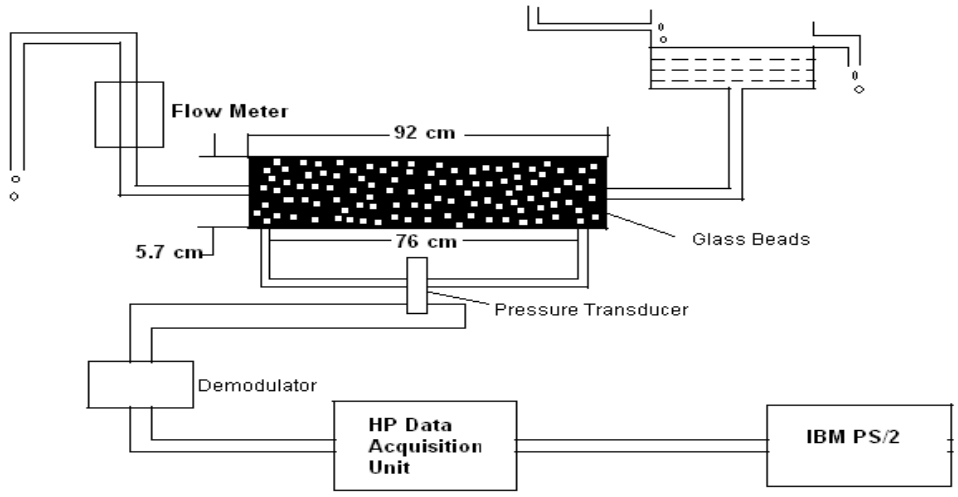

Fig. 2.13: Figure of the experimental set up after Kececioglu and Jiang (1994).

2.1.3. Field Based Studies

Goswami (1968) led a field based examination in the coastal aquifer at Digha in Purba Midnapur [Figure 2.14]. To characterize the dispersion and development of the saline and fresh groundwater, a geohydrological study was done by sinking Auger bore holes and testing the water quality. The investigation territory was seen to comprise of fine to coarse grain sand with intermittent delicate soft clay lenses.

From the chemical investigation, the interface between freshwater and saline water was drawn for every one of the well areas. The proportion of chloride/bicarbonate was utilized as an index for saline water ingression. The regular and yearly variety of the interface was likewise explored. For day by day tidal wavering, minor developments of the interface were watched. It was watched that wide deviations from the hypothetical "Herzberg Ratio" have been notified in this area. The profundity of the interface in the examination was substantially less than that computed based on the Ghyben-Herzberg guideline [Figure 2.15].

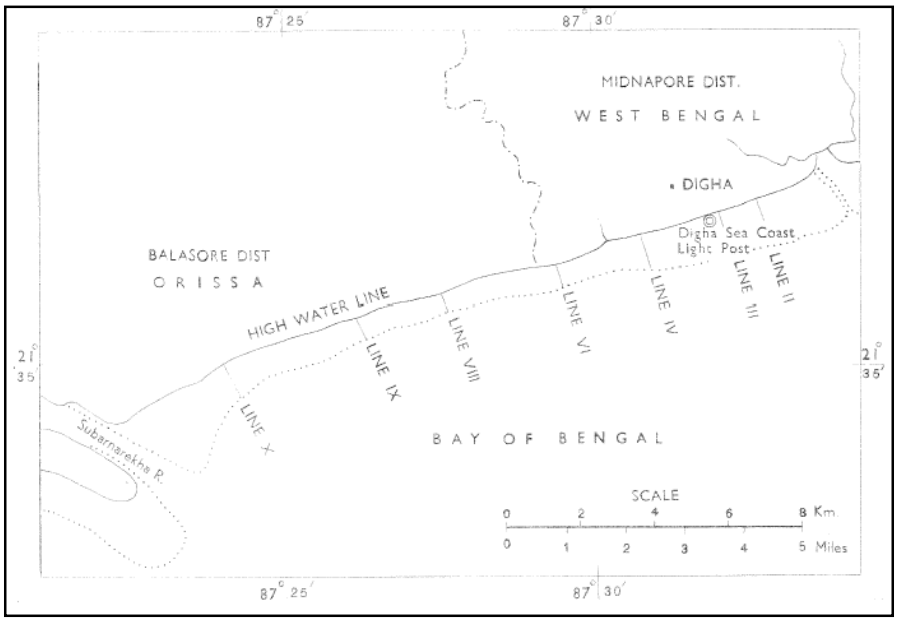

Fig. 2.14: Map showing the study area selected by Goswami (1968).

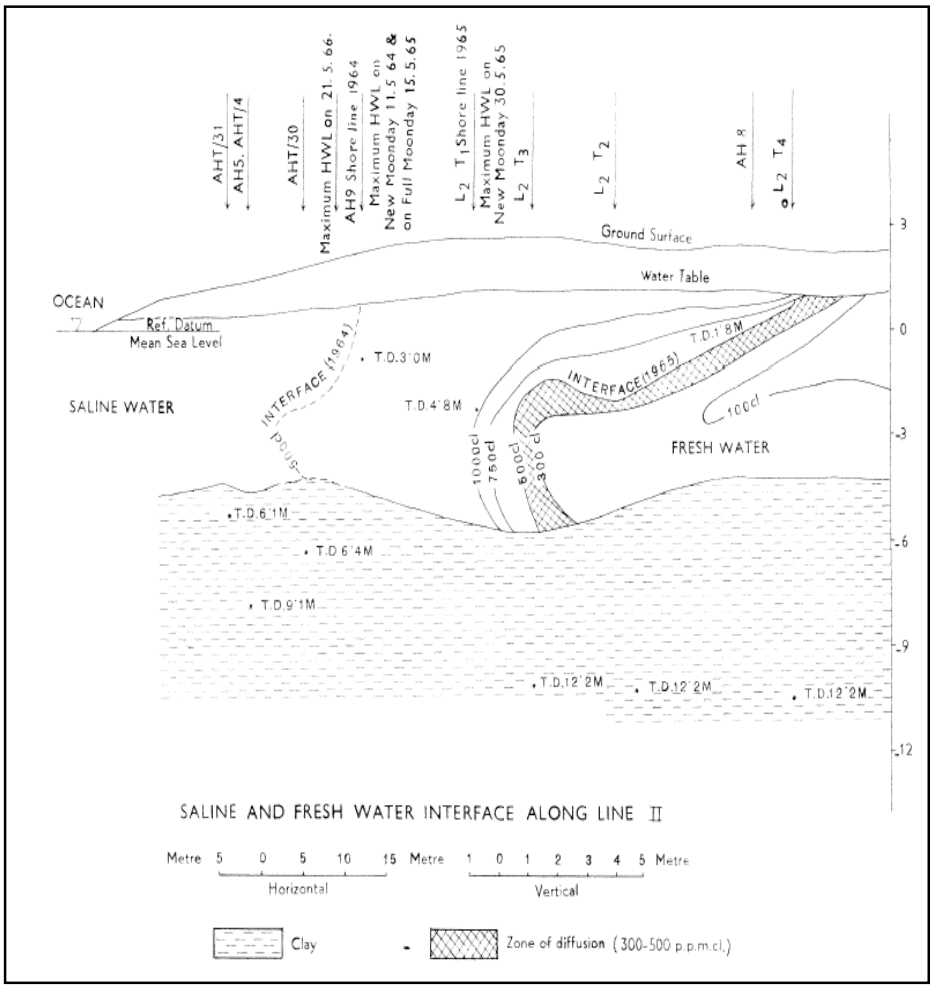

Fig. 2.15: A typical view showing the saltwater-freshwater interface (Goswami, 1968).

Fetter (1972) developed an equation for the 2D steady state position of the saline water interface in a phreatic aquifer underneath a maritime island assuming Dupuit's approximations. He presented an analytical solution by solving the equation for certain simple geometric boundaries. He suggested utilizing the model for multilayered aquifers by assuming an average conductivity to apply for the islands of any shape by means of a numerical solution. The model was effectively used to create the known position of the saline water interface underneath the South Fork of Long Island in New York.

Barlow (2003) investigated a considerable field construct consider with respect to groundwater quality and stream in Atlantic coast, USA, in the reference of saline water ingression. He also discussed the detection, supervision and administration techniques of the saltwater ingression in the USA, Atlantic coast.

A basic investigation of groundwater and coastal biological communities together with the problem and occasion has additionally been examined by the author. The author likewise developed line of equivalent chloride concentration in groundwater at Southwestern Florida [Figure 2.16]. The yearly variation of an average chloride concentration is presented in Figure 2.17 and also the profile for water salinity and temperature with depth [Figure 2.18].

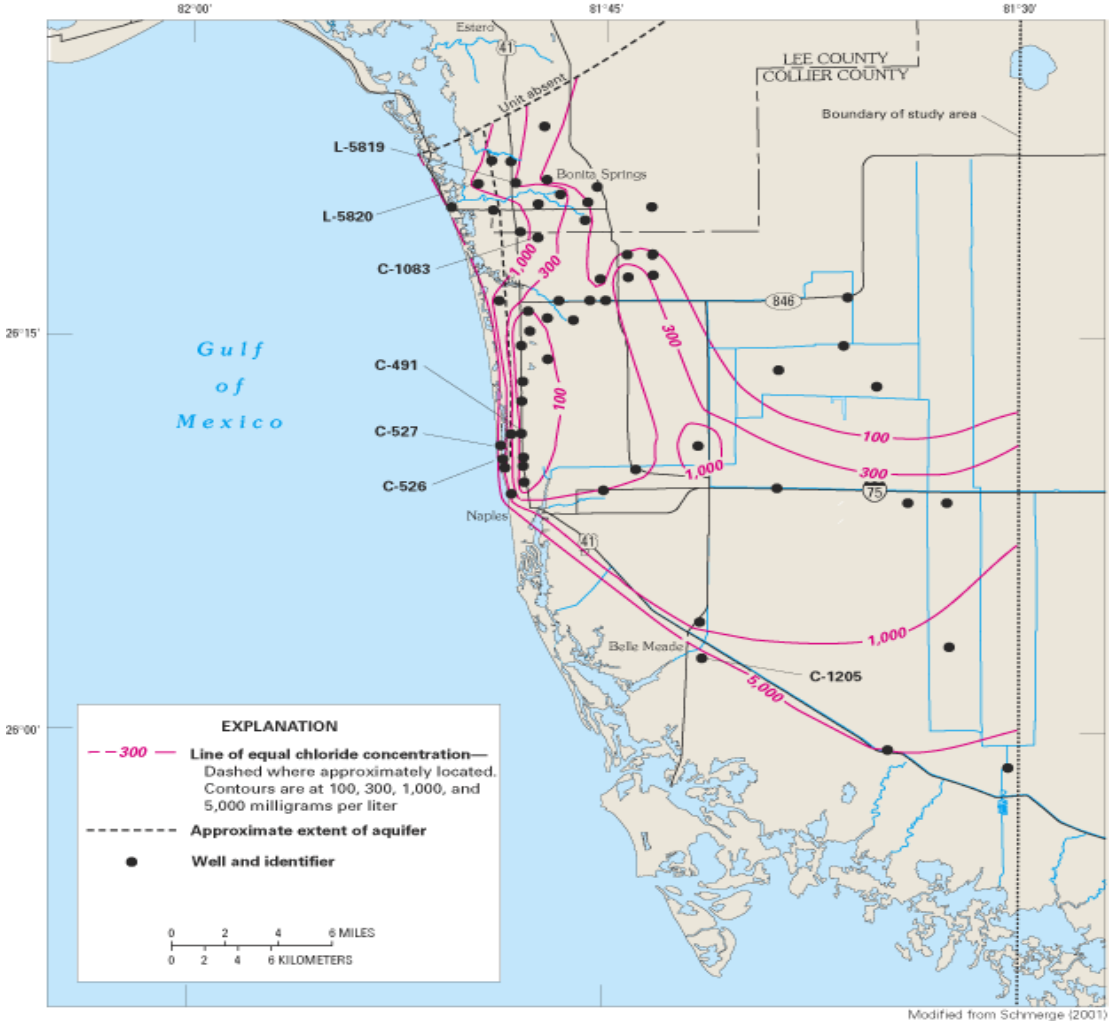

Fig. 2.16: Chloride concentration contours in southwestern Florida (Barlow, 2003).

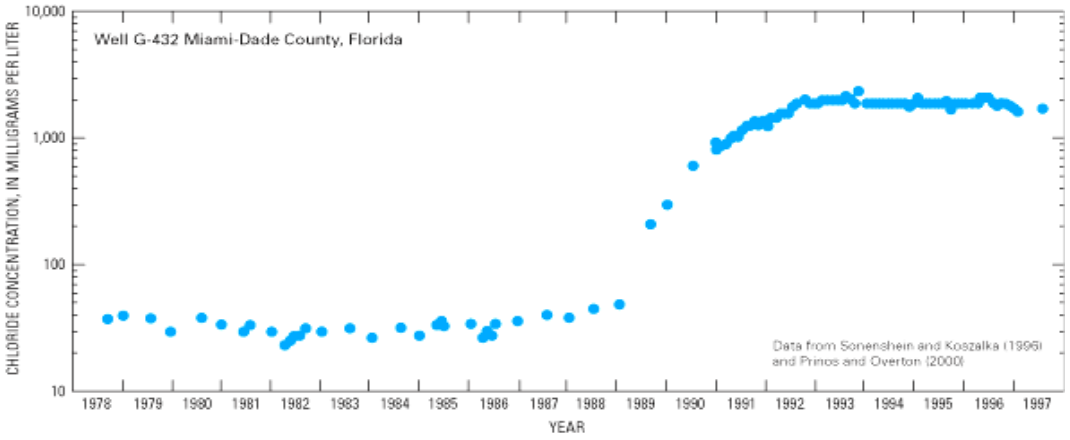

Fig. 2.17: Yearly variation of chloride concentrations in Florida (after Barlow, 2003).

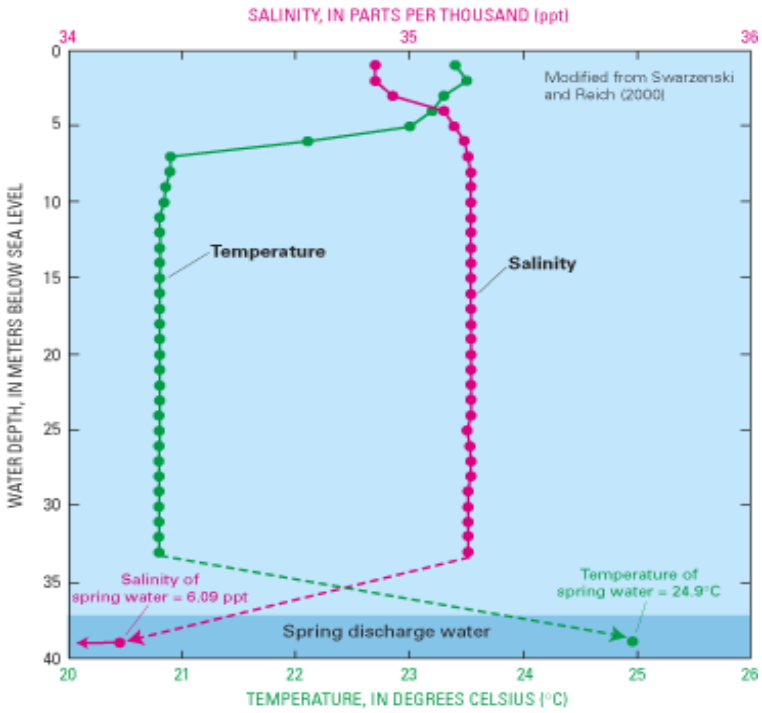

Fig. 2.18: Typical profile of water salinity and temperature with depth (Barlow, 2003).

Raghubabu *et al.* (2004) conducted field study in the coastal zone of Srikakulam, Guntur and Nellore of Andhra Pradesh districts and Pulicat Lake in the north to Cape Comarine in the south of Tamil Nadu, identified as coastal sandy soils. In most of these coastal sandy soils, there prevail a shallow depth of good quality water with the freshwater floating at a depth of 0.5 m - 3.0 m below ground level and thickness of 3 - 4 m above saline water/clay layers. These waters cannot be extracted in high qualities by conventional tube well because of saline water underlying the area. He suggested that the skimming well with horizontal collector framework was a feasible answer for preventing saline water ingression into the inland freshwater aquifer. The author claimed that this technology can be accepted and adopted in coastal sandy soils of Andhra Pradesh, Tamil Nadu, Orissa and West Bengal.

Chandra (2005) conducted field study on surface geophysical data and borehole logging had been conducted in the coastal tracts of India with varied objective. Electrical resistivity measurements surface in addition to bore hole had been the generally extensively utilized techniques. The groundwater quality interface and the spatial disposition of freshwater aquifer upto 300 m depth had been successfully identified. The case study from coastal tracts manifests the applications and limitations of the resistivity techniques and the essentiality of techniques of integrating other geophysical to take out ambiguities had been conducted.

Papadopoulou *et al.* (2005) investigated a field based work with respect to examination and control of saline water ingression in the industrial area of the City of Herakleio in Greek islands. The geology and saline zone of the study area [Figure 2.19] were mapped from the geophysical measurement [Figure 2.20]. Additionally the reasonableness of various administration strategies were proposed to control the saltwater ingression, particularly artificial recharge by injection well [Figure 2.21].

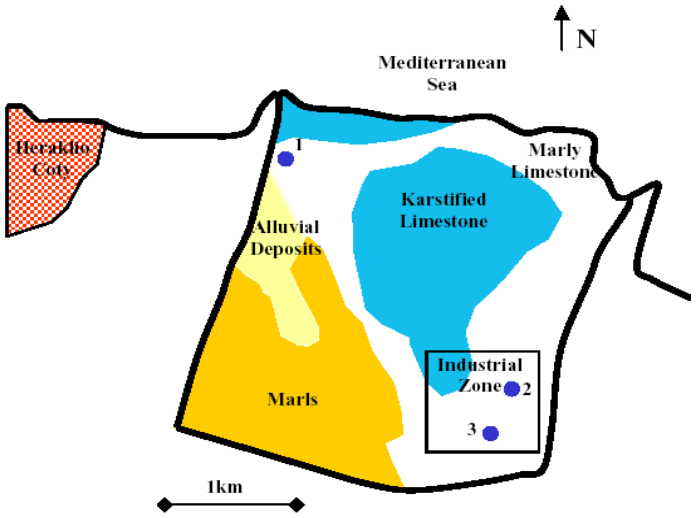

Fig. 2.19: Geological map and study area (after Papadopoulou *et al.*, 2005).

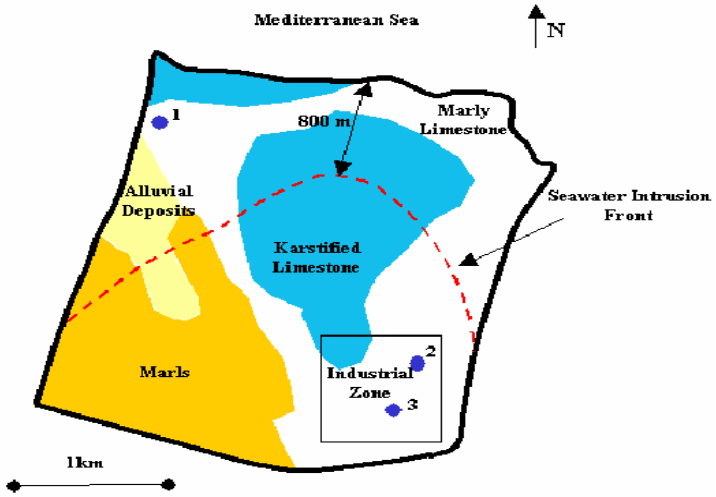

Fig. 2.20: Simulated saltwater front (after Papadopoulou *et al.*, 2005)

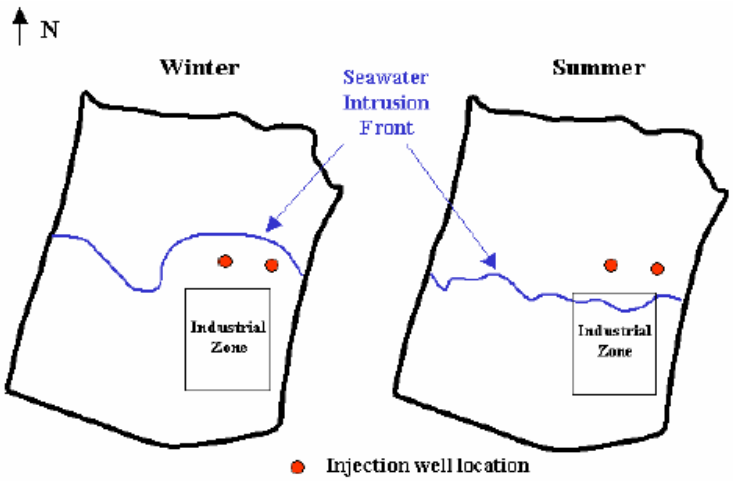

Fig. 2.21: Recharge by injection wells (after Papadopoulos *et al.*, 2005)

Chachadi (2005) studied the seawater ingression in the North Goa. A pointer based model was exhibited to survey and quality the susceptibility extent of seaside aquifers to saline water ingression because of unreasonable groundwater extraction or conceivable ascent in the ocean level. The new strategy GALDIT, of aquifer Vulnerability mapping because of seawater ingression had been effectively used to evaluate the degree of aquifer contamination because of ocean water ingression.

Gallardo and Marui (2007) carried out field based predictive modelling to assess the relevance to groundwater flow and the fresh- saline water interface in connection to the development activities at the coastal front plain of Tokaimura, Japan. The impact of the advancement on the stream and salinity patterns was studied. The simulation outcome was validated against field measurements. The model depicted suitably the groundwater progression and the shape and development of the saltwater front, although a slight underestimation was noted. Results from this study can be connected to other coastal sites under anthropogenic influence constituting a valid reference for guiding and management decisions.

Werner and Simmons (2009) built up a basic applied system to give a first-arrange appraisal of seawater ingression changes in seaside unconfined aquifers because of sea-level rise. Two conceptual models were tested: (1) flux controlled frameworks, in which ground water release to the sea is determined in spite of changes in sea level, and (2) head-controlled frameworks, whereby ground water extraction or surface character keep up the head condition in the aquifer in spite of sea level changes. The conceptualization expects unfaltering state conditions, a sharp interface seawater-freshwater transition zone, homogeneous and isotropic aquifer properties, and steady recharge. On account of consistent flux conditions, the higher boundary for seawater ingression because of sea level ascent (up to 1.5 m is tested) was no more noteworthy than 50 m for regular estimations of recharge, hydraulic conductivity and depth of the aquifer. This was in striking differentiation to the steady head cases, in which the extent of salt water toe movement is on the order of hundreds of meters to quite a few kilometers for the same sea-level ascent.

Olufemi *et al.* (2010) conducted field study for evaluation of groundwater quality and saline water ingression in coastal aquifers of Lagos Metropolis, Nigeria. In this examination, the coastal aquifers of Lagos city were chosen for an evaluation of its groundwater quality and effect of saline ingression. Water samples gathered along the coastal area were subjected to different physicochemical investigations. Results acquired were contrasted with permissible values for drinking water expressed by Federal Environmental Protection Agency (FEPA) and World Health Organization (WHO). The outcomes show that all the water samples were essentially hard (extend 522.14– 1233.34 mg/l). The salinity was outlined by conductivity estimations. Three examples had specific conductance over as far as possible for freshwater. The examples anyway met as far as possible for drinking water for the other tested parameters.

Bianchi *et al.* (2011) studied hydrogeological examinations in the Grosseto Province (southern Tuscany, Italy) mean to build up a right model for the management of coastal aquifers, which were influenced via seawater ingression because of overexploitation for different purposes. This examination refreshes and incorporates hydrogeological learning of the zone; furthermore, it proposes an observing system and corrective measures. Finished investigations uncover the presence of coexisting flow frameworks of various rank which permit the mixing of freshwater and saltwater, both shallow (recent) and deep (old), in different extents. Hydraulic head estimations uncover the critical effect of pumping on the flow of groundwater, with the formation of a negative hydraulic head in territories of serious withdrawal (water supply frameworks, fish farms). The definition of calculated models for the aquifers permitted the improvement of numerical models for hydrodynamic and hydrochemical simulations, which give helpful data on the general development of frameworks under various stress conditions. The examination evaluated plans to check seawater ingression, considering the characteristics of the multi-aquifer arrangement of the Albegna plain and of the nearby carbonate aquifer. A system of existing wells and additional monitoring wells was distinguished for quality and amount observing of aquifers.

Sherif *et al.* (2012) conducted field work a shot at groundwater pumping from Kalbha and Fujairah coastal aquifer of the United Arab Emirates (UAE) had augmented appreciably amid the most recent two decades to meet the farming water demands. Because of the absence of normal recharging from precipitation and the excessive pumping, groundwater levels had declined essentially causing an ingression of seawater in the coastal aquifer of Wadi Ham. Accordingly, numerous directing wells in the coastal zone had been ended and various agriculture fields had been abandoned. MODFLOW was utilized to simulate the groundwater flow and survey the seawater ingression in the coastal aquifer of Wadi Ham. The model was calibrated against a five-year dataset of past groundwater levels and approved against an additional eleven-year dataset. The impacts of pumping on groundwater levels and seawater ingression were researched. Results demonstrated that diminishing the pumping from Khalbha well field will decrease the seawater ingression into the south-eastern part of the aquifer. Under the present groundwater pumping rates, the seawater will keep on migrating inland.

Ayolabi *et al.* (2013) examined geophysical and geochemical systems to outline give confirms that the coastal aquifers in the study area had been encroached by saltwater

from the adjoining Lagos lagoon. The resistivity information were obtained with a terminal dividing (a) that fluctuate between 1.6 to 8 m, and development factor *n* of 30. The depth reversed models got from inversion of the fifteen resistivity information got in the zone revealed considerable effect of the lagoon water on the aquifers showed as low resistivity for the most part beneath 7 Ωm. A combination of four diverse electrode arrays – Schlumberger, Wenner, Dipole-dipole and pole– dipole, with no less than three conveyed at each site (except for three traverses – traverses 13, 14 and 15), yield better level and vertical determination, having depth scope of 36– 226 m with 1.6– 8 m electrode spacing utilized. The depicted geoelectric layers were compared with logs from both boreholes situated inside the campus. Confirmation from geochemical investigation of borehole and the lagoon water samples supported the ERT result. Dynamic reduction altogether TDS and EC from the lagoon to the coastal aquifer supports progressive intrusion of the inland aquifers by the encroaching lagoon water. What's more, comparable pattern was seen in overwhelming metal dissemination Pollution Index (PI) plot recommending conceivable underground flow of water from the lagoon to the aquifers. From this examination, it was concluded that unreasonable groundwater withdrawal and potentially the decrease of groundwater slopes which enables saline-water to move freshwater in the aquifer of the explored territory are in charge of the saline water ingression watched.

Das *et al.* (2014) conducted field investigation on effect of water quality in piyali stream, sundarbans, india because of saline water ingression. The Sundarbans, an UNESCO Heritage site contains a vast mass of rural populace which relies upon its usual resources for sustainability. Salinity is normal issue in the Sundarbans. The Piyali River is a tributary of the Matla River which releases into the Bay of Bengal. The Basin of Piyali River, an estuarine stream with general tidal convergence, with extraordinary accentuation on Kultali block of the Sundarbans had been decided for using the water of the Piyali River amid dry months. Ocean water contains chlorides with different salts that can be harmful to rural harvests and drinking water quality as they surpass the drinking water norms. An endeavour had been made to research whether there was any degree of the salt water ingression to the Piyali River from Matla River amid pre monsoon season which by implication confirms legitimate working of sluice gate alongside assurance of physico-chemical parameters to identify the water is fit for irrigation and drinking purpose. Water tests from various areas of the Piyali River had been analyzed for their substance in regards to salinity, chloride, total dissolved solids, total solids, turbidity, electrical conductivity and pH keeping in mind the end goal to enhance management options.

Sahu (2014) studied the status and review of soil structures of Purba Midnapur, West Bengal.The Purba Medinipur district has a vast expanse of younger alluvial soils. It is separated into three parts. First, there is a strip of purely deltaic country composed of younger alluvial soils or Entisols bordering the Rupnarayan River and the Hugli River. The second division consists of the coastal alluvial soils of Entisols group. Much of the area is salifereous and must be protected from the attacks of the ocean by banks. There is a long narrow and elongated strip of saline and alkali soils of Aridisols group, stretching from Digha to the east of the Haldi River. The remaining portion consists of older

alluvium belonging to Alfisols group beside the Western portion near Egra and in a very small part to the northwest along the river Kangsabati. The work basically deals with the status of soil and related problems in Purba Medinipur district.

Adedotun *et al.* (2015) studied on the significant endeavour at depicting nearness and parallel degree of saline water ingression into aquifers at the easternmost piece of Dahomey basin which falls basically in the sedimentary territory of Ondo State of Nigeria. 61 water tests were gathered from hand burrowed wells, shallow boreholes, and lakes over the investigation territory and analyzed for important parameters, for example, as pH, conductivity, total hardness, calcium hardness, magnesium hardness, total dissolved solids, alkalinity and concentrations of the following anions and cations; chloride, calcium, Sulphate, bicarbonate, magnesium and sodium. Comparable salinity was computed from the water test investigation comes about. The hydrochemical examination comes about uncovers conceivable saline water ingression in the coastal zone, particularly the southeastern part and Agbabu in the north central part of the investigation region as obvious from high concentration values of chloride (372 - 1500 mg/l), alkalinity (105 - 330 mg/l), equivalent salinity (135 - 2808 mg/l), total dissolved solid (181 - 1005 mg/l), high pH values (4.4 - 8.6 pH) and conductivity values (541 - 1500 μs/cm).

Grundmann *et al.* (2016) investigated field contemplate on control saltwater ingression in coastal dry locales and its societal implications for cultivation. The activities of farmers and in addition the improvement of fitting administration methodologies, an exact overview with partners and physically based demonstrating of the groundwater-agribusiness hydro-framework connections was taken into considerations. The examination was exemplarily researched for the south Batinah area in the Sultanate of Oman, which was influenced by saltwater ingression into a coastal aquifer framework because of over extraction of groundwater for irrigation.

Toste *et al.* (2017) investigated global temperature prediction to increase in the end of the century and one of the primary consequences of this warming is the sea level rise.

Considering the vulnerabilities on coastal frameworks and water resources, it is vital to assess the potential impacts of this ascending in coastal territories, since the saline ingression on streams would be strengthened, prompting issues identified with water quality. In this unique circumstance, the present work meant to confirm saline water ingression changes along an imperative stream, São Francisco Canal, situated in Rio de Janeiro State, Brazil. For this reason, a hydrodynamic modeling was performed utilizing SisBaHiA, considering diverse ocean levels and tide conditions. As per the outcomes, it was confirmed the increase on saline ingression and higher salinity esteems because of an ocean level ascent of 0.5 m. These outcomes demonstrate that new licenses for water withdrawals must be painstakingly dissected as the fluvial flow assumes a critical part to contain the saltwater ingression on the considered waterway. As needs be, it is suggested the assessment of environmental change impacts keeping in mind the end goal to reduce coastal vulnerability, and the utilization of this topic on ecological authorizing and regional arranging, integrating water scheduling with coastal management.

Alfarrah and Walraevens (2018) contemplated groundwater overexploitation and seawater ingression in coastal territories of arid and semi-arid area in Libya experienced dynamic seawater ingression in the coastal aquifers since the 1930s in light of its regularly expanding water requirement from underground water resources. Tripoli city is a common territory where the pollutant of the aquifer as saltwater ingression is exceptionally created. Sixty-four groundwater tests were gathered from the investigation zone and analyzed for specific parameters that show salinization and contamination of the aquifer. The outcomes exhibit high estimations of the parameters Electrical Conductivity, Na^+, K^+, Mg^{2+}, Cl^- and SO_4^{2-}, which can be credited to seawater ingression, where Cl^- is the significant toxin of the aquifer. The water types as indicated by the *Stuyfzand Groundwater Classification* are for the most part $CaCl_2$, NaCl and Ca/Mg mix. These water types show that groundwater chemistry is changed by cation exchange reactions amid the mixing procedure amongst freshwater and saline water. The concentrated withdrawal of groundwater from the aquifer decreases freshwater discharge to the ocean, makes drawdown cones and lowering of the water table to as much as 25 m underneath mean ocean level. Irrigation with nitrogen composts and household sewage and development of contaminants in regions of high hydraulic gradients inside the drawdown cones most likely are in charge of the high NO_3^- fixation in the area.

2.2 Inferences from available Literatures

From the previous section, it is evident that significant research and development has already been conducted by various scientists, researchers and field engineers at various parts of the world in the field of examination and control of saline water ingression into coastal aquifers and other important zones.

Amongst the important works, the generally important assistance is briefly reviewed. Starting from the year of 1935 to till 2018, a total of 48 papers have been studied. These contributions are broadly classified into three categories, viz., theoretical contributions (analytical and numerical studies), lab based test works and field-based investigations.

As watched, the distinctive kinds of hypothetical works that have been done are comprehensively in view of two classes, for example, (i) to be specific utilizing the sharp interface idea e.g. Wang (1965), Gupta and Gaikwad (1987), Reilly and Goodman (1987), Motz (1992), Mahesha (2001), Mahesha (2009), Goswami (1968) and Gallardo and Marui (2007), (ii) using the brackish interface idea e.g. Li and Yeh (1968), Pinder and Cooper (1970) and Xue *et al.* (1995) and Mohan and Pramada (2005).

Research facility based laboratory works have been finished include Bennett *et al.* (1968), Mughal and Awan (1977), Fand *et al.* (1987), Schincariol and Schwartz (1990) and Kececioglu and Jiang (1994). However it may be observed that a particular research facility laboratory work to show contemplate in light of saltwater ingression and resulting freshwater recharge into a characteristic permeable media is yet to be done. Also, the studies on the alteration of hydraulic conductivity of aquifer materials with saline concentration with period of submergence are limited.

Field based investigations have been led by different analysts such as Goswami (1968), Fetter (1972), Barlow (2003), Raghubabu *et al.* (2004), Chandra (2005), Chachadi (2005), Papadopoulou *et al.* (2005), Gallardo and Marui (2007), Werner and Simmons (2009), Olufemi *et al.* (2010), Bianchi *et al.* (2011), Sherif *et al.* (2012), Ayolabi *et al.* (2013), Das *et al.* (2014), Sahu (2014), Adedotun *et al.* (2015), Grundmann *et al.* (2016), Toste *et al.* (2017) and Alfarrah and Walraevens (2018). Merely Goswami (1968) has examined the nature and position of the interface and depicted the fresh and saline groundwater bodies inside the aquifer of Digha shoreline, Purba Midnapur, West Bengal, India. The profundity of the interface was observed to be considerably less than that ascertained based on the Ghyben-Herzberg rule.

Das *et al.* (2014) carried out field study on impact of water quality in Piyali River, Sundarbans, India by reason of saline water ingression. Sahu (2014) studied the status and review of soil structures of Purba Midnapur. However, the work is not details analysis for estimation and remedial measures of saline water ingression in the area concern and the given model is in need of updation.

Discontinuity do exist in information with respect to the modelling of the hydrogeology, aquifer framework, subsurface stratification, water quality parameters, pre-monsoon, post-monsoon profundity on water level and pre- monsoon piezometric surface contour of the investigation region of Purba Midnapur.

Also simulation of groundwater level at coastal zones of Purba Midnapur by Visual MODFLOW software has been done for prediction for future groundwater level and salt water flow intrusion path/s. Major variables like density, viscosity, temperature and saline concentration etc. have not been determined in the coastal zone of Purba Midnapur of current interest so far. These components are considered over in the present examination.

Raghubabu *et al.* (2004) suggested that the skimming with horizontal collector framework was a practical answer for controlling saline water ingression into the inland freshwater aquifer. Mohan and Pramada (2005) examined the saline water ingression on the South Chennai aquifer and a model was developed. Suitable predictions were done up to the time of 2010. As recommended, sensible management procedures, for example, modernizing the existing tanks, development of a semi-pervious obstruction and control rate of discharge or permissible pumping amounts would be of assistance in optimisation the seawater intrusion in the territory.

Papadopoulou *et al.* (2005) proposed distinctive administration situations to anticipate facilitate entrance of the saline water ingression front in the industrial zone of the City of Herakleio in Greek islands. Artificial recharge of freshwater is proposed as a feature of the prevention of saline water encroachment.

From the detail survey of these past research works, it is observed that there is an obvious deficiency in the research on saline water intrusion in coastal belts of West Bengal district in India. Therefore a careful thorough and detailed investigation has been done to study about the basic fundamentals of saline water intrusion into coastal aquifers of Purba Midnapur and its causes, subsequent effects and thereby the remedial measures.

2.3 References

Abd-Elhamid, H.F. and Javadi, A.A. (2008). Mathematical Model to Control Saltwater Intrusion in Coastal aquifers. Proceeding of Geo-Congress, New Orleans, Louisiana, USA.

Adedotun, I.A., Gregory, O.O. and Obasanmi, A.A. (2015). Hydrochemical Investigation of Saline Water Intrusion into Aquifers in Part of Eastern Dahomey Basin, Southwestern Nigeria. *Journal of Environment and Earth Science*, Vol. 5, No. 11, pp. 138-153.

Alfarrah, N. and Walraevens, K. (2018). Groundwater Overexploitation and Seawater Intrusion in Coastal Areas of Arid and Semi-Arid Regions. *Water*, Vol. 10, Iss. 2, Art. 143, pp. 1-24.

Andrade, J.S., Costa, U.M.S., Almeida, H.A. and Stanley, H.E. (1999). Inertia Effects on Fluid through Disordered Porous Media. *Physical Review Letters,* Vol. 82, Iss. 26, pp. 5249-5252.

Ayolabi, E.A., Folorunso, A.F., Odukoya, A.M. and Adeniran, A.E. (2013). Mapping saline water intrusion into the coastal aquifer with geophysical and geochemical techniques: The University of Lagos campus case (Nigeria). *SpringerPlus*, Vol. 2, 433, pp. 1-14.

Barlow, P.M. (2003). Ground Water in Freshwater-Saltwater Environments of the Atlantic Coast. Circular 1262, U.S. Geological Survey, Reston, Virginia, USA.

Bennett, G.D., Mundorff, M.J. and Hussain, S.A. (1968). Electric Analog Studies of Brine Coning Beneath Freshwater Wells in the Punjab Region, West Pakistan. *Geological Survey Water Supply Paper* 1608-J.

Bianchi, S., Nocchi, M. and Salleolini, M. (2011). Hydrogeological investigations in southern Tuscany (Italy) for coastal aquifer management. *AQUA mundi*, Am03028, pp. 53-70.

Chachadi, A.G. (2005). Seawater Intrusion Mapping Using Modified GALDIT Indicator Model-a Case Study in Goa. *Jalvigyan Sameeksha,* Vol. 20, pp. 1-14.

Chan, T.P. and Govindraju, R.S. (2003). A New Model For Soil Hydraulic Properties Based on A Stochastic Conceptualization of Porous Media. *Water Resources Research*, Vol. 39, Iss. 7, pp. 1-5.

Chandler, R.L. and Mcwhorter, D.B. (1975). Interface Upconing Beneath a Pumping Well. *Groundwater*, Vol. 13, No. 4, pp. 354-359.

Chandra, P.C. (2005). Geophysical Investigation for Groundwater in Coastal Tracts. *Jalvigyan Sameeksha,* Vol. 20, pp. 1-14.

Charmonman, S.C. (1965). A solution of the pattern of fresh-water flow in an unconfined coastal aquifer. *Journal of Geophysical Research*, Vol. 70, No. 12, pp. 2813-2819.

Das, S., Nayek, M., Das, S., Dutta, P., Mazumdar, A. (2014). Impact on Water Quality in Piyali River, Sundarbans, India due to Saline Water Intrusion. *Indian Journal of Environmental Protection*, Vol. 34, No. 12, pp. 1010-1019.

Fand, R.M., Kim, B.Y.K., Lam, A.C.C. and Phan, R.T. (1987). Resistance to the Flow of Fluids through Simple and Complex Porous Media Whose Matrices are Composed

of Randomly Packed Spheres. *Journal of Fluids Engineering*, Vol. 109, Iss. 3, pp. 268-274.

Fetter, C.W.Jr. (1972). Position of Saline Interface Beneath Oceanic Islands. *Water Resources Research,* Vol. 8, Iss. 5, pp. 1307-1315.

Gallardo, A.H. and Marui, A. (2007). Modeling the Dynamics of the Freshwater-Saltwater Interface in Response to Construction Activities at a Coastal Site. *International Journal of Environmental Science & Technology*, Vol. 4, Iss. 3, pp. 285-294.

Goswami, A.B. (1968). A Study of Salt Water Encroachment in the Coastal Aquifer at Digha, Midnapore District, West Bengal, India. *Bulletin, International Association of Scientific Hydrology,* Vol. 13, No. 3, pp. 77-87.

Grundmann, J., Al-Khatri, A. and Schütze, N. (2016). Managing saltwater intrusion in coastal arid regions and its societal implications for agriculture. *Proceedings of IAHS,* 373, pp. 31–35.

Gupta, A.D. and Gaikwad, V.P. (1987*).* Interface Upconing due to a Horizontal Well in Unconfined Aquifer. *Groundwater*, Vol. 25, No. 4, pp. 466-474.

Inoue, M. and Nakayama, Y. (1998). Numerical Modeling of Non-Newtonian Fluid Flow in a Porous Medium using a three Dimensional Periodic Array. *Journal of Fluids Engineering*, Vol. 120, Iss. 1, pp. 131-135.

Jones, P.H., Hendricks, E.L., Burdge, I. and others (1956). Water Resources of Southwestern Louisiana. *Geological Survey Water-Supply Paper 1364*, Washington, USA, p. 460.

Kececioglu, I. and Jiang, Y. (1994). Flow through Porous Media of Packed Spheres Saturated With Water. *Journal of Fluids Engineering,* Vol. 116, Iss. 1, pp. 164-170.

Li, W. and Yeh, G. (1968). Dispersion at the Interface of Miscible Liquids in a Soil. *Water Resources Research,* Vol. 4, Iss. 2, pp. 369-377.

Mahesha. A. (2001). Effect of Strip Recharge on Sea Water Intrusion into Aquifers. *Hydrological Sciences-Journal-des Sciences Hydrologiques,* Vol. 46, No. 2, pp. 199-210.

Mahesha, A. (2009). Conceptual Model for the Safe Withdrawal of Freshwater from Coastal Aquifers. *Journal of Environmental Engineering,* Vol. 135, No. 10, pp. 980-988.

Millham, N.P. and Howes, B.L. (1995). A Comparison of Methods To Determine K in a Shallow Coastal Aquifier. *Groundwater*, Vol. 33, No. 1, pp. 49-56.

Mohan, S. and Pramada, S.K. (2005). Management of South Chennai Coastal Aquifer System-A Multi Objective Approach. *Jalvigyan Sameeksha,* Vol. 20, pp. 1-14.

Motz, L.H. (1992). Salt water Upconing in an Aquifer Overlain by a Leaky Confining Bed. *Groundwater,* Vol. 30, No. 2, pp. 192-198.

Mughal, I. and Awan, N.M. (1977). Upconing of Salt Freshwater Interface Beneath Wells in Freshwater Zones. *CEWRE Publication 005.*

Muskat, M. (1937). The Flow of Homogeneous Fluids through Porous Media. University of Michigan, McGraw-Hill Book Company, USA.

Muskat, M. and Wyckoff, R.D. (1935). An Approximate Theory of Water Coning in Oil Production. *Transactions of the AIME,* Vol. 114, Iss. 1, pp. 144-163.

Olufemi, A.G. (2010). Assessment of groundwater quality and saline intrusions in coastal aquifers of Lagos Metropolis, Nigeria. *Journal of Water Resource and Protection*, Vol. 2, No. 10, pp. 849-853.

Papadopoulou, M.P., Karatzas, G.P. and Koukadaki, M.A. (2005). Modeling the Saltwater Intrusion Phenomenon in Coastal Aquifers - A Case Study in the Industrial Zone of Herakleio in Crete. *Global Nest Journal*, Vol. 7, No. 2, pp 197-203

Pinder, G.F. and Cooper, H.H. (1970). A Numerical Technique for calculating the Transient Position of Salt Water Front. *Water Resources Research,* Vol. 6, Iss. 3, pp. 875-882.

Raghubabu, M., Prasad, B.R. and Srikanth, I. (2004). Subsurface Skimming Techniques for Coastal Sandy Soils. Bulletin No. 1/04: 18 pp. AICRP Saline Water Scheme, Bapatla, AP, India.

Rudraiah, N. (1985). Coupled Parallel Flow in a Channel and a Bounding Porous Medium of Finite Thickness. *Journal of Fluids Engineering,* Vol. 107, Iss. 3, pp. 322-329.

Rudraiah, N., Venkatachalappa, M. and Siddalingappa, B. (1986). The Damping of Internal Gravity Waves in a Continuously Stratified Turbulent Fluid in Non-Darcy Flow. *Arabian Journal for Science and Engineering*, Vol. 11, Iss. 1 pp. 101-110.

Sahu, A. (2014). Status of Soil in Purba Medinipur District, West Bengal– A Review. *Indian Journal of Geography & Environment,* Vol. 13, pp. 121-126.

Schincariol, R.A. and Schwartz, F.W. (1990). An Experimental Investigation of Variable Density Flow and Mixing in Homogeneous and Heterogeneous Media. *Water Resources Research*, Vol. 26, Iss. 10, pp. 2317-2329.

Schmorak, S. and Mercado, A. (1969). Upconing of Freshwater – Sea Water Interface below Pumping Wells- Field Study. *Water Resources Research*, Vol. 5, Iss. 6, pp. 1290-1311.

Sherif, M., Kacimov, A., Javadi, A. and Ebraheem, A.A. (2012). Modeling Groundwater Flow and Seawater Intrusion in the Coastal Aquifer of Wadi Ham, UAE. *Water Resources Management*, Vol. 26, No. 3, pp. 751–774.

Toste, R., Rosman, P.C.C. and deFreitas, A.V. (2017). Saline Intrusion Response to Sea Level Rise and Its Implications on Water and Coastal Management: A Case Study in Brazil. *Journal of Water Resource and Protection*, Vol. 9, pp. 510-522.

Wang, F.C. (1965). Approximate Theory for Skimming Well Formulation in the Indus Plain of West Pakistan. *Journal of Geophysical Research*, Vol. 70, No. 20, pp. 5055-5063.

Werner, A.D. and Simmons, C.T. (2009). Impact of Sea-Level Rise on Sea Water Intrusion in Coastal Aquifers. *Groundwater*, Vol. 47, No. 2, pp. 197-204.

Xue, Y., Xie, C. and Wu, J. (1995). A Three Dimensional Miscible Transport Model for Seawater Intrusion in China. *Water Resources Research,* Vol. 31, Iss. 4, pp. 903-912.

CHAPTER - 3

(Objectives and Methodology)

- Objectives
- Methodology
- Sequence of Execution
- References

3.1 Objectives

The research carried out under the purview of this thesis has aimed towards analysis and remedial measure of saline water ingression in the coastal aquifers of Purba Midnapur District of West Bengal in India. The specific objectives of the entire research conducted and the methodology followed are presented in this chapter. The objectives of this research are sequentially enumerated below:

- To perform theoretical analysis on saline water encroachment into coastal aquifers, for determining the safe discharge from shallow vertical and horizontal wells considering upconing and to present a practical and feasible design methodology for extraction of groundwater in coastal zone with anticipation of adequate recharge.

- To conduct laboratory experiments for investigating the pattern of intrusion of saline water and comprehensive recharge of fresh water into natural soil media, the variation of its hydraulic conductivity with saline concentration and period of submergence.

- To develop the sub-surface stratification, piezometric surface contour, aquifer system, subsurface stratification and saline water ingression in the coastal zones of Purba Midnapur.

- To study and simulate the piezometric surface contour levels at coastal zones of Purba Midnapur district by visual MODFLOW software.

- To conduct field investigations including hydro-geological site characterisation and groundwater quality assessment in the study area and it's modelling by taking the different parameters of chemical properties of the water samples along the coastal areas of the study area.

- To develop a cost effective methodology for management and control of saline water ingression into coastal aquifer and to apply the methodology so developed in a selected site of the study area for adequate quantification.

- To suggest aquifer improvement plan of Purba Midnapur district as groundwater legislation in succession that may facilitate in recharging the aquifer zones control the risk of saline water encroachments and improve the quality of groundwater in respect to salinity.

- To search alternative source/s to meet the future demand of fresh water in the area - the surface water may be collected from Subarnarekha River and distributed after proper treatment for various purposes.

3.2 Methodology

In order that the objectives, as stated, are fulfilled, the research methodology described in this thesis is divided into five distinct phases, such as: theoretical analysis, laboratory experimentations, field works, groundwater level simulation from software computations and development of a suitable control technique from the viewpoint of saline water intrusion. These different phases are sequentially described step-by-step below:

3.2.1 Theoretical Analysis

- The saline water ingression is a common phenomenon in coastal environment. Whenever the groundwater is withdrawn from coastal aquifer, the possibility of upconing is initiated and simultaneously the interface is shifted towards the withdrawn point. The problem of upconing is more severe for deep wells. Therefore the relevant analytical formulations have been developed for safe withdrawn of groundwater from a vertical well considering upconing anticipation with Ghyben-Herzberg (Drabbe and Ghijben, 1889) assumptions and Dagan and Bear (1968) analysis. Using this model, the variation of safe well discharge was studied at varying fresh water head above mean sea level.

- As an alternative to conventional vertical wells, adoption of qanat-well structures (a combination of horizontal wells with central vertical riser) produces more yields and reduces the problem of upconing. An analytical study has been carried out to investigate the maximum yield from such qanat-well structure considering effect of upconing.

- Also theoretical formulations have been established for different shape of interface and length of saline water intrusion, width of ocean front etc.

- The Forchheimer's formula has been expanded in terms of modified Reynolds number and friction factor with different saline concentration at varying temperature. The two coefficients in Forchheimer's formula have been found out by analytical derivation.

3.2.2 Laboratory Experiments

Experiments on NaCl solution and natural soil are performed at the Hydraulics Laboratory of Contai Polytechnic Institute in Purba Midnapur. Brief descriptions of experiments so performed are sequentially given below:

- The variation of kinematic viscosity and density of saline water with saline concentration and different temperature are studied.

- Using falling head permeameter, the variation of hydraulic conductivity of natural soil for different periods of submergence in saline water have been studied.

- The pattern of intrusion of the NaCl solution in the course of the natural soil and the consequence of adequate fresh water recharge are investigated by means of a series of laboratory model tests developed specifically for this purpose. By means of this model test, the following studies are performed: (i) identification of flow pattern of saline water in its interaction with fresh water through natural soil, (ii) identification of interface / mixing zone pattern between saline water and fresh water, (iii) determination of shape of phreatic line and its time variation and (iv) estimation of flow velocity of saline water through porous medium.

3.2.3 Field Investigations

During the field investigations, soil bore-log sample and water samples from deep tube wells have been collected as for the present research programme of the coastal zone of Purba Midnapur district. The investigations were conducted in the sequence mentioned below:

- The hydro-geological study and the sub surface stratification in the Purba Midnapur district have been conducted by using the available sub-surface and hydro-geological data from the Public Health Engineering Department, Government of West Bengal, India. Comprehensive and in-depth routine wise analyses of the available field data have been performed.

- A review on the management and improvement of groundwater condition of Purba Midnapur district have been done and the following research have been performed: (i) depth of water level in Purba Midnapur during pre-monsoon and post-monsoon period, (ii) brackish water in the aquifers below sand dunes, (iii) hydro-geological/geochemical condition in coastal tracts of Purba Midnapur district, (iv) piezometric surface contour of study area, (v) spatial variation of aquitards and aquifers and (vi) three dimensional view of piezometric surface of the study area.

- In the coastal area of Purba Midnapur district at the selected deep tube well locations the water samples have been collected to determine the quality of the coastal groundwater. Chemical analyses were done in the State Water Investigation Directorate of Government of West Bengal located at Sech Bhavan in Kolkata. A thorough and comprehensive analysis of the available field data have been carried out and probable paths of the saline water intrusion in the study area are traced. Collection and compilation of data were done to obtain the

relevant geotechnical and geo-hydraulic properties of the subsoil existing in these coastal aquifers.

- The variation of saline concentration in the coastal area of Purba Midnapur district is assessed. Thus a series of contour surfaces have been obtained. The contours of chloride content, specific conductivity and total dissolved solids are estimated as well.

3.2.4 Software Simulation of Groundwater Level

- Visual MODFLOW 2000 software has been utilized to analyze the groundwater level simulation in Purba Midnapur.

- The pumping well discharge data, at two different time period of 2002 and 2012, have been collected from Public Health Engineering under Government of West Bengal.

- The simulated data for the year 2012 based on the data of 2002 and the observed data of 2012 are compared and a correlation coefficient is found out to indicate data validity.

- Also simulated ground water level data of 2019, 2020, 2021, 2022 and 2023 based on well discharge data of 2002 and 2012 are correlated for its justification.

- This work focuses the prediction of future groundwater levels in the perspective of potential groundwater management scenarios in the region concerned.

3.2.5 Management and Control of Saline Water Intrusion

- A convenient cost effective methodology for control of saline water intrusion into coastal aquifers has been developed. This methodology consists of withdrawal of groundwater by suitably designed qanat-well structure for withdrawn of fresh water coupled with rainwater recharge by recharge ponds and recharge wells. The technique so developed is successfully applied to a specific site in the study area. Adequate quantifications have been carried out and important observations are obtained there from.

- The study area has been divided into six zones for aquifer improvement planning based on the soil characteristics of aquifers and status of piezometric surface and imposing certain restriction of abstraction of groundwater by deep tube wells in the area concern, will help in recharging the aquifer, and control the danger of saline water intrusion and enhance the quality of groundwater.

- Other plan of solution to meet the fresh water demand in future in the area, using alternative freshwater sources has also been encouraged, the existing rivers of Rupnarayan are collected and distribution to the various purpose after proper treatment.

3.3 Sequence of Execution

The entire research is commenced, stepwise performed and completed following a definite sequence for the steps of execution. The sequence of execution is illustrated in Figure 3.1.

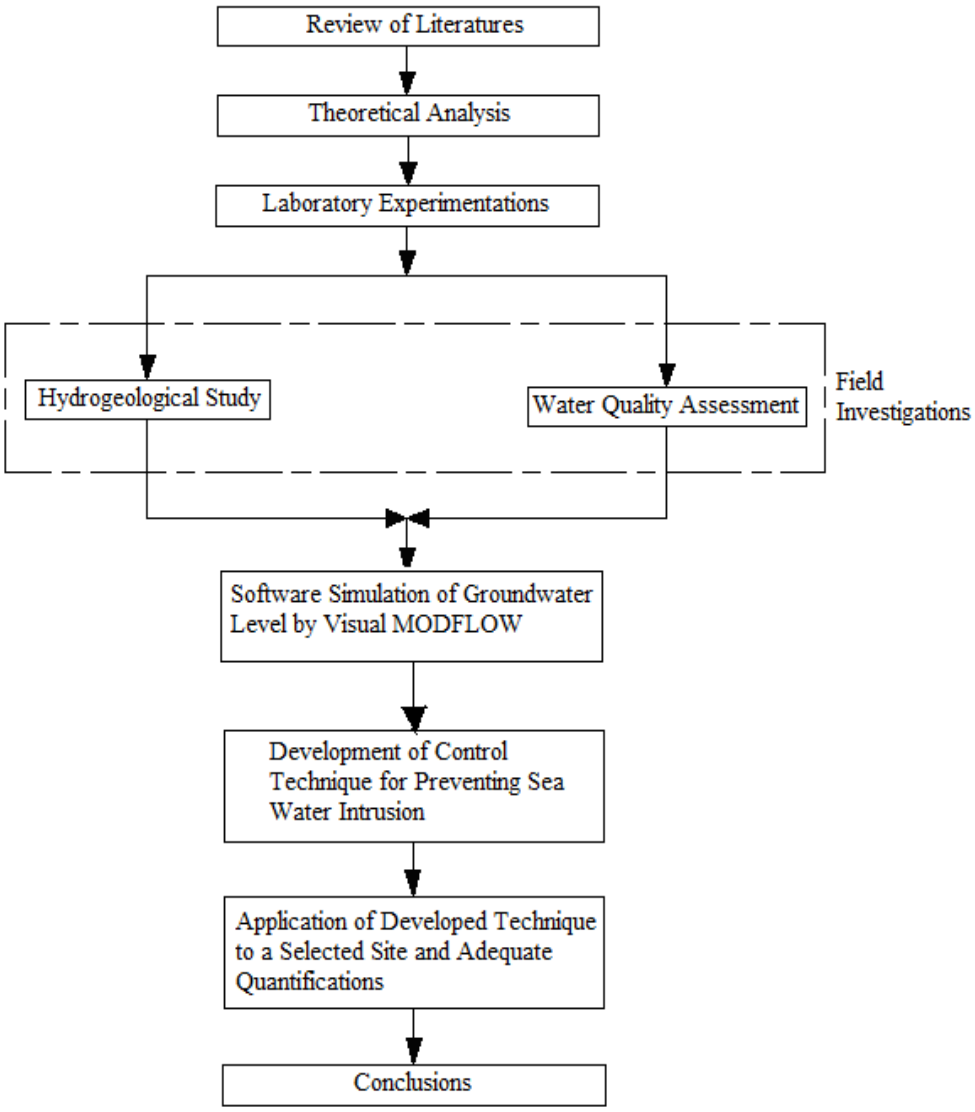

Fig. 3.1: Sequence of execution of this research programme.

3.4 References

Dagan, G. and Bear, J. (1968). Solving the Problem of Local Interface Upconing in a Coastal Aquifer by the Method of Small Perturbations. *Journal of Hydraulic Research*, Vol. 6, Iss. 1, pp. 15-44.

Drabbe, J. and Ghijben, W.B. (1889). Nota in verband met de voorgenomen putboring nabij Amsterdam. Tijdschrift Kon. K. Instituut van ingenieurs, The Hague. Tijdschrift. The Hague. pp. 8-22.

CHAPTER - 4

(Linear and Non-Linear Flow Through Granular Porous Media: Governing Theories)

- Background
- Types of Porous Media
- Properties of Flow through Porous Media
- Types of Flow through Porous Media
- Relationship between *A* and *B*
- Determination of Velocity using Forchheimer's Law
- Expansion of Forchheimer's Equation in Terms of *A* and *B*
- Expression for Velocity at Varying Salinity and Temperature
- Expansion of Forchheimer's Law by Modified Reynolds Number and Friction Factor
- References

4.1 Background

A brief review of literatures as mentioned in the Chapter 2 indicates that significant researches were conducted on linear and non-linear flow through a porous media. Thus physical understanding of flow pattern of saline water intrusion to fresh coastal aquifers is essential in the related field. The suggested values of A and B as per Ergun (1952) and the relation between them are determined. The Forchheimer law making velocity as the subject of formula is calculated. The Forchheimer law in terms of modified Reynolds number and modified friction factor is finally derived. The governing non-linear flow equation that is the Forchheimer equation has been modified and expressed in terms of saline concentration at different temperatures.

4.2 Type of Porous Media

Most of the materials are permeable when observed at a proper length scale. Illustrations go from permeable silicon, which is permeable on the nanometre scale to limestone cavity and underground stream framework on the kilometre scale. Anyway of this work it can be set under two classifications.

Classification 1: This class incorporates those permeable media which has no individual molecule yet comprise of a specific structure. The state of the framework is twisted under the liquid stream conditions. The best case of this class is sponge.

Classification 2: This classification incorporates permeable media, for example, sand or glass beads packed in a settled volume. In this sort of permeable media singular particles get deformed from their unique position for the period of the flow of liquid. Sand and glass beads might be contrast in their properties, i.e., surface irregularity and size of the particles. Surface and dimension of the glass beads are smoother and more uniform as compared to the sand particles. Stream of liquid through a permeable medium is essentially represented by its porosity and the hydraulic conductivity.

4.3 Properties of Flow through Porous Media

The properties which govern the flow through a porous media are sequentially described below:

Porosity: Porosity is a dimensionless amount indicated by ϕ. It is the proportion of void space to the aggregate volume of material. It manages how much liquid an immersed material can contain and has a vital effect on expand properties of the material. Consider a point in a three dimensional flow region denoted by $x_i = (x_1, x_2, x_3)$ where x_i (i = 1 to 3) are the coordinate of the point. Let V_t be the total volume containing both fluid and solid which might be each sphere or cube with centre at x_i. Let V_v be the volume of voids. Then the porosity ϕ of such porous medium is defined as

$$\phi = \text{void volume / total volume} = V_v/V_t \quad (<1)$$

Permeability: Permeability is a measure of the capacity of a material to pass on liquid under a hydraulic gradient. Permeability is an element of permeable media as it were.

Hydraulic conductivity: It might be characterized as the liquid speed per unit hydraulic gradient. It is a component of both the permeable medium and liquid. It is signified as K and in scientific term.

$$K = -\frac{V}{dh/dx} \tag{4.1}$$

where, $dh/dx =$ hydraulic gradient, K= hydraulic conductivity (m/s) and V= mean velocity of flow or volume rate of flow per unit area (m/s).

Owing the collapse at the current occasion to achieve in excess of a tolerably legitimate expression relating the coefficient of penetrability to the geometric qualities of soil, refinement in K are barely justified. In any case, due to the impact that the thickness and consistency of the pore liquid may apply on the subsequent speed, it is some an incentive to confine that component of K which is reliant on these properties. We introduce the physical permeability k_0 (in cm^2), which is a consistent exemplifying the structural features qualities of the medium and is free of the property of the liquid. The connection between the porosity and the coefficient of penetrability as given by Muskat (1946) is

$$K = \frac{k_0 \gamma_w}{\mu} \tag{4.2}$$

where, γ_w is the unit weight of the fluid and μ is the coefficient of viscosity. Substituting Equation (4.2) in to the equation of Darcy's law, we obtain

$$K = k_0 \frac{\gamma_w}{\mu} \frac{dh}{dx} \tag{4.3}$$

Table 4.1: Some typical values of coefficient of permeability.

Soil type	Coefficient of permeability K (cm/s)
Clean gravel	1.0 and greater
Clean sand (coarse)	1.0 - 0.01
Sand (mixture)	0.01 - 0.005
Fine sand	0.05 - 0.001
Silt	0.0005 - 0.00001
Clay	0.000001 and smaller

This demonstrates the discharge speed is in reverse equivalent to the viscosity liquid. Equation (4.3) might be utilized when dealing with more than one fluid or with temperature variations. In the ground water and seepage problems encountered in civil engineering where we are fundamentally intrigued by the stream of a solitary moderately incompressible liquid subject to little changes in temperatures, it is additional suitable to utilize Darcy's law with K as in Equation (4.1).

In soft computing language the difference between the coefficients of permeability and hydraulic conductivity are given in Equations (4.4-4.7).

If, $$f = f(g) \tag{4.4}$$

where, this expression represents that hydraulic conductivity is a function of soil property.

If, $$\phi = \phi(g, h) \tag{4.5}$$

where, this expression represents that the coefficient of permeability is another function of soil and fluid both property.

If, $$q_i = -k_0 \frac{\partial h}{\partial x_i} \quad (i = 1, 2, 3) \tag{4.6}$$

This k_0 depends on the properties of both hard and liquid parts of permeable media and is given by

$$K = \frac{k_0 \rho g}{\mu} \tag{4.7}$$

where, g is the gravity acceleration. This k_0 is autonomous of the properties of liquid and depends on the porosity. The some typical values of coefficient of permeability are given in Table 4.1.

Relative Density: The looseness and solidity of sandy soils can be demonstrate quantitatively by relative density D_r defined by the Equation (4.8).

$$D_r = \frac{\gamma_{d\ \max} - \gamma_d}{\gamma_{d\ \max} - \gamma_{d\ \min}} \times 100\% \tag{4.8}$$

where, $\gamma_{d\ \max}$ = sand in its highest unit weight; $\gamma_{d\ \min}$ = sand in its lowest unit weight; and γ_d = sand in its in-situ condition unit weight.

Specific Gravity: Specific gravity of a material is described as the ratio of its mass of an equal volume of water at reference temperature, 4°C. So, to estimate the specific gravity of used sand, density bottle method has been used. The formula for specific gravity (G) is given in Equation (4.9).

$$G = \frac{(M_2 - M_1)}{(M_2 - M_1) - (M_3 - M_4)} \tag{4.9}$$

where, M_1 = mass of empty bottle; M_2 = mass of bottle + dry sand; M_3 = mass of bottle + sand + water; and M_4 = mass of bottle + water.

4.4 Types of Flow through Porous Media

Depending upon the Reynolds number, flow through porous media can be broadly categorized as (1) laminar flow and (2) turbulent flow.

4.4.1 Laminar Flow

There are numerous occurrences of flow of liquid through permeable media. For instance, the development of water, oil, and gaseous petrol through the ground, drainage underneath dams and expansive structures, flow during packed towers in some chemical procedure, filtration, this rely upon this flow. The speed of these cases is generally so little and flow entries so thin that laminar flow might be accepted positively. The laminar move through permeable media can be either linear or non-linear as explored by numerous in their independently led tests. Anyway the consequences of Darcy and Forchheimer are generally challenging.

4.4.1.1 Linear Flow

Linear flow administrations comprise of Darcy and pre-Darcy flow. Anyway as the affectability of accessible instrumentation isn't adequate to calculate the mainly low pressure gradient and velocities, only Darcy flow is analyzed.

4.4.1.1(a) Darcy or Linear Flow

In 1856 the French designer Henri Darcy developed probes the stream of water through a pipe packed with sand and found that specific conditions the volume rate of flow through the pipe was corresponding to the negative of the pressure gradient. This relationship which is called Darcy's law can be expressed as given in Equation (4.10).

$$V = -K\frac{dh}{dx} \tag{4.10}$$

The negative sign in the equation indicates that the flow is always in the direction of decreasing head. Resulting research has adjusted the Darcy law to incorporate the fluid viscosity and can be expressed as in Equation (4.11).

$$V = -\frac{K}{\mu}\frac{dp}{dx} \tag{4.11}$$

The estimation of K in the condition depends on the viscosity of liquid as well as on the size and geometrical course of action of the strong partials in the in the permeable material. It is thus complicated to forecast the value of K proper to the specific arrangement of conditions. As the Darcy's law communicates a linear equation, the flow administered by this law certainly is a linear flow. The Reynolds number relating to the lower and upper bound of Darcy regime can be assigned by $R_{e\mathrm{DL}}$ and $R_{e\mathrm{DH}}$, respectively.

4.4.1.1(b) Range of Validity of Darcy's Law

Visual perception of colour infused into fluids drove Reynolds in 1883, to infer that the regulation of the flow was subject to its speed. At little speed the stream seemed methodical, in layers, that is, laminar. With expanding speeds, Reynolds observed a mixing between the colour and water; the pattern of stream ends up unpredictable, or turbulent. Inside the scope of laminar stream, Reynolds found a straight proportionality to exist between hydraulic gradient and speed of stream, in keeping the Darcy's law. At

turbulence, the hydraulic gradient moved toward the square of speed. This interpretation suggests an illustration of the hydraulic gradient as given in Equation (4.12).

$$i = av + bv^n \tag{4.12}$$

where, a and b are consists and n is between 1 and 2. From studies of the flow of water through columns of shot of uniform size, Lindquist reports n to be exactly 2. Whatever the exact request of n, tests has shown decisively that for little speeds (inside the laminar range), Darcy's law gives a precise display of the flow inside a permeable medium.

There remains now the condition of the estimation of the laminar range of the stream and the augmentation to which genuine stream frameworks through soils are incorporated. Such a standard is outfitted by Reynolds R_e (a pure number relating inertial to viscous force), characterized as given in Equation (4.13).

$$R_e = \frac{\rho V_s d}{\mu} \tag{4.13}$$

where, V_s = superficial flow velocity; d = mean sand diameter.

Particle Reynolds number for Darcy flow: $10^{-5} < R_e < 2.3$.

Particle Reynolds number for Forchheimer flow: $5 < R_e < 80$.

Forchheimer flow is widely-regarded as being the primary to recommend a non-linear relationship between the pressure gradient and fluid velocity for Reynolds number greater than the upper Darcian Reynolds number. In 1901 he proposed a second order Equations (4.14-4.16) to fit exploratory information as takes after.

$$-\frac{dh}{dx} = \frac{1}{\gamma}\left(AV + BV^2\right) \tag{4.14}$$

$$\text{or,} \qquad -\frac{dp}{dx} = AV + BV^2 \tag{4.15}$$

$$\text{or,} \qquad -\frac{dp}{dx} = A\frac{(1-\phi)^2}{\phi^3}\frac{\mu V}{d^2} + B\frac{(1-\phi)}{\phi^3}\frac{\rho V^2}{d} \tag{4.16}$$

where γ = specific weight; V = volume rate of flow per unit area, A and B are dimensionless constants and the pertinence of the Equation (4.16) to various porous media are reliant on the constants A and B. The values of dimensionless constants A and B are suggested by Ergun (1952).

A foremost inadequacy of Forchheimer's equation is that they cannot adequately account for the combined effect of the geometric and viscosity and hence the empirical constants contained therein must be re determined for each specific porous medium.

4.4.1.2 Forchheimer or Non-linear Flow

Linear or Darcy stream is a declaration of strength of viscous forces exerted by the strong permeable matrix on the interstitial liquid and is of constrained relevance. Be that as it may, non-Darcy or post Darcy stream is influenced by inertia forces and turbulence. Forchheimer flow is broadly viewed similar to the first to propose a non- linear connection between the pressure gradient and fluid velocity for $R_e > R_{e\text{DH}}$

4.4.2 Turbulent Flow

The term turbulent or Post Forchheimer flow alludes to stream for which $R_e > R_{eFH}$, that is, for Reynolds number higher than those for which Forchheimer stream happens. There is a translation from laminar to turbulent stream to be particle Reynolds number (R_{eFH}).

4.5 Relationship between *A* and *B*

The suggested values of A and B as per Ergun (1952) are given in Figure 4.1 for the ranges A= 150 to 180 and B= 1.75 to 1.8. From Figure 4.1, the relation between A and B are found linear as shown in Equation (4.17).

$$B=0.0017A+1.5 \tag{4.17}$$

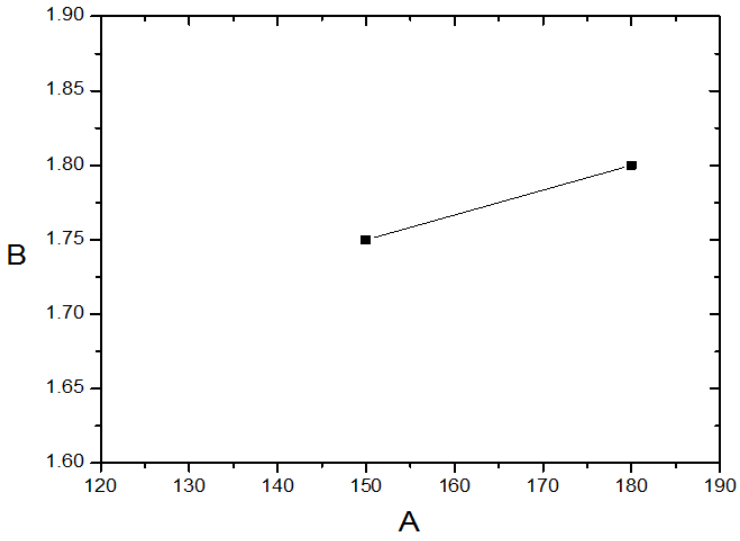

Fig. 4.1: Graph showing relation between A and B.

4.6 Determination of Velocity using Forchheimer's Law

The non-linear Forchheimer's Equation (4.18) is rewritten [Equations (4.19-4.20)] making velocity as independent variable.

$$-\frac{dh}{dx}=\frac{1}{\gamma}(AV+BV^2) \qquad \text{or,} \qquad i=\frac{1}{\gamma}\left(AV+BV^2\right) \tag{4.18}$$

$$\text{or,} \qquad V=-\frac{A}{2B}\left(1\pm\sqrt{1+\frac{4B\gamma i}{A^2}}\right) \tag{4.19}$$

Expanding $\left(\sqrt{1+\frac{4B\gamma i}{A^2}}\right)$ by binomial expansion, the following equation is obtained.

$$\sqrt{\left(1+\frac{4B\gamma i}{A^2}\right)}=1+\frac{1}{2}\left(\frac{4B\gamma i}{A^2}\right)-\frac{1}{8}\left(\frac{4B\gamma i}{A^2}\right)^2+\frac{1}{16}\left(\frac{4B\gamma i}{A^2}\right)^3-\frac{5}{128}\left(\frac{4B\gamma i}{A^2}\right)^4 \tag{4.20}$$

Truncating the right hand side of Equation (4.20) after the fifth term and substituting the same in Equation (4.19), the expression for velocity is determined [Equation (4.21)].

$$V = \frac{A}{2B}\left[\frac{1}{2}\left(\frac{4B\gamma i}{A^2}\right) - \frac{1}{8}\left(\frac{4B\gamma i}{A^2}\right)^2 + \frac{1}{16}\left(\frac{4B\gamma i}{A^2}\right) - \frac{5}{128}\left(\frac{4B\gamma i}{A^2}\right)^4\right] \tag{4.21}$$

The reason for taking negative sign is obvious because V=0 at i=0. It is usually sufficient for a non-linear analysis to consider up to the quadratic term only and in that case the expression for V is given by Equations (4.22-4.23)

$$V = \frac{A}{2B}\left[\frac{1}{2}\left(\frac{4B\gamma i}{A^2}\right) - \frac{1}{8}\left(\frac{4B\gamma i}{A^2}\right)^2\right] \tag{4.22}$$

or $$V = \frac{\gamma i}{A} - \frac{B\gamma^2 i^2}{A^3} \tag{4.23}$$

4.7 Expansion of Forchheimer's Equation in Terms of *A* and *B*

With the simplification of Equation (4.23), it can be written as Equations (4.24-4.25).

$$V = \frac{\gamma i}{A} - \frac{B}{A^3}(\gamma i)^2 \tag{4.24}$$

$$V = \frac{\gamma i \phi^3 d^2}{A(1-\phi)^2 \mu}(i) - \frac{B}{A^3}\frac{\phi^6 \rho d^5 \gamma^2}{(1-\phi)^5 \mu}(i)^2 \tag{4.25}$$

Substituting Ergun's B in terms of A in Equation (4.25)

$$V = \left\{\frac{\phi^3 d^2 g}{A(1-\phi)^2 \nu}\right\}(i) - \left\{\frac{(0.0017A + 1.5)}{A^3}\frac{\phi^6 d^5 g^2}{(1-\phi)^5 \nu}\right\}(i)^2 \tag{4.26}$$

4.8 Expression for Velocity at Varying Salinity and Temperature

The terms for kinematic viscosity can be replaced into Equation (4.26) relating to saline concentration for different temperatures as obtained from the graphs showing variation of kinematic viscosity versus saline concentration at different temperatures.

(1) Expression of velocity in terms of saline concentration at temperature of 17.5 ^{0}C can be obtained by putting $\nu = 0.0006\,x^3 - 0.0269\,x^2 + 0.4689\,x + 7.5339$.

(2) Expression of velocity in terms of saline concentration at temperature of 26^{0}C can be obtained by putting $\nu = 0.0006\,x^3 - 0.0258\;x^2 + 0.463\,x + 7.3933$.

(3) Expression of velocity in terms of saline concentration at temperature of 32^{0}C can be obtained by putting $\nu = 0.0006\,x^3 - 0.025\,x^2 + 0.4535\,x + 7.381$.

(4) Expression of velocity in terms of saline concentration at temperature of 40^{0}C can be obtained by putting $\nu = 0.00003\,x^4 - 0.0011\,x^3 + 0.0005\,x^2 + 0.4359\,x + 6.6042$.

(5) Expression of velocity in terms of saline concentration at temperature of 45^{0}C can be obtained by putting $\nu = 0.00004\,x^4 - 0.002\,x^3 + 0.0217\,x^2 + 0.2577\,x + 6.4157$.

4.9 Expansion of Forchheimer's Law by Modified Reynolds Number and Friction Factor

Rewriting the Equation (4.16)

$$-\frac{dp}{dx} = A\frac{(1-\phi)^2}{\phi^3}\frac{\mu V}{d^2} + B\frac{(1-\phi)}{\phi^3}\frac{\rho V^2}{d} \tag{4.27}$$

Dividing both sides by $B\frac{(1-\phi)}{\phi^3}\frac{\rho V^2}{d}$, Equation (4.27) becomes

$$-\frac{dp}{dx}\frac{d\phi^3}{BV^2(1-\phi)\rho} = \frac{A(1-\phi)\mu}{Bd\rho V} + 1 \tag{4.28}$$

The left hand side of the Equation (4.28) can be compared with Darcy Weisbach's friction factor C_f **[**Equation (4.29)].

Darcy Weisbach's friction factor $C_f = \frac{\nabla p}{L}\frac{D}{\nu V^2}\frac{2g}{\rho}$ (4.29)

$$= \frac{\nabla p}{L}\frac{D}{\nu V^2}\frac{\text{numerical value}}{\rho}$$

Hence the term $-\frac{dp}{dx}\frac{d\phi^3}{BV^2(1-\phi)\rho}$ can be written as a form of friction factor and can be called modified friction factor C_f'. So, the term modified friction factor can be expressed as given in Equation (4.30).

$$C_f' = -\frac{dp}{dx}\frac{\phi^3 d}{BV^2\rho(1-\phi)} \tag{4.30}$$

Similarly the term $\frac{B}{(1-\phi)}\frac{\rho V d}{\mu}$ can be written as modified Reynolds number (R_e') as compared to actual Reynolds number $R_e = \frac{\rho V d}{\mu}$.

So, modified R_e can be written as given in Equation (4.31).

$$R_e' = \frac{B}{(1-\phi)}\frac{\rho V d}{\mu} \tag{4.31}$$

Thus modified friction factor **(** C_f' **)** can be written as given in Equation (4.32).

$$C_f' = \frac{1}{R_e'} + 1 \tag{4.32}$$

4.10 References

Ergun, S. (1952). Fluid Flow through Packed Column. *Chemical Engineering Progress,* Vol. 48, No. 2, pp. 89-94.

Forchheimer, P.H. (1901). Wasserbeweguing durch Boden, *Zeitschrift fur Acker und Pflanzenbau*, Vol.45, pp. 1782-1788.

Muskat, M. (1937). The Flow of Homogeneous Fluids through Porous Media. University of Michigan, McGraw-Hill Book Company, USA.

CHAPTER - 5

(SALINE WATER INTRUSION AND EXTRATION-THEORETICAL ANALYSIS)

- Saline Water Intrusion
- Shape of Interface and Length of Saline Water Intrusion
- Width of Ocean Front through Freshwater Discharge to Ocean
- Ghyben-Herzberg Assumptions
- Theory of Upconing and Well Discharge
- Recasting of Equation for Safe Yield from Well
- Upconning beneath Crossed Qanat-Well with Vertical Riser
- References

5.1 Saline Water Intrusion

Saline water ingression in fresh groundwater aquifer happens in the region of seaside areas at whatever point saline water dislodges or blends with freshwater. This circumstance normally happens in coastal areas having hydraulic connection with ocean when the rate of extraction in the wells breaks the regular hydrodynamic equilibrium [Figure 5.1]. This saline water ingression into freshwater aquifers is probably going to cause significant issues in the event that such aquifer is tapped for local water supply or for water system.

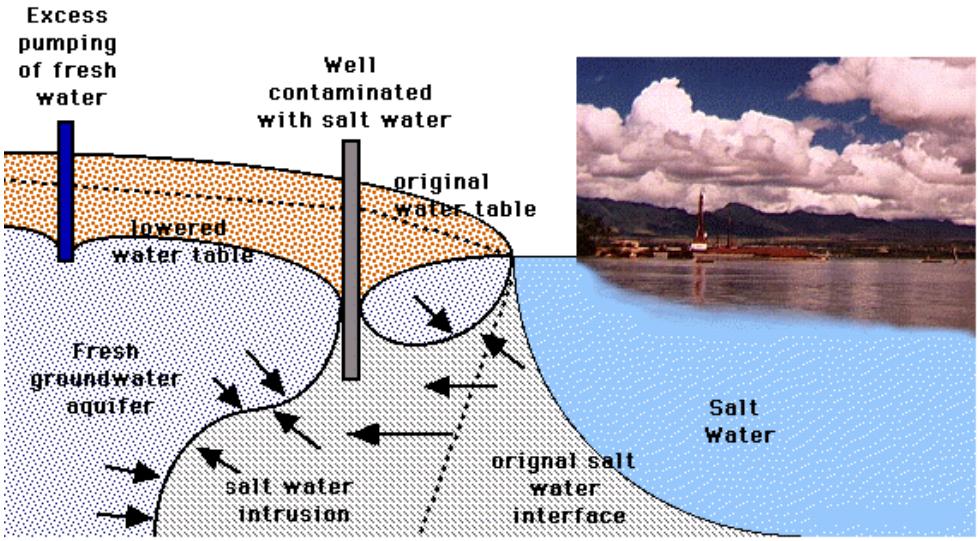

Fig. 5.1: Saline water intrusion in coastal aquifer.

5.1.1 Submarine Groundwater Discharge

Groundwater permeates from the surface gradually downwards through aquifers in the earths subsurface and inevitably discharges into lakes, streams, and the waterfront Ocean. The discharge of groundwater straightforwardly into marine waters is called submarine groundwater discharges (SGD). The impact of submarine groundwater discharges depends upon two components (i) Ecology of coastal system (ii) Contaminants carried by ground water. The French Engineer, Henry Darcy, first measures submarine groundwater discharge, given by $Q = K.i.A$ where Q = discharge in m^3/sec, i = hydraulic gradient, A = area of cross-section of aquifer in m^2, K = aquifer hydraulic conductivity in m/sec.

5.1.2 Diffusion Zone or Mixing Zone

The interface between freshwater and saline water is not sharp but has a narrow mixing zone along the interface. Normally this mixing zone is created from ocean tides, seasonal water table fluctuation, movement of freshwater and saline water and also from molecular diffusion (Wentworth, 1948; DeWiest and Davis, 1966).

5.1.3 Finite Thickness of Brackish Transition Zone

The thickness of brackish transition zone varies from 1 m to more than 100 m, concentrated pumping in Honolulu-Pearl Harbour area of Hawaii has created localized transition zones more than 300 m thick (Todd, 1980). From field measurement and experimental studies, as per Todd the thickness of transition zone becomes greatest near the shoreline. Normally in brackish transition zone the saline concentration increases with depth from freshwater to saline water.

5.1.4 Relative Salinity

In the brackish transition zone, the salinity of the ground water increases gradually with depth of the aquifers from freshwater to saline water. The distribution of salinity varies with depth and the relative salinity S_R as percentage is calculated as follows.

$$S_R = \left(\frac{C - C_f}{C_s - C_f} \right) \tag{5.1}$$

where C is the salinity at a particular depth within the brackish transition zone and C_f and C_s are the salinity of the freshwater and saline water, respectively.

5.2 Shape of Interface and Length of Saline Water Intrusion

The shape of interface is of parabolic nature and it is similar to Dupuit's parabola and is given by Rumer and Harleman (1963).

$$y = \sqrt{2\left(\frac{q}{K'} \right) x + 0.55\left(\frac{q}{K'} \right)^2} \tag{5.2}$$

$$K' = K\left(\rho_s - \rho_f \right) / \rho_f = K\left(G_s - 1 \right) = 0.025K \tag{5.3}$$

where, q = freshwater flow per unit width of ocean front, K = permeability of aquifer, ρ_s = density of saline water, ρ_f = density of freshwater, x, y = coordinates of the interface with the origin at the contact of mean sea level with land surface [Figure 5.2].

Applying boundary conditions ρ_f =1000 kg/m^3 and ρ_s = 1025 kg/m^3 on Equation (5.2) and Equation (5.3)

$$y = 0, \;\; x_0 = -0.275\left(q / K' \right) \tag{5.4}$$

The total length of intrusion measured from $x = 0$, is given by Figures 5.2 and 5.4.

$$2qL = K' H^2 \qquad \text{where } H = \text{thickness of aquifer}$$

$$x = 0, \; y_0 = 0.741\left(q / K' \right) \tag{5.5}$$

$$L = K' H^2 / 2q \qquad \text{when} \quad K > H \tag{5.6}$$

$$H^2 = 2qL / K' \qquad \text{or,} \;\; H = \sqrt{2qL / K'} \tag{5.7}$$

Replacing H by b in Equation (5.6), the seaward freshwater flow is given by

$$q = K' b^2 / 2L \tag{5.8}$$

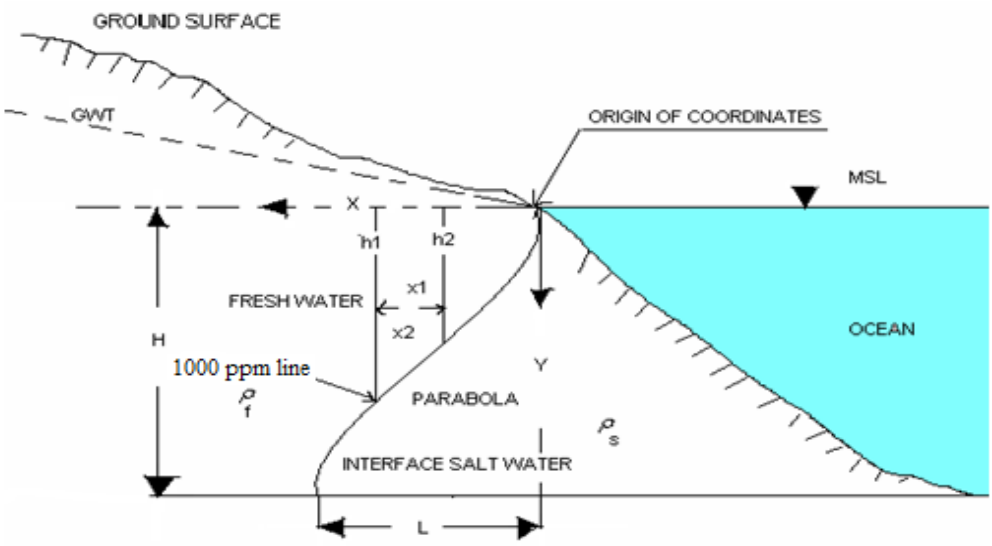

Fig. 5.2: The parabolic shape of interface between saline water and freshwater.

5.3 Width of Ocean Front through Freshwater Discharge to Ocean

Glover (1964) developed the following approximate equation for the shape of the freshwater and saline water interface.

$$y^2 - \frac{2qx}{K'} - \frac{q^2}{K'^2} = 0 \tag{5.9}$$

$$K' = K\left(\rho_s - \rho_f\right)/\rho_f = K\left(G_s - 1\right) = 0.025K \tag{5.10}$$

$$x = 0, y_0 = q/K' \tag{5.11}$$

$$y = 0,\ x_0 = q/2K' \tag{5.12}$$

where x_0 = width of ocean front through which freshwater discharge to ocean [Figure 5.3]. If the coordinate distances (x, y) from the shoreline to any point on the interface are found, the freshwater lost into the sea (q) can be determined. The saline water wedge in confined aquifer is given in Figure 5.4.

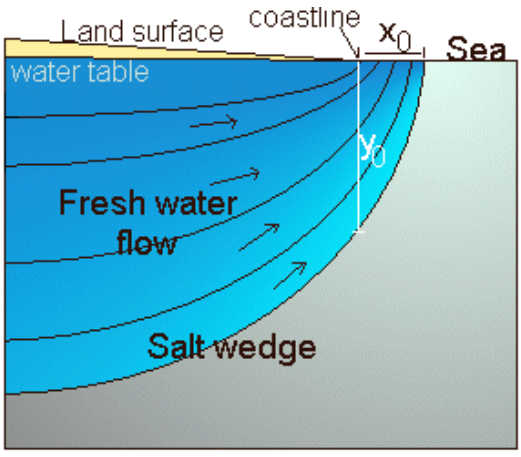

Fig. 5.3: Diagram interface (salt wedge) at the seacoast (after Glover, 1964)

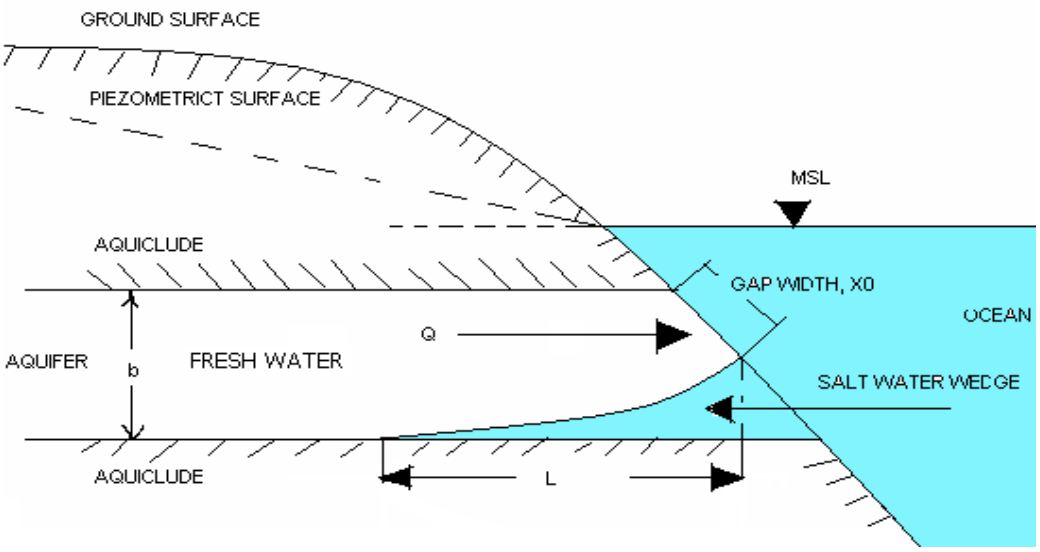

Fig. 5.4: Saline water wedge in a confined aquifer.

5.4 Ghyben-Herzberg Assumptions

In a sedimentary structure, ruled by exchange of fluvial and marine regimes, develops a complex groundwater stream demonstrate. The groundwater stream towards the ocean under common slope through the stack of sediment is blocked or altered by the obstruction of salt water or by charging of salt water from tidal attacks. This has offered ascend to a captivating situation with an assortment of circumstances in the dispersion of freshwater and saline water aquifers like saline water underlying or overlying freshwater in water table aquifers, or isolated by impenetrable or cracked confining layers, freshwater substituting with saline water isolated by impenetrable layers and freshwater along the side reviewing into saline water under both water table or confined conditions.

The relationship in a water table aquifer has been brought out by Ghyben - Herzberg principle (Drabbe and Ghijben, 1889). Saline water ingression happens in all coastal front aquifer. Pumping of freshwater expands the saline water ingression. This apparent fact is called saline water intrusion. The limit amongst saline and freshwater is known as the "interface" [Figure 5.5].

At the point when balance between saline water and freshwater in coastal aquifers is achieved, the profundity of the interface beneath mean sea level is given by the Drabbe and Ghijben (1889) under the accompanying assumptions:

- The aquifer is uniform, identical and unconfined nature.
- Freshwater and saline water is isolated by sharp interface.
- There is no immediate fresh groundwater flow to the ocean.
- There is no blending zone between the freshwater and saline water.

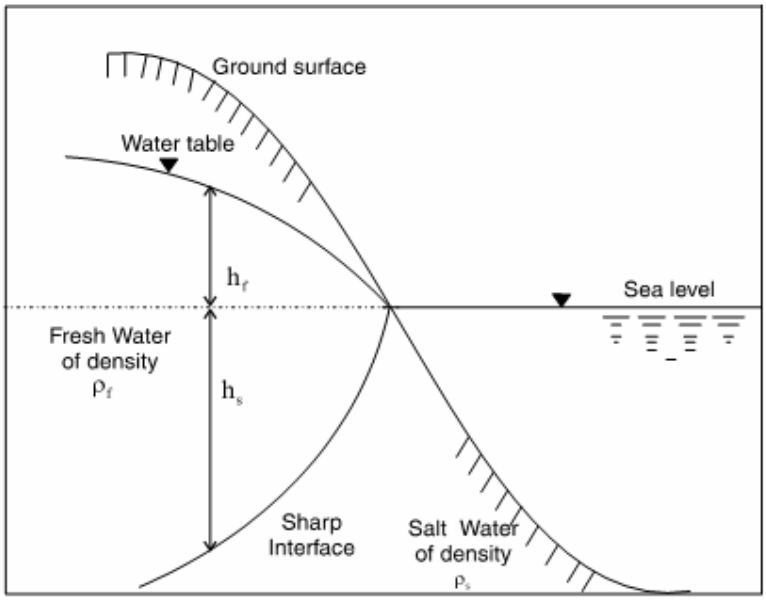

Fig. 5.5: Saline water intrusion and interface as per Ghyben-Herzberg principle.

Pressure of freshwater from water table is equal to pressure intensity of saline water from mean sea level at the same point of interface.

$$\rho_f g\left(h_s + h_f\right) = \rho_s g h_s \tag{5.13}$$

$$\text{or,} \quad h_s = \frac{\rho_f}{\rho_s - \rho_f} h_f \tag{5.14}$$

$$\text{Now,} \quad h_s = 40 h_f \tag{5.15}$$

where, $h_s =$ depth of the interface below sea level, and $h_f =$ elevation of the phreatic level above sea level.

5.5 Theory of Upconing and Well Discharge

A standout amongst the most emotional types of saline water ingression happens in coastal regions that are needy upon groundwater for their consumable water and water system needs. The most widely recognized situation includes the over-pumping of the freshwater aquifer. This reduces the head difference at the saline water-freshwater interface and induces the flow of saline water into the freshwater system. This is frequently exacerbated by inadequate recharge to the freshwater aquifer, which can happen in the midst of dry spell. The freshwater aquifers "float" over the saline water at the interface because of thickness contrasts in the two separate water sources. The saline water tends to shape a wedge under the freshwater that expands inland. As saline water ingression happens, this wedge broadens assist inland and is seen at shallower profundities. The outcome is that wells that beforehand delivered freshwater can see an expansion in chloride focus that makes the well unusable for water system or consumable employments. In coastal aquifers, where freshwater lying above saline

water, is pumped by a well, the interface ascends underneath the well because of drawdown of groundwater table around the well because of which weight on the interface is decreased and saline water ascends as a funnel shaped underneath the well [Figures 5.6 and 5.7]. This phenomenon is known as upconing. On the off chance that the highest point of the conical mound achieves the well, saline water will stream out of the well, which is an exceptionally unfortunate fact.

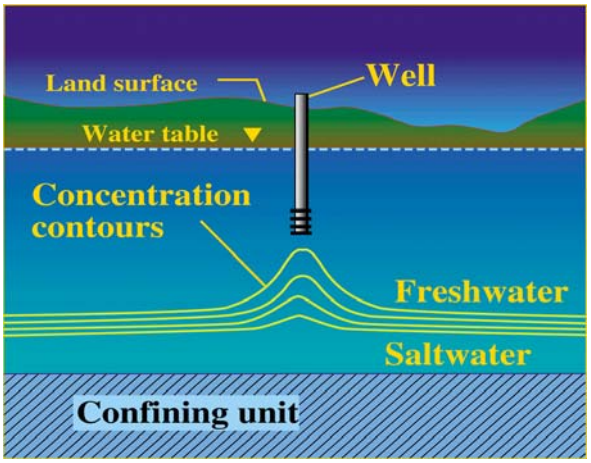

Fig. 5.6: Diagram presentation of saline water upconing diagram after Barlow (2003).

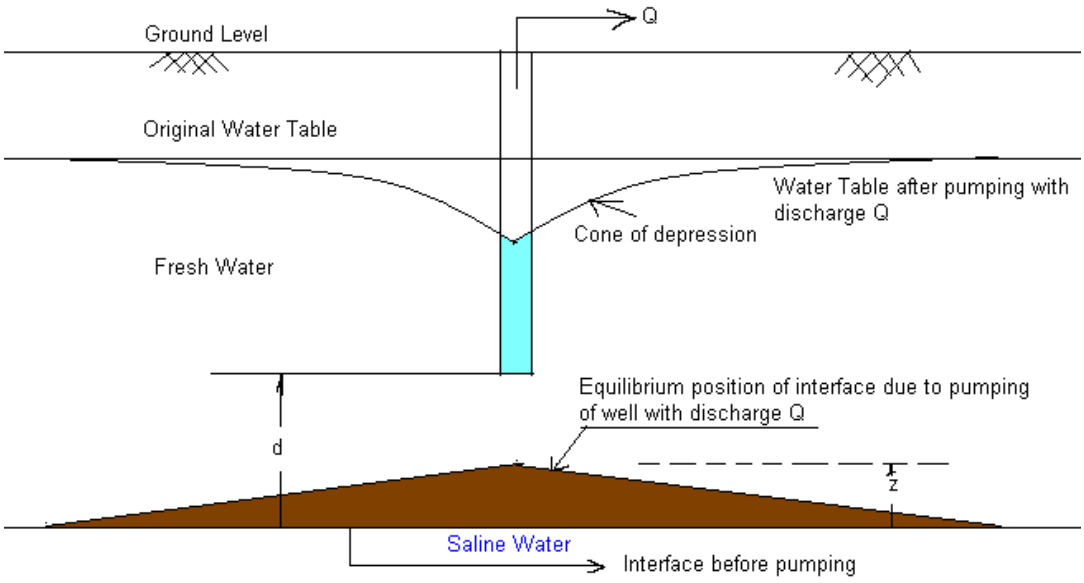

Fig. 5.7: Upconing of saline water beneath a pumped well.

Dagan and Bear (1968) gave a mathematical expression for determining the height of the cone "Z_t" below the well. The formula is as follows:

$$Z_t = \frac{\rho_f Q}{2\pi\left(\rho_s - \rho_f\right)K_x d}\left[1 - \frac{2\rho_f \theta h_f}{2\rho_f \theta d + \left(\rho_s - \rho_f\right)K_z t}\right] \tag{5.16}$$

where, Z_t = Rise of cone at time t; Q = Discharge of well; d = Depth of inter face below the bottom of the well, before pumping; K_x = Hydraulic conductivity of aquifer in horizontal direction; K_z = Hydraulic conductivity of aquifer in vertical direction; θ = porosity of aquifer; t = Time since start of pumping.

When $t \rightarrow \infty$, the equilibrium height, Z_∞ of the cone is given by

$$Z_\alpha = \frac{\rho_f Q}{2\pi(\rho_S - \rho_f)K_x d} \tag{5.17}$$

If $Z_\infty = d$, i.e. if the well is to discharge saline water, then putting value of $Z_\infty = d$ in Equation (5.17),

$$d = \sqrt{\frac{\rho_f Q}{2\pi(\rho_s - \rho_f)K_x}} \tag{5.18}$$

From Ghyben- Herzberg relation, the depth of interface below the well, before pumping is given by

$$d = h_f\left[\left(\frac{\rho_f}{\rho_s - \rho_f}\right)+1\right] - d_w \tag{5.19}$$

Equating the right-hand sides of Equations (5.18) and (5.19), Equation (5.20) is obtained.

$$\sqrt{\frac{\rho_f Q}{2\pi(\rho_s - \rho_f)K_x}} = h_f\left[\left(\frac{\rho_f}{\rho_s - \rho_f}\right)+1\right] - d_w \tag{5.20}$$

where, d_w = depth of well from original undisturbed water table.

Putting for ρ_f = 1 kg/m^3, ρ_s = 1.025 kg/m^3 in Equation (5.20), making Q the subject of the formula, the following equation is obtained.

$$Q = 0.157K_x(41h_f - d_w)^2 \tag{5.21}$$

From Equation (5.21), it is seen that for a homogeneous aquifer the safe discharge from the well is increased with increase in freshwater head h_f above mean sea level, and the safe discharge from well is increased with decrease in depth of well (d_w) below the original undisturbed freshwater table. The result as mentioned in Table 5.1 has been obtained by applying Equation (5.21) in the programme, as mentioned in *Appendix A*.

5.5.1 Output Results from Well Discharge Analysis

Using the theory developed, a case study based on field data has been carried out. The depth of freshwater zone is varied from 5 m to 120 m below the original undisturbed freshwater table, keeping in view the subsoil condition in the district of Purba Midnapur. The hydraulic conductivity of the subsoil in the horizontal direction is taken as an average value of 25m/day in the site near Contai and Digha regions. The output results obtained using the computer program documented and Qanat-well discharges at different hydraulic heads in course and fine texture is presented in Table 5.1.

Table 5.1: Well discharge at different freshwater head for various values of the depth of well (hydraulic conductivity of soil, K_x = 25 m/day).

d_w (m) → h_f (m) ↓	05	10	20	40	60	80	100	120
0.0	98.1	392.5	1570.0	6280.0	14130.0	25120.0	39250.0	56520.0
0.4	510.1	160.8	50.9	2186.1	7461.3	15876.5	27431.7	42126.9
0.8	3033.4	2040.4	643.1	203.5	2903.9	8744.3	17724.7	29845.1
1.2	7668.0	6031.3	3346.6	332.2	457.8	3723.4	10129.0	19674.6
1.6	14414.0	12133.6	8161.5	2572.3	123.1	813.9	4644.7	11615.5
2.0	23271.3	20347.2	15087.7	6923.7	1899.7	15.7	1271.7	5667.7
2.4	34240.0	30672.2	24125.3	13386.5	5787.6	1328.8	10.0	1831.2
2.8	47320.0	43108.4	35274.1	21960.5	11786.9	4753.3	859.7	106.1
3.2	62511.3	57656.1	48534.4	32645.9	19897.6	10289.2	3820.8	492.4
3.6	79813.9	74315.0	63905.9	45442.7	30119.5	17936.3	8893.1	2989.9

From the results in Table 5.1, the figures are plotted and it is concluded that initially well discharge increases as freshwater head above mean sea level increases when depth of well from original undisturbed water table is 5 m**,** 10 m, 20 m, 40 m curves respectively as shown in Figure 5.9. In Figure 5.9, the opposite observation is noted, the discharge attend maximum initially at minimum freshwater head, after that the well discharge decreases, as freshwater head increases, attend zero discharge after that the well discharge increases as freshwater head above mean sea level increases, but in small magnitude as for 60 m, 80 m, 100 m, and 120 m curves respectively. As regards to the developed formulations for safe yield of vertical well considering upconing in coastal regions and the relevant hypothetical case study, it may be concluded that initially the well discharge increases with freshwater head above mean sea level following fairly a parabolic pattern. Also, at zero discharge, the variation of the depth of well with the freshwater head above mean sea level follows parabolic pattern with positive gradually increasing slope. The Zero discharge at different freshwater head for various values of the depth of well and Hydraulic conductivity of aquifer is shown in Table 5.2 below from the table curves are plotted, as for Figure 5.8.

Table 5.2: The variation of freshwater head at different depth of well at zero discharge.

Sl. No.	Well Depth (d_w) (m)	Freshwater Head (h_f) (m)
01	05	1
02	40	3.5
03	100	7

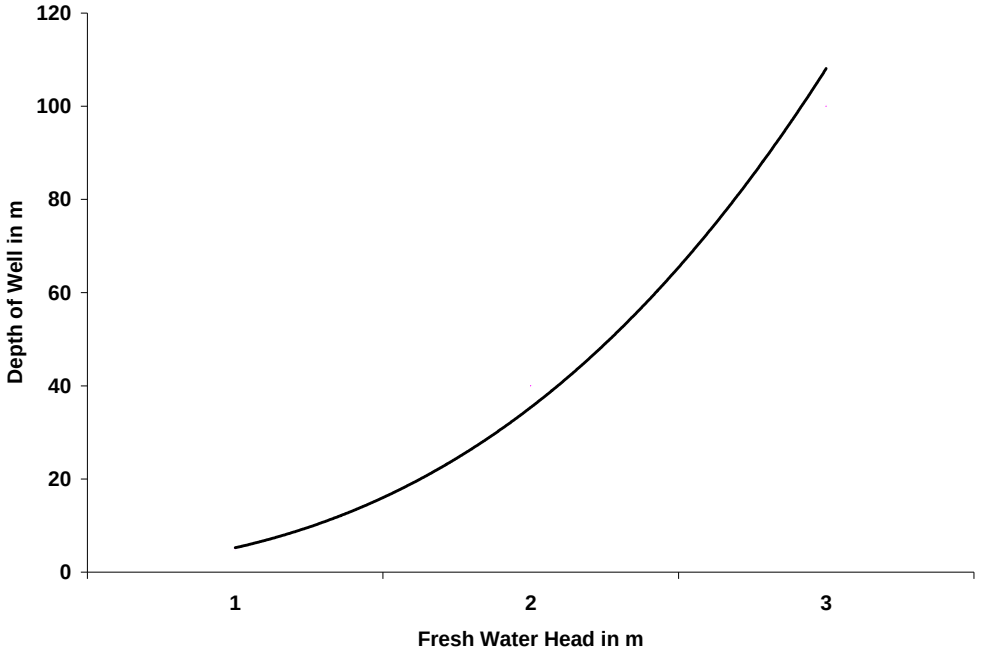

Fig. 5.8: True curves for depth of well versus freshwater head at zero discharge.

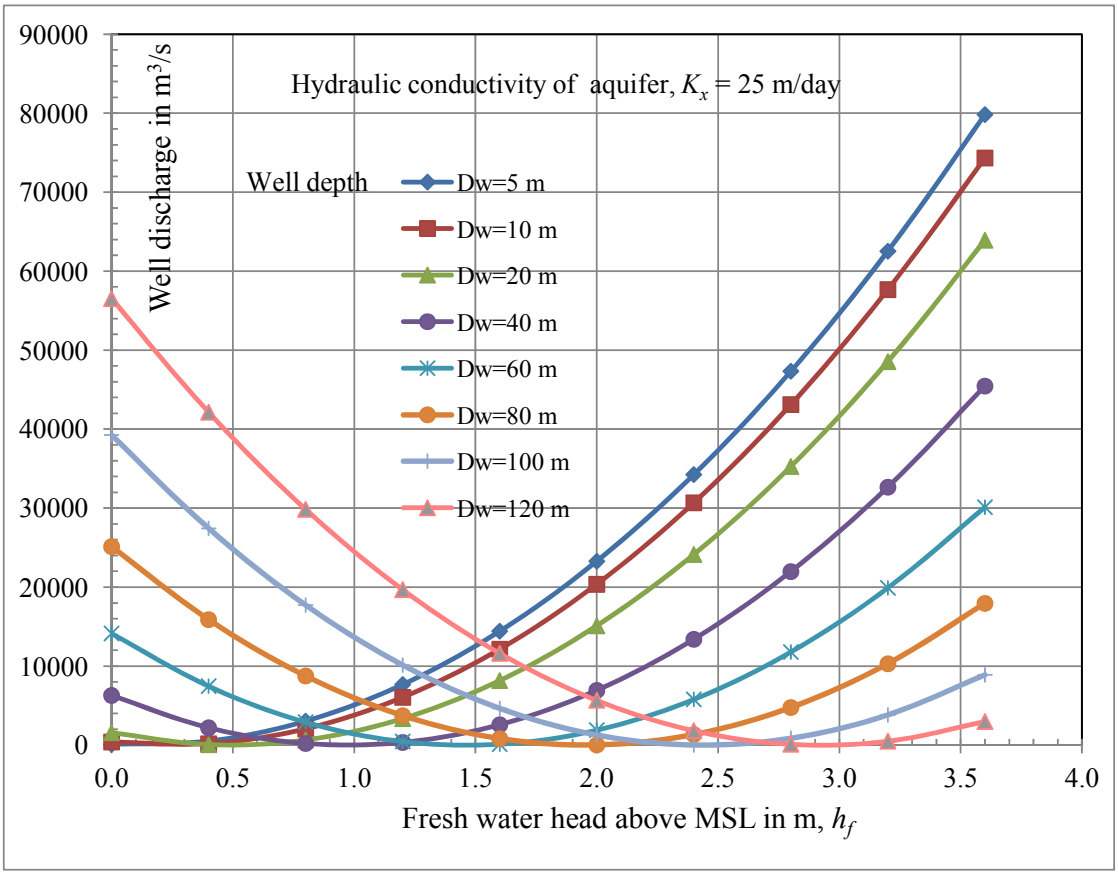

Fig. 5.9: True curves for variation of well discharge versus freshwater head.

Safe Yield Analysis

In the south eastern part of coastal areas of Purba Midnapur district namely Nandigram and Haldia are covered by unconsolidated sediments of recent age and it is represented by vast plains of fluvial and marine deposits. In the coastal region the recent sediments are characterized by a group of yellow or brown medium to sandy soil, the hydraulic conductivity is more than Digha and Contai site. The hydraulic conductivity of the subsoil in the horizontal direction is taken as an average value of [K_x = 3.512×10^{-4} m/s, Laboratory test] 30.34 m/day. The output results obtained using the computer program documented is presented in Table 5.3. The true curves for variation of well discharge versus freshwater head at different depth of well are plotted in Figure 5.10.

Table 5.3: Safe yield from wells at different freshwater head for various values of the depth of wells (hydraulic conductivity of soil, K_x=30.34 m/day).

d_w (m)→ h_f (m)↓	05	10	20	40	60	80	100	120
0.0	119.07	476.30	1905.20	7620.80	17146.80	30483.20	47630.00	68587.20
0.4	618.99	195.09	61.73	2652.80	9054.27	19266.14	33288.42	51121.08
0.8	3681.04	2475.99	780.37	246.91	3523.86	10611.20	21508.94	36217.09
1.2	9305.19	7319.02	4061.12	403.14	555.55	4518.37	12291.58	23875.20
1.6	17491.45	14724.15	9903.99	3121.48	149.36	987.65	5636.34	14095.43
2.0	28239.83	24691.39	18308.97	8401.93	2305.29	19.05	1543.21	6877.72
2.4	41550.32	37220.75	29276.06	16244.49	7023.33	1612.56	12.19	2222.22
2.8	57422.92	52312.22	42805.27	26649.17	14303.48	5768.18	1043.29	128.79
3.2	75857.63	69965.80	58896.59	39615.97	24145.74	12485.92	4636.49	597.47
3.6	96854.46	90181.49	77550.02	55144.87	36550.11	21765.77	10791.81	3628.26

5.6 Recasting of Equation for Safe Yield From Well

$$h_f + H - d_w = d \tag{5.22}$$

where, $H = \sqrt{2ql/K'}$. Putting the value of H in Equation (5.22), Here l is the total length of saline water intrusion.

$$h_f + \sqrt{\frac{2ql}{K'}} - d_w = \sqrt{\frac{\rho_f Q}{2\pi\left(\rho_s - \rho_f\right)K_x}} \tag{5.23}$$

$$Q = \frac{2\pi\left(\rho_s - \rho_f\right)K_x}{\rho_f}\left(h_f + \sqrt{\frac{2ql}{K'}} - d_w\right)^2 \tag{5.24}$$

Applying Boundary condition for ρ_f = 1000 kg/m^3 and ρ_s = 1025 kg/m^3 on Equation (5.24) and then putting $K^{/} = 0.025K$,

$$Q = 0.157K_x\left(h_f + \sqrt{\frac{2ql}{0.025K}} - d_w\right)^2 \tag{5.25}$$

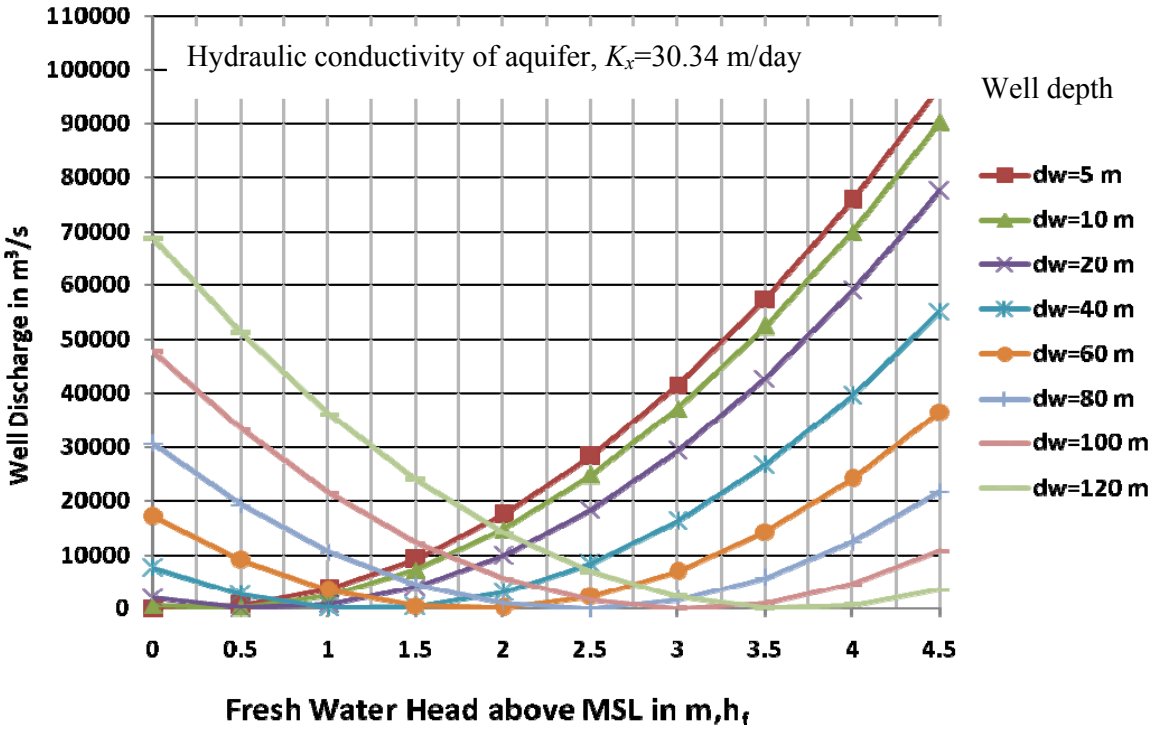

Fig. 5.10: True curves for variation of well discharge versus freshwater head

5.7 Upconning beneath Crossed Qanat Well with Vertical Riser

In coastal regions, deep tube wells are not preferable because of possibility of upconing of saline water. Shallow tube wells or deep tube wells with low discharge might be utilized; however the discharge being low may not get the job done to convene proposed requirements. In this unique circumstance, horizontal infiltration galleries called qanats combined with vertical risers can be built in the freshwater zone to maintain a strategic distance from issues with related with upconing. The qanats are stone product or PVC pipe having holes (5 mm diameter) settlement of 0.2 m to 1.5 m measurement, set at a profundity of 1 m to 5 m with rock pressing and wire nets at close interims so water can seep with low speeds into the gallery. This water can be drawn out and used while adequately safeguarding the nature of groundwater [Figure 5.11]. More details are described in Chapter 10. The qanat-well structures combined with vertical risers are as a practical answer for the issue of upconing underneath deep vertical wells. The deep vertical wells may not be feasible in several situations and qanats coupled with vertical risers can be successfully used in such cases.

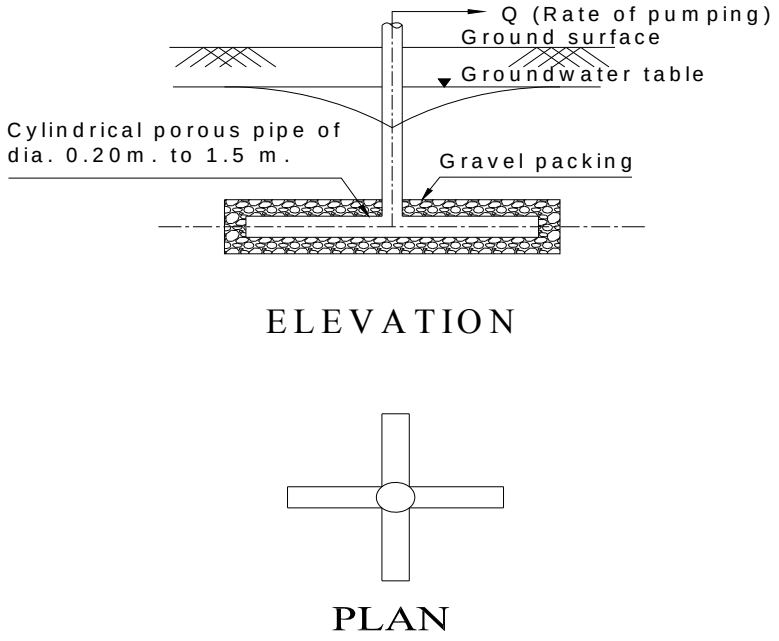

Fig. 5.11: Plan and elevation of a four legged qanat well structure.

5.8 References

Barlow, P.M. (2003). Ground Water in Freshwater-Saltwater Environments of the Atlantic Coast. Circular 1262, U.S. Geological Survey, Reston, Virginia, USA.

Dagan, G. and Bear, J. (1968). Solving the Problem of Local Interface Upconing in a Coastal Aquifer by the Method of Small Perturbations. *Journal of Hydraulic Research*, Vol. 6, Iss. 1, pp. 15-44.

DeWiest, S.N. and Davis, R.J. (1966). *Hydrogeology*. John Wiley and Sons, New York, p. 463.

Drabbe, J. and Ghijben, W.B. (1889). Nota in verband met de voorgenomen putboring nabij Amsterdam. Tijdschrift Kon. K. Instituut van ingenieurs, The Hague. Tijdschrift. The Hague. pp. 8-22.

Glover, R.E. (1959). The Pattern of Fresh Water Flow in a Coastal Aquifers. *Journal of Geophysical Research*. Vol. 64, Iss. 4, pp. 457-459.

Glover, R.E. (1964). *Groundwater Movement*. U.S. Bureau of Reclamation, Engineering Monograph, 31.

Rumer, R.R.Jr. and Harleman, D.R.F. (1963). Intruded Salt Water Wedge in Porous Media. *Journal of the Hydraulics Division*, Vol. 89, Iss. 6, pp. 193-220.

Todd, D.K. (1980). Groundwater Hydrology. 2nd edition. John Wiley and Sons, New York, USA. p. 245.

Wentworth, C.K. (1948). Growth of the Ghyben-Herzberg transition zone under a rinsing hypothesis. *Eos, Transactions American Geophysical Union*, Vol. 29, Iss. 1, pp. 97–98.

CHAPTER - 6

(Laboratory Tests to Determine Salinity Factors)

- Background
- Preparation of Sodium Chloride Solution
- Determination of Kinematic Viscosity of Saline Concentration
- Determination of Density of Saline Concentration
- Determination of Darcy's Coefficient
- Procedure to Determination Darcy's Coefficient
- Analysis Results
- Determination of Forchheimer Coefficients
- Experimental Setup
- Experimentation for Forchheimer's Velocity
- Soil Properties
- Hydraulic Conductivity and Forchheimer's Coefficients
- Rheological Characteristics of Saline Water
- Results and Discussions
- References

6.1 Background

The fresh groundwater contamination by saline water intrusion has become an alarming problem. It threatens all countries depending on groundwater abstraction from coastal zones. At present significant researches on saline water intrusion into coastal aquifers are in advancement. Some the significant contributions by previous researchers are briefly discussed below.

Li and Yeh (1968) determined a theoretical report on the distribution miscible fluids move through a permeable media. Mughal and Awan (1977) analyzed the issue of upconing of the freshwater and saline water interface below a drain using the Hele-Shaw model. They considered the freshwater and saline water as immiscible liquids with sharp interface. Fand *et al.* (1987) directed an exploratory examination for the resistance from the stream of liquids through straightforward and complex permeable media whose frameworks were made out of randomly packed spheres. Kececioglu and Jiang (1994) led an exploratory examination for move through permeable media of packed spheres immersed with water.

Xue *et al.* (1995) proposed a finite element technique to study the three dimensional miscible transport models for saline water ingression in a phreatic aquifer with a transition zone. Millham and Howes (1995) provided a relationship of the various methods to estimate hydraulic conductivity (K) in a shallow coastal aquifer including tidal damping, tracer, slug, permeameter and grain size analysis. Inoue and Nakayama (1998) conducted a numerical modelling of a non-Newtonian liquid move through a permeable medium utilizing a three dimensional cluster.

Andrade *et al.* (1999) explored the source of the deviations from the established Darcy law by numerical simulation of the Navier-Stokes conditions in two-dimensional uncombed permeable media. They connected the Forchheimer condition as a phenomenological model to relate the varieties of the contact factor for various porosities and stream conditions. Chan and Govindaraju (2003) projected an innovative model for soil hydraulic properties in view of a stochastic conceptualization of permeable media.

But no considerable studies have been done so far on the change in hydraulic conductivity of the aquifer soil due to long term contact with saline water. The present study involves in experimental determination of hydraulic conductivity of well graded fine sand by means of falling head permeameter after submerging it in sodium chloride solution at a specified concentration and for a specified period of submergence. The variation of hydraulic conductivity of the sand sample with saline concentration and period of submergence is studied.

The results and their interpretations of the experimentation on hydraulic conductivity of sand submergence under saline water have been presented briefly. The work also deals with determination of Forchheimer coefficients. The physical properties of saline water are estimated using laboratory tests. The flow pattern of seepage due to saline water intrusion and freshwater recharge into granular porous medium has been investigated by means of standard model tests.

6.2 Preparation of Sodium Chloride Solution

Pure sodium chloride and distilled water have been collected, the maximum solubility of sodium chloride has been determined for different saline concentration. It comes as 35.7×10^4 mg/l and other five unsaturated sodium chloride solutions such as 30.7×10^4 mg/l, 25. 7×10^4 mg/l, 20.7×10^4 mg/l, 15.7×10^4 mg/l, and 10.7×10^4 mg/l have been prepared and kept in separate bottles for experimentations.

6.3 Determination of Kinematic Viscosity of Saline Concentration

For determining kinematic viscosity, Saybolt viscometer, which is available in the hydraulic laboratory, has been used. The procedure adopted in measuring kinematic viscosity at different temperature is as follows:

- A sample measuring 60 ml sodium chloride solution with a known saline concentration has been poured into the Say bolt viscometer.
- With the help of a thermostat the temperature of the solution has been adjusted to the required value.
- A thermometer has been used for accurate measurement of temperature.
- Time taken by the solutions to completely evacuate the viscometer chamber has been measured with the help of a stop watch.

An expression of kinematic viscosity as a function of time (t) i.e. $v = C_1t + C_2/t$ (where v is viscosity, C_1 and C_2 are constants) has been used for measuring kinematic viscosity with the known value of time (t) for a particular solution.

Following with the above procedure, the results obtained are tabulated in Table 6.1 and subsequently the graphs, both true and best fit curves are plotted (Figures 6.1 to 6.5).

Table 6.1: Variation of kinematic viscosity with salinity and temperatures

Kinematic viscosity v (10^{-7} m^2/s)							
Temperature (°C)	Saline concentration (10^4 mg/l)						
	0	10.7	15.7	20.7	25.7	30.7	35.7
17.5	7.540	10.220	10.610	11.700	12.020	15.101	18.620
26	7.400	10.100	10.540	11.650	11.980	15.000	18.410
32	7.383	10.060	10.250	11.550	11.920	14.970	18.260
40	6.598	10.440	10.810	11.370	11.550	13.150	17.580
45	6.401	9.876	10.064	10.440	10.620	11.180	15.680
51	5.805	7.188	7.481	7.770	8.545	9.118	11.180

It is observed from the graphs that the kinematic viscosity increases with the increase of saline concentration. Initially the variation is considerable but gradually there is a tendency of stabilisation. Another set of true and best fit curves for observing the

variation of viscosity at varying temperature of sodium chloride solution for different saline concentration are plotted [Figures 6.6 to 6.7].

In accordance with the Meteorological Survey Department of India, the average temperature in atmosphere sometimes rises up to 51°C. Although the soil temperature may be slightly lower than as compared to the atmospheric temperature, the laboratory experiments have been conducted at a temperature range of 10.7°C to 51.0°C.

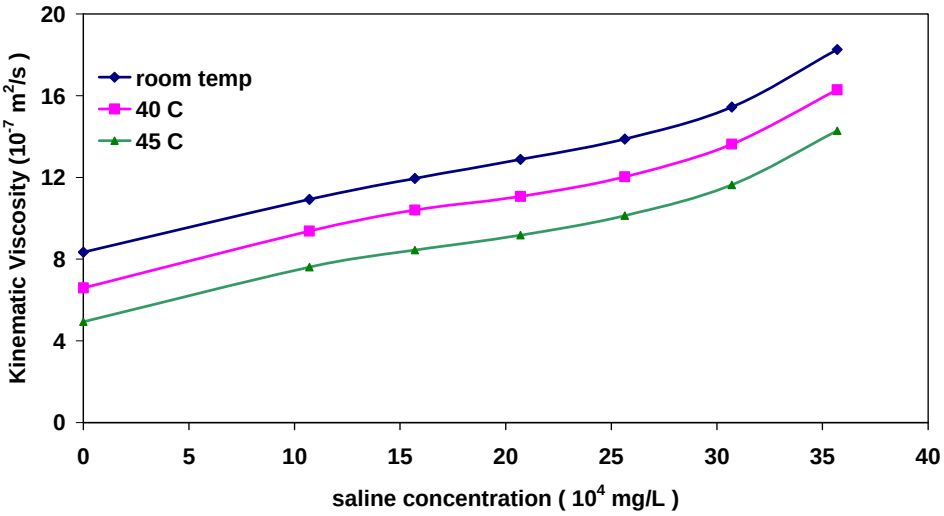

Fig. 6.1: True curves showing the variation of kinematic viscosity at different saline concentration of sodium chloride solution at varying temperatures.

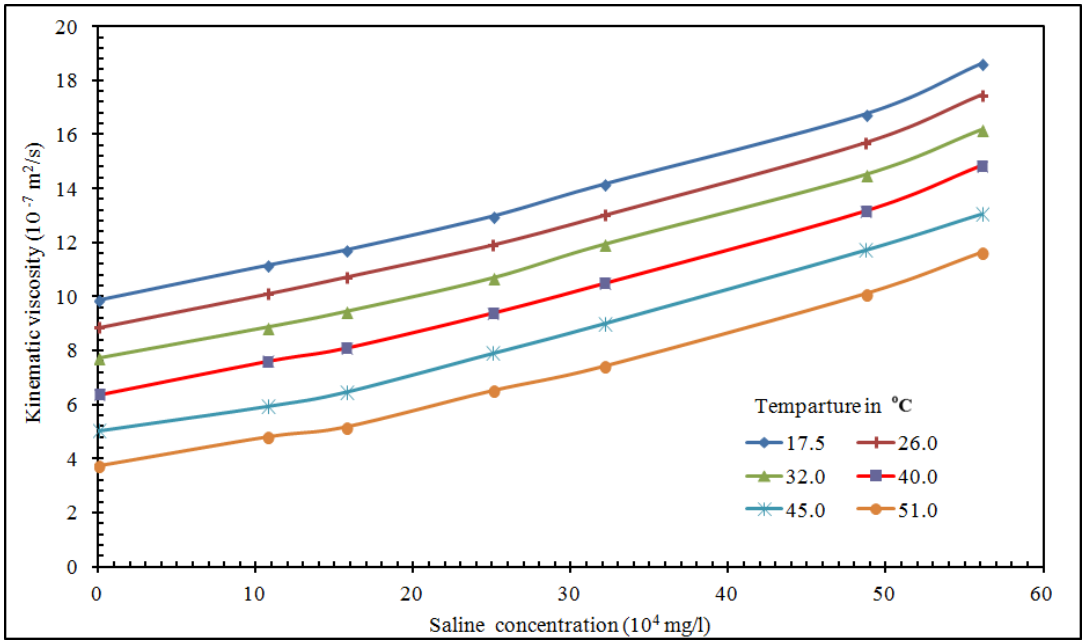

Fig. 6.2: Best fit curves showing the variation of kinematic viscosity at different saline concentration of sodium chloride solution at varying temperatures.

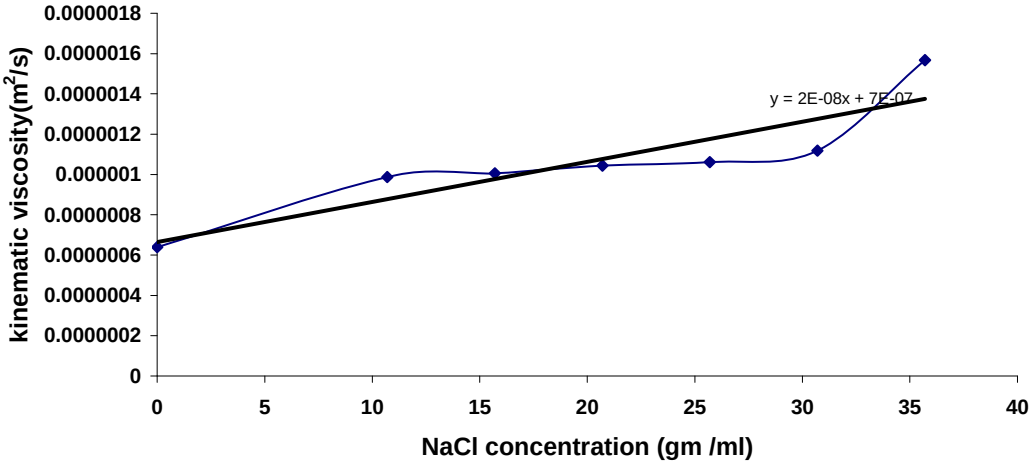

Fig. 6.3: Variation of kinematic viscosity at different sodium chloride concentration in water at 45°C.

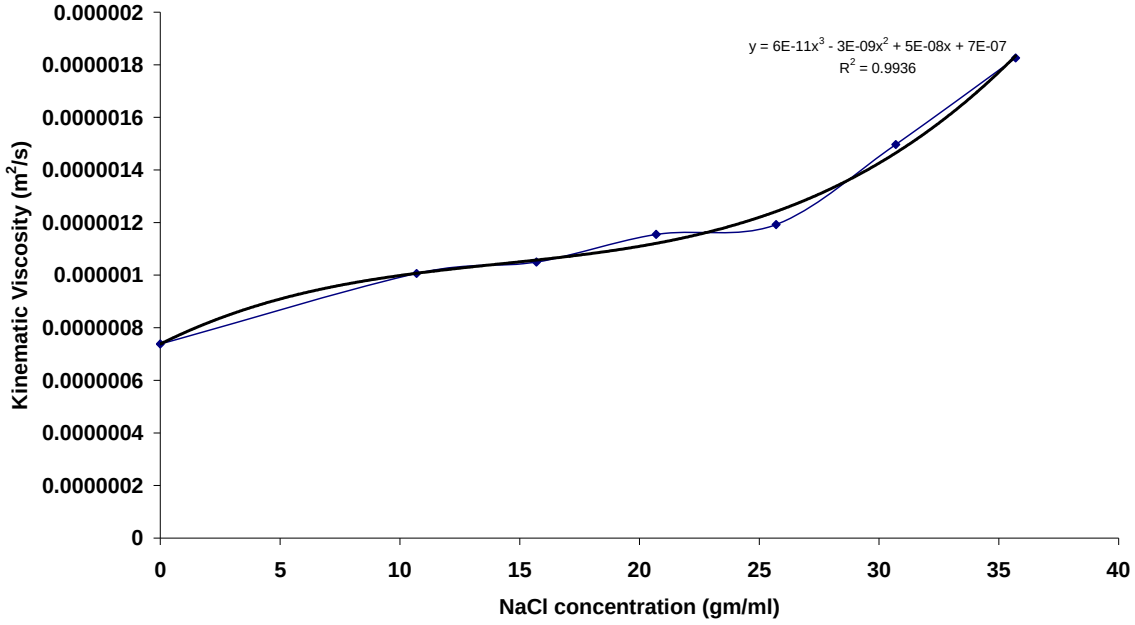

Fig. 6.4: Pattern showing the increase of kinematic viscosity with the increase of sodium chloride concentration in water at room temperature.

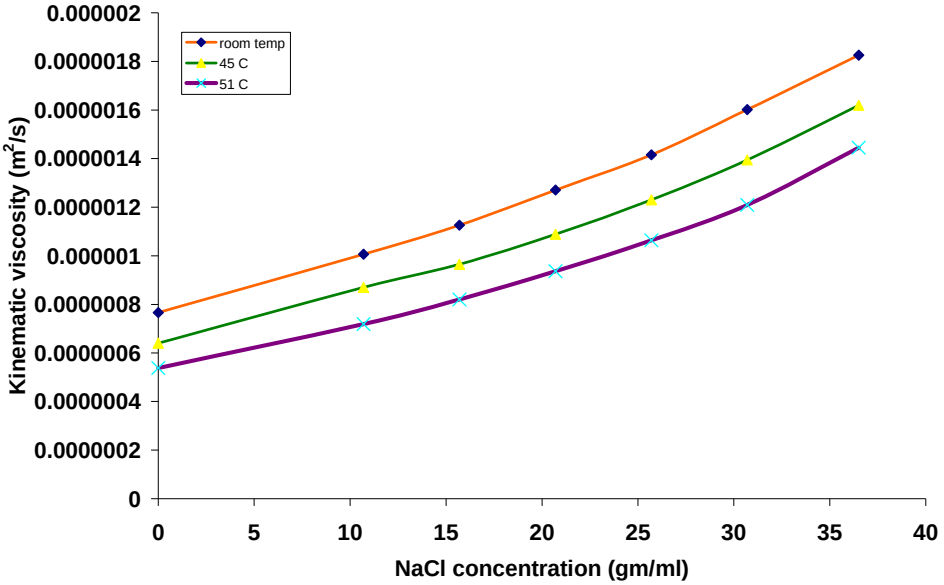

Fig. 6.5: Variation of kinematic viscosity at varying sodium chloride solution concentration at different temperatures.

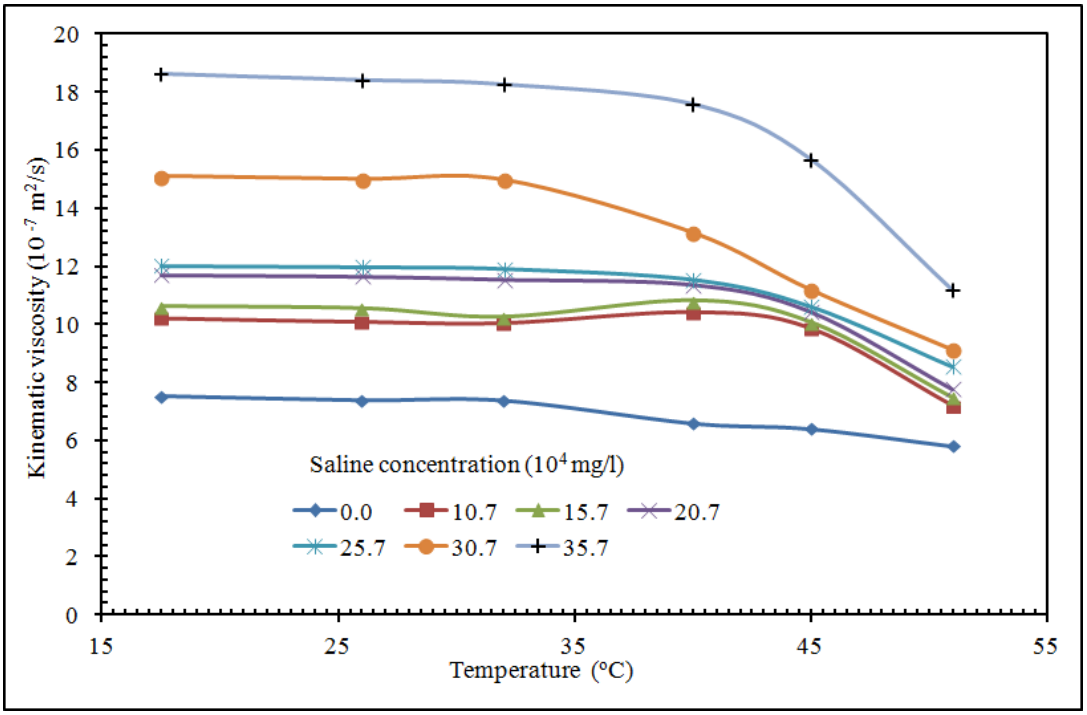

Fig. 6.6: True curves showing the variation of kinematic viscosity at varying temperature of sodium chloride solution for different saline concentration.

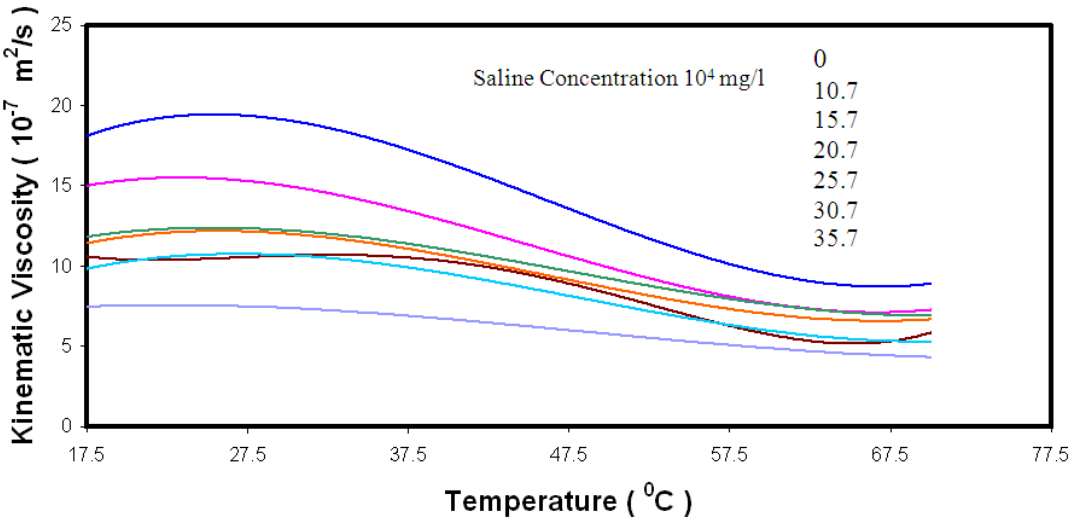

Fig. 6.7: Best fit curves showing the variation of viscosity at varying temperature of sodium chloride solution for different saline concentration.

6.4 Determination of Density of Saline Concentration

The experiment to find out specific gravity of saline concentration for sodium chloride solution at different temperatures has been conducted by Westphal balance. The simple Archimedes principle is the basis for the measurement of specific gravity.

While conducting experiments, every care has been taken in getting the best possible accurate results. Then subsequently densities of solutions have been determined. The result thus obtained are tabulated in Table 6.2 and the corresponding true and best fit curves of density versus saline concentration of sodium chloride solutions at different temperatures are plotted in Figures 6.8 to 6.13.

It is observed from the graph that density increases with the increase in saline concentration. A separate graph showing the true curve for variation of density versus temperature of sodium chloride solution for different saline concentration is also shown in Figure 6.14.

Table 6.2: Variation of density of saline concentration at different temperatures.

Density (kg/m^3)							
Temperature (^{0}C)	Saline concentration (10^4 mg/l)						
	0	10.7	15.7	20.7	25.7	30.7	35.7
10	1001.0	1107.78	1125.74	1157.68	1125.64	1189.61	1204.58
20	998.5	1097.80	1121.75	1146.70	1168.56	1187.62	1197.60
25	998.0	1087.82	1118.76	1144.70	1167.66	1187.62	1197.60
30	998.0	1077.84	1117.76	1137.72	1167.66	1187.62	1197.60

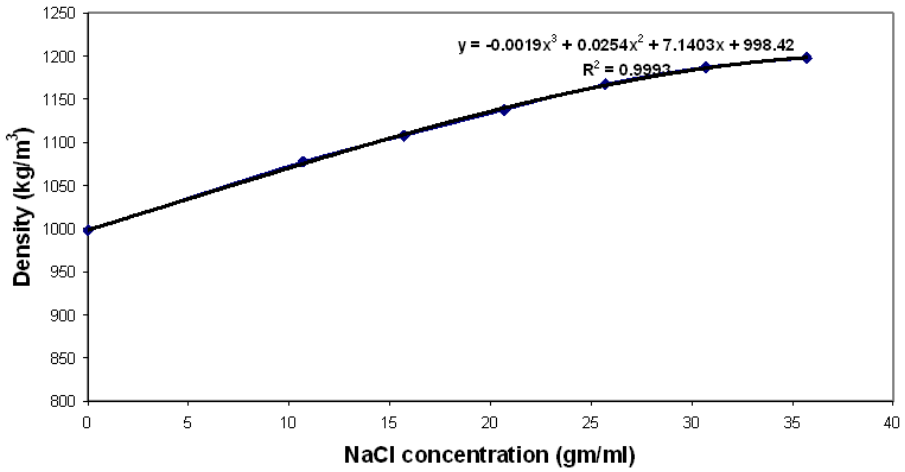

Fig. 6.8: Variation of density at different sodium chloride concentration in water. (Here, x is sodium chloride concentration in saline water; y is density of saline water)

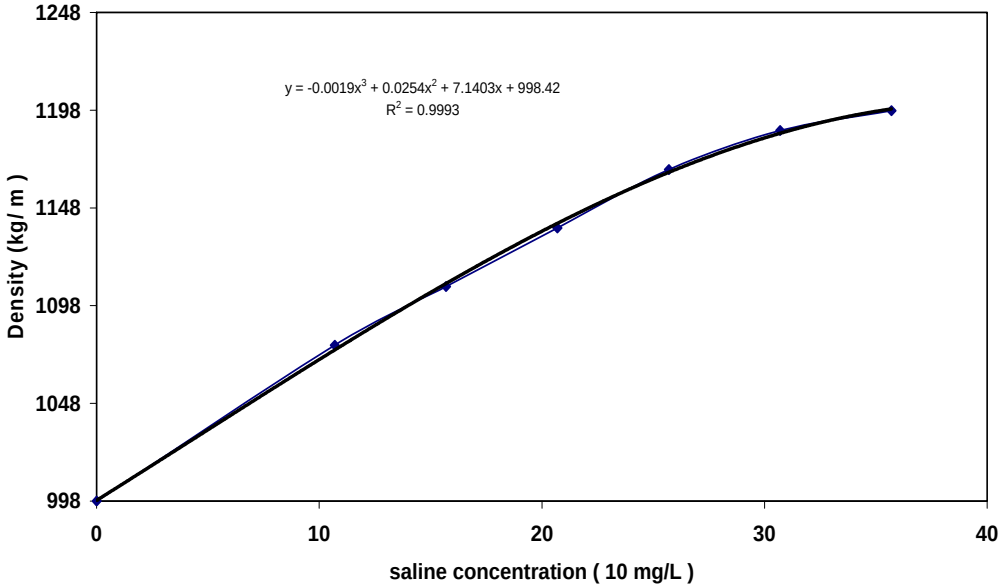

Fig. 6.9: True curve showing variation of density at varying saline concentration of NaCl.

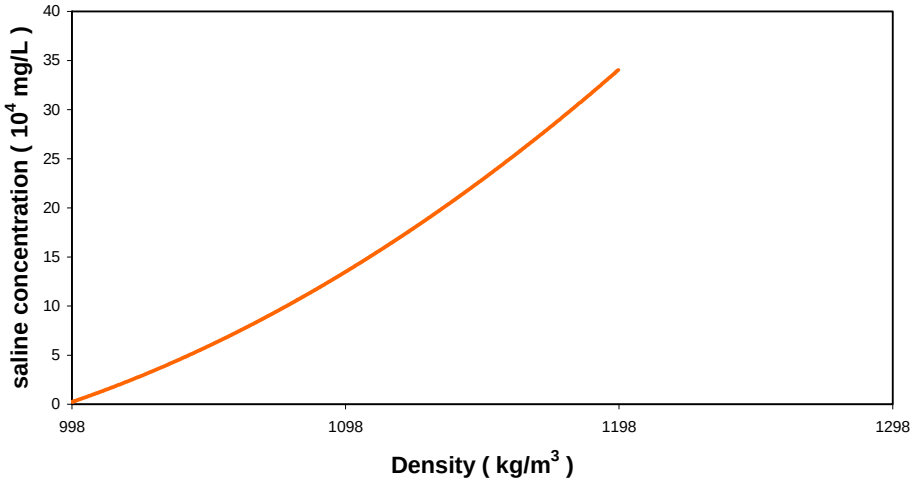

Fig. 6.10: Variation of saline concentration at different density of NaCl solution.

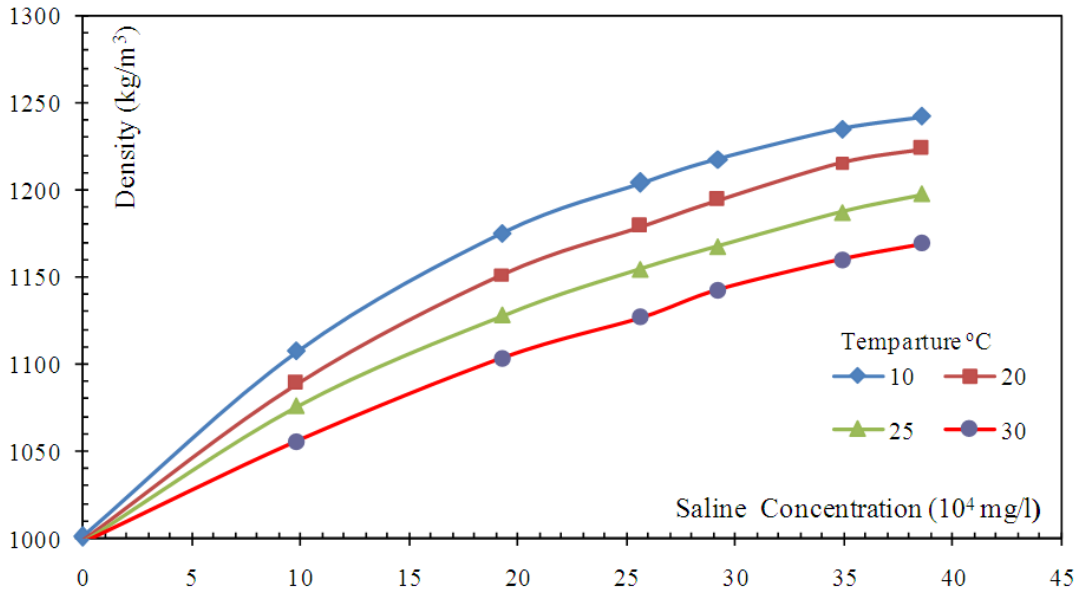

Fig. 6.11: True curves showing the variation of density at different saline concentration of sodium chloride solution.

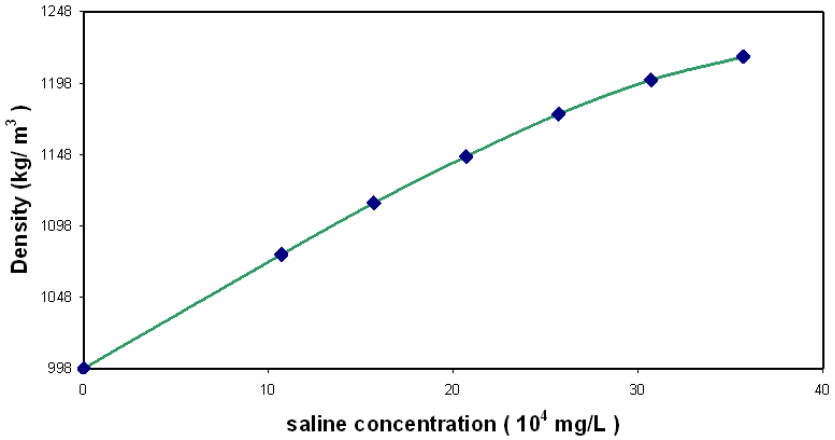

Fig. 6.12: True curve showing the variation of density at different saline concentration of sodium chloride solution.

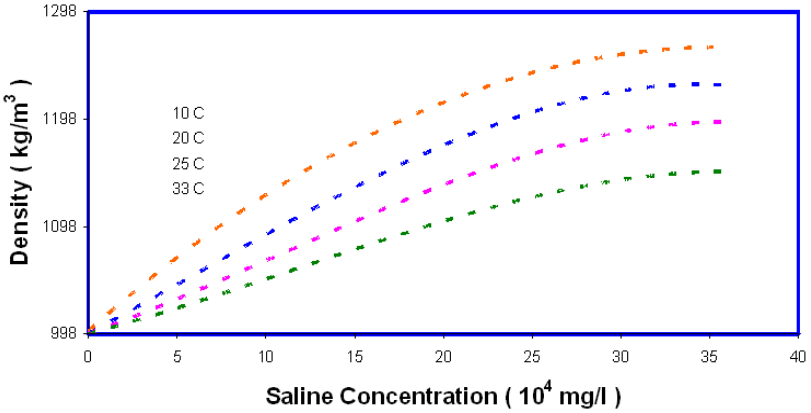

Fig. 6.13: Best fit curves showing the variation of density at different saline concentration of sodium chloride solution at varying temperatures.

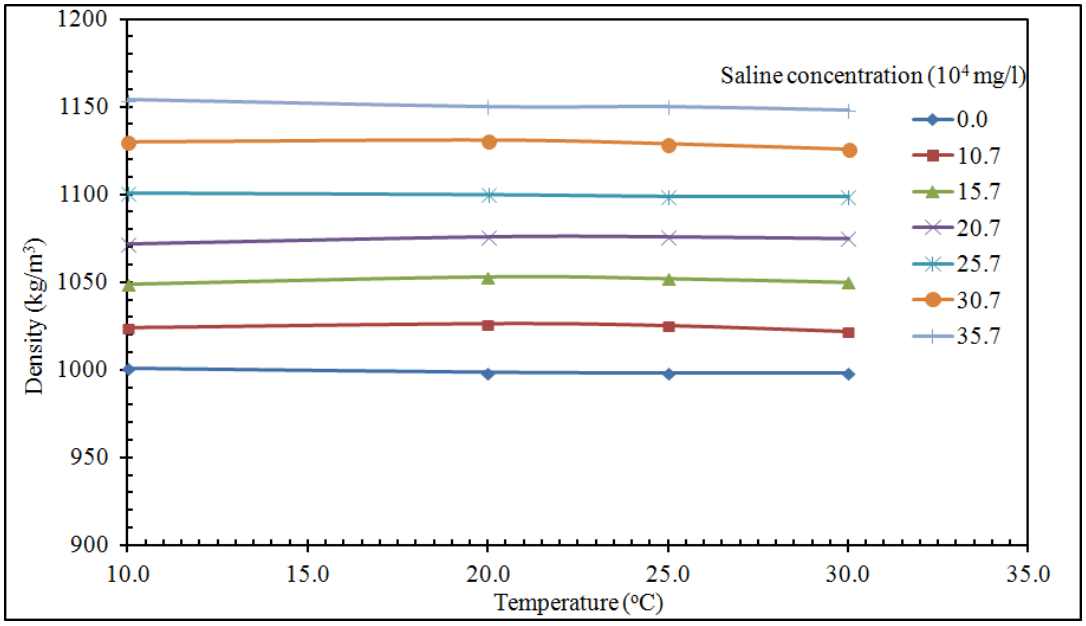

Fig. 6.14: True curves showing the variation of density at different temperature of sodium chloride solution for different saline concentration.

6.5 Determination of Darcy's Coefficient

The experiment to determine hydraulic conductivity has been conducted. The description of apparatus and procedure has been described below.

6.5.1 Description of Apparatus

The saturated hydraulic conductivity of a sand sample can be best measured by a falling head permeameter. A sketch of this apparatus is shown in Figure 6.15 the sand sample is contained within a Perspex tube of cross-sectional area A_1 with inlet and out let and filters at the top and bottom. The inlet to this tube (cross-sectional area A_1) is connected by a small bore tube of cross-sectional area A_2 through which water flows. Water flowing through the sand sample is collected at a bottom tank. The out level must be in level with the bottom of sample.

6.6 Procedure to Determine Darcy's Coefficient

At the start of the test (time $t = 0$), the water level in the upper (small bore) tube is at a height h_1 above the permeameter outlet. The water level in the upper tube falls as water flows through the sand sample. At the end of the test ($t = T$) the water level in the upper tube has fallen to a height h_2 above the permeameter.

At a general time t ($0< t < T$) the water level is at a general height h ($h_2< h< h_1$). Applying Darcy's law at a general time t, to the sand sample.

$$V = k_0 i \qquad \text{or} \qquad \frac{q}{A_1} = k_0 i$$

$$\text{or} \quad q = A_1 k_0 i = A_1 k_0 \frac{h}{L} \tag{6.1}$$

In the small bore tube $q = A_2 V$

But the velocity $v = -\frac{dh}{dt}$ So $q = -A_2 \frac{dh}{dt}$ (6.2)

From Equations (6.1-6.2)

$$\frac{dh}{dt} = -\left(\frac{A_1}{A_2}\right)\left(\frac{k_0}{L}\right)h$$

Integrating between limits at t=0, h=h_1 and t=T, h=h_2

$$\int_{h_1}^{h_2} \frac{dh}{h} = -\left(\frac{A_1 k_0}{A_2 L}\right)dt$$

$$k_0 = \frac{A_2 L}{A_1 T} \ln\left(\frac{h_1}{h_2}\right) \tag{6.3}$$

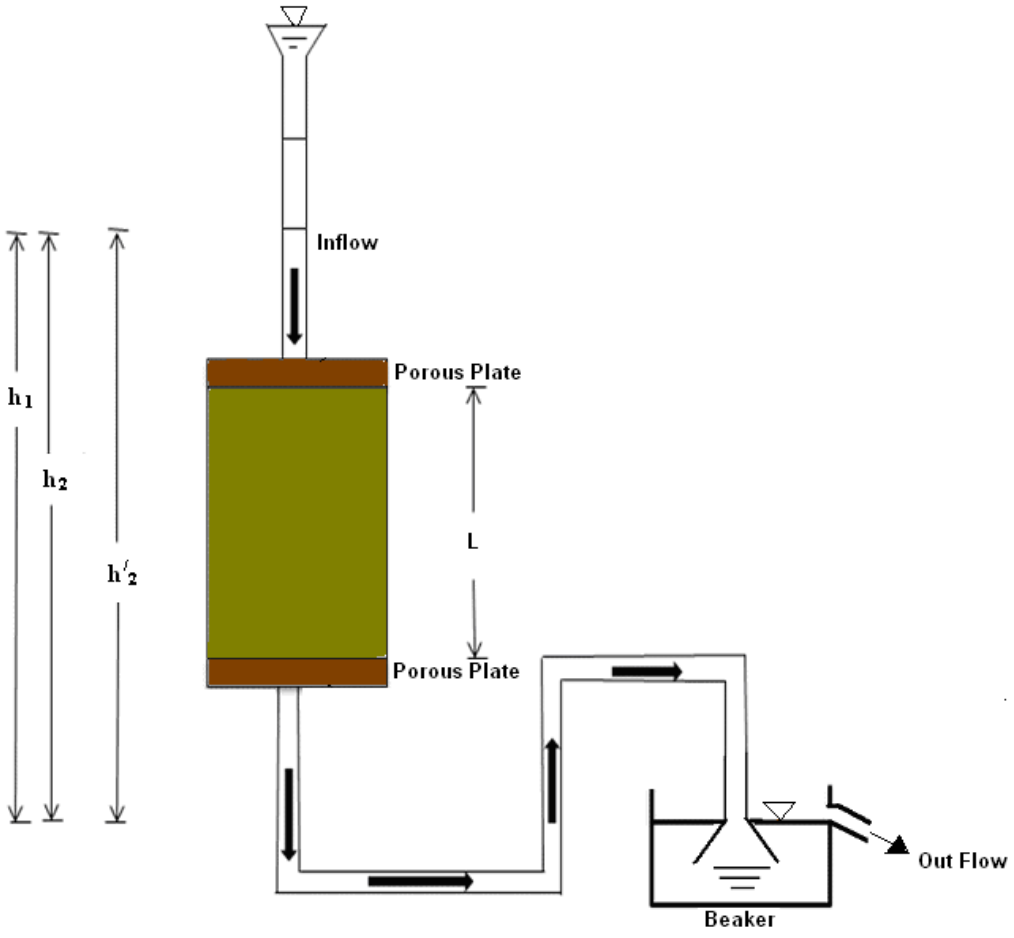

Fig. 6.15: Falling head permeameter.

6.6.1 Test Material

The sample is sieved through a set of sieves of gradually diminishing opening sizes. The percent finer corresponding to each sieve is determined and the results have been displayed in Table 6.3.

Table 6.3: Test results of sieve analysis.

I.S. sieve (mm)	Diameter of grain (mm)	Weight retained (gm)	Percentage retained	Cumulative percentage retained	Percentage finer
2.360	2.360	3.0	0.6	0.6	99.4
1.180	1.180	15.5	3.1	3.7	96.3
0.600	0.600	59.5	11.9	15.6	84.4
0.425	0.425	225.0	45.0	60.6	39.4
0.300	0.300	134.0	26.8	87.4	22.6
0.150	0.150	53.0	10.6	98.0	2.0
0.075	0.075	8.0	1.6	99.6	0.4

6.6.2 Determination of Hydraulic Conductivity of Porous Media

The experiments to determine hydraulic conductivity have been done by preparing samples of well graded sand submerged in different percentage of saline concentration that is 0%, 25%, 50% and 100% for different period of time that is 0, 1, 3, 4, 7 and 14 days by a falling head permeameter.

6.6.3 Procedure to Determine Hydraulic Conductivity

As the head of water during the test in the falling head permeameter is not constant, Darcy's law cannot be used directly in computing the hydraulic conductivity from the data obtained. The relationship expressing the hydraulic conductivity in terms of data from falling head test can be determined as below.

A= Area of the mould (specimen)
a = Area of standpipe
h = Head at given time t
h_1= Head at beginning of test
h_2= Head at end of test
L= Length of specimen
T= Elapsed time during which head falls from h_1 to h_2

In the falling head test, the water is allowed to flow through the specimen until as much air as possible has been removed from the soil. When ready to start the test the water is allowed to fall in the standpipe to some head h_1 at which time a stop watch is started.

When the head fallen to some head h_2, the watch is stopped to determine the time t. As the head decreases, the velocity of the water through the specimen decreases. At some head h between h_1 and h_2 the velocity $v=k_0h/L$. During an interval of time dt the head will fall a distance dh and the quantity of water dq flowing through the specimen can be expressed by Darcy's law.

$$k_0 = \frac{aL}{AT}\ln\left(\frac{h_1}{h_2}\right) \tag{6.4}$$

Following the above equation is used for the determination of hydraulic conductivity of sand sample submerged in deferent salinity the graphs have been plotted. The results of falling head permeameter test are tabulated in Table 6.4.

Table 6.4: Results of falling head permeameter test.

Hydraulic conductivity (cm/s)	Salinity concentration (%)	Period of submergence (days)	Hydraulic conductivity (cm/s)	Salinity concentration (%)	Period of submergence (days)
0.013500	0	0	0.009660	0	4
0.005936	25	0	0.003260	25	4
0.002460	50	0	0.000780	50	4
0.001450	100	0	0.000697	100	4
0.009780	0	1	0.009600	0	7
0.003700	25	1	0.002870	25	7
0.002400	50	1	0.000710	50	7
0.000767	100	1	0.000580	100	7
0.009680	0	3	0.009600	0	14
0.003400	25	3	0.002610	25	14
0.000800	50	3	0.000685	50	14
0.000760	100	3	0.000474	100	14

6.7 Analysis of Results

Pure sodium chloride and distilled water have been collected. The maximum solubility of sodium chloride has been determined which come as 35.7×10^4 mg/l and other five unsaturated sodium chloride solutions such as 30.7×10^4 mg/l , 25.7×10^4 mg/l , 20.7×10^4 mg/l , 15.7×10^4 mg/l ,and 10.7×10^4 mg/l , have been prepared and kept in separate bottles for experimentations. The graphs as plotted in Figures 6.16-6.17, shows the variation of hydraulic 50% saturation, afterwards it approaches stabilization. Variation of hydraulic conductivity with time indicates that hydraulic conductivity decreases as the period of submergence in different concentration of sodium chloride solution increases, but rate of decrease of hydraulic conductivity is quite slow for the samples, which have been submerged in sodium chloride solutions for more three days. Conductivity with the percentage of saturated salinity concentration indicates that hydraulic conductivity

decreases sharply with the increase in percentage of saturated salinity concentration upto and kept in separate bottles for experimentations.

From the observation made on the laboratory experimentation with falling head permeameter in case of the flow of sodium chloride solution through sand, it may be concluded that the hydraulic conductivity decreases with saline concentration as well as period of submergence. The rate of decrease is sharp when the saline concentration lie in the range of 0-40% and gradually stabilizes thereafter. On the other hand this rate of reduction is high enough when the periods of submergence lie in the range of 0-4 days with a gradual stabilization thereafter.

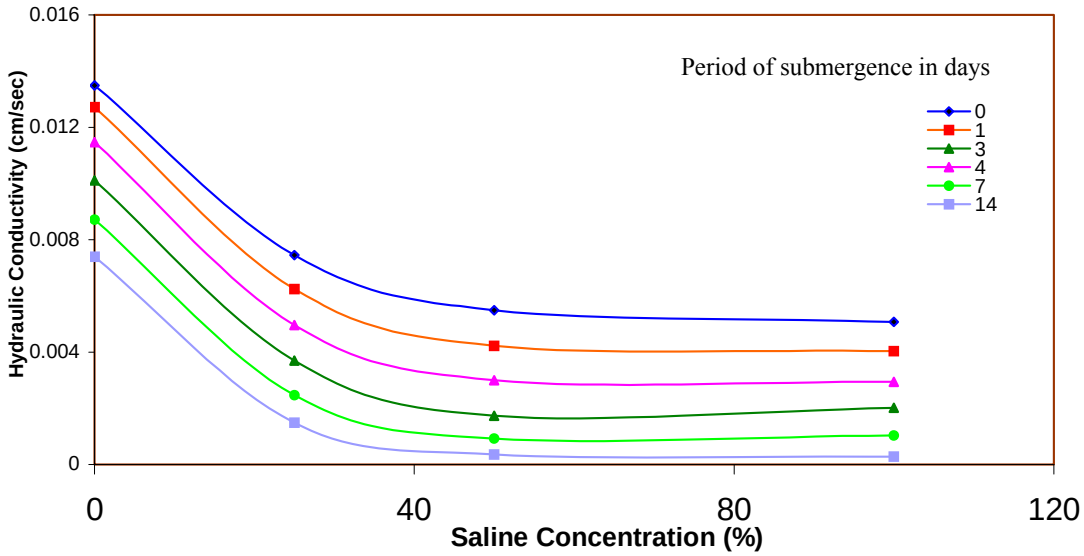

Fig. 6.16: Variation of hydraulic conductivity at different saline concentration for different period of submergence.

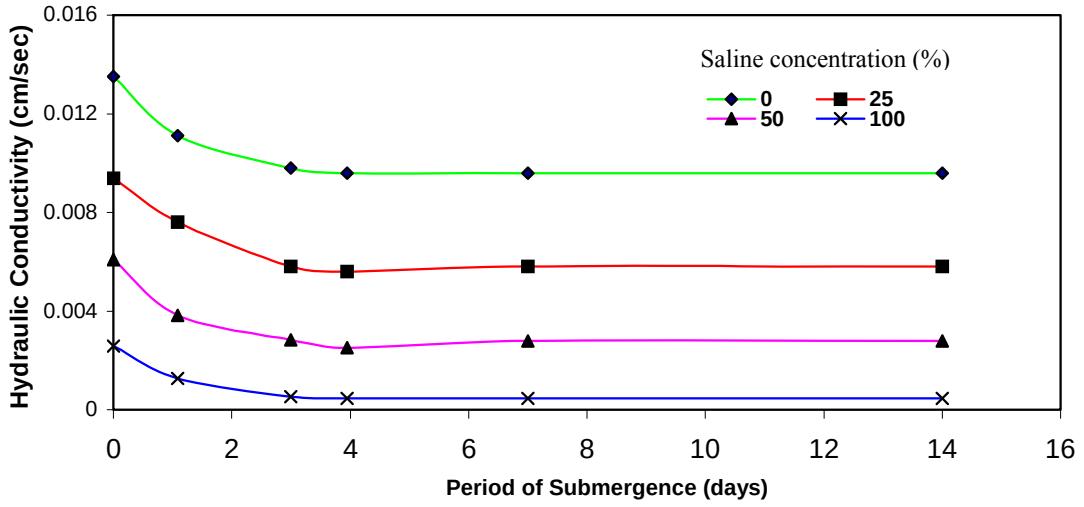

Fig. 6.17: Variation of hydraulic conductivity at different period of submergence for different saline concentration.

6.8 Determination of Forchheimer Coefficients

In case of Forchheimer flow, the mean flow velocity V may be expressed as shown in Equation (6.5) by binomially expanding the quantity within the root and neglecting the cubic and higher order term. Thus,

$$V = \frac{\gamma i}{a} - \frac{b\gamma^2 i^2}{a^3} \tag{6.5}$$

But, when i=0, V=0; hence negative sign is taken into consideration. Thus,

$$V = K_1 i + K_2 i^2 \tag{6.6}$$

where, K_1 and K_2 are the coefficients, are to be find out. Now for the calculation considering two Equations (6.7-6.8),

$$V_1 = K_1 i_1 + K_2 i_1^{\,2} \tag{6.7}$$

$$V_2 = K_1 i_2 + K_2 i_2^{\,2} \tag{6.8}$$

where, V_1 and V_2 are the velocities for the two set of experiments, i_1 and i_2 are the hydraulic gradient for corresponding set of experiments. Now solving these two equations - the values of K_1 and K_2 are obtained and from this values the Forchheimer's coefficients are determined which are comparable to theoretical values.

6.9 Experimental Setup

In order to carry out model tests so as to study the pattern of seepage in regards to saline water intrusion and freshwater recharge into natural porous medium, an experimental setup has been developed. A sketch of this apparatus is shown in Figure 6.18. A photographic view of this test setup is presented in Figure 6.19. The entire setup has been fabricated with 5 mm thick transparent Perspex sheet. It mainly consists of inlet tank, a rectangular open channel, a gate and outlet tank. In the middle of the open channel, a sliding gate is provided which is capable to a unidirectional up-down movement which is governed by a rope and pulley arrangement. The function of this gate is to provide variable opening of the flow passage. The hydraulic connection between the two tanks with the channel is done by cast iron pipes with inlet and outlet valves. One of the side walls of the central channel is graduated with square grid so as to trace the phreatic line of salt water and also the interface between saline water and freshwater. The side walls of the two tanks are also graduated so as to measure the inlet and outlet heads. The entire setup is fixed on a wooden table.

6.9.1Test Procedure

Initially, the central channel is filled with the porous medium upto the desired level. The gate level is adjusted as per requirement. The gate is to be inserted within the porous medium with extreme such that the porosity of the medium gets disturbed to a minimum.

In one of the two tanks, salt water having a specified saline concentration is poured upto the desired head. For visualization purpose, this salt water should be preferably coloured by an inert material. The valve between this tank and the channel is opened and a stopwatch is started. It should be ensured that the valve between the other tank and the channel is fully closed. After regular interval, the pattern of intrusion is noted from the coordinate's phreatic line corresponding to the seepage of saline water. After hydraulic stabilization is achieved, the heads at the upstream and the downstream ends as well as the coordinates of the stabilized phreatic line are noted. The other tank is then filled up with freshwater upto desired head and the valve is opened. The continuous flow of water in this inlet tank should be ensured. At regular intervals, the shifting of the locations of the surface of salt water is also noted.

6.9.2 Experiments on Stratified Fluid

These experiments have been done in the Hydraulics Laboratory by using the above mentioned experimental setup. The experiments have been conducted by two separate methods (a) saline water intrusion and (b) freshwater recharge.

During experimentations, distilled water has been used as the freshwater. Since all the hydraulic characteristics of the same are standardised, these are not determined separately.

6.9.2.1 Saline Water Intrusion

First of all, the sand is poured into the open channel by uniform falling method. Pure sodium chloride is dissolved into distilled water at a specified concentration so as to obtain the saline water. Then from the downstream tank, coloured saline water is fed into the open channel.

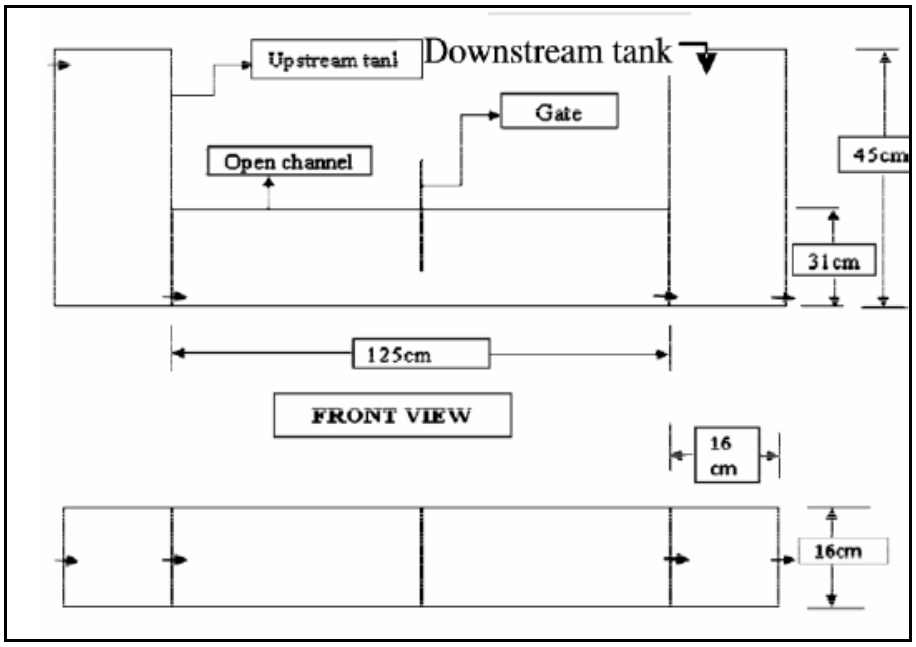

Fig. 6.18: Schematic diagram of the experimental setup.

A small quantity of potassium permanganate ($KMnO_4$) is used as the colouring dye such that its presence does not significantly affect the density and other hydraulic property of the solution. After completion of intrusion of saline water into the model, the readings for denoting the position of the streamline are taken. Some pictures are shown in Figure 6.19 and the normalised values of the ordinates are tabulated in Table 6.5. The results and discussion are given thereafter.

Fig. 6.19: Saline water intrusion into the open channel.

Table 6.5: Normalised values of X and Y coordinates for saline water intrusion at varying time.

Point No.	Normalized values of X-coordinates	Normalized values of Y-coordinates at varying time (T in hours)						
		$T = 2$	$T = 6$	$T = 14$	$T = 16$	$T = 19$	$T = 22$	$T = 34$
1	0.0083	0.500	0.613	0.750	0.750	0.750	0.772	0.863
2	0.0416	0.450	0.590	0.727	0.770	0.770	0.818	0.909
3	0.08	0.409	0.545	0.659	0.770	0.770	0.840	0.932
4	0.125	0.386	0.486	0.613	0.704	0.727	0.795	0.795
5	0.166	0.340	0.441	0.568	0.659	0.650	0.727	0.750
6	0.208	0.260	0.363	0.523	0.609	0.636	0.682	0.704
7	0.25	0.136	0.318	0.386	0.545	0.591	0.613	0.613
8	0.291	0.136	0.272	0.341	0.386	0.545	0.568	0.568
9	0.333	0.113	0.163	0.25	0.295	0.309	0.477	0.523
10	0.375	0	0.127	0.204	0.25	0.272	0.341	0.341
11	0.416	0	0.136	0.136	0.204	0.227	0.272	0.316
12	0.458	0	0.113	0.113	0.182	0.204	0.272	0.318
13	0.5	0	0.9	0.113	0.182	0.204	0.272	0.295
14	0.542	0	0	0	0.182	0.204	0.275	0.275
15	0.583	0	0	0	0.204	0.204	0.227	0.295
16	0.625	0	0	0	0.182	0.182	0.222	0.272
17	0.666	0	0	0	0.172	0.172	0.204	0.250
18	0.708	0	0	0	0.113	0.113	0.182	0.204
19	0.75	0	0	0	0	0.113	0.136	0.182
20	0.791	0	0	0	0	0	0.113	0.136
21	0.875	0	0	0	0	0	0	0.118
22	0.916	0	0	0	0	0	0	0.113

6.9.2.2 Freshwater Recharge

After complition of saline water intrusion the freshwater recharge has been started. From the upstream tank the freshwater have been recharged by operating the valves of pipe lines. During experimentations, distilled water has been used as the freshwater. Since all the hydraulic characteristics of the same are standardized, these are not determined separately. In similar way, the streamline coordinates are taken and the normalised values are tabulated in Table 6.6. the reading has been taken from upstream side. Some picture are shown in Figure 6.20 for showing the freshwater recharge stream lines. The results and discussion are given in the next section.

Fig. 6.20: Freshwater recharge in to the open channel.

For model test, two different sets of experiments, one for saline water intrusion and another for freshwater recharge have been conducted. The heads were applied 20 cm and 30 cm, respectively. The test results are presented in Table 6.5, Figures 6.22 and Table 6.6, Figure 6.23, respectively.

6.10 Experimentation for Forchheimer's Velocity

For constant hydraulic gradient (i) and for various saline concentration, fluids are taken to conduct this experiments. By volumetric method, following velocities are taken, $V_1 = 0.257\times10^{-3}$ m/s, $V_2 = 0.14\times10^{-3}$ m/s and $V_3 = 0.116\times10^{-3}$ m/s, where V_1, V_2 and V_3 are velocities for diefferent saline cocentrations i.e., for diefferent kinematic viscosities (ν). The results are tabulated in Table 6.7. Taking theoretical cosiderations, another table has been shown (Table 6.8) in comparison to theoretical and experimental velocity.

Table 6.6: Normalised values of *X* and *Y* coordinates for freshwater recharge at varying time.

Point No.	Normalized values of *X*-coordinates	Normalized values of *Y*-coordinates at varying time (*T* in hours)						
		T=2	*T*=6	*T*=14	*T*=16	*T*=19	*T*=22	*T*=34
1	0.0083	0	0	0	0	0	0	0
2	0.0416	0	0	0	0	0	0	0
3	0.080	0.090	0	0	0	0	0	0
4	0.125	0.136	0.090	0	0	0	0	0
5	0.166	0.191	0.113	0.090	0	0	0	0
6	0.208	0.222	0.136	0.113	0.09	0	0	0
7	0.250	0.258	0.204	0.136	0.113	0.09	0	0
8	0.291	0.277	0.227	0.204	0.136	0.09	0	0
9	0.333	0.295	0.277	0.227	0.227	0.136	0.09	0
10	0.375	0.295	0.277	0.277	0.285	0.227	0.113	0
11	0.416	0.295	0.285	0.285	0.295	0.354	0.285	0.090
12	0.458	0.328	0.295	0.295	0.354	0.398	0.295	0.136
13	0.500	0.328	0.328	0.328	0.398	0.558	0.398	0.285
14	0.542	0.341	0.354	0.354	0.558	0.586	0.558	0.586
15	0.583	0.386	0.398	0.398	0.586	0.698	0.586	0.698
16	0.625	0.568	0.586	0.586	0.698	0.772	0.698	0.772
17	0.666	0.615	0.698	0.698	0.772	0.818	0.840	0.840
18	0.708	0.704	0.772	0.772	0.818	0.840	0.840	0.909
19	0.750	0.727	0.818	0.818	0.840	0.909	0.909	0.932
20	0.791	0.750	0.840	0.840	0.909	0.909	0.932	1
21	0.875	0.772	0.909	0.909	0.909	0.932	1	1
22	0.916	0.909	0.909	0.909	0.932	1	1	1
23	0.958	0.909	0.932	0.932	1	1	1	1
24	1	0.909	1	1	1	1	1	1

Table 6.7: Experimental velocities.

Salinity concentration ($\times 10^4$) (mg/l)	Kinematic viscosity ($\nu \times 10^{-7}$) (m^2/s)	Velocity ($V \times 10^{-3}$) (m/s)
0	10	0.257
31.3	15	0.140
35.7	18.4	0.116

Table 6.8: Results from experimental and theoretical studies.

Modified friction factor (C_f')	Velocity	
	Experimental ($V_{exp}\times10^{-3}$) (m/s)	Theoretical ($V_{th}\times10^{-3}$) (m/s)
4.809	0.257	0.2560
11.488	0.140	0.1458
16.520	0.116	0.1200

6.11 Soil Properties

6.11.1 Visual Characteristics

Shaking test is called dilatancy test. It helps to distinguish silt from clay since silt is more permeable than clay. Dispersion test is useful for making a rough estimate sand, silt and clay present in a material. Conducting above mentioned test, the used sand is found well graded, light yellow coloured.

6.11.2 Grain Size Distribution

The grain size distribution curve is illustrated in Figure 6.21. From the sieve analysis, the mean grain size d_{50} is determined to be 0.6 mm.

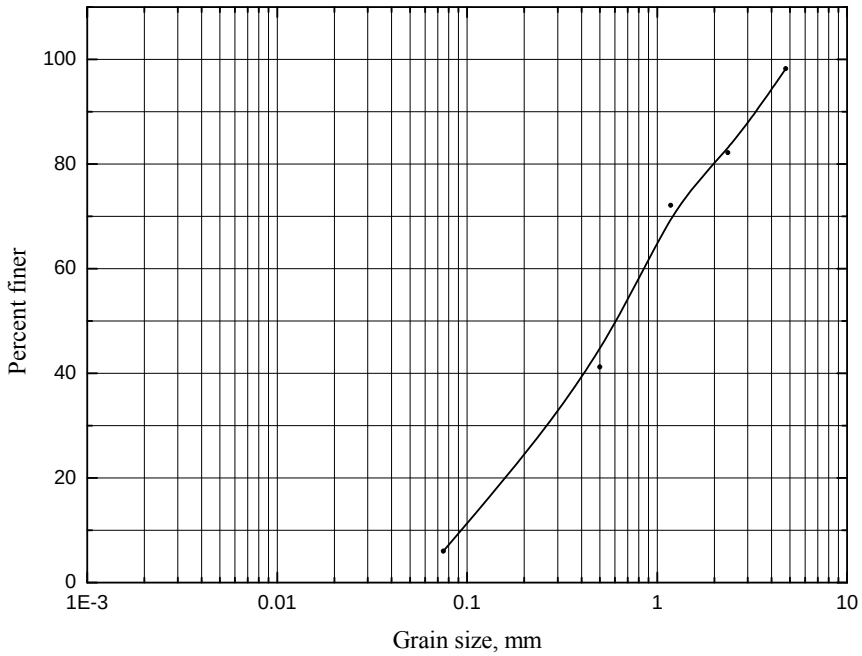

Fig. 6.21: Grain size distribution curve by sieve analysis.

6.11.3 Other Properties

The following values of sand properties are found from data obtained from the laboratory experiments.

- The specific gravity of the used sand is (G_s) = 2.655 at temperature 27 ^{0}C.
- The unit weight of the used sand is (γ_s) = 14.7 kN/m^3.
- The relative density (D_r) i.e., Looseness and Denseness of the used sand are 29.59% and 70.4%, respectively.

6.12 Hydraulic Conductivity and Forchheimer's Coefficients

Using falling head permeameter and applying Equation (6.4), the hydraulic conductivity is found out to be 0.5936×10^{-4} cm/sec. Before finding out the Forchheimer's coefficients, the Reynolds number has to be checked. Operating the gate of the channel another reading has been taken and from this value again checked the Reynolds number which is in the range of Forchheimer's flow. Then applying the Equations (6.7) and (6.8) the values of K_1 and K_2 has been found out and such values are displayed in Table 6.9.

Table 6.9: Values of Forchheimer's coefficients.

Hydraulic gradient (i)	Velocity ($V\times10^{-3}$) (m/s)	Forchheimer's coefficients (K_i)
0.22	0.257	$K_1 = 0.1168\times10^{-2}$
0.24	0.2796	$K_2 = 0.6327\times10^{-2}$

6.13 Rheological Characteristics of Saline Water

6.13.1 Relation between Reynolds Number and Friction factor

The graphical representations have been shown in the Figure 6.24. From the theoretical consideration, which is described in Chapter 4 (Expansion of Forchheimer's law in terms of modified Reynolds number and modified friction factor) and the experimental results the modified Reynolds number and modified friction factor have been found out. The results are plotted in Figure 6.25.

6.13.2 Velocity at different Kinematic Viscosity

The kinematic viscosity has been found out according to different saline concentration and for that velocities are also found out which are tabulated in Table 6.7. Graphical representation has been shown in Figure 6.26. The time variation of normalized y-coordinates of the interface at different locations is shown in Figure 6.27.

6.13.3 Forchheimer's Velocity with respect to Modified Friction Factor

From the theoretical consideration, which is described in Chapter 4 and conducting required experiments, the following results have been found. The results of experimental and theoretical values are tabulated in Table 6.8. One comparison plot has been shown in Figure 6.28.

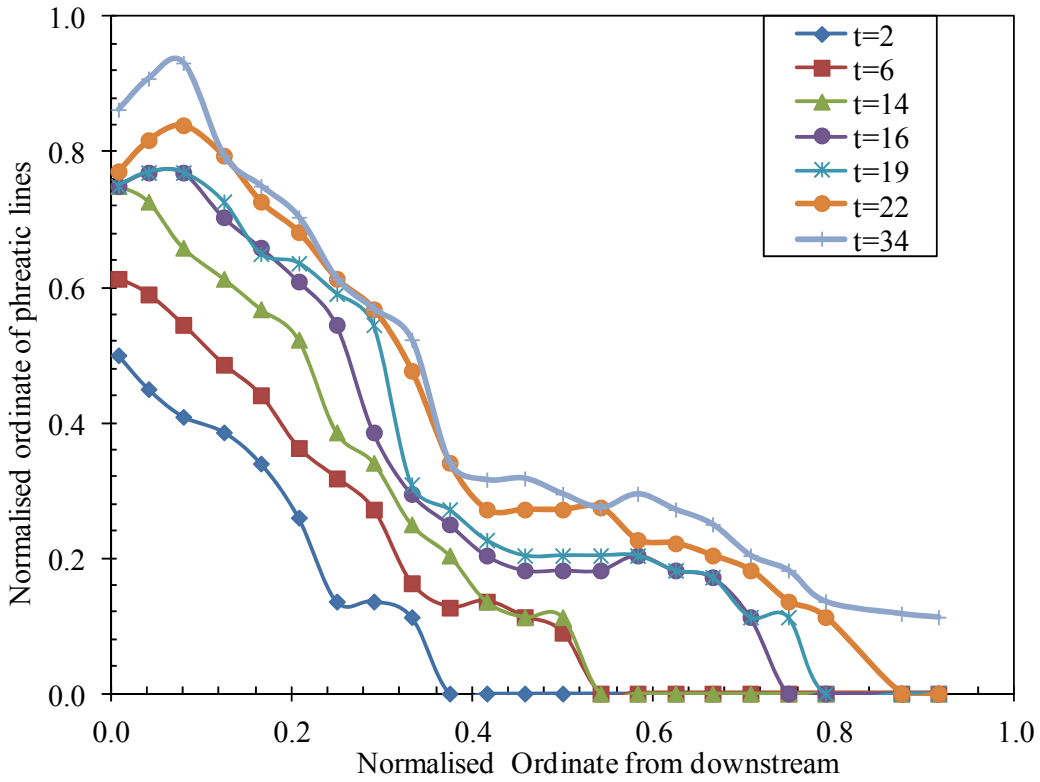

Fig. 6.22: Graphical representation of the experimental results for saline water intrusion. (Here, *t* = time interval of saline water intrusion from tank to the channel)

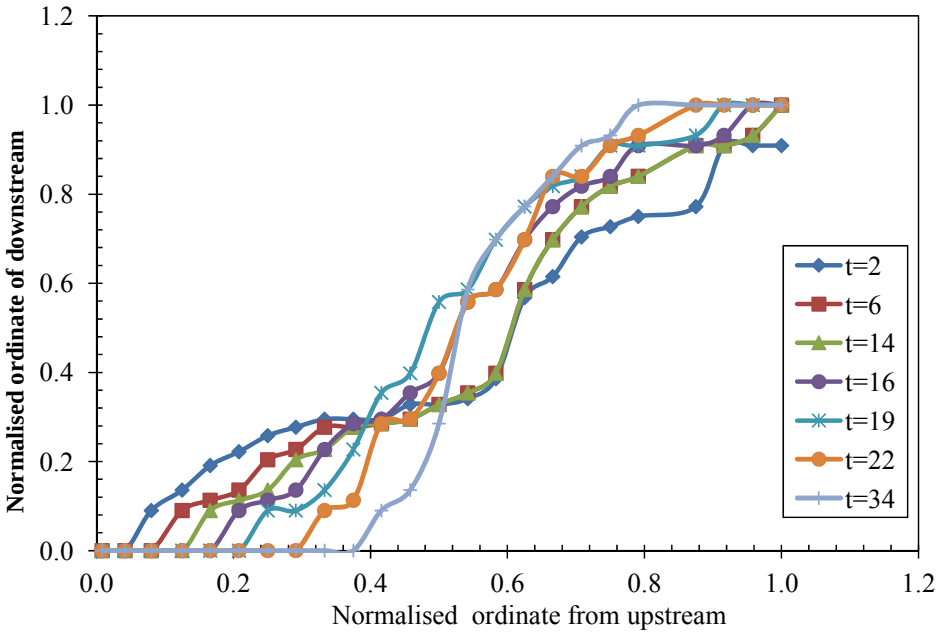

Fig. 6.23: Graphical representation of the experimental results for freshwater recharge.

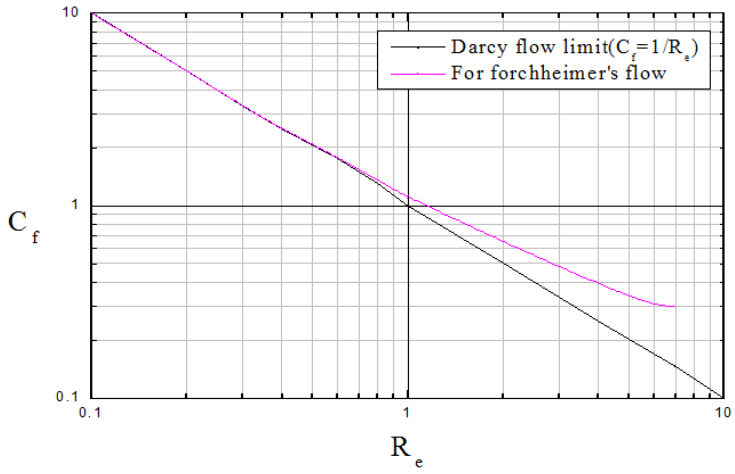

Fig. 6.24: Friction factor, Reynolds number relation.

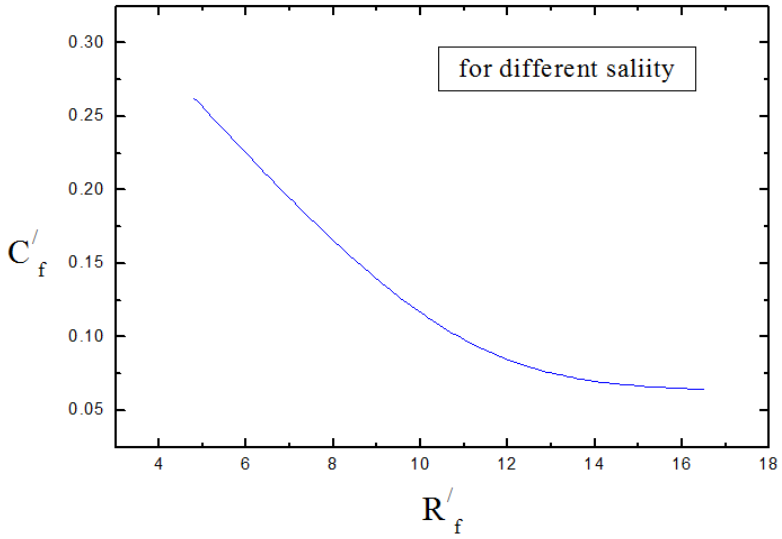

Fig. 6.25: Variation of modified Reynolds number versus modified friction factor.

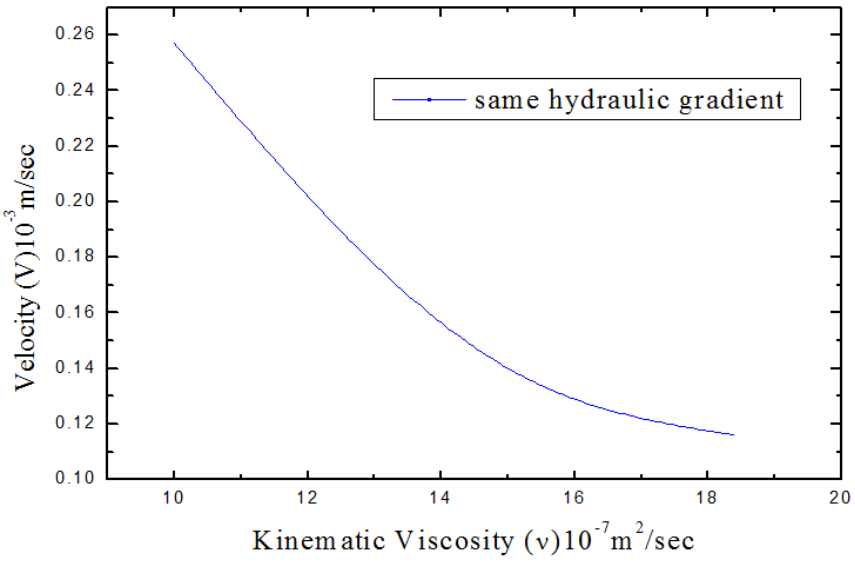

Fig. 6.26: Kinematic viscosity versus experimental velocity.

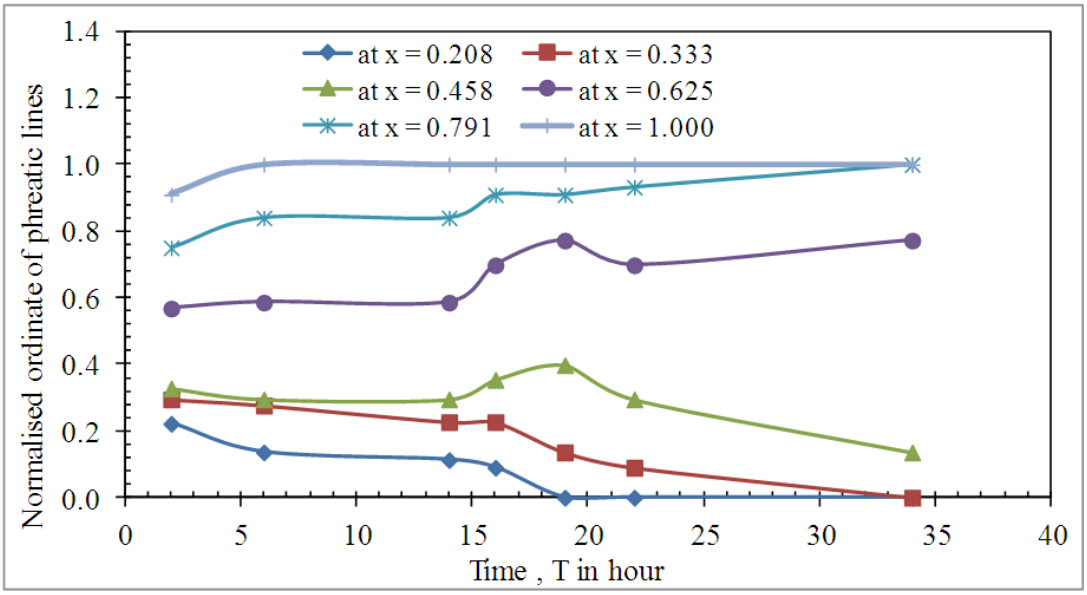

Fig. 6.27: Graphical representation of the stratified fluid (in constant ordinate values from upstream) in various times versus normalised value of abscissa.

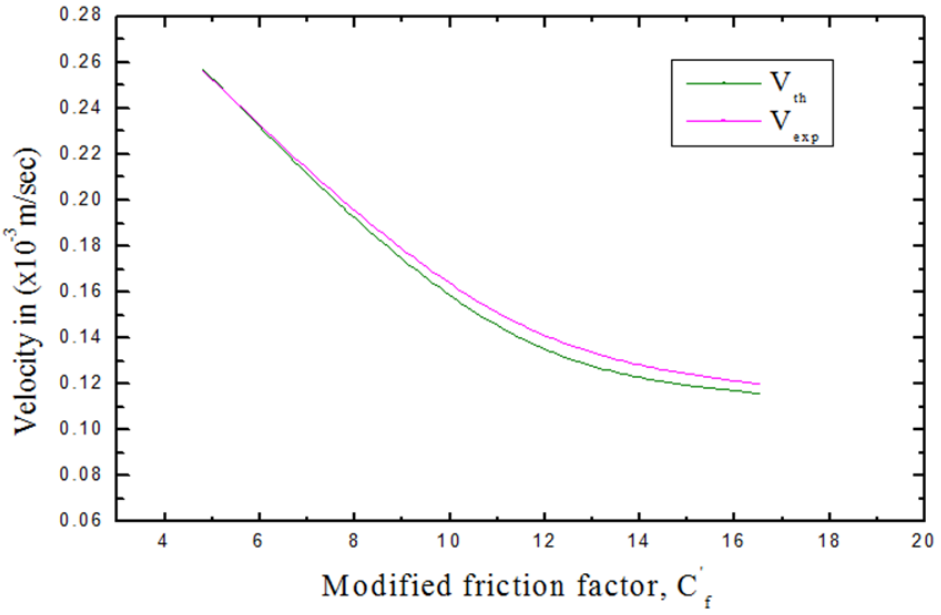

Fig. 6.28: Forchheimer's velocity obtained from theoretical and experimental study with respect to modified friction factor.

6.14 Results and Discussion

From the entire investigation the following results are obtained:

- The experiments regarding variation of kinematic viscosity of sodium chloride solution for different saline concentration at different temperature and variation of density for the same saline concentration have been conducted and relevant curves

have been plotted. It is observed from the graph that the viscosity decreases with the temperature and increases with saline concentration. Similarly the density increases with the increase in saline concentration.

- From the observations made on the results of the laboratory experiments with falling head permeameter in case of flow of sodium chloride solution through sand, it may be concluded that the hydraulic conductivity decreases with saline concentration as well as with period of submergence. The rate of decrease of hydraulic conductivity is sharp when the saline concentration lies in the range of 0-40% and gradually stabilises thereafter. Also, this rate of reduction is high enough when the period of submergence lies in the range of 0-4 days with a gradual stabilisation thereafter.
- For model test, two different sets of experiments, one for saline water intrusion and another for freshwater recharge have been conducted. The heads were applied 20 cm and 30 cm, respectively. The test results are presented in Table 6.5, Figures 6.22 and Table 6.6, Figure 6.23, respectively. The X -coordinates are normalized by the distance between inlet and outlet points of the channel. The Y -coordinates, on the other hand, are normalized by the head applied in saline water intrusion. The phreatic lines of the saline water intrusion and the interfaces in freshwater recharge are observed to be in irregular pattern as depicted in Figures 6.22 to 6.23. In case of saline water intrusion, the phreatic line at any time instance slopes down from the inlet end with a sudden change in slope at a normalized distance of 0.3 m to 0.5 m. With the advent of time, the phreatic line translates gradually towards the other end of the channel. For freshwater recharge, the interface gradually slopes towards the downstream end in advent of time. The time variation of normalized *y*-coordinates of the interface at different locations is shown in Figure 6.27. Although of irregular pattern, the slopes are observed to be sufficiently small. More importantly, significant diffusion between fluids of two different densities is observed to take place indicating absence of any sharp interface at mixing zone.
- From model tests; the friction factor and Reynolds number for Darcy's and Forchheimer's flow have been studied. The Reynolds number increases as the friction factor decreases. And also from the plotted curves for modified Reynolds number versus modified friction factor, it can be said that, modified friction factor C_f' and modified Reynolds number R_e' are changing inversely proportional way.

6.15 References

Andrade, J.S., Costa, U.M.S., Almeida, H.A. and Stanley, H.E. (1999). Inertia Effects on Fluid through Disordered Porous Media. *Physical Review Letters,* Vol. 82, Iss. 26, pp. 5249-5252.

Chan, T.P. and Govindraju, R.S. (2003). A New Model for Soil Hydraulic Properties Based on A Stochastic Conceptualization of Porous Media. *Water Resources Research*, Vol.39, Iss.7, pp.1195-1208.

Fand, R.M., Kim, B.Y.K., Lam, A.C.C. and Phan, R.T. (1987). Resistance to the Flow of Fluids through Simple and Complex Porous Media Whose Matrices are Composed of Randomly Packed Spheres. *Journal of Fluids Engineering*, Vol. 109, No. 3, pp. 268-274.

Forchheimer, P.H. (1901). Wasserbeweguing durch Boden, *Zeitschrift fur Acker und Pflanzenbau*, Vol.45, pp. 1782-1788.

Inoue, M. and Nakayama, Y. (1998). Numerical Modeling of Non-Newtonian Fluid Flow in a Porous Medium using a three Dimensional Periodic Array. *Journal of Fluids Engineering*, Vol. 120, Iss. 1, pp. 131-135.

Kececioglu, I. and Jiang, Y. (1994). Flow through Porous Media of Packed Spheres Saturated With Water. *Journal of Fluids Engineering,* Vol. 116, Iss. 1, pp. 164-170.

Li, W.H. and Yeh, G.T. (1968). Dispersion at the Interface of Miscible Liquids in a Soil. *Water Resources Research,* Vol. 4, Iss. 2, pp. 369-377.

Millham, N.P. and Howes, B.L. (1995). A Comparison of Methods to Determine K in a Shallow Coastal Aquifier. *Groundwater*, Vol. 33, Iss. 1, pp. 49-56.

Mughal, I. and Awan, N.M. (1977). Upconing of Salt Fresh water Interface Beneath Wells in Fresh Water Zones. *CEWRE Publication 005.*

Rudraiah, N. (2001). Non-Linear Study of Stratified Fluid through Porous Media. *Journal of Porous Media,* Vol. 4, Iss. 2, pp. 127-136.

Xue, Y., Xie, C. and Wu, J. (1995). A Three Dimensional Miscible Transport Model for Seawater Intrusion in China. *Water Resources Research,* Vol. 31, Iss. 4, pp. 903-912.

CHAPTER - 7

(Field Investigation-I: Hydrogeology and Subsurface Stratification)

- Groundwater Movements and Aquifer System
- Aquifers` Materials
- Groundwater Recharge
- Groundwater and Wells
- Groundwater Flow Patterns in Multilayer Coastal Aquifer
- Soil Properties
- Sub-Surface Geology
- Hydrogeology of Purba Midnapur
- Saline Water Intrusion towards Piezometric Surface
- References

7.1 Groundwater Movements and Aquifer System

Groundwater is fresh water (from rain or softening ice and snow) that splashes into the dirt and is put away in the small spaces (pores) amongst rocks and particles of soil. Groundwater represents almost 95 percent of the country's fresh water assets. It can remain underground for a huge number of years, or it can rise to the top and help fill waterways, streams, lakes and wetlands. Groundwater can likewise rise to the top as a spring or is pumped from a well. Both of these cases are basic ways to get groundwater for drinking. Groundwater is the source of water supply for around 50 percent of our cities, localities, and framings. Groundwater is put away in the modest open spaces amongst shake and sand, soil, and rock. How well inexactly organized rock, (for example, sand and rock) holds water relies upon the measure of the stone particles. Layers of inexactly organized particles of uniform size, (for example, sand) tend to hold more water than layers of rock with materials of various sizes. This is on account of little rock materials settle in the spaces between bigger rock materials, diminishing the measure of open space that can hold water. Porosity (how well rock material holds water) is likewise influenced by the state of rock particles. Round particles will pack more firmly than particles with sharp edges. Material with rounded shaped has more open space and can hold more water. Groundwater is found in two zones [Figure 7.1]. The unsaturated zone, promptly beneath the land surface, contains water and air in the open spaces, or pores. The saturated zone, a zone in which every one of the pores and rock particles are packed with water, underlies the unsaturated zone. The highest point of the saturated zone is known as the water table. Salt water also enters underground aquifer along coastal belt where hydraulic gradients slope downwards in an inland direction [Figures 7.2-7.3]. The level of water table ascents and falls as indicated by the measure of rainfall, recharge and snowmelt that happen consistently, in India is higher in the post-monsoon time and at its lower in the pre-monsoon time.

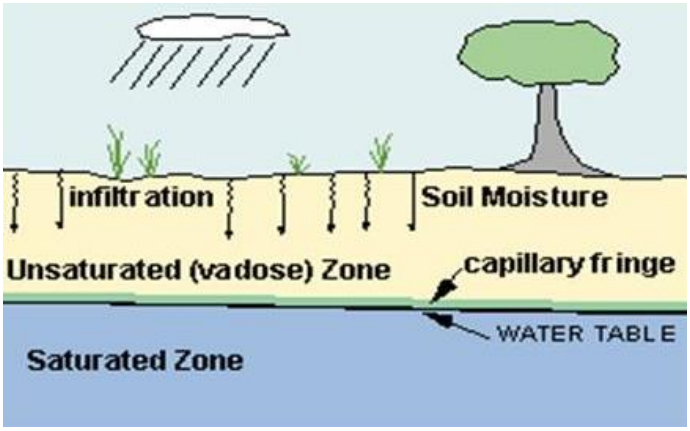

Fig. 7.1: Different zones through which groundwater moves.

Different types of soil and rock vary in the size of the spaces for water to move through. It is easier for water to move through bigger spaces, so water flows through it quickly. Then again, the spaces in mud are small to the point that no water travels through. The

layers of rock are solid to the point that they do not give water a chance to travel through. Others are brittle or have bunches of enormous breaks. On the off chance that the breaks are associated with each other, at that point water can move through the rock.

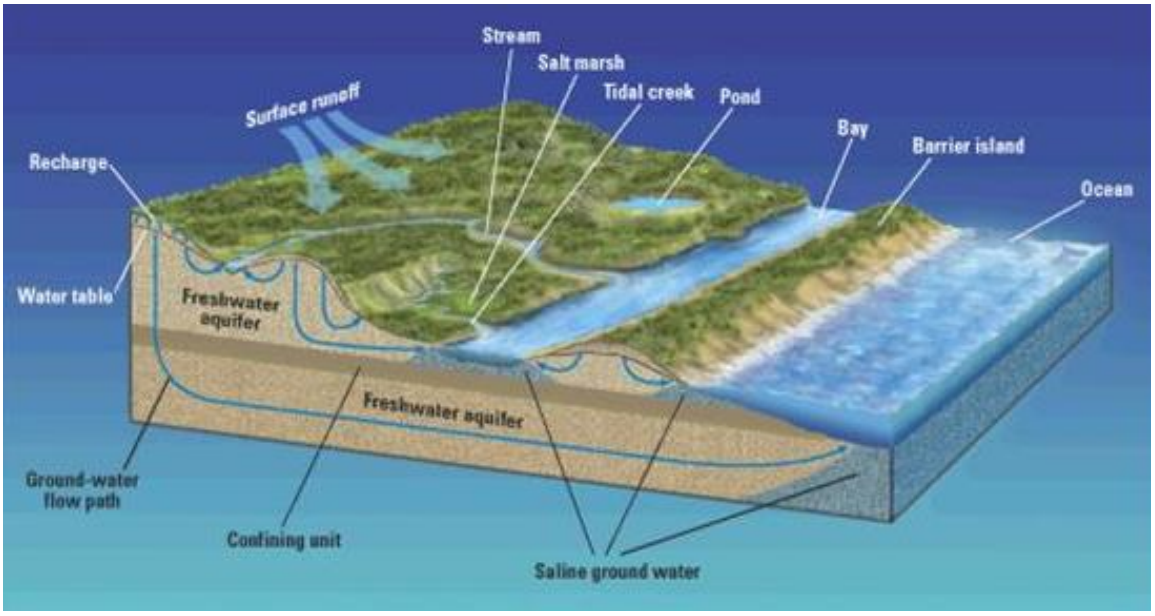

Fig. 7.2: Groundwater flow paths in coastal aquifer.

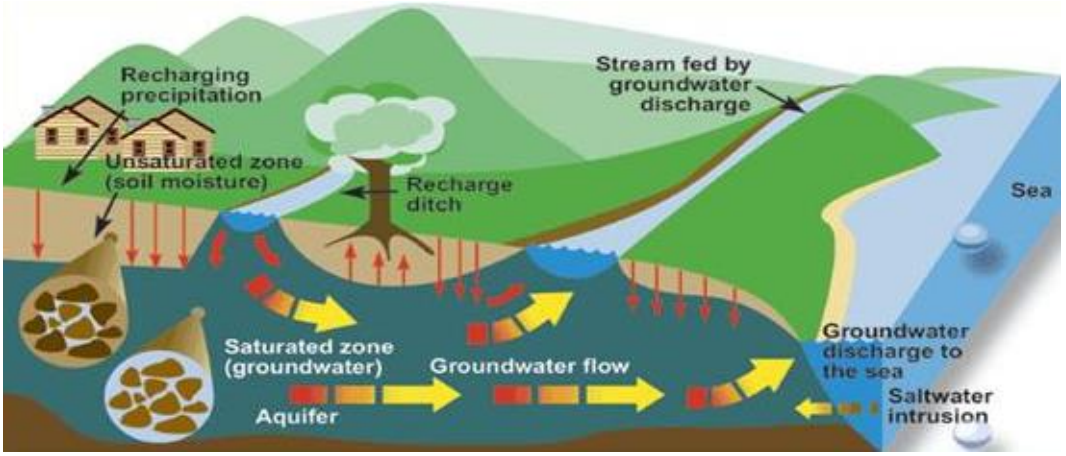

Fig. 7.3: Groundwater discharge and saline water intrusion towards coastal aquifer.

7.2 Aquifer Material

A permeable material, for example, sand, rock, and gravel that enable water to travel through it is called an aquifer. Aquifers can be confined or unconfined. Confined aquifers have non-permeable layers above and beneath the aquifer zone [Figures 7.4-7.5]. On the basis of transmissibility, the saturated geologic formations are arranged in a descending order Aquifer-Aquitard-Aquiclude-Aquifuge. These are described below:

- ***Aquifer***

  Saturated water bearing lithological arrangement stores water as well as yields adequate amount of groundwater. In this manner an aquifer transmits water

effectively because of its high permeability. Unconsolidated stores, for example, sand, rock, sandstone and limestone frame great aquifers.

- ***Aquitard***

  A geological stratum, impenetrable nature which transmits water at an ease back rate contrasted with an aquifer. A clay lenses underlined with sand.

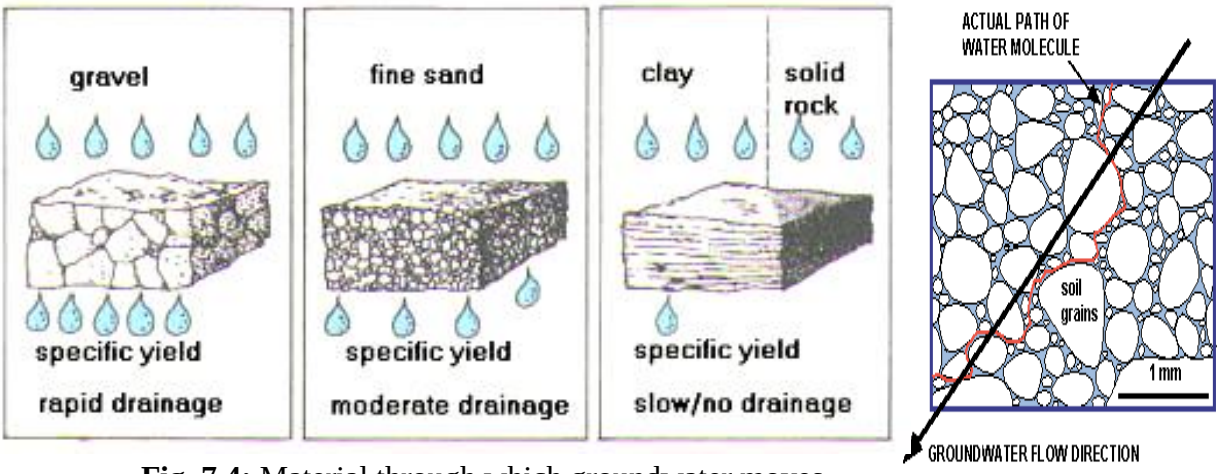

Fig. 7.4: Material through which groundwater moves.

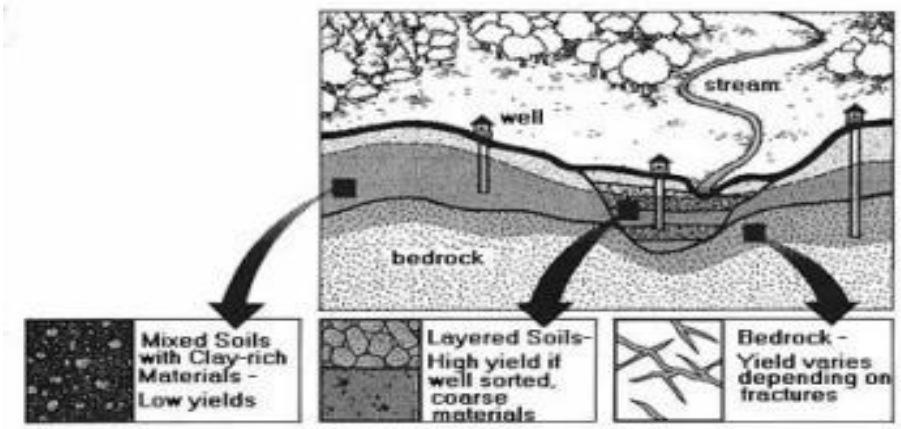

7.5: Aquifer material.

- ***Aquiclude***

  It is a lithological stratum which can store water but cannot transmit water in considerable amounts. Clay is an example of an aquiclude.

- ***Aquifuge***

  It is a lithological stratum which is neither permeable nor porous. There is no interconnected opening and hence this layer neither absorbs nor transmits water. Massive compact rock for example basalt, granite etc with any fractures is an aquifuge.

- ***Perched Aquifer***

  It is special type of aquifer which is sometimes found in an unconfined aquifer [Figure 7.6].

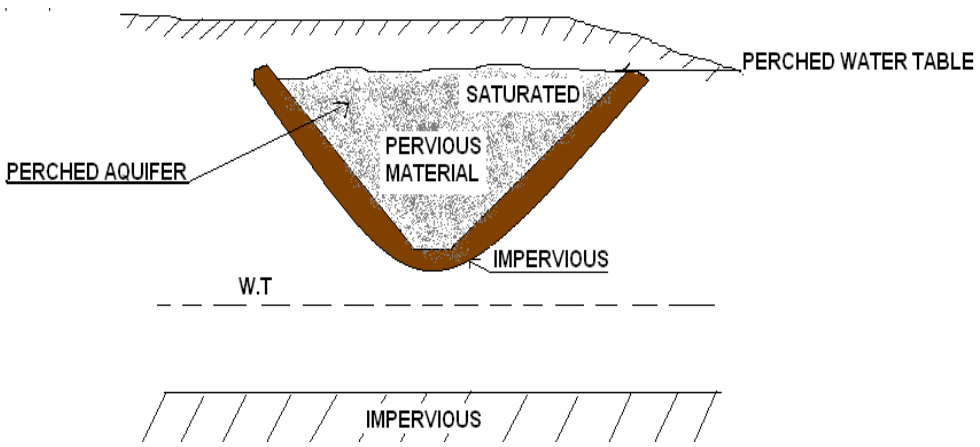

Fig. 7.6: Perched aquifer.

7.3 Groundwater Recharge

Precipitation and snowmelt can either be runoff in streams or soak into the ground. The procedure of water soaking into the ground to develop into groundwater is known as groundwater recharge.

The surface area where water absorbs is known as the recharge area. There are a few different ways that groundwater may be recharged by rain.

- Rain infiltrates where it falls and the aquifer water table is normally recharged by rain [Figure 7.7].
- Rain absorbs into ground and then goes through into deep stratum to recharge a confined aquifer.
- Rain is not absorbed so it keeps running off into streams. At the point when a stream flows through a region that enables water to absorb a portion of the water from the stream may leak down to recharge the aquifer beneath.

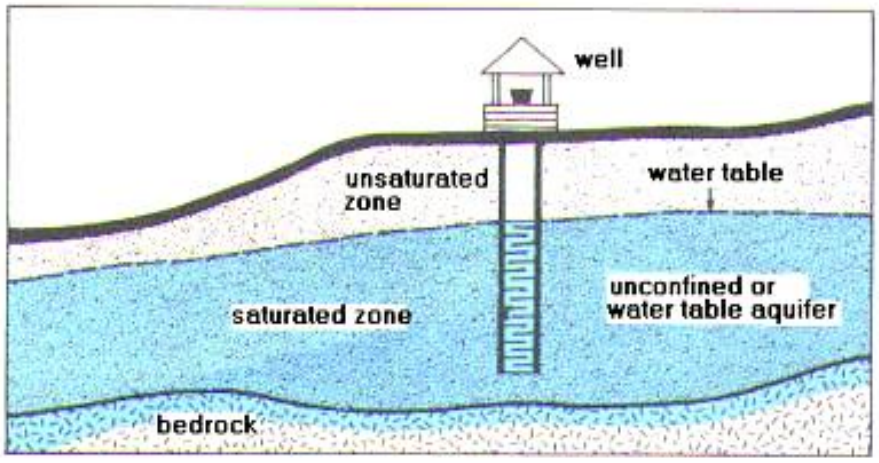

Fig. 7.7: Unconfined or water table aquifer.

7.3.1 Unconfined or Water Table Aquifer

Aquifers that are not bound under pressure are called unconfined or water table aquifers. The water level in a well is same as the water table outside the well.

7.3.2 Confined or Artesian Aquifer

Groundwater that ends up caught under impermeable soil or rock might be experiencing pressure. This is known as a confined or artesian aquifer [Figure 7.8]. A well that penetrates a kept aquifer is known as an artesian well. Water pressure in the confined aquifer will make water in the well transcend the aquifer level. The extreme level that the water in the well will ascend to is known as the potentiometer surface, or potential water level. On the off chance that this is higher than the highest point of the well, the well will overflow.

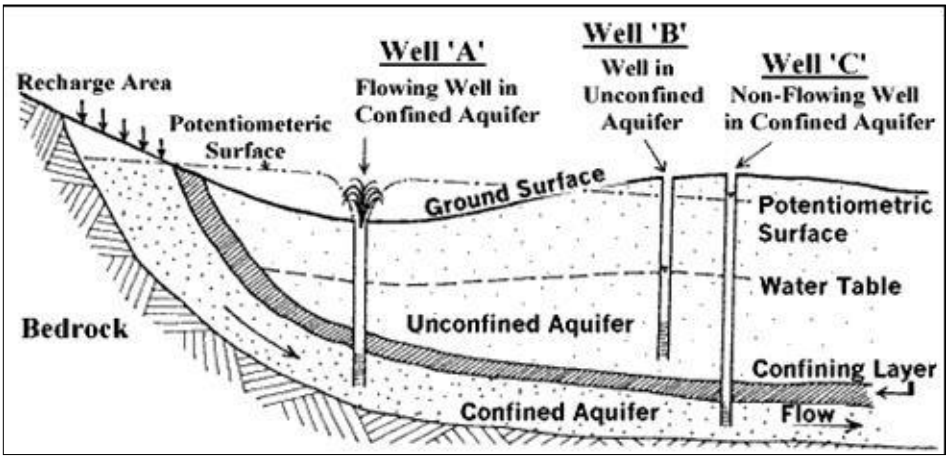

Fig. 7.8: Confined or artesian aquifer.

7.4 Groundwater and Wells

Pumping from a well in a water table aquifer brings down the water table close to the well. This region is known as a cone of depression. The land region over a cone of depression is known as the area of influence. Groundwater streams towards the well into the cone of depression. This can alter the characteristic course of groundwater stream inside the zone of influence around the well.

7.4.1 Induced Recharge

The cone of depression from a well may reach out to a close-by stream or lake. This brings down the water table underneath the stream or lake level. As a result, the stream or lake begins to lose water to the groundwater aquifer in near the well. This is known as induced recharge [Figure 7.9].

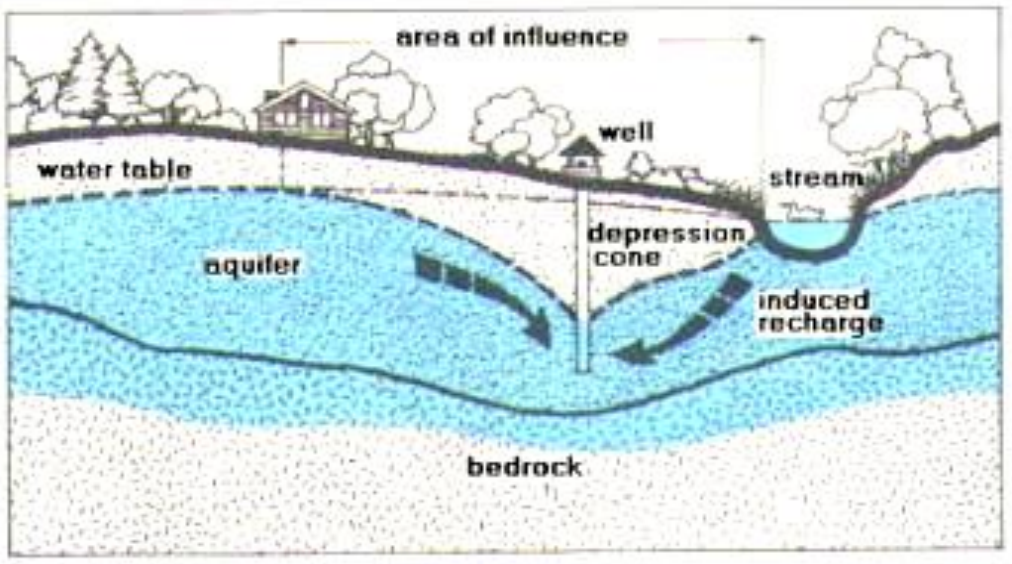

Fig. 7.9: Induced recharge.

7.4.2 Well Contribution Zone

A groundwater recharge zone that is the resource of water for a well is known as the contribution zone or catchments zone. This may incorporate just a segment of a bigger aquifer recharge zone. The zone of influence because of well pumping, that overlies the cone of depression, may reach out past the contribution zone. Induce recharge from well pumping causes groundwater to stream towards the well that would not ordinarily contribute water to a well [Figure 7.10].

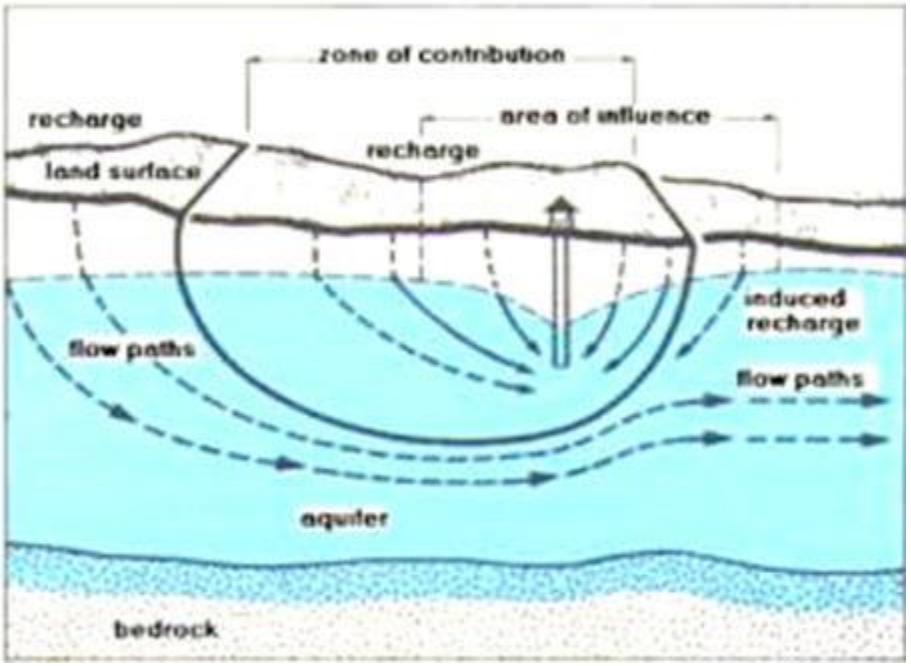

Fig. 7.10: Well contribution zone.

7.4.3 Groundwater Drainage Area

Groundwater in unconfined aquifers, that do not have impermeable soil or rocky layers between the aquifer and the land surface, for the most part streams into a similar stream waste bowl where it is found. Bound or artesian aquifers, which exist at more prominent profundity, might be a piece of a local groundwater stream framework that may not compare with the surface drainage [Figure 7.11].

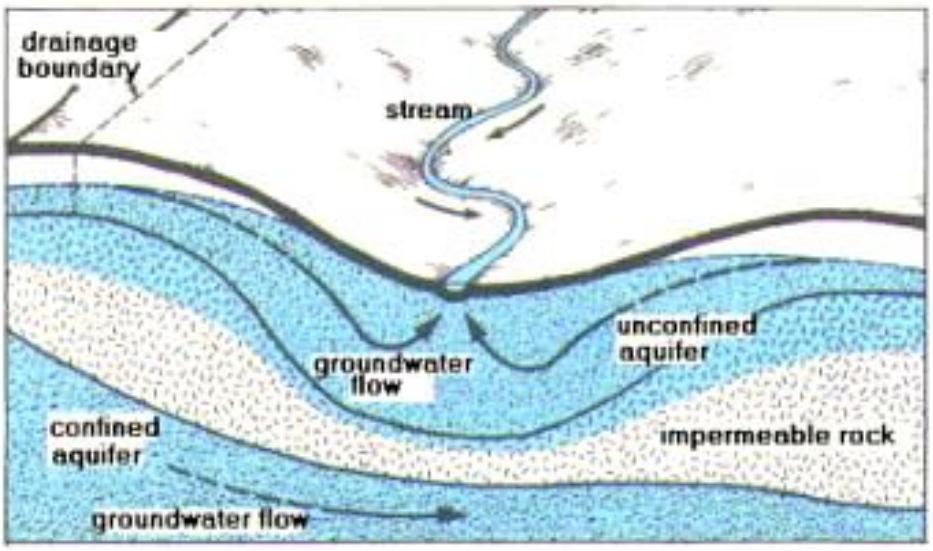

Fig. 7.11: Groundwater drainage area.

7.4.4 Groundwater Depletion

On account of groundwater extraction, bringing down of the water table is inescapable for pressure driven reasons. In any case, the size and physical appropriation of the bringing down will rely upon local conditions, e.g., the positions of the wells, the structures and nature of the aquifers, recharge conditions, etc. Typical consequents impacts of water table lowering are:

- Drying up of environmentally vital wetlands.
- Decreases in soil moisture content (field limit), with plant-particular effects on plant cover (change in the regular and cultivated greenery) and with significant impacts on the fauna
- Total lowering of groundwater storage amid maintained droughts (dried up shallow wells)
- Dried away of springs and waterways (Rivers and lakes dry up between rains),
- Intrusion of saline water into aquifers close to coasts.

7.5 Groundwater Flow Patterns in Multilayer Coastal Aquifer

Aquifers and confining units are mapped based on the level of differentiation in hydraulic conductivity among geologic units (Sun and Johnston, 1994). Generally, there

is a close correlation between the type of geologic formation and its water-yielding properties. For example, unconsolidated sands and gravels, sandstones, and lime stones generally are real wellsprings of groundwater supplies (aquifers), while beds of sediment and clay basically as binding units (Heath, 1984).

Aquifers inside the Atlantic beach front zone change in estimate from nearby scale aquifers that are a couple of square kilometers or less in areal extent to multilayer, local scale aquifers that are a tens of thousands of square miles in areal extent. In numerous regions, unconfined aquifers that are near land surface are underlain by at least one confined aquifers that might be in part or totally segregated from the land surface by confined units. Despite the fact that these multilayer, local aquifer frameworks might be broken locally, they act hydrologically as a solitary framework on a regional scale (Sun and Johnston, 1994).

Fresh groundwater interacts with saline groundwater at the offshore edges of waterfront aquifers. The offshore furthest reaches of freshwater in a specific aquifer is controlled by the measure of freshwater moving through the aquifer, the thickness and hydraulic properties of the aquifer and nearby confined units, and the relative densities of saline water and freshwater, among different factors. On account of its lower density, freshwater has a tendency to stay over the saline (saltwater) zones of the aquifer, despite the fact that in multilayered aquifer frameworks, offshore streaming freshwater can discharge upward through confining units into overlying saline water [Figure 7.12].

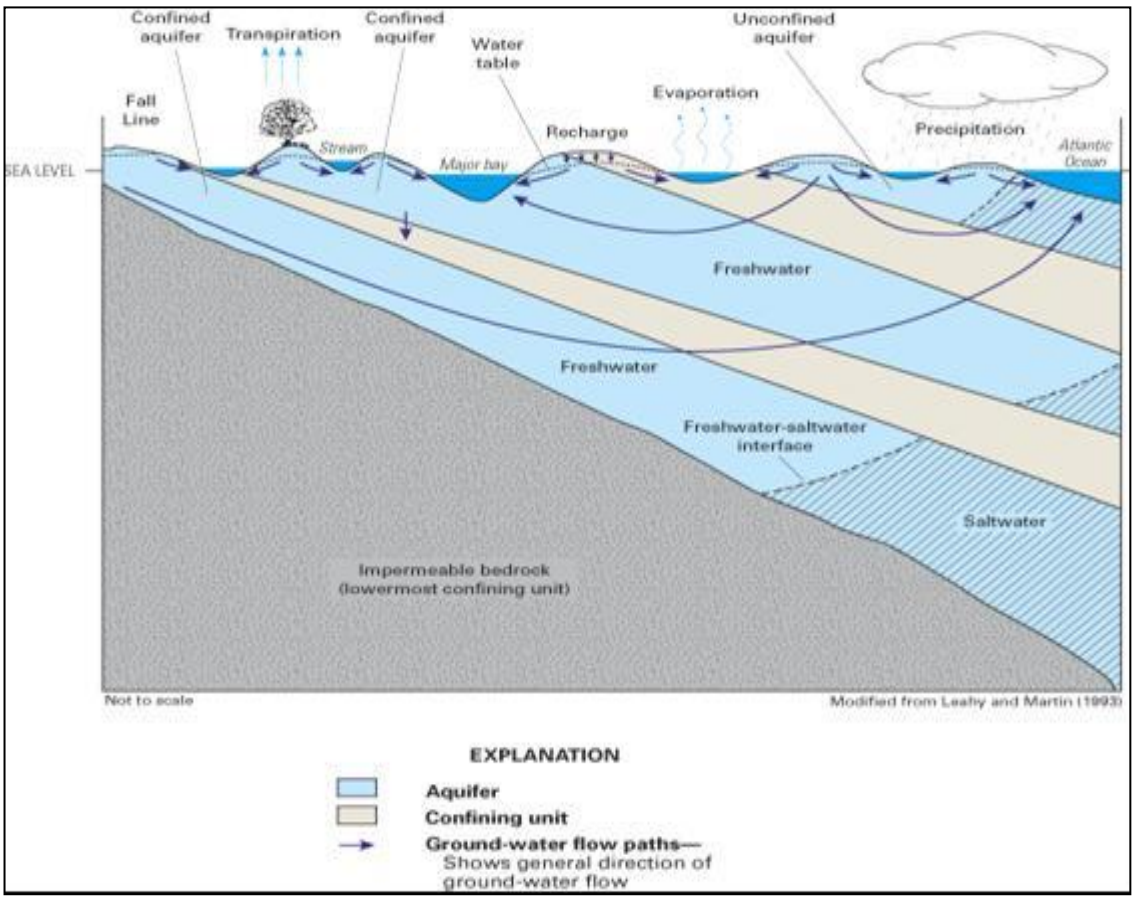

Fig. 7.12: Groundwater flow patterns in a multilayer, regional aquifer system.

7.5.1 Fernandina Permeable Zone

The aquifers isolated by a less penetrable confined unit (the "center binding unit") that confines development of water between the two aquifers [Figure 7.13]. Much of the aquifer system is overlain by an upper confining unit that, where present, limits the amount of recharge to the system. Where the upper confining unit is thin or absent, recharge is plentiful and ground-water circulation is high. In these areas of high recharge and vigorous circulation, groundwater readily dissolves the carbonate rocks that make up the aquifer system, creating large and highly permeable conduits that store and transmit tremendous volume of groundwater.

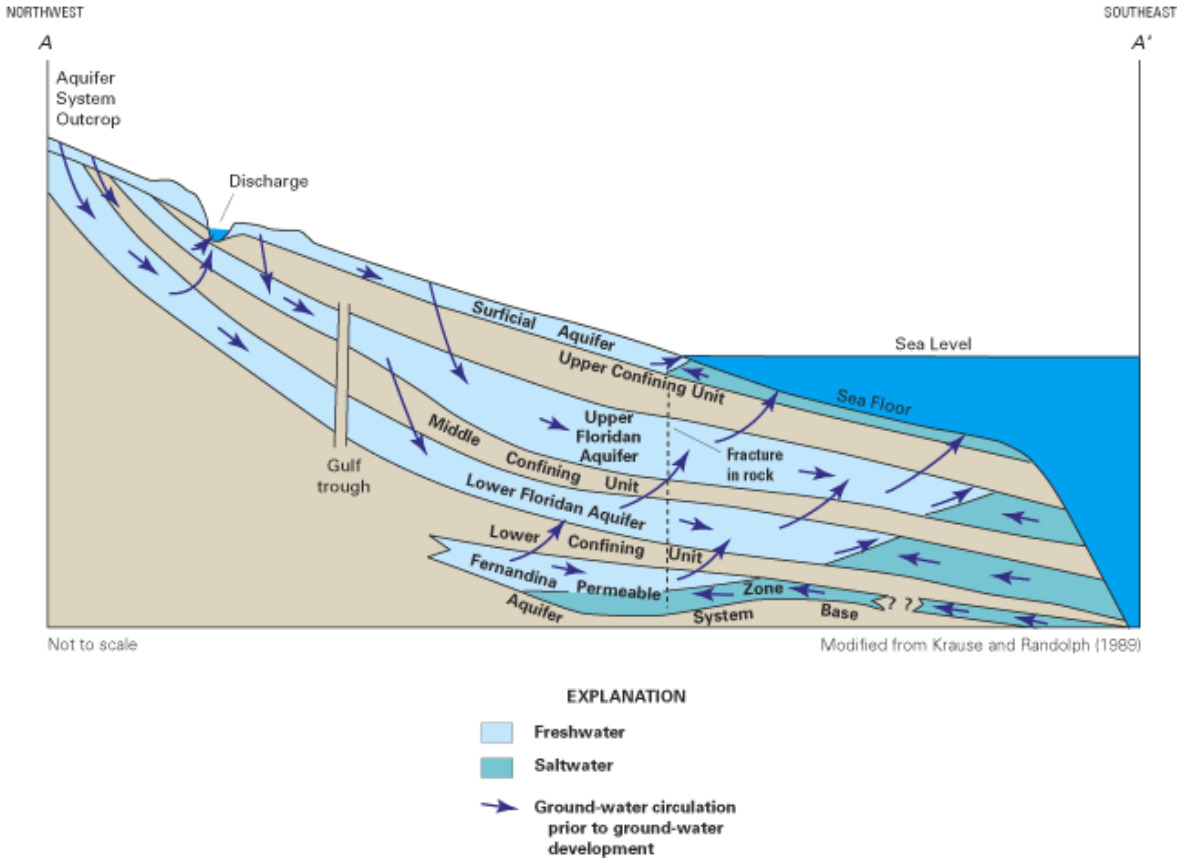

Fig. 7.13: The Fernandina permeable zone.

7.6 Soil Properties

On the off chance that the specific gravity of the soil grains of a saturated soil is assumed or estimated and if the water content is know, some valuable information such as the void ratio, porosity, saturated unit weight and bulk density of the soil can be calculated. The below mention definition are used to define the structure or status of the soil.

Void ratio = $e = V_v / V_s$, the volume of the void (V_v) and the volume of the solids (V_s) in the specimen.

Porosity, $\eta = V_v / V$, the volume of the void (V_v) and the total volume in the specimen ($V = V_v + V_s$). Also, $\eta = e/(e + 1)$

Water content, $w = (W_w / W_s)$, it is the ratio between the weight of water (W_w) in the soil specimen and the weight of solids (W_s) or dry weight of the same specimen.

7.6.1 Soil Classification and Identification

A soil may be classified according to its texture as gravel, sand, silt or clay. A natural soil consists of one more of these general types and may contain a varying amount of organic material. Accordingly, if silt identified as "sandy silt", "gravel silt", or "organic silt", it implies that the soil is primarily silt having fairly comparable as pure silt whereas the adjectives are used for the soil constituents of less power. The major types are differentiated according to their size as per Massachusetts Institute of Technology (M.I.T.) classification or I.S. 1498-1959 [Figure 7.14].

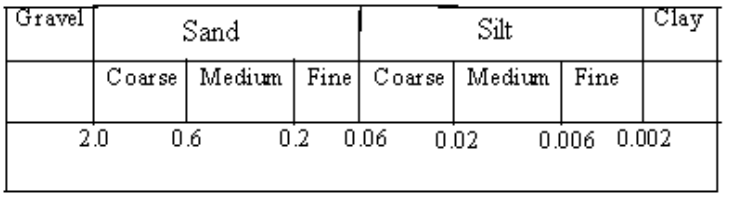

(a) M.I.T. Classification or I.S.:1498-1959 recommended classification.

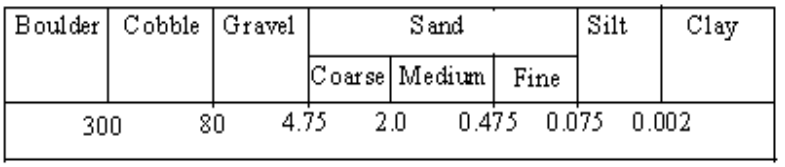

(b) I.S.: 1498-1970 recommended classification.

Fig. 7.14: Grain-size soil classification scale (in mm).

Large size grains that are coarser than gravel are called cobbles, pebbles and granules. Grains of very large sizes, over about 30 cm, are called boulder. Porosities of specific materials, approximate ranges, were listed by Davis (1969) are given in Table 7.1. The individual soil particles of sands and rock can be recognized by the naked eye or a hand focal point, while particles of silt and mud can be distinguished just by a magnifying lens or all the more regularly by an electron magnifying lens. Sand and gravels belong to the coarse-grained group (macroscopic), whereas silts and clays belong to the fine-grained group (macroscopic). Coarse-grained soils are usually cohesionless whereas fine-grained soils exhibit plasticity because of their cohesive properties (except for cohesionless silts such as the powdery "rock flour"). The major types of fine-grained soils are inorganic silts (plastic and nonplastic), inorganic clays, organic silt, and organic clays, plastic silts contain minute flake-shaped (also plate like and sometimes needle like) particles.

Clays and plastic sediments comprise of tiny or sub minute drop formed crystalline minerals that are described by their colloidal properties (plasticity, cohesion, and ability to absorb ions). Some clays are non crystalline. Organic materials contain finely isolated

particles of organic matters (shells, rotted plants, and creature living beings). The colour of the soil varies from dark grey to black depending on the amount of organic matter and its stage of decay. Usually it is not necessary to differentiate between organic silt and organic clays. Both types are generally recommended to as "organic soils" such soils have a high degree of compressibility.

Table 7.1: Approximate ranges of porosity of grains.

Type of Grain	Porosity %	Type of Grain	Porosity %
Silts and clays	50-60	Dense solid rock	<1
Fine sand	40-50	Fractured and weathered igneous rock	2-10
Medium sand	35-40	Permeable, recent basalt	2-5
Coarse sand	25-35	Vesicular lava	10-50
Gravel	20-30	Tuff	30
Sand and gravel mixes	10-30	Sandstone	5-30
Glacial till	25-45	Carbonate rock with original and secondary porosity	10-20

Table 7.2: Porosity, void ratio, and unit weight of typical soils in natural state.

Description	Porosity η (%)	Void Ratio e (--)	Water Content w (%)	Unit Weight γ_d (t/m^3)	Unit Weight γ (t/m^3)
Uniform sand, loose	46	0.85	32	1.43	1.89
Uniform sand, dense	34	0.51	19	1.75	2.09
Mixed-grained sand, loose	40	0.67	25	1.59	1.99
Mixed-grained sand, dense	30	0.43	16	1.86	2.16
Glacial till, very mixed-grained	20	0.25	9	2.12	2.32
Soft glacial clay	55	1.20	45	…..	1.77
Stiff glacial clay	37	0.60	22	…..	2.07
Soft slightly organic clay	66	1.90	70	…..	1.58
Very soft, mostly organic clay	75	3.00	110	…..	1.43
Soft bentonite	84	5.20	194	…..	1.27

w = water content when saturated, in percent of dry weight, γ_d = unit weight in dry state, γ = unit weight in saturated state (Terzaghi, 1943).

Organic soils have variable specific gravities, but they are usually less than 2.0. Pure quartz sand has a specific gravity of 2.66. While the normal types of inorganic clays have a specific gravity ranging between 2.3 to 2.9 with an average of 2.7. Since inorganic silts and clays cannot be easily differentiated visually, simple manual field tests are actually performed. These tests should be supplemented by standard physical tests in order to properly identify and classify these soils. The results of the standard physical soil tests

supplement and /or correct the driller's field log. The Porosity, void ratio, and unit weight of typical soils in natural state is given in Table 7.2.

Permeability

Several formulae are available which make use of mechanical analysis data for determination of hydraulic conductivity or velocity of water through aquifer samples (Wenzel, 1942). The critical-size parameter used in these formulae is the effective size of grain (d_{10}). If all grains are of the effective size diameter, the sand would transmit the same amount of water that it actually does. This size parameter is related to K (hydraulic conductivity in m/day) as given in Equation (7.1).

$$K = Cd^2_{10}\left(0.70 + 0.03t\right) \tag{7.1}$$

where C= a constant having a value ranging from 1200 for very uniform clean sands to 400 for very closely packed sand containing considerable amounts of alumina or iron, d_{10} = effective size in mm and t = temperature in ^{0}C. Change in the temperature of water cause appreciable changes in the hydraulic conductivity of the water-bearing materials due to changes in the viscosity of water. Hydraulic conductivity of various water-bearing materials, especially of those lack significant differences, may be compared (Table 7.3).

7.7 Sub-Surface Geology

The Purba Midnapur district [Figure 7.15] of West Bengal is located to the southwest of Kolkata and shares the western border of the state of Orissa. The district involves 4736 km^2 area and circumscribed by Paschim Midnapur and Bankura districts of West Bengal in the north, Hooghly, Howrah and 24-Paragnas areas of West Bengal in the east, Bay of Bengal in the south and Mayurbhanj and Balasore districts of Orissa in the southwest. The district lies roughly between 21°38' North to 22°30' North latitudes and between 87°2' East and 88°11' East longitudes. The district is densely populated with 5.5 lakhs population enumerated in 2011 census. The district is subdivided into five subdivisions namely Haldia, Contai, Tamluk, Egra, Panskura. The district head quarter is located at Tamluk town. A few noteworthy and minor waterways navigate the district. Waterway Kasai crosses through the Panskura town and the modern town of Haldia. Kasai River after its confluence with Kalaghai River is known as Haldi River and it ultimately joins the river Hooghly. Rupnarayana River flows towards Eastern border of the district and joins Bay of Bengal. The other major river Subarnarehka passes through the south-western periphery of the district. Here the most part of groundwater basin area is under Ganga basin with the remaining is under the Subarnarehka River basin. The Purba Midnapur has been shaped in the last couple of thousands of years by the persistent supply of sediment stacked from immense catchments which is stored into a dying down basin, incompletely fluvial and somewhat marine, under shifting vitality conditions. The coastal part is covered by unconsolidated sediments of recent age (Table 7.4) and it is represented by vast plains of fluvial and marine deposits. In the coastal region the recent sediments are characterized by a group of yellow or brown coloured sediments. Again

yellowish or brown sediments are underlain by greyish white sand sequence. The similar types of sediments are also perceived in inland areas.

Lithology of bore holes has been drilled in the Purba Midnapur district in three phases. In the first phase, soil log data of Egra, Daxin Danki, Sarda, Marisda, Balgeria, Nilpur, Digha, Chandipur, Sutahata, Tamluk and Khejuri have been analysed. In the second phase, soil log data of Kalindi, Ratanpur, Amarshi Kasba, Kamarda, Serkhanchak, Mukutshila, Routara, Pichabani and Basantia soil have been analysed. The soil samples locations are given in Figure 7.18. The third phase Baghaput and Sofiabad, Contai is described at the section 7.7.1. It is observed from the lithology of bore holes that the same group of aquifers continued from the inland part of the district up to the coast. It is also seen that there is considerable lateral variation, i.e. the individual layer of sand, laterally changes its grade from sandy to silt/clay.

Table 7.3: Estimations of physical parameters related with different kinds of aquifer materials [Todd (1980) after Johnson (1967), Morris and Johnson (1967)].

Material	Porosity (%)	Specific Yield (%)	Hydraulic Conductivity (m/day)
Coarse gravel	28 [r]	23	150 [r]
Medium gravel	32 [r]	24	270 [r]
Fine gravel	34 [r]	25	450 [r]
Coarse sand	39	27	45 [r]
Medium sand	39	28	12 [r]
Fine sand	43	23	2.5 [r]
Silt	46	8	0.08 [h]
Clay	42	3	0.0002 [h]
Fine-grained sandstone	33	21	0.2 [v]
Medium-grained sandstone	37	27	3.1 [v]
Limestone	30	14	0.94 [v]
Dolomite	26		0.001 [v]
Dune sand	45	38	20
Loess	49	18	0.08 [v]
Peat	92	44	5.7 [v]
Schist	38	26	0.2 [v]
Shale	6		
Slate			0.00008 [v]
Till (predominantly silt)	34	6	
Till (predominantly sand)	31	16	0.49 [r]
Till (predominantly gravel)		16	30 [r]
Tuff	41	21	0.2 [v]
Basalt	17		0.01 [v]
Weathered gabbros	43		0.2 [v]
Weathered granite	45		1.4 [v]

[v] - Indicates vertical measurement of hydraulic conductivity, [h] - indicates vertical measurement of hydraulic conductivity, [r] - indicates measurement on a repacked sample

Table 7.4: Stratigraphic succession of Purba Midnapur.

Rock type	Geological age
Alluvium	Recent
Older alluvium	Pleistocene
Siwalik group	Miocene-pliocene

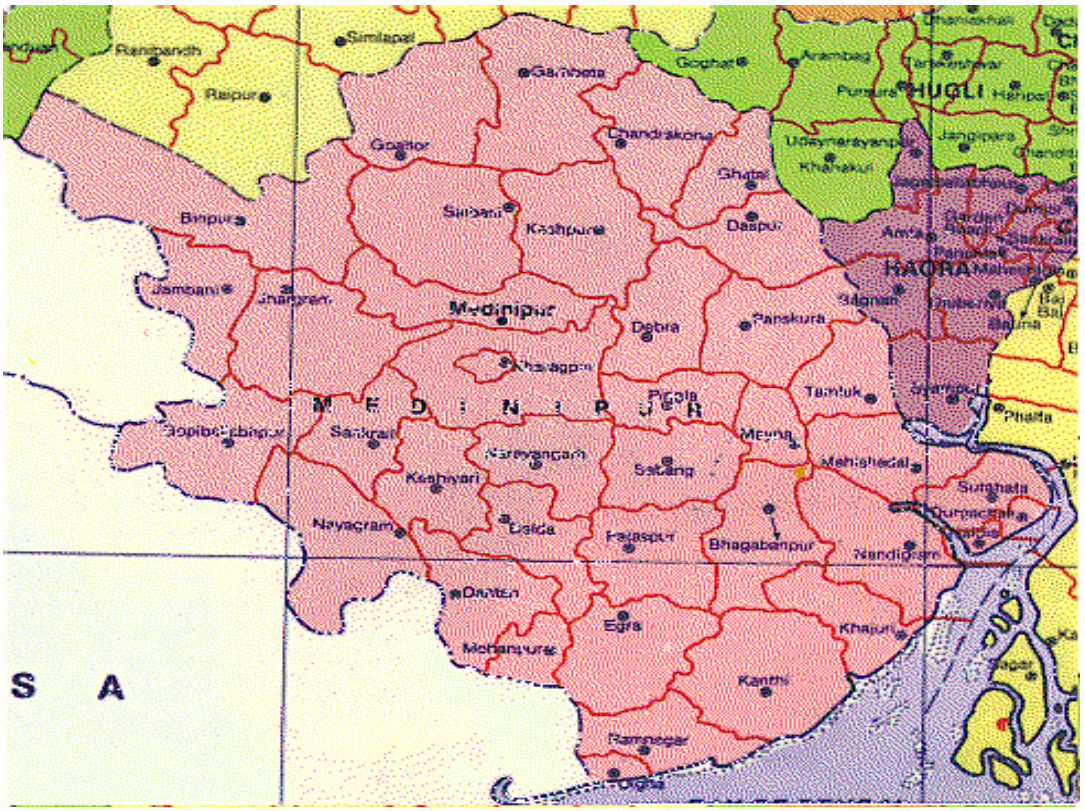

Fig. 7.15: Different blocks of Midnapur district.

It is also observed that the three different types of formations encountered in various, bore holes in different part of the district belong to different geological ages, from tertiary to the recent. The unconsolidated current silt is basically a succession of earth, sand and rock displaying wide variety in review and shading. Usually these sediments are characterized by shades of grey, brown and yellow colour. The sand is of quartz feldspathic material often associated with gravel, calcareous shelly material. The unconsolidated sediments are very thick (300 m) close to the coast. These horizons occurring at different depths form the aquifers. The aquifers are regionally extensive. Unconsolidated recent sediments are mainly in the eastern and coastal parts of the district and are seen to reduce in thickness towards inland. The aquifers position at different bore hole locations is given in Table 7.5. The thickness of recent sediments about 25 m at Panskura, 50 m at Tamluk, 30 m at Nandigram, 35 m at Contai, 50 m at Haldia, 80 m at Khejuri, 90 m at Dariyapur. On the coastal side thick sand horizons are met at Khejuri and Dariyapur but these thick sand horizons are laterally discontinues towards southeast, i.e. Haldia, Sutahata etc. Towards Daxin Danki, Bodra and Digha (south-eastern part) a thick sand horizon is divided into several small horizons by intervening clay lenses.

Table 7.5: Aquifer positions at different borehole locations.

Stratum	Tapping zone (m bgl)	General features	Quality of water
BOREHOLE-1: EGRA			
I	47-50	Sand fine to medium grained, yellow in colour	Fresh
II	104-107	Sand very coarse with few kankar and feldspar fragments grey in colour	Fresh
III	175-178	Sand to medium to coarse with block mineral fragments	Fresh
BOREHOLE-2: DAXIN DANKI			
I	191-194	Sand fine to medium with mica and mineral fragments grey in colour	Brackish
II	237-240	-Do-	Brackish
BOREHOLE-3: SARDA			
I	45-46	Sand very fine to fine with mica, yellowish in colour	Saline
II	86-89	Sand a mixture of fine medium and coarse grained brownish colour	Saline
III	170-172	Sand fine to coarse grained, greyish white in colour	Saline
BOREHOLE-4: MARISDA			
I	106-107	Sand fine to medium grained, grey in colour	Brackish
II	155-168	-Do-	Saline
III	187-189	-Do-	Saline
BOREHOLE-5: NILPUR			
I	20-23	Sand medium to coarse grained, yellow in colour	Saline
II	99-102	Sand fine to medium grained, yellow in colour	Saline
III	159-162	-Do-	Brackish
IV	195-198	-Do-	Brackish
BOREHOLE-6: BALGERIA			
I	49-52	Fine to medium sand	Brackish
II	105-108	-Do-	Brackish

BOREHOLE-7: DIGHA

Stratum	Tapping zone (m bgl)	General features	Quality of water
I	45-48	Sand fine to coarse grained with mica yellow in colour	Brackish
II	103-106	Sand, clay, quartz, feldsper, mica, pyroxene, grey colour	Saline

BOREHOLE-8: CHANDIPUR

I	74-79	Sand fine to medium with feldsper, pyroxene, mica greyish white colour	Saline
II	116-119	Sand fine to coarse grained with feldsper, pyroxene, mica brownish yellow colour	Brackish
III	194-197	Sand fine to coarse grained	Brackish

BOREHOLE-9: SUTAHATA

I	68-71	Sand fine to medium grained grey colour	Brackish
II	108-111	-Do-	Saline
III	159-162	-Do-	Saline

BOREHOLE-10: TAMLUK

I	92-95	Sand fine to coarse grained wit quartz, feldspar, pyroxene, mica brownish colour	Brackish
II	122-125	Sand fine to coarse yellow colour	Fresh
III	161-164	-Do-	Fresh

BOREHOLE-11: KHEJURI

I	30-33	Sand very fine grained yellowish grey colour	Brackish
II	59-64	-Do-	Fresh
III	195-198	-Do-	Fresh

The information available from the bore holes - different type of sediments down to a depth of 300 m has been identified. Greyish white sand clay belonging to upper tertiary is encountered from 121 m to 200 m below ground level (bgl) at Marisda, from 102 m to 200 m at Sarda, 66 m to 300 m at Digha, 82 m to 200 m at Khejuri and 105 m to 200 m bgl at Egra, in the eastern part, 142 m down to a depth of 300 m at Tamluk, 66 m to 300 m bgl at Sutahata.

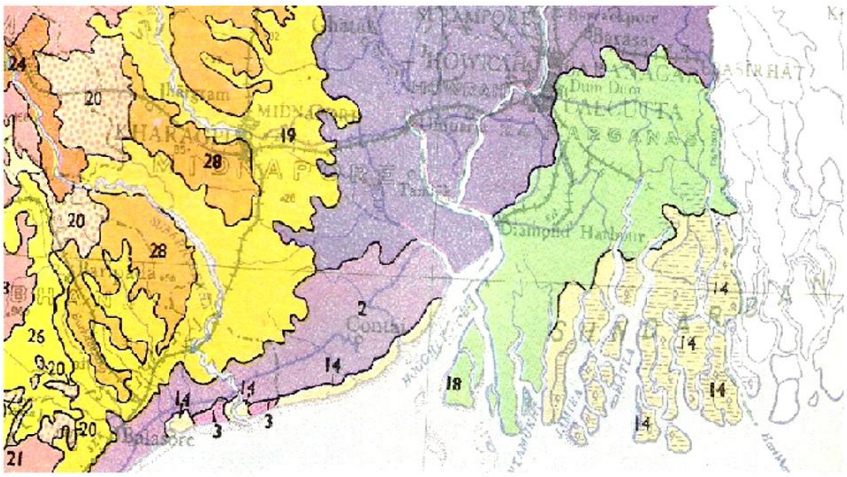

Fig. 7.16 (a): The soil profiles of some portion of East Coast of India (NATMO, 2013).

Fig. 7.16 (b): Index of soil profiles displayed in Figure 7.16(a).

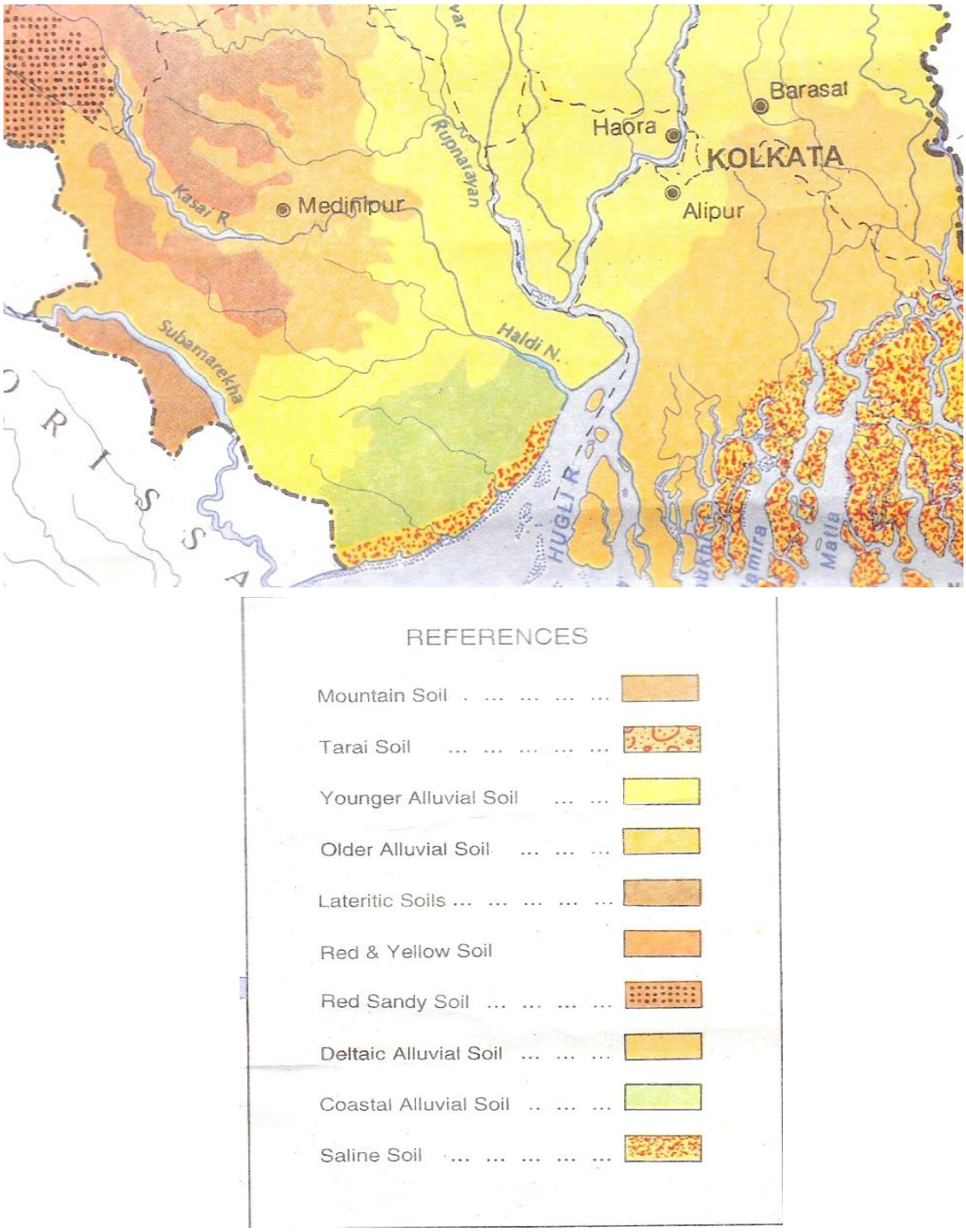

Fig. 7.17: The soil profiles of Pubra Midnapur (NATMO, 2013).

These greyish white sand and clay horizons are overlain brownish yellow and grey colored sand and clay horizons of Holocene. These sediments occur from 15 m to 121 m below ground level at Marisda, 12 m to 102 m below ground level at Sarda, 21 m to 66 m below ground level at Digha, 06 m to 139 m below ground level at Bhupatinagar, 0 to 75 m below ground level at Egra, 63 m to 66 m below ground level at Sutahata and 93 m to 142 m below ground level at Tamluk.

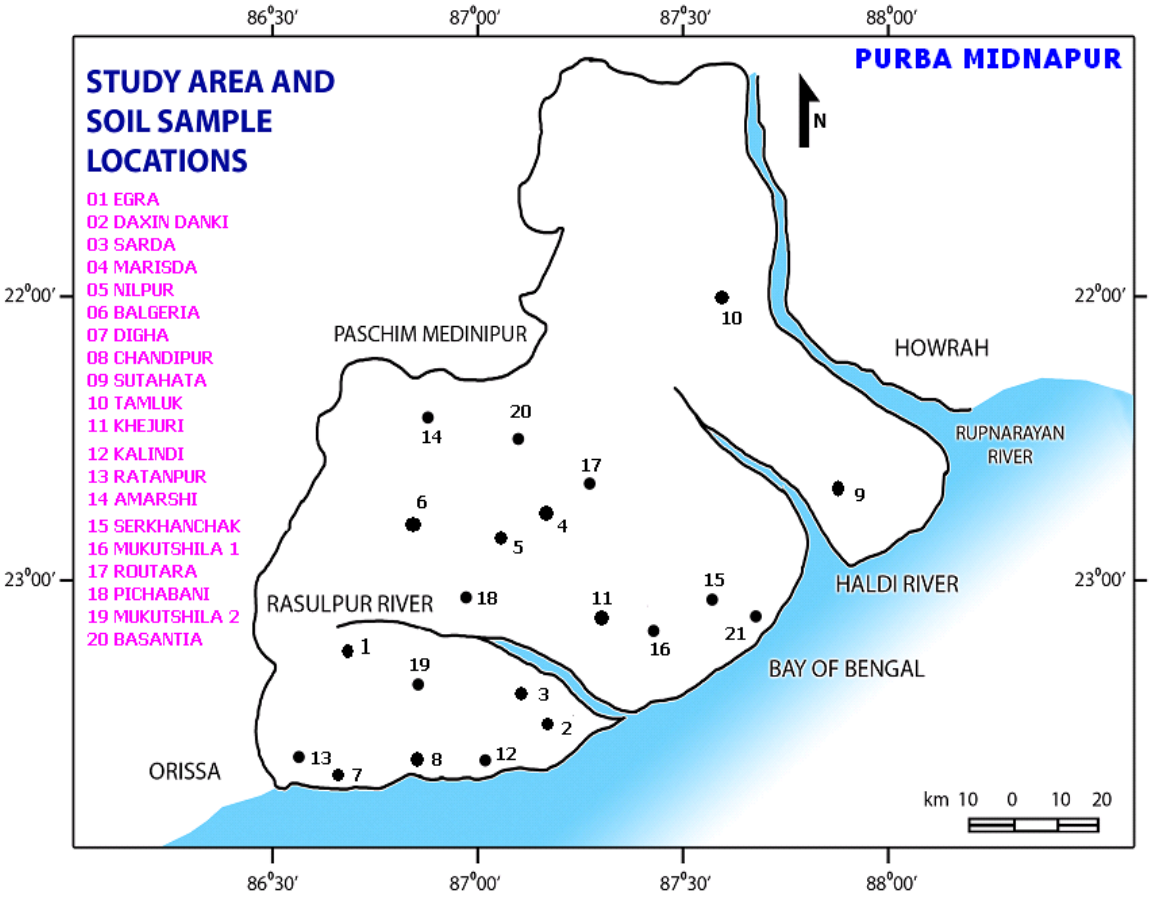

Fig. 7.18: Soil sampling locations.

Table 7.6: Lithology of Borehole No. 12 at Kalindi.

Stratum	Depth range (m)	Nature of formation	Hydraulic conductivity (m/day)	Remarks
1	00.00 to 26.95	Clay blackish	4.1×10^{-5}	-
2	26.95 to 29.40	Coarse Sand brownish	1.84×10^{2}	-
3	29.40 to 62.83	Clay light black	4.2×10^{-3}	-
4	62.83 to 72.35	Coarse sand light yellow	2.23×10^{2}	-
5	72.35 to 108.28	Clay light black	4.1×10^{-5}	-
6	108.28 to 156.91	Fine and medium sand greyish	4.2×10^{2}	(Zone A)
7	156.91 to 161.71	Sticky clay	4.1×10^{-5}	-
8	161.71 to 185.70	Medium sand greyish	1.84×10^{2}	(Zone B)
9	185.70 to 197.91	Clay mixed with Sand	4.1×10^{-5}	-
10	197.91 to 200.45	Clay blackish	4.2×10^{-3}	-

It is discovered that the upper soil of Purba Midnapur is of quaternary root and comprises of rotating stores of dirt and sand of marine inception. Likewise with every single marine store, adjusted grains and high porosity are overwhelming attributes. The northern part of the area comprises of a blend of alluvial and marine stores [Figure 7.16(a-b) and 7.17]. Also there is a great spatial heterogeneity in the aquifer, which makes any predictive method for calculating the depth of saline water intrusion futile.

Analysis of electrical logging data has been done for Ratanpur site and the corresponding results are displayed in Table 7.6. Electrical logging using multi-electrode system has been used to delineate the boundary of granular and non-granular layers and to decipher the interface of fresh and saline water. Analysis of electrical logging results depicts the following:

- Electrical logging is done upto depth of 198 m bgl and shows presence of mainly two zones containing granular sediments saturated with groundwater, disposition of which are between 102-150 m and 159-189 m bgl. To facilitate discussion these two zones are designated as A and B, respectively.
- Further observation shows that granular zone above 60 m contains inferior quality groundwater due to proximity of inferior quality groundwater. Zone A may not be recommended for tapping in the present case and zone B is the only zone left for tapping.
- Tube well assembly may be lowered tapping zone B with strainer position between 162 m -183 m bgl (21 m of strainer length) to obtain groundwater of good quality and quantity. To prevent contamination of tube well water by inferior quality water from above, the portion of the bore hole between 78 m – 90 m below ground level may be sealed by impervious material (bentonite balls).
- As per the results given in Table 7.7 and electrical logging analysis, tubewell assembly may be lowered tapping zone A within strainer position between 199.13 m to 203.78 m to obtain good quality of groundwater. As shown in Table 7.8, the electrically logged multi-electrode system mainly shows that groundwater contained upto 123 m below ground level is inferior in nature and best portion available for tapping lies in between 216 - 249 m below ground level and hence, strainer position can be placed anywhere in between 216 - 249 m below ground level (Zone A).

Table 7.7: Lithology of Borehole No. 13 at Ratanpur.

Stratum	Depth range (m)	Nature of formation	Hydraulic conductivity (m/day)	Remarks
1	00.00 to 10.21	Top sand yellow	3.28×10^{2}	-
2	10.21 to 24.29	Clay mixed with sand	4.2×10^{-3}	-
3	24.29 to 42.84	Medium and coarse sand yellow	1.84×10^{2}	-
4	42.84 to 79.70	Morum mixed with clay and sand	4.2×10^{-2}	-
5	79.70 to 129.90	Clay blackish mixed with sand	4.2×10^{-3}	-
6	129.90 to 152.90	Fine to medium sand greyish	4.1×10^{1}	-
7	152.90 to 171.49	Clay blackish	4.1×10^{-5}	-
8	171.49 to 189.78	Fine to medium sand greyish	4.1×10^{1}	-
9	189.78 to 199.13	Clay blackish	4.1×10^{-5}	-
10	199.13 to 203.78	Medium to coarse sand greyish	4.1×10^{1}	(Zone A)
11	203.78 to 210.64	Sandy clay	4.1×10^{-2}	
12	210.64 to 240.85	Medium and fine sand greyish	4.2×10^{-3}	-

Analysis of electro-logging results has also been done for Kamarda and Serkhanchak and subsequent lithlogy logs are displayed in Tables 7.9 and 7.10, respectively. It is

recommended that the tubewell assembly may be lowered between 134.1 to 228.6 m and 192- 216.4 m, respectively for these two sites to obtain good quality of groundwater.

In the logging depth electrical log reveals the presence of several small zones as highlighted in Table 7.11, only one prominent zone containing granular sediments saturated with groundwater disposition of which is between 213 m to 270 m bgl. Further analyses of the geophysical data show groundwater contained in granular sediments within 195 m are saline in quality and there is no prominent barrier separating the saline zone and fresh water zone except poly bed below 195 m bgl. As such, yield may be kept to minimum to prevent saline water impregnation from above. Tube well assembly may be lowered tapping the zone between 228 m to 254 m below ground level for moderate to good quality and quantity of ground water. The portion of the bore hole between 191 m to 213 m, may be sealed by impervious materials to prevent percolation of inferior quality groundwater from above.

Analysis of electrical logging results for Routara is illustrated in Table 7.12 (a) and Table 7.12 (b). It is recommended for the tapping zone-F in between 175.5 m to 217.5 m to obtain good quality groundwater.

Table 7.8: Lithology of Borehole No. 14 at Amarshi Kasba.

Stratum	Depth range (m)	Nature of formation	Hydraulic conductivity (m/day)	Remarks
1	00.00 to 10.06	Clay	4.1×10^{-5}	-
2	10.06 to54.93	Fine sand yellow	4.1×10^{1}	-
3	54.93 to 57.37	Clay	4.1×10^{-2}	-
4	57.37 to 66.51	Medium to coarse sand	1.84×10^{2}	-
5	66.51 to 127.36	Fine to medium sand greyish	1.94×10^{2}	-
6	127.36 to 205.10	Clay mixed with kankar	4.1×10^{-5}	-
7	205.10 to 252.41	Fine to medium sand greyish	1.84×10^{2}	(Zone A)
8	252.41 to 263.59	Sandy clay	4.2×10^{-1}	-
9	263.59 to 272.50	Clay	4.1×10^{-5}	-

Table 7.9: Lithology of Borehole No. 15 at Kamarda.

Stratum	Depth range (m)	Nature of formation	Hydraulic conductivity (m/day)	Remarks
1	00.00 to 6.10	Clay brown sticky	4.1×10^{-5}	-
2	6.10 to 9.14	Sand fine grey	4.1×10^{1}	-
3	9.14 to 12.19	Clay grey sticky	4.1×10^{-5}	-
4	12.19 to 27.43	Sand fine grey	4.1×10^{1}	-
5	27.43 to 79.25	Clay brown sticky	4.1×10^{-5}	-
6	79.25 to 106.68	Sand medium to coarse brown	1.84×10^{2}	-
7	106.68 to 128.02	Clay grey sticky	4.1×10^{-5}	-
8	128.02 to 134.11	Sand mixed with clay grey	1.94×10^{2}	-
9	134.11 to 228.66	Sand medium to coarse white	1.84×10^{2}	(Zone A)

Table 7.10: Lithology of Borehole No. 16 at Serkhanchak.

Stratum	Depth range (m)	Nature of formation	Hydraulic conductivity (m/day)	Remarks
1	00.00 to 3.00	Surface soil	4.12×10^{-5}	-
2	3.00 to 21.00	Clay grey silty	4.23×10^{-5}	-
3	21.00 to 30.50	Clay mixed with sand	4.24×10^{-5}	-
4	30.50 to 76.00	Clay	4.12×10^{-5}	-
5	76.00 to 106.50	Clay grey sity	4.27×10^{-5}	-
6	106.50 143.00	Sand medium brownish	1.94×10^{2}	-
7	143.00 to 149.5	Sand fine to medium greyish	1.84×10^{2}	-
8	149.5 to 161.5	Clay grey silty	4.1×10^{-5}	-
9	161.5 to 167.50	Sand fine brownish	1.74×10^{2}	-
10	167.50 to 182.9	Sand medium brownish	1.64×10^{2}	-
11	182.9 to 192.00	Sand medium greyish	1.87×10^{2}	-
12	192.00 to 216.4	Sand fine to medium greyish	1.94×10^{2}	(Zone A)

Table 7.11: Lithology of Borehole No. 17 at Mukutshila.

Stratum	Depth range (m)	Nature of formation	Hydraulic conductivity (m/day)	Remarks
1	00.00 to 4.57	Surface soil	4.1×10^{-5}	-
2	4.57 to 18.89	Clay	4.2×10^{-5}	-
3	18.89 to 32.96	Medium to coarse sand yellowish	1.84×10^{2}	-
4	32.96 to 62.28	Clay	4.1×10^{-5}	-
5	62.28 to 139.35	Medium sand	1.84×10^{2}	-
6	139.35 to 146.15	Clay with kankar	4.1×10^{-3}	-
7	146.15 to 171.47	Medium to coarse sand yellowish	1.84×10^{2}	-
8	171.47 to 185.00	Clay	4.1×10^{-5}	-
9	185.00 to 189.58	Sandy clay	4.3×10^{-1}	-
10	189.58 to 221.43	Clay	4.1×10^{-5}	-
11	221.43 to 280.35	Fine to medium sand greyish	1.84×10^{2}	(Zone A)
12	280.35 to 289.28	Sediment	3.92×10^{-1}	-

Table 7.12(a): Lithology of Borehole No. 18 at Routara.

Stratum	Depth range (m)	Nature of formation	Hydraulic conductivity (m/day)	Remarks
1	00.00 to 2.10	Clay surface	4.1×10^{-5}	-
2	2.10 to 7.50	Fine sand greyish	4.2×10^{1}	-
3	7.50 to 11.10	Fine sand yellowish	4.1×10^{1}	-
4	11.10 to 13.50	Clay yellowish	4.1×10^{-5}	-
5	13.50 to 22.20	Sand fine to medium yellowish	1.84×10^{2}	-

6	22.20 to 37.50	Clay yellowish sticky	4.2×10^{-5}	-
7	37.50 to 57.60	Sand coarse greyish with laterite	4.3×10^{1}	-
8	57.60 to 65.40	Clay yellowish	4.2×10^{-5}	-
9	65.40 to 115.50	Coarse sand yellowish	1.94×10^{2}	-
10	115.50 to 129.30	Clay greyish	4.2×10^{-5}	-
11	129.30 to 152.10	Sand medium greyish	1.84×10^{2}	-
12	152.10 to 175.50	Clay greyish	4.2×10^{-5}	-
13	175.50 to 217.50	Sand coarse to medium greyish	1.84×10^{2}	(Zone A)
14	217.50 to 256.50	Clay greyish hard	4.2×10^{-5}	-

Table 7.12 (b): Lithology of Routara.

Sl. No.	Nature of formation	Zones	Depth (m)
1	Clay	A	2.10 m to 11.10 m
2	Sand (fine)	B	13.50 m to 22.20 m
3	Sand (fine to medium)	C	45.60 m to 57.60 m
4	Sand (coarse)	D	65.40 m to 115.50 m
5	Sand (medium)	E	129.30 m to 152.10 m
6	Sand (coarse to medium)	F	175.50 m to 217.50 m

Table 7.13: Lithology of Borehole No. 19 at Pichabani.

Stratum	Depth range (m)	Nature of formation	Hydraulic conductivity (m/day)	Remarks
1	00.00 to 04.57	Pasty clay blackish	4.2×10^{-5}	-
2	04.57 to 18.70	Sandy clay black	4.3×10^{-3}	-
3	18.70 to 32.70	Fine to medium sand yellow	1.84×10^{2}	-
4	32.70 to 37.04	Very fine sand	1.74×10^{2}	-
5	37.04 to 46.08	Loose clay with sand	1.44×10^{2}	-
8	46.08 to 69.15	Very coarse sand light yellow	4.2×10^{-5}	-
9	69.15 to 73.68	Sand mixed with clay	3.28×10^{2}	-
10	73.68 to 119.61	Fine sand yellow	4.1×10^{-1}	-
11	119.61 to 142.30	coarse sand grey	1.94×10^{2}	-
12	142.30 to 160.92	Loose clay black	2.67×10^{2}	-
13	160.92 to 183.17	Very coarse sand	4.11×10^{-5}	(Zone A)
14	183.17 to196.70	Pasty clay blackish	4.2×10^{-5}	-
15	196.70 to 236.45	Very fine sand grey	1.84×10^{2}	-
16	236.45 to 249.92	Black clay	4.2×10^{-5}	-
17	249.92 to 277.38	Fine sand grey	1.84×10^{2}	-
18	277.38 to 286.78	Loose black clay	4.2×10^{-5}	-
19	286.78 to 296.00	Very fine sand grey	4.1×10^{1}	-
20	296.00 to 305.28	Black loose clay	4.2×10^{-5}	-

In the logging depth there are several zones containing granular sediments but due to their proximity to the near surface and saline water bearing condition, the zones above 138 m below ground level are not discussed here but their disposition are shown in Table 7.13. The saline water and fresh water interface is near 138 m below ground level. Zone upto 90 m contains high salinity content groundwater while zone upto 138 m contains comparatively less saline water. On geophysical consideration, there are two zones, which may be tapped for moderate to good quality and quantity of groundwater. The dispositions of these zones are between 153 m to 180 m, 189 m to 225 m below ground level, marked in Table 7.13. There is a small zone of granular sediments below 240 m but to its small extension, this zone is not discussed further as it may not have any importance as a potential aquifer. If desired, the tube well assembly may be lowered with strainer position between 160.50 m to 178.50 m and 191 m to 222 m for moderate to good quality and quantity of groundwater. The portion of bore hole near 150 m may be sealed by cement or sticky clay to restrict impregnation of saline water from above.

Table 7.14: Lithology of Borehole No. 20 at Mukutshila Tubewell 2.

Stratum	Depth range (m)	Nature of formation	Hydraulic conductivity (m/day)	Remarks
1	00.00 to 3.04	Surface subsoil	4.21×10^{-5}	-
2	3.04 to 12.06	Clay sticky	4.1×10^{-5}	-
3	12.06 to 36.81	Fine sand brownish	4.1×10^{-1}	-
4	36.81 to 41.33	Fine sand mixed with clay	4.1×10^{-5}	-
5	41.33 to 50.71	Clay sticky	4.43×10^{-5}	-
6	50.71 to 64.73	Sand very fine light yellow	4.2×10^{-5}	-
7	64.73 to 80.49	very fine Sand	4.3×10^{-1}	-
8	80.49 to 97.03	Sand medium brownish	4.2×10^{-1}	-
9	97.03 to 106.41	Sandy clay	1.94×10^{2}	-
10	106.41 to 111.08	Sand medium brownish	2.92×10^{2}	-
11	111.08 to 129.02	Sand fine mixed with gravel	1.84×10^{2}	(Zone A)
12	129.02 to 142.97	Sand coarse sticky clay	1.94×10^{2}	-
13	142.97 to 156.87	Clay dark grey little sand	4.2×10^{-5}	-
14	156.87 to 170.92	Sand coarse	4.22×10^{-5}	(Zone B)
15	170.92 to 180.02	Sand fine grey	3.84×10^{2}	-
16	180.02 to 192.64	Clay sticky	4.2×10^{-1}	-
17	192.64 to 224.35	Sand very fine light yellow	4.24×10^{-1}	-
18	224.35 to 233.47	Sand coarse yellowish	3.64×10^{2}	(Zone C)
19	233.47 to 242.39	Sand medium	1.67×10^{2}	-
20	242.39 to 269.65	Sand coarse grey to light	3.54×10^{2}	-

Analysis of the geophysical data, shown in Table 7.14, clearly reveals that in the logging at depth of 300 m there are mainly three granular zones which contain moderate to good quantity of groundwater. Apart from these, there are other insignificant zones of granular

sediments whose position have been shown in the plate but have not been discussed in the report. The disposition of the three granular zones as stated above is between 105 m to 123 m, 155.4 m to 174 m and 189 m to 285 m. To facilitate discussion these zones have been designated as zones A, B and C respectively as highlighted in Table 7.14.

The interface of saline and fresh water is near 90 m below ground level and granular sediments above this zone contains mineralized water which in all probability unsuitable for human consumption. Further analysis shows that zone A though contain moderate quality of groundwater but this zone is very near to zones of transition and accordingly this zone is not recommended for tapping in this case. Zone B does not show very promising picture as a zone of good source of groundwater. Moreover, there is a change of texture of granular sediments which has made the zone of good source of groundwater further limited apart from its small extension as a whole. Thus, this zone B is suitable for recommendation for tapping.

Table 7.15: Lithology of Borehole No. 21 at Basantia.

Stratum	Depth range (m)	Nature of formation	Hydraulic conductivity (m/day)	Remarks
1	00.00 to 4.57	Top soil clay	4.1×10^{-5}	-
2	04.57 to 14.81	Very fine sand light black	4.2×10^{-1}	-
3	14.81 to 52.60	Fine sand brown	4.23×10^{-1}	-
4	52.60 to 105.05	Clay with sand blackish	4.1×10^{-3}	-
5	105.05 to 123.85	Coarse sand	3.84×10^{2}	-
6	123.85 to 152.13	Clay with sand greyish	4.1×10^{-2}	-
7	152.13 to 165.96	Fine to medium sand greyish	4.2×10^{-1}	-
8	165.96 to 179.87	Fine sand light yellow	4.1×10^{-1}	-
9	179.87 to 203.27	Fine sand greyish	4.3×10^{-1}	-
10	203.27 to 226.47	Fine to medium sand greyish	4.1×10^{2}	-
11	226.47 to 258.70	Medium to coarse sand light yellow	1.84×10^{2}	(Zone A)
12	258.70 to 299.08	Clay light grey	4.2×10^{-5}	-

As shown in Table 7.15, in the logging depth of 286 m, there are several zones containing granular sediments of different texture. The dispositions of these zones are shown. The interface of fresh water and saline water is near 87 m below ground level. Groundwater above this zone is saline and should not be tapped for human consumption. The zones after 90 m are suitable for tapping for medium to good quality of groundwater. The entire bore hole is covered by granular sediments of different texture and in true sense there is no clay barrier. The zone after 90 m to 120 m may not be tapped in the present case as it is near the saline boundary. The portion between 210 m to 240 m below ground level is good quality and quantity of groundwater for tapping. To prevent percolation of contaminated water from above the portion between 114 m to 132 m may be sealed by cement or sticky clay.

7.7.1 Bore Hole Location at Baghaput, Junput and Sofiabad, Contai

After each standard penetration test, sufficient quantities of disturbed samples have been collected from split spoon sampler. Disturbed samples have been also collected from auger when it is operated. These samples have been preserved in the polythene packets. Labelled properly and sent to laboratory for identification and testing [Figure 7.19].

7.7.2 Sub Soil Characteristics of Coastal Area of Purba Midnapur

The sub soil of the location as revealed by the present investigation may be broadly divided in the following strata [Figures 7.20-7.21].

Stratum-IA: This stratum consisting of very loose yellowish grey silt fine sand. This layer is found only for borehole (B.H.) 2 and started from the ground level for B.H. 2 and continued up to the maximum depth of 0.08 m for the same bore hole. The average thickness of this stratum may be taken as 0.08 m approximately. The soil in this stratum is non cohesive in nature with no plasticity. The angle of internal friction (ϕ) of soil for this layer may be taken as 28^0.

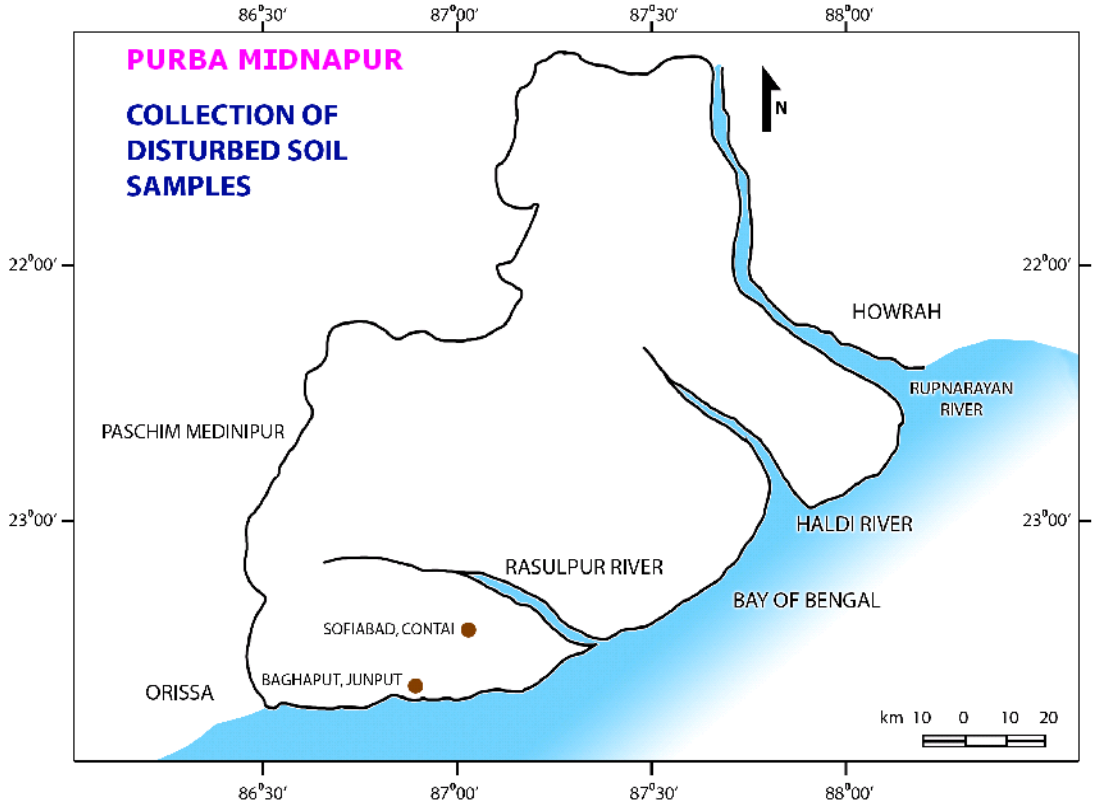

Fig. 7.19: Disturbed soil-sample location at Baghaput, Junput and Sofiabad, Contai.

The Poisson's ratio (μ) for this layer may be taken as 0.30. The relative density of this layer (D_γ) may be taken as 20%. This layer will undergo mainly immediate settlement under imposed load if any. The bulk density of soil for this layer may be taken as 1.80 t/m^3 on an average.

Standing water level: Standing water level for this location is taken. During the fieldwork, the average standing water level at the borehole location is found on an average of 1.89 m below the existing ground level. Tables 7.16-7.18 show the soil characteristics at boreholes locations in Baghaput School, Junput. Here auger boring was done of 200 mm bolehole diameter. At B.H. locations 1, 2 and 3 measured groundwater levels were 1.95 m, 1.87 m and 1.95 m, respectively.

Table 7.16: Soil characteristics at B.H. 1

Sl. No.	Stratum symbol	Depth range (m)	Description of stratum
1	I	0.0 - 4.0	Soft to medium light yellowish grey or light Bluish grey silty clay.
2	II	4.0 - 22.0	Medium whitish grey silty fine sand. Some percentage of clay found at 15.00 m and 18.00 m depth.
3	III	22.0 - 30.6	Stiff to very stiff light yellowish grey sandy clay.

Table 7.17: Soil characteristics at B.H. 2

Sl. No.	Stratum symbol	Depth range (m)	Description of stratum
1	AI	0.0 - 0.8	Very loose yellowish grey silty fine sand.
2.	I	8.0 - 2.8	Medium whitish grey silty fine sand. Some percentage of Clay found at 15.00 m & 18.00 m depth.
3.	II	2.8 - 13.0	Medium whitish grey silty fine sand.
4.	III	13.0 - 30.6	Stiff to very stiff light yellowish or bluish grey sandy silty clay.

Table 7.18: Soil characteristics at B.H. 3

Sl. No.	Stratum symbol	Depth range (m)	Description of stratum
1	I	0.0 - 3.5	Soft to medium light yellowish grey or light Bluish grey silty clay with sand
2.	II	3.5 - 13.0	Medium whitish grey silty fine sand.
3.	III	13.0 - 30.6	Stiff to very stiff light yellowish or bluish grey sandy silty clay.

Stratum-I: This stratum is basically a soft to medium light yellowish/ bluish grey silty clay layer with mixture of some percentage of sand. This layer started from ground level for B.H. 1 and B.H. 3 but from 0.80 m for B.H. 2 below the existing ground level and continued up to a maximum depth of 4.00 m depth for B.H. 1 below the existing ground level. The average thickness of this layer may be taken as 3.17 m. The soil in this stratum is cohesive in nature and of high plasticity character. As per IS classification this layer may be named as CI type. The bulk density of soil for this layer may be taken as1.83 t/m^3 on an average.

Stratum-II: This stratum consisting of medium whitish grey silty fine sand. Some percentage of clay is found between 15.00 to 18.00 m depth below the ground level for B.H. 1 only. This layer is started from the minimum depth of 2.80 m for B.H. 2 and continued up to the maximum depth of 22.00 m for the B.H. 1. The average thickness of this stratum may be taken as 12.57 m approximately. The soil in this stratum is non cohesive in nature with no plasticity. Field N value varies from 4 to 50 m. The angle of internal friction (ϕ) of soil for this layer may be taken as 32° The Poisson's ratio (μ) for this layer may be taken as 0.30. The relative density of this layer (D_γ) may be taken as 45%. This layer will undergo mainly immediate settlement under imposed load if any. The deformation modulus of soil (E_d) for this layer may be taken as 1683.50 t/m^3. The bulk density of soil for this layer may be taken as 1.88 t/m^3 on an average.

Stratum-III: This stratum consisting of stiff to very stiff yellowish/bluish grey sandy silty clay/sand clay layer. This layer is found to exist from a minimum depth of 13 m for B.H. 2 and B.H. 3 only below the existing ground level and continued upto the full depth of exploration i.e. 30.6 m. The average thickness of this layer may be taken as 14.55 m. The soil in this stratum is cohesive in nature having intermediate to high plasticity characteristics. This layer posses only unconfined cohesion (C) but no angle of internal friction ($\phi=0^0$). From the laboratory test, the C value of this layer may be taken as 10.02 t/m^2 from the unconfined compression test on undisturbed and remoulded soil samples. The bulk density of soil for this layer may be taken as 1.89 t/m^3 on an average.

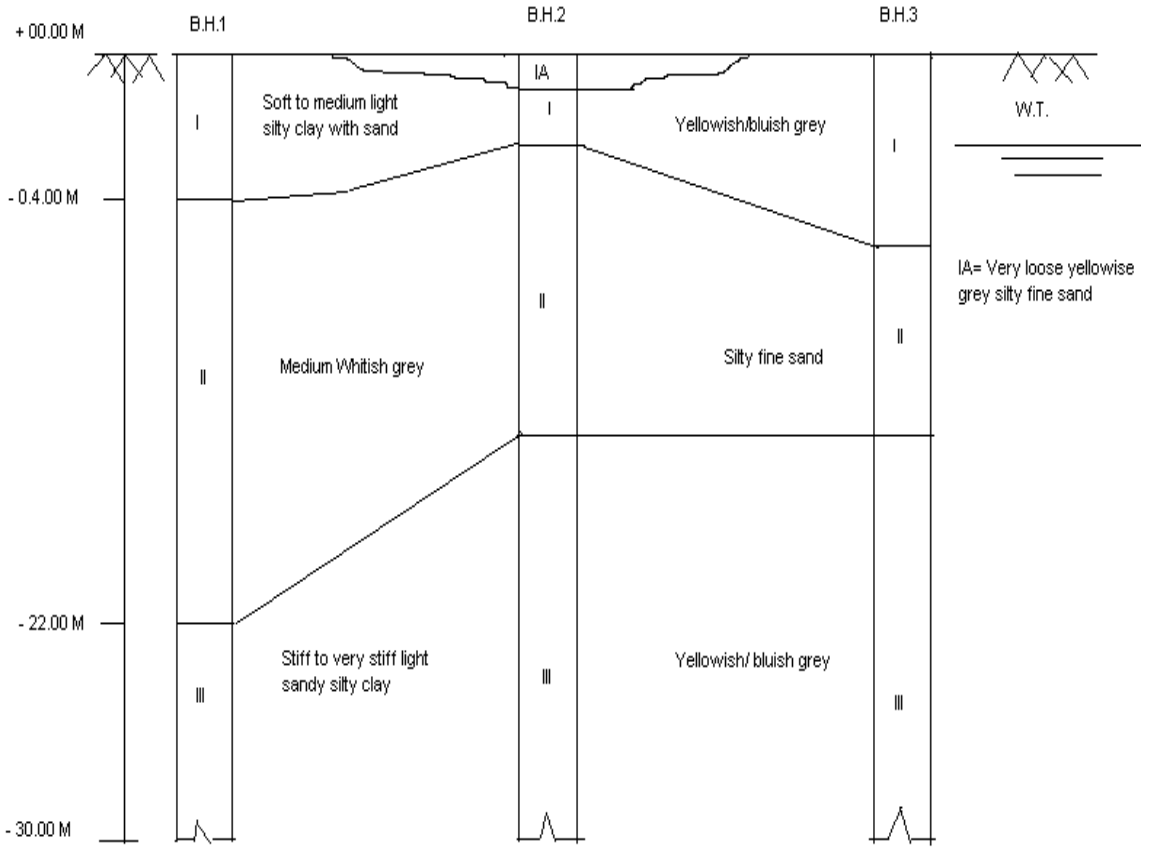

Fig. 7.20: Sub-Soil profile log at Baghaput, Junput, Contai.

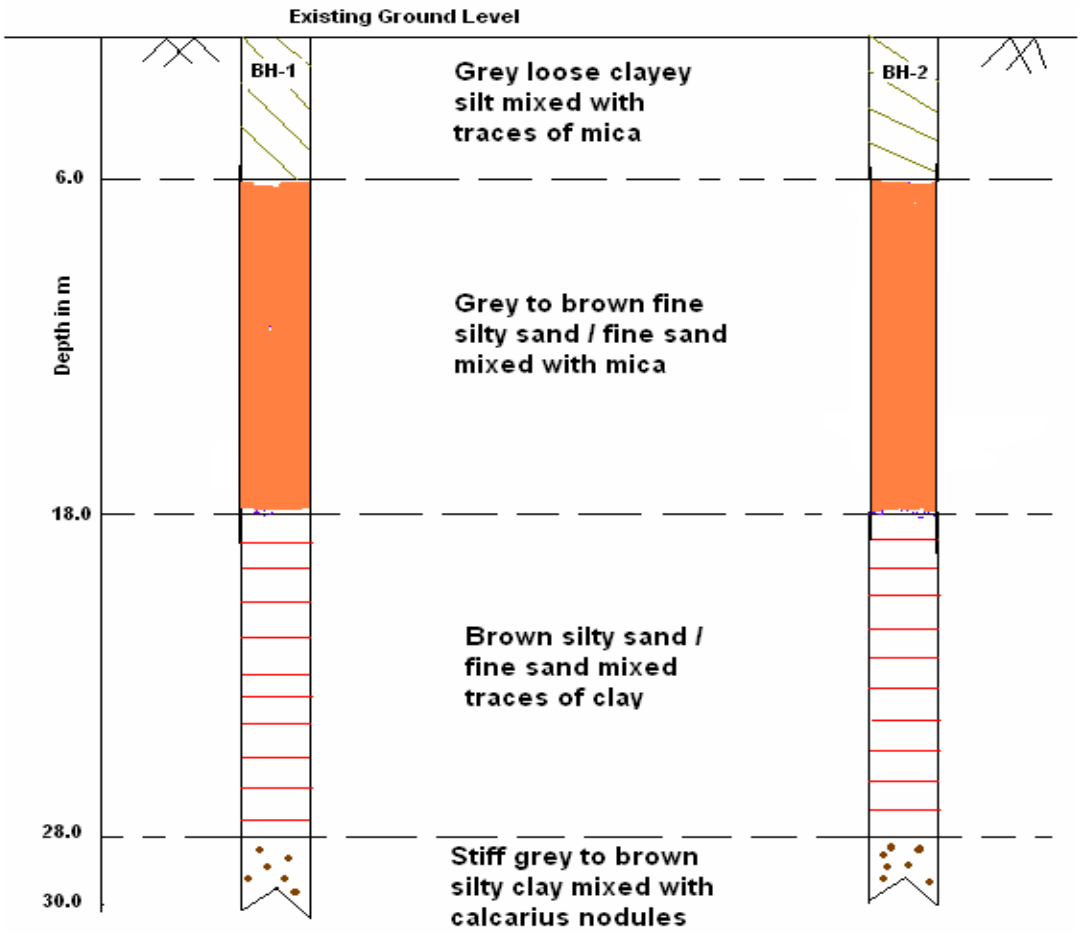

Fig. 7.21: Sub-soil profile log at Sofiabad, Contai.

7.8 Hydrogeology of Purba Midnapur

The aim of the present study is to bring out the stratigraphy, strength characteristics of the sub soil and hydrology of the site, by conducting borehole studies including in-situ tests and laboratory investigations at Baghaput water supply scheme in Purba Midnapur. The area belongs to the southern part of the largest delta of the world. This delta was formed by the deposits from innumerable river systems in the past. Some originated from large track of Himalayan Mountains, some from the old peninsular on the West and some from Garo hills on the east. The long stretch of the Indo-Gangetic alluvial plains culminated in to the great delta of Bengal, formed and extended southwards gradually by the river systems of mighty Ganga-Brahmaputra and their tributaries [Figure 7.23]. The sub-surface deposits in the region thus represent typical deltaic characters comprising sands, silts and clays with some sporadic organic concentrations down to great depths. To be precise, it can be mentioned that this region contains two types of deposits as (i) The normal silty clay deposits formed under back swamp condition, which cover most of the area, (ii) the sandy river belt deposits left by the ancient meandering rivers which occurs in stretches.

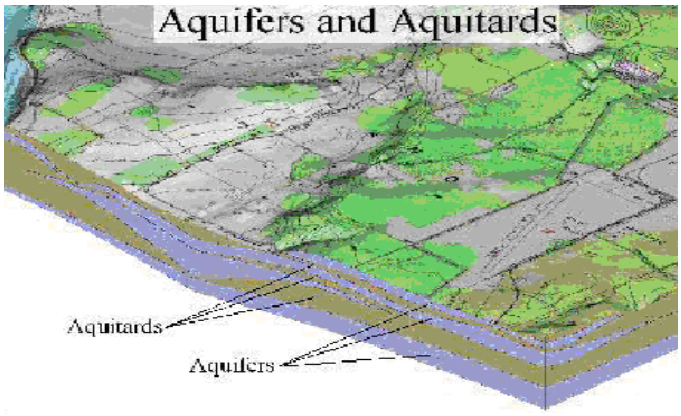

Fig. 7.22: Example of spatial variation of aquitards and aquifers.

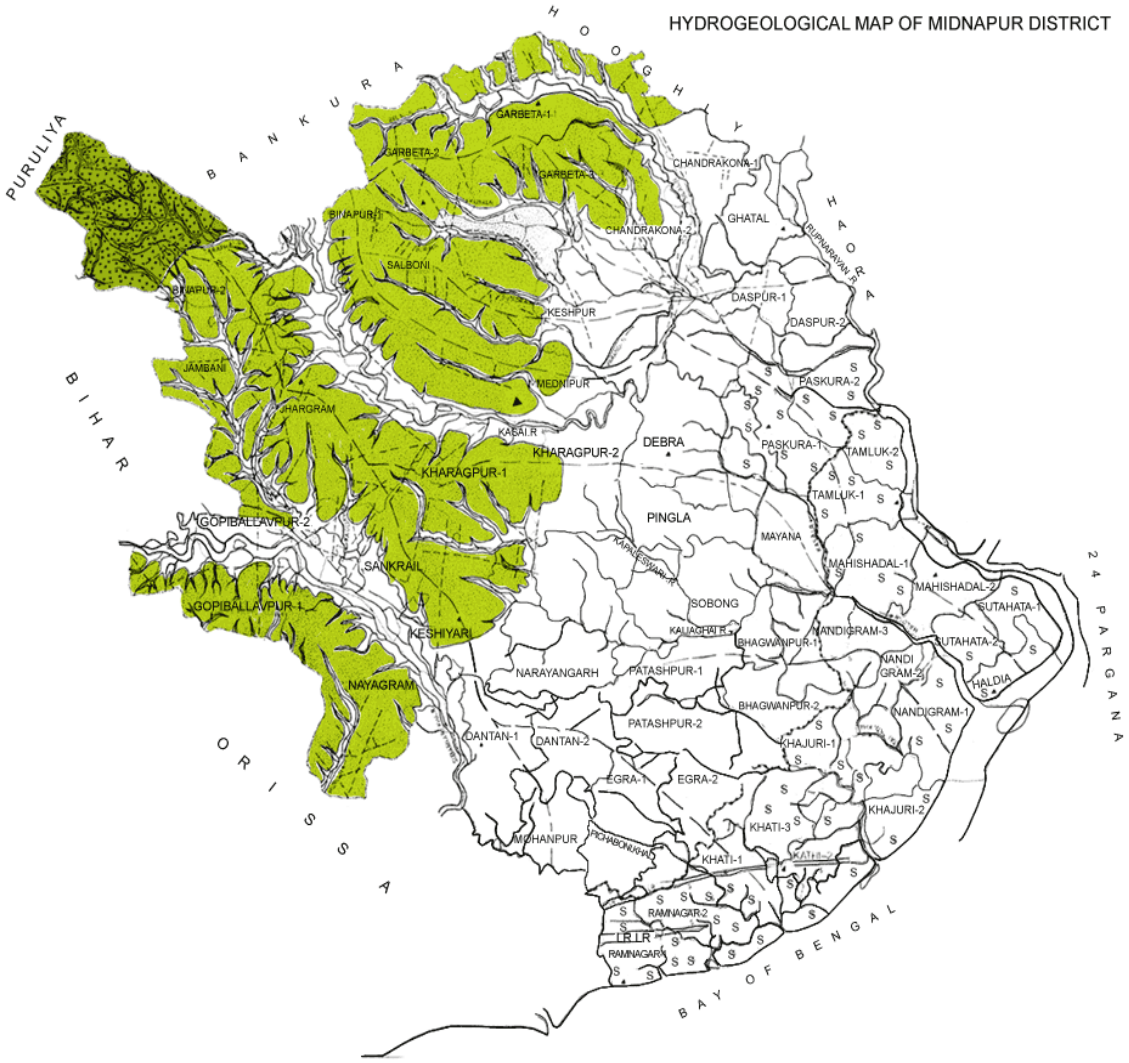

Fig. 7.23: Hydro-geological map of Midnapur (NATMO, 2013).

An example sketch is given in Figure 7.22 showing aquifers and aquitards which vary spatially in both thickness and elevation. There might be a quite few aquifers introduce and every aquifer will have diverse hydraulic features attributes (recharge, pressure, capacity and so forth) and propensity to saline water ingression. The pressure driven qualities can change altogether starting with one area then onto the next, even inside a solitary aquifer. This inconstancy and multifaceted nature of our groundwater framework presents vulnerability in fathoming antagonistic circumstances. As a result, water resource planning and management efforts have primarily relied on review of water use proposals on an individual site specific basis.

7.8.1 Groundwater Level in 2014

Groundwater improvement and administration considers in parts of Purba Midnapur district has been attempted to think about the expansion of saline aquifers and impact of high tsunamis on phreatic aquifers and to consider the effect of extensive scale groundwater improvement on groundwater management including saline water intrusion. Groundwater level in Purba Midnapur district changes from 3 to 14 m below ground level for the period of pre monsoon period [Figure 7.25] and 4-12 m below ground level in post monsoon period [Figure 7.26], beneath the sand dune clay bed happen down the profundity of 70 m below ground level level. Adjustment of sand and clay bed happens down to a profundity of 450 m below ground level. By and large salty water found in every one of the aquifers underneath sand ridges up to the profundity of 450 m below ground level over a little region around Contai. Fresh water aquifer is located inside 120 to 300 m below ground level towards south east of Contai in Mukundpur, Baijapur and Sophiabad. The hydro geological/geochemical condition in coastal tracts of Purba Midnapur is shown in Figure 7.24.

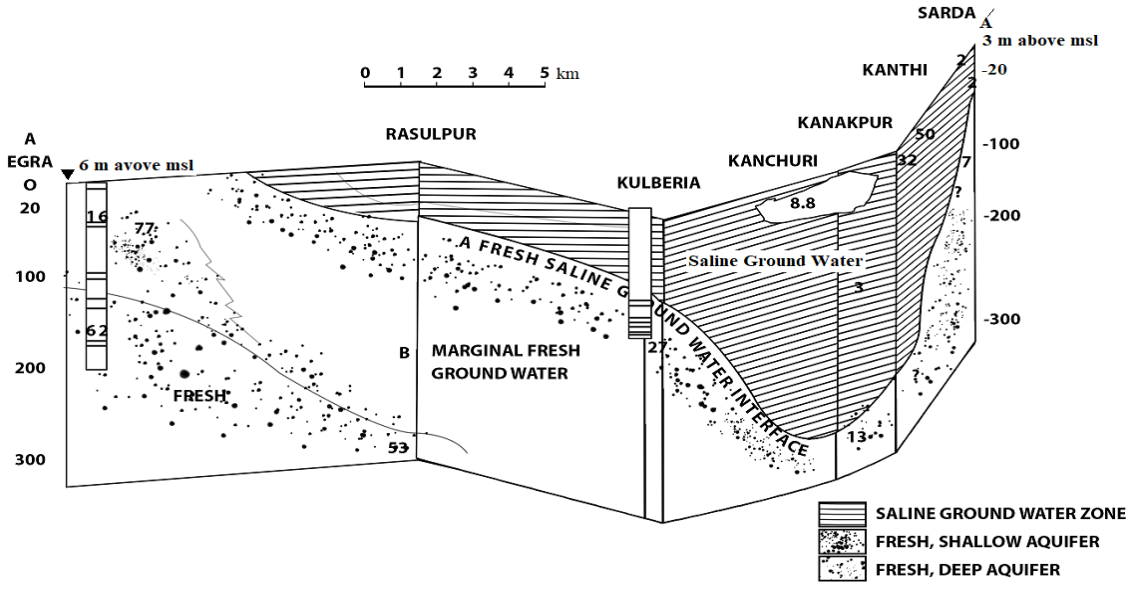

Fig. 7.24: Hydro geological/geochemical condition in coastal tracts of Purba Midnapur.

- Fresh water is deficient in a few places in the definite investigation zone of Contai I, II and III blocks where the tube well is not possible because of high saline content.

- Desiltation of existing lakes in Contai territory is recommended.
- Construction of new lakes in the waste land zone.

Haldia Industrial Complex in Purba Medinipur district has been informed, subsequently aimless withdrawal of groundwater has been limited. Haldia Development Authority has masterminded to supply the surface water to take care of the water demand. Hence, roof top rain water harvesting structures should be adopted for conservation of rain water in industrial sector for non drinking purposes.

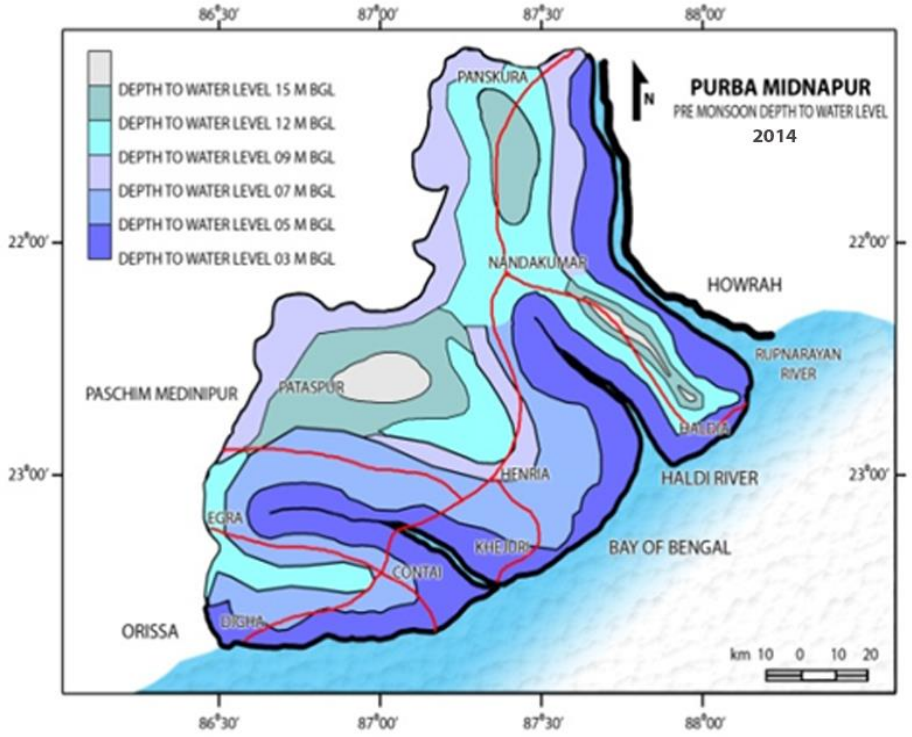

Fig. 7.25: Pre-monsoon groundwater level contours.

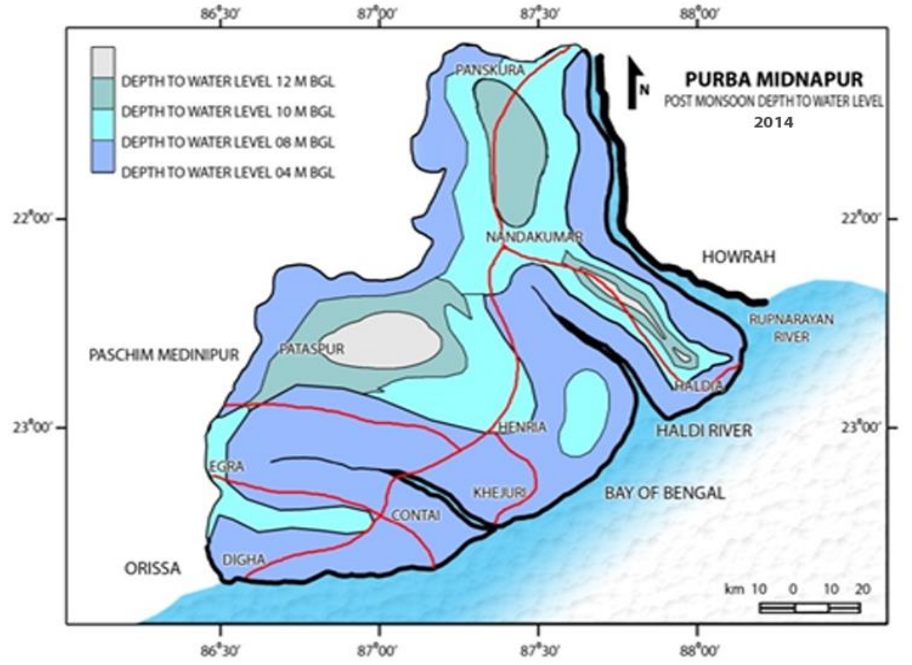

Fig. 7.26: Post-monsoon groundwater level contours.

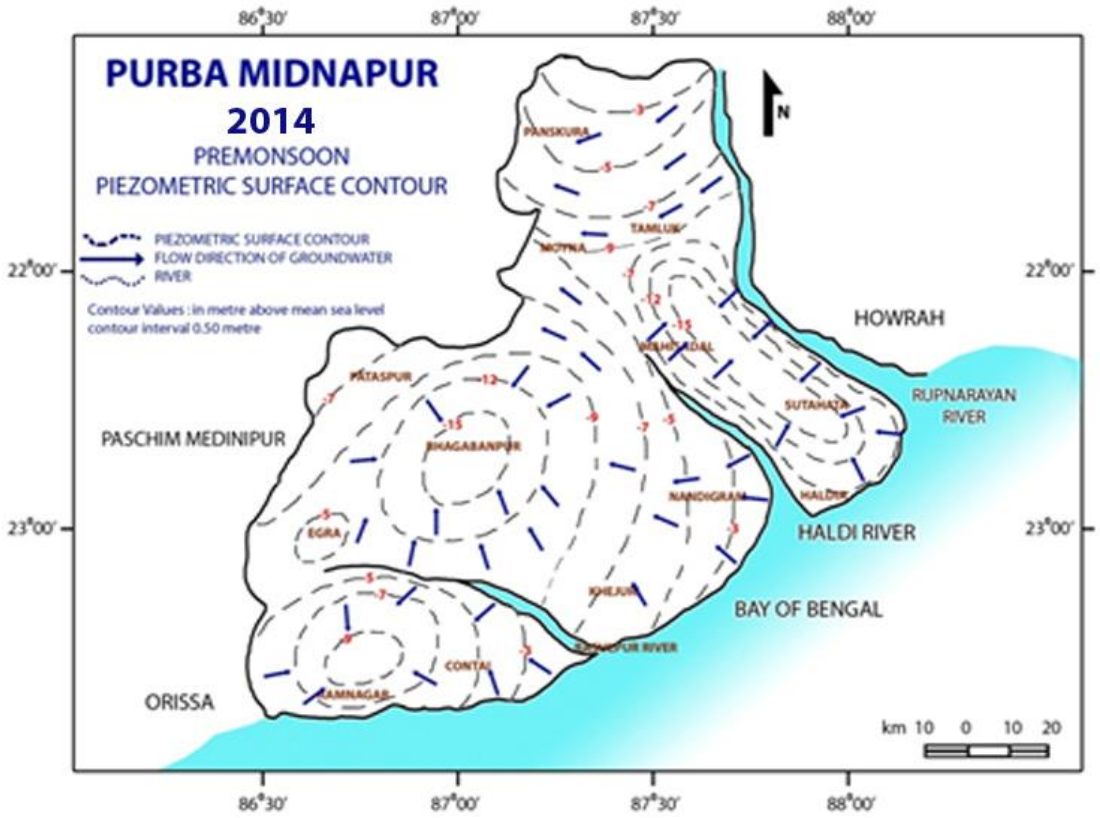

Fig. 7.27: Pre-monsoon piezometric surface contours.

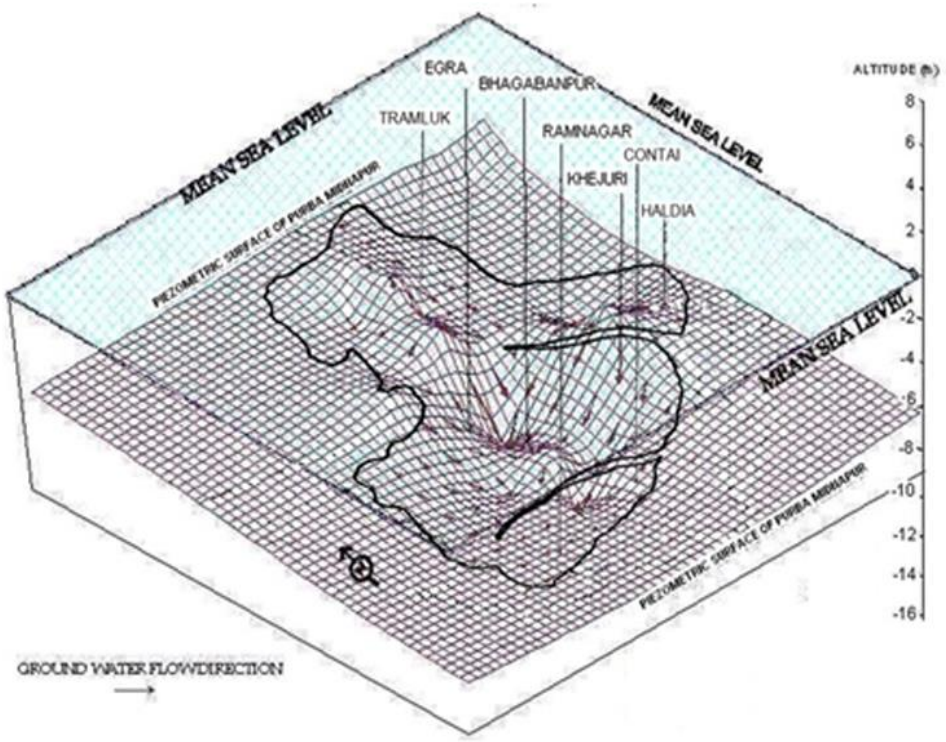

Fig. 7.28: Three dimensional view of piezometric surface during pre-monsoon, 2015.

7.8.2 Results and Discussion

For the year 2014 and 2015 [Figures 7.27-7.28], the pre-monsoon piezometric surface contours demonstrate depressions close Ramnagar, Bhagbanpur and Sutahata. In the predominant climatic situation in the zone, the pre-monsoon condition is extreme added critical at the post- monsoon condition. Consequently, assessment of the potential for salinisation is completed considering the pre- monsoon condition. It is obvious that the Ramnagar region which incorporates the traveller resort of Digha and the town of Contai, is extremely inclined to saline water ingression just like the Sutahata territory which incorporates the modern town of Haldia. Prompt and pressing measures are expected to push back saline water intrusion in these zones.

7.9 Seawater Intrusion towards Piezometric Surface

The main components and relationships between fresh and saline water in the coastal zone of Purba Midnapur district are assumed as follows:

- The presence of a saline front and lenses of fresh water in the upper aquifer.
- The presence of a saline wedge in deeper aquifers.
- The existence of hydraulic continuity between groundwater and saline water where most important cases are (a) and (b), as shown diagrammatically in Figure 7.29(a) and the distribution in the groundwater is shown in Figure 7.29(b).

The saline front is controlled in the upper aquifer (case a) by regional flow of groundwater towards the sea as well as the prevailing recharge conditions. Fresh water lenses may form in this ‘case a’, overlying the saline water. Minor seasonal changes may take place in these relationships between fresh and saline water only under natural conditions. Major abstraction has of groundwater may change this phenomenon adversely. Excess abstraction of groundwater, for irrigation upstream, will cause the movement of saline front inland, consequence of which pumping of brackish and saline groundwater in more southerly wells will be beginning. In the same manner, excess withdrawal or badly planned abstraction of water from the fresh water lenses will cause upconing of saline water and with the effect of making wells go saline. Digha, Khejuri, Nandigram and Contai are already facing these problems where saline intrusion is also occurring in the deeper aquifer. Problem is less significant in the ‘case b’ regarding the relationship between groundwater and saline river water. In this ‘case b’ the interchange of fresh water in the river and the groundwater is very low because:

- The hydraulic gradient between the two is low.
- Upper aquifer hydraulic conductivities are also comparatively low.

Thus while dry season groundwater abstraction takes place in a time when river water salinity is at its highest in upstream waters, there is no guarantee that it will be drawn into nearby wells. Also, because there is a base flow recession between October and January, any incoming saline water is likely to be flushed back out again.

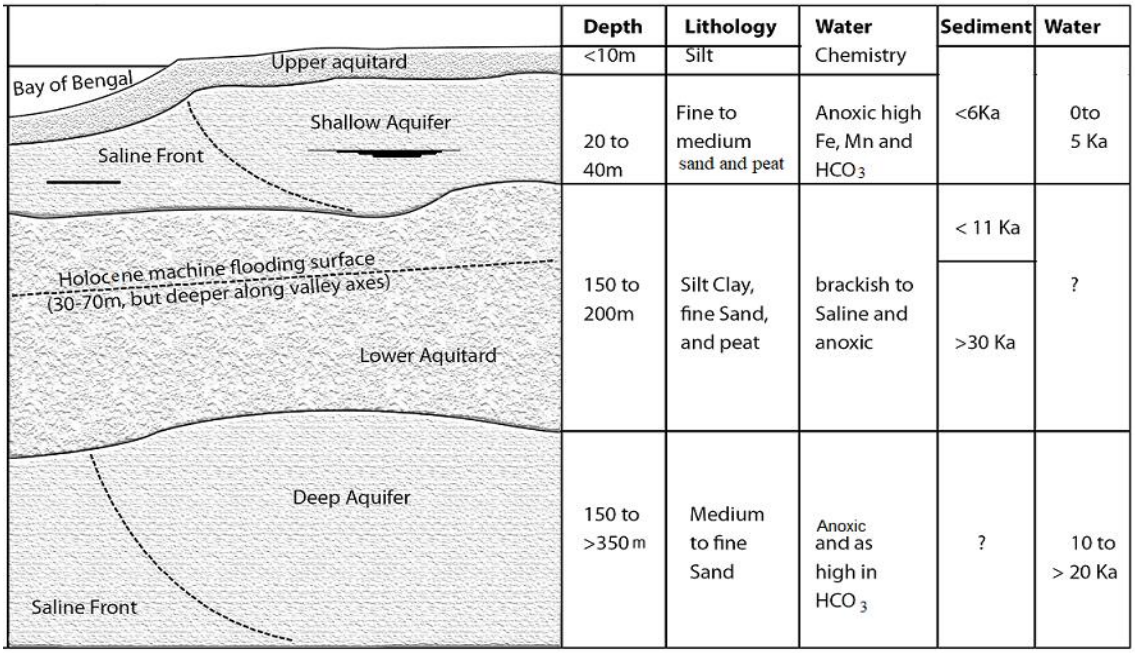

	Depth	Lithology	Water Chemistry	Sediment	Water
Upper aquitard	<10m	Silt			
Shallow Aquifer	20 to 40m	Fine to medium sand and peat	Anoxic high Fe, Mn and HCO_3	<6Ka	0to 5 Ka
Lower Aquitard	150 to 200m	Silt Clay, fine Sand, and peat	brackish to Saline and anoxic	< 11 Ka >30 Ka	?
Deep Aquifer	150 to >350 m	Medium to fine Sand	Anoxic and as high in HCO_3	?	10 to > 20 Ka

Fig. 7.29: (case a) Schematic of aquifer stratigraphy in the coastal zone of Purba Midnapur.

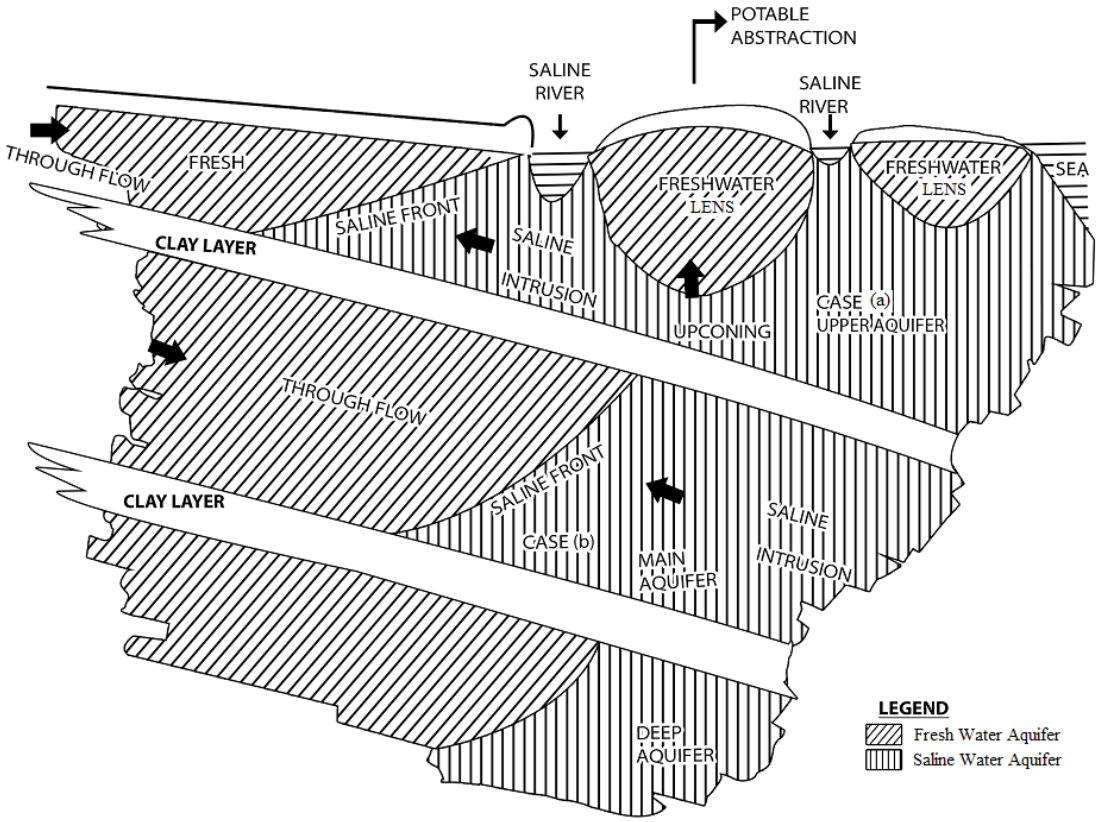

Fig. 7.29 (case b): Salinity distribution and process in the coastal zone of Purba Midnapur.

7.10 References

Barlow, P.M. (2003). Ground Water in Freshwater-Saltwater Environments of the Atlantic Coast. Circular 1262, U.S. Geological Survey, Reston, Virginia, USA.

Davis, S.N. (1969). Porosity and permeability of natural materials in DeWiest, R.J.M., ed., *Flow through porous media*. Academic Press, New York, USA, pp. 54-89.

Heath, R.C. (1984). Groundwater Regions of United States. *U.S. Geological Survey Water Supply Paper* 2242, p. 78.

Johnson, A.I. (1967). Specific yield--compilation of specific yields for various materials. *U.S. Geological Survey Water Supply Paper* 1662-D.

Krause, R.E. and Randolph, R.B. (1989). Hydrology of the Floridan aquifer system in southeast Georgia and adjacent part of Florida and South Carolina. *US Geological survey professional paper* 1403-D, p. 65.

Morris, D.A. and Johnson, A.L. (1967). Summary of hydro- logic and physical properties of rock and soil materials, as analyzed by the Hydrologic Laboratory of the U.S. Geological Survey, 1948-60. *Geological Survey Water-Supply Paper* 1839–D, p. 42.

NATMO (2013). NATMO Publications. National Atlas and Thematic Mapping Organisation. Department of Science and Technology, Government of India.

Sun, R.J., and Johnson, R.H. (1994). Regional aquifer system analysis program of the U.S. Geological Survey, 1978-1992: *U.S. Geological Survey Circular* 1099, p. 126.

Terzaghi, K. (1943). Theoretical Soil Mechanics, Wiley, New York, USA.

Todd, D.K. (1980). Groundwater Hydrology. (Second edition). Wiley, New York, USA

Wenzel, L.K. (1942). Methods for Determining Permeability of Water Bearing Materials, with Special References to Discharging Well Methods. *U.S. Geological Survey Water Supply Paper* 887, p. 192.

CHAPTER - 8

(Simulation of Groundwater Levels)

- Background
- Introduction
- Survey of Literatures
- The Study Area
- Numerical Modelling
- About MODFLOW
- Input Data Description
- Simulation GWLs for 2012
- Comparison between Simulated and Actual GWLs for 2012
- Simulated GWLs for 2019-2023 based on 2002 Data
- Simulated GWLs for 2019-2023 based on 2012 Data
- Correlation Coefficient
- Simulated GWLs for 2019-2023 based on 2002 and 2012 Data
- Prediction of Groundwater Flow Path
- Significant Remarks
- References

8.1 Background

The Groundwater modelling tool is a significant tool for solving many groundwater related problems. Visual MODFLOW is one of such tool that utilizes a finite difference method to answer the problems. In this chapter Visual MODFLOW 2000 software has been utilized to study the groundwater level simulation in Purba Midnapur district of West Bengal in India. The data of pumping well discharge has been collected at two different time period of 2002 and 2012 from Public Health Engineering Department under Government of West Bengal. The simulated data for the year 2012 based on the measured data of 2002 and the observed data of 2012 have been compared and a correlation coefficient is found out to signify data validity. Also simulated groundwater level data of 2019 to 2023 based on well discharge data of 2002, 2012 and combined data of 2002 and 2012 have been correlated for its justification. The groundwater flow occurs from south to north direction of Purba Midnapur, as the saline water intrusion from the Bay of Bengal takes place into the aquifers towards inland direction. In the real field situation saline water encroachments have affected the aquifers and it has covered up to 50 km of location from Kalindi (near sea shore) to Nandakumar (inland) location. This chapter focuses on the prediction of future groundwater levels (GWLs) as a potential groundwater management scenario in the region concern.

8.2 Introduction

Groundwater modelling is a technique that can examine numerous groundwater issues. Numerical groundwater tool is a significant tool for many hydrologists. Presently numerous programs have been developed as a part of groundwater modelling. A model might be easy version of an actual globe system; the first step in building a model is to make an approximate model. It consists of sets of assumptions that represent real world structural work, the transportation process, the principal process governing them and the significant medium properties.

Next, the reasonable model is deciphered in numerical model through governing equations with related limit and boundary conditions. An answer can be acquired by making an interpretation of it into numerical model and composing a computer programming code for explaining it.

Governing flow equation for MODFLOW:

$$\frac{\partial}{\partial x}\left(K_{xx}\frac{\partial h}{\partial x}\right)+\frac{\partial}{\partial y}\left(K_{yy}\frac{\partial h}{\partial y}\right)+\frac{\partial}{\partial z}\left(K_{zz}\frac{\partial h}{\partial z}\right)+W=S_s\frac{\partial h}{\partial t} \qquad (8.1)$$

where, K_{xx}, K_{yy}, K_{zz} are the hydraulic conductivities along the x, y, z axes which are parallel to the major axes of hydraulic conductivity; h is the piezometric head; W is the volumetric flux per unit volume signifying to source/sink terms; S_s is the specific storage coefficient characterized as the volume of water discharged from storage per unit change in head per unit volume of porous material.

MODFLOW software is used to simulate the aquifer frameworks where (a) the flow is in saturated condition, (b) Darcy's law applies, (c) the density of groundwater is constant, and (d) the principal direction of hydraulic conductivity or transmissivity does not change within the aquifer framework. These types of situations are met in numerous aquifer frameworks for which groundwater flow analysis is very much significant. For these kinds of systems - simulation can be done using MODFLOW software for a wide range of hydrologic characteristics and processes.

Consistent state and transient stream can be simulated in unconfined aquifers, confined aquifers, confining units. An assortment of highlights, for example, reservoirs, channels, rivers, springs, wells, evapo-transpiration and recharge from precipitation and irrigation can also be simulated. At least four different solution methods had been implemented to answer the numerical methods involving finite difference equations. The accessibility of diverse approaches permits the customer to adopt most efficient approach to solve numerical equations.

MODFLOW software simulates groundwater flow in aquifer frameworks utilizing the finite difference method. In this strategy an aquifer framework is separated into rectangular squares by a lattice as appeared in Figure 8.1. The grid of block is organized by rows, columns and layers and each block is commonly called a 'cell'.

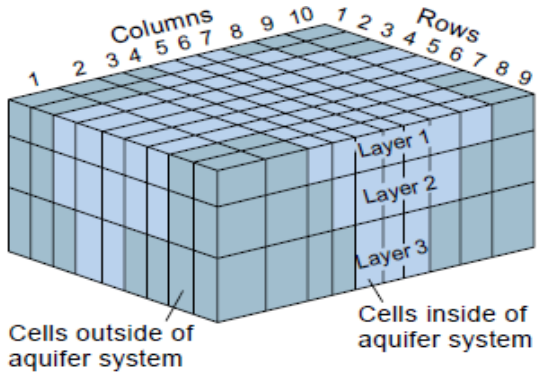

Fig. 8.1: Example of model grid for three dimensional groundwater flows.

For every cell inside the volume of the aquifer framework, the client must indicate the aquifer properties likewise the client must determine data identifying with wells, waterways and other inflow outflow characteristics for cells comparing to the position of the features. MODFLOW utilizes the contribution to develop to settle conditions of the groundwater stream in the aquifer framework. The arrangement comprises of head (groundwater level) at each cell in the aquifer framework (aside from cells where head is indicated as known as input data sets) at interims known as 'time steps'. The head can be printed or put away in a computer storage appliance for any time step. Hydrologists normally utilize water levels from a model layer to develop form maps for assessment with comparative maps from field information. They also evaluate calculated groundwater levels at various places within the cells with the observed field data to estimate model error. The procedure of adjusting model input values to reduce model

error is mentioned to as model calibration. Notwithstanding water levels, MODFLOW computes a water budget plan for the whole aquifer framework. The budget records inflow and outflow of the aquifer framework for all hydrologic characters that include or expel water.

8.3 Survey of Literatures

Groundwater is a growing problem in every part of our country. Because of enlarged population, industries, and simultaneously increased demand groundwater is suitable insufficient and groundwater level is becoming lower day by day.

The review of previous researches has been done on a global basis with due emphasis given on Indian scenario. The important contributions from different scientists on groundwater simulation using MODFLOW are discussed here.

Toth (1963) discovered hypothetically the presence of hierarchically nested groundwater stream frameworks like local, intermediate and regional. They also investigated that the recharge at different depths, isotropic environmental conditions, vegetations, hydrochemistry and surface water flow pattern. Freeze and Witherspoon (1966) were the first to use in three dimensions in heterogeneous, anisotropic conditions, investigate water table configuration. They estimated hydraulic conductivity and also found out the discharge and recharge from a basin. Freeze (1971) prepared a transient unsaturated model to research the connection between penetration rates, water table ascent and base stream hydrograph and furthermore to examine the most extreme basin yield under recharge and discharge conditions. Sun and Johnston (1994) estimated to illustrate flow framework and simulate the groundwater flow to observe the changes in land use and groundwater development.

Computer models were practiced in almost all cases where United States Geological Survey (USGS, 2000) three dimensional finite difference models (Trescott, 1975) and the USGS MODFLOW models (McDonald and Harbaugh, 1988) were applied. Jin-Sheng *et al.* (2002) built up a three dimensional groundwater stream model to simulate the region's groundwater flow through a limited distinct strategy utilizing Visual MODFLOW groundwater simulation interface.

Based on the parameters for the calibrated model, the agricultural water saving potentiality and its influence on the groundwater were analysed. Al-Salamah *et al.* (2011) used MODFLOW model for the Saq Aquifer in Buraydah area of Saudi Arabia. From this model results significant cone of depression was found if the excessive pumping rates for that condition prevail. This management scheme was recommended to adopt for the future protection of groundwater resources in Kingdom of Saudi Arabia. Dhar *et al.* (2009a-e, 2010) and Das *et al.* (2014) worked on the impact on groundwater due to saline water intrusion in coastal regions of South 24 Parganas in West Bengal. Since long years back, the coastal areas of Purba Midnapur was located near lower region of Rajmahal and Singbhum. The coastal area of Purba Midnapur was constructed by stratified layers which are framed through the deposition of sediments and stones in

years after years carrying through Ganga, Bhagirathi and other rivers. In some previous literatures it was discussed that groundwater recharging will be increased due to increase in rainfall.

Gao (2011) had approached and proved that using of MODFLOW can make the model numerically steady and more effective. Numerous lines of confirmations for model calibrations ought to be examined when demonstrating groundwater stream frameworks with complex conditions to guarantee the exactness and illustration of the model. Ismail *et al.* (2013) had developed a horizontal well or radial collector well establishment in shallow aquifers to develop water withdrawal rates in Pintu Geng well field in Kelantan, Malaysia and simulated utilizing the drainage package of Visual MODFLOW groundwater model. An ideal pumping rate was considered during modelling. The result accomplished the desired drawdown of under 2 m in a region of 300 m encompassing the Pintu Geng horizontal collector well.

Takounjou *et al.* (2011) did the detail modelling of groundwater flow and particle tracking to determine the groundwater flow and molecule movement in the shallow unconfined aquifer of the Upper Anga'a waterway watershed. A steady state groundwater stream simulation was completed utilizing Visual MODFLOW programming. Malik *et al.* (2012) calculated to coordinate the watched drawdowns with model computed drawdowns utilizing distinctive estimations of aquifer parameters in the Gurgaon district of Haryana state in India using MODFLOW. Varalakshmi *et al.* (2014) had built up a three dimensional groundwater stream model for the Osmansagar and Himayathsagar catchments - a semiarid hard shake rock zone in India with two reasonable layers. Under transient conditions utilizing visual MODFLOW programming for the period 2005 to 2009, the 15-20 m top layer was a weathered zone, trailed by second 20-25 m layer cracked zone in view of hydro-geophysical examinations and borehole lithologs.

Lakshmi and Narayanan (2015) had revealed the suitability of MODFLOW software under various hydro-geological conditions. MODFLOW is easy to analyze the two dimensional, three dimensional groundwater flow system. Lasya and Inayathulla (2015) had built up a model for Jakkur catchment in Bangalore city. The model was kept running in both steady state and transient stream conditions. The model was calibrated by changing the hydraulic conductivity esteems by experimentation technique. Their model additionally demonstrated the anticipated versus watched groundwater head. They additionally created zone budget. Korkmaz *et al.* (2016) determined using MODFLOW under Groundwater Modelling System (GMS) software.

For adjustment of hydraulic conductivities, the parameter evaluation model was utilized. Through steady-state examination, surge inclined regions were resolved in the city of Eskisehir (Turkey). Singh and Shukla (2016) performed a simulation model using Arc SWAT model inputs in VISUAL MODFLOW groundwater system for parametric, sensitivity analysis with hydraulic conductivity values. Calibrated and approved model additionally utilized for future groundwater level expectations in potential groundwater administration situations in Sai Gomti interfluve district in India.

8.3.1 Inferences from Available Literatures

From the previous section, it is evident that significant researches and development have already been done by various scientists, engineers and researchers at various parts of the globe in the field of analysis. Lakshmi and Narayanan (2015) suggested the appropriateness of MODFLOW software under different hydro-geological conditions. MODFLOW is easy to analyse the two dimensional, three dimensional groundwater flow system. In their study they proposed a grading system and procedure of using MODFLOW software and discussed general procedure for determination of the results. However, the groundwater level simulation of Purba Midnapur district of West Bengal, India for future prediction has not yet studied by using MODFLOW. But in this present study, the use of Visual MODFLOW programming has been done successfully to predict of future groundwater level obtained by simulation 2017 for Purba Midnapur district of West Bengal, India and also comparison of predicted data with existing data had been done successfully.

8.4 The Study Area

The area to be modelled for this study is coastal part of Purba Midnapur. Figure 8.2 shows the exact location of Purba Midnapur. The latitude of the study area is located between 21^0 38' North and 22^0 30' North latitudes and between 87^0 27' East and 88^0 11' East longitudes. The local calculated model has been created for the region with couple of assumptions of aquifer layers and hydraulic properties.

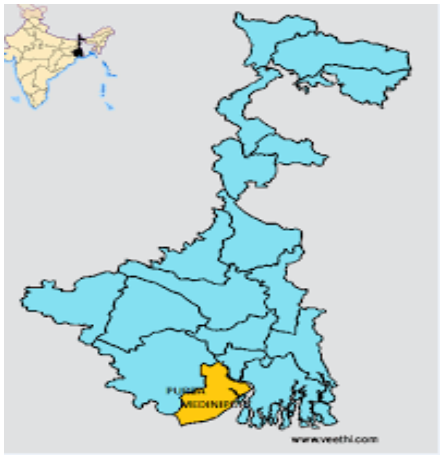

Fig. 8.2: Map showing the location of the **s**tudy area.

Deterministic groundwater models like MODFLOW normally necessitate the solution of partial differential equations. A general type of the condition relating the transient stream of a compressible liquid in a non-homogeneous anisotropic aquifer is obtained by incorporate Darcy's law with the continuity equation. The three dimensional development of groundwater of steady density through permeable medium might be

depicted by the partial differential equation (McDonald and Harbaugh, 1988). A conceptual model is a depiction of aquifer system every now and again as a square chart or cross area. The entire aquifer framework might be comprised of few aquifer layers. The soil types in the study area mostly loamy clay soil, coastal saline soil, clay loamy soil. For the conceptual model it is assumed that silty clayey layer is in between sandy loam layers.

8.5 Numerical Modelling

Groundwater modelling is proficient by utilizing a three dimensional Visual MODFLOW 2000, a modelling program created by United States Geological Survey (USGS). This is the most broadly utilized finite difference groundwater model and considered a standard for groundwater modelling. The advancement of input documents is assembled utilizing Visual MODFLOW a regularly utilized pre-processor of information that is utilized to accelerate and encourage the improvement of the MODFLOW model. The model space was created using 30×30×3 grids. For the entire site, there are 30 rows, 30 columns and three layers with general uniform grid spacing. The wells are modelled using Visual MODFLOW model. Vertically the grids are refined to three layers.

Horizontally finer spacing is considered for well field in Purba Midnapur, with a specific end goal to handle horizontal well designed diameter. The horizontal well refining process is only limited to immediate area around the Purba Midnapur well field. The discretisation of modelled area consists of 30 columns and 30 rows. The area nearby the modelled area is made inactive. Table 8.1 shows the parameters used in Visual MODFLOW software during calibration of the program.

A digitized diagram of the examination region is superimposed on the modelled region as a base diagram. The model composed of three layers. It includes layer I (sandy loam layer which is upper aquifer), layer II (silty clay layer which is an aquitard) and layer III (sandy loam layer which is lower aquifer) in Purba Midnapur coastal areas. The less permeable layer is modelled with reasonable hydraulic conductivity 10^{-7} m/s. A value between 5-20% of yearly precipitation is prescribed as calculate of recharge (Waterloo, 2006).

Based on this regulation, recharge is set equivalent to 12% of normal yearly precipitation after subjection to modification all through the model adjustment and approval created. Visual MODFLOW is run in steady state condition then it calibrates hydraulic heads on a yearly basis. One set of data consists of eight well discharge data for the year 2002 and other set of data consists of 30 well discharge data for the year 2012. Table 1 represents the parameters which were used for the calibrated model. All the wells are within the modelled area. Model calibration basically consists of minimizing the mistake amongst anticipated and watched heads. Recharge rate was 12% of rainfall which is 180 mm/year (Waterloo, 2006).

Table 8.1: Parameters applied for calibration (Ismail *et al*., 2013).

Parameters	Value		
	Zone -I	Zone II	Zone-III
K_x (m/s)	0.006	0.0006	0.006
K_y (m/s)	0.006	0.0006	0.006
K_z (m/s)	0.0006	0.00006	0.0006
S_s	10^{-5}	10^{-5}	10^{-5}
S_y	0.27	0.27	0.27
Recharge	18% of average yearly rainfall = 180 mm		
Total porosity	0.20	0.20	0.20
Effective porosity	0.11	0.11	0.11

Note: K_x or K_{xx} is the hydraulic conductivity towards horizontal direction in m/s, S_y is the specific yield and Recharge indicates rainfall in mm.

8.6 About MODFLOW

Visual MODFLOW is the most total, and easy to understand, demonstrating condition for reasonable applications in three-dimensional groundwater stream and contaminant transport simulation. This completely coordinated package joins great systematic apparatuses with an intelligent menu structure. Simple to-utilize graphical devices enable:

- appropriate allocate model properties and limit conditions
- run display simulations for stream and pollutant transport
- calibrate the model utilizing manual or computerized systems
- optimize pumping and alleviative well rates and areas
- visualize the outcomes utilizing 2D or 3D illustrations.

The model info parameters and results can be pictured in 2D (cross-area and plan view) or 3D whenever amid the improvement of the model or the showing of the outcomes. For complete three-dimensional groundwater flow and contaminant transport displaying, Visual MODFLOW is the best software package accessible.

New Highlights in Visual MODFLOW

- MIKE 11 Integration
- PHT3D Integration
- MT3DMS 5.1 Integration

Pumping Well Optimization

A portion of the normal situations include:

- Limiting the mass expulsion cost of a pump-and-treat groundwater remediation framework while keeping up capture of a contaminant plume.

- Maximizing the pumping rate at least one water supply wells while keeping up a base drawdown level in the aquifer.
- Maximizing the pumping rate at least one water supply wells while keeping up the concentration of a determine pollutant below a specified level.

MODFLOW data sets

Visual MODFLOW v.4.0 has an altogether enhanced bringing in process that supports MODFLOW-2000 data set. This new procedure uses an adjusted adaptation of the USGS utility (MF96to2K.EXE) to change over MODFLOW-96 and MODFLOW-88 informational indexes into MODFLOW-2000 format and after that imports the MODFLOW-2000 data set into the Visual MODFLOW graphical condition.

Property Zones and Recharge Zones from Polygon Shape Files

Visual MODFLOW acquainted the capacity with import and introduce conductivity and storage zone disseminations from outer information sources including XYZ ASCII, TXT documents, MS Access, MDB records, MS excel, XLS records, Surfer, GRD documents, and ESRI Point and line .SHP documents. Visual MODFLOW v.4.0 stretches out this ability to extra model properties including initial heads, initial concentrations, and dispersivities. The capacity to map property zones and recharge zones from ESRI Polygon.shp records is additionally included.

Importing and Editing Layer Surface Elevations

Visual MODFLOW v.4.0 gives a drastically enhanced arrangement of devices for importing, making, and changing layer surface rises for finite difference model grid, imports USGS DEM document.

Importing and Displaying Site Map Images

The pictures were required to be in BMP form, and it was just conceivable to see one site outline at once.

Creating a New Model

To create a new model, selected file and new from the main menu screen of Visual MODFLOW. Create new model window will appear, after generating a new model save option has appeared and then saved the data.

Project Outline

The project outlines window will show up which is isolated into a few segments.

- The project information frame allows us to enter an optional project title, a project description, and detailed project information by press on the details button.

- The flow simulation outline enables us to choose the flow type for a project utilizing the pick list, and the appropriate flow numeric engine and simulation type utilizing the draw down menus (if accessible).
- The units outline enables us to choose the coveted units for every factor utilizing the draw down menus.

Flow Simulation

For the flow simulation, selected a flow type from the pick list. The flow type selected will automatically edit the numeric engine pick list, so only compatible flow numeric engines are displayed. On account of saturated (variable density), variably saturated, and vapor, just a single Flow numeric engine is appropriate.

Flow Options

The following flow option window allows me to configure all options related to the flow model. The flow option window is separated into various sections.

Model Domain

The following model domain window allows me to configure all options related to the default model grid.

Selecting the Model Region

Next operation is to choosing a model locale that includes the accompanying assignments:

- Orienting the model network along the central bearing of groundwater stream.
- Selecting the general size of the model space from a large area.

After refining the grid, putting the well discharge data and hydraulic conductivity data, now it becomes time to run the model.

Run Section - Model Run Settings

The Run section is where the model simulations are 'launched' (started) and it provides access to the run settings for the numeric engines chosen for flow, particle tracking, contaminant transport, and parameter estimation simulations as shown in Figure 8.3.
The top menu bar of the Run segment contains the following menu items.

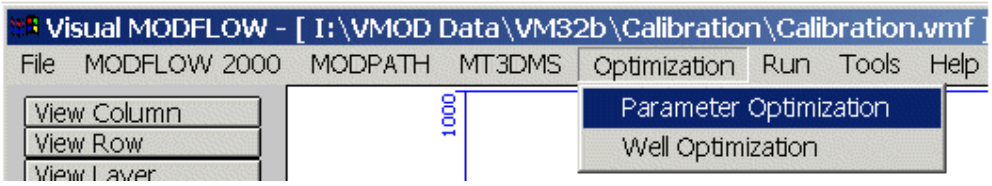

Fig. 8.3: Model Run settings window.

Since the steady-state flow simulation is chosen, Visual MODFLOW will set up the informational collection for an unfaltering state stream simulation and will naturally utilize the information from the first time period (only) of every limit condition and pumping well characterized in Visual MODFLOW to run the model to accomplish stream balance (i.e. a period free arrangement since all data sources are steady).
Next section comes is to run the model.

Running the Model – VMEngines

To run a simulation with any or every single numeric motor, it is required to choose Run from the top menu bar of the Run area and the Engines to Run window will show up as appeared in Figure 8.4.

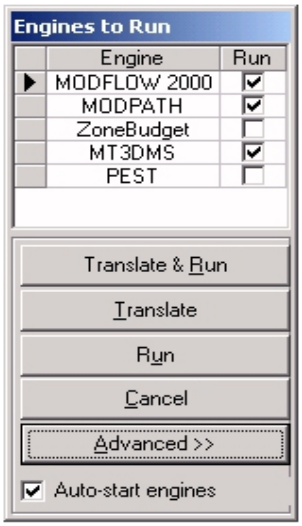

Fig. 8.4: Running the model window.

For this section MODFLOW 2000 was run only. The output segment of Visual MODFLOW is opened by choosing output from the top menu bar of the Main Menu as shown in Figure 8.5. After entering the output segment, Visual MODFLOW will consequently stack the accessible output records for Head (.hds), Drawdown (.ddn) and concentration (.ucn) for all output times. Once these information records are stacked, the Output screen will show up with the accompanying things in the best menu bar.

Fig. 8.5: Output section in top menu bar.

Note that if client ran an undertaking utilizing both MODFLOW and MT3D, and afterward in a later simulation you ran just MODFLOW and did not run MT3D, just the Flow information would be refreshed, not the concentration data. Subsequently, after entering the Output menu, the accompanying output data arning window will show up. It cautions you that the recently estimated heads (.hds) record is more up to date than the

already computed MT3D (.ucn and .obs) documents, on the grounds that MT3D was excluded in the present run.

Limitation

The water must have a steady thickness, density, dynamic viscosity (and consequently temperature) all through the demonstrating area (SEAWAT is an adjusted form of MODFLOW which is intended for density-dependent groundwater flow and transport). The principal components of anisotropy of the hydraulic conductivity have been used in MODFLOW. This tensor does not allow non-orthogonal anisotropies, as could be normal from stream in fractures. Parallel anisotropy for a whole layer can be demarcated to by the coefficient "TRPY.

8.7 Input Data Description

Total eight numbers of wells were chosen to collect discharge data of 2002 from the Contai and Digha sub-division area. These data were collected from the Public Health Engineering Directorate under Government of West Bengal. These collected data have been utilized as input data as shown in the Table 8.2. The location map of the wells is shown in Figure 8.6. The values of discharge data of 2002 for eight groundwater monitoring wells are simulated for the year 2012. The groundwater levels for the entire area are obtained from the software MODFLOW simulation.

Table 8.2: Pumping well discharge rates at different locations of study area in 2002.

Sl . no.	Name and location of well	Pumping discharge rate (m^3/day)
1	Kalindi water supply (SW1)	2362
2	Sherkhanchawk (SW2)	2671
3	Ratanpur (SW3)	2226
4	Pichabani (SW4)	3725
5	Majha (SW5)	2671
6	Basantia High School (SW6)	3157
7	Mukutshila (SW7)	2998
8	Majha 2 (SW8)	1417

Time duration of 10 years has been given to the software as the initial input for simulation. The model is calibrated with 30×30×3 grid size. That means the entire study area is uniformly graded with 30 rows 30 columns and 3 layers. A digitized map of the study area is entered in drawing interchange format. To get better results finer grading at well location of the eight monitoring well locations are prepared. For setting purpose, the elevation of ground surface, bottom of layer 1, bottom of layer 2, bottom of layer 3 are imported. The interpolation used for throughout the process is found inverse of the

distance. Apart from the input values specified in Table 8.2 for calibration phase other inputs that are entered was the discharge data of eight numbers of groundwater monitoring wells. After proper grid spacing specified for the entire study area the site location is looked like this in digitized format as shown in Figure 8.7. The river boundary condition of Bay of Bengal exists to the southern part of Purba Midnapur site location.

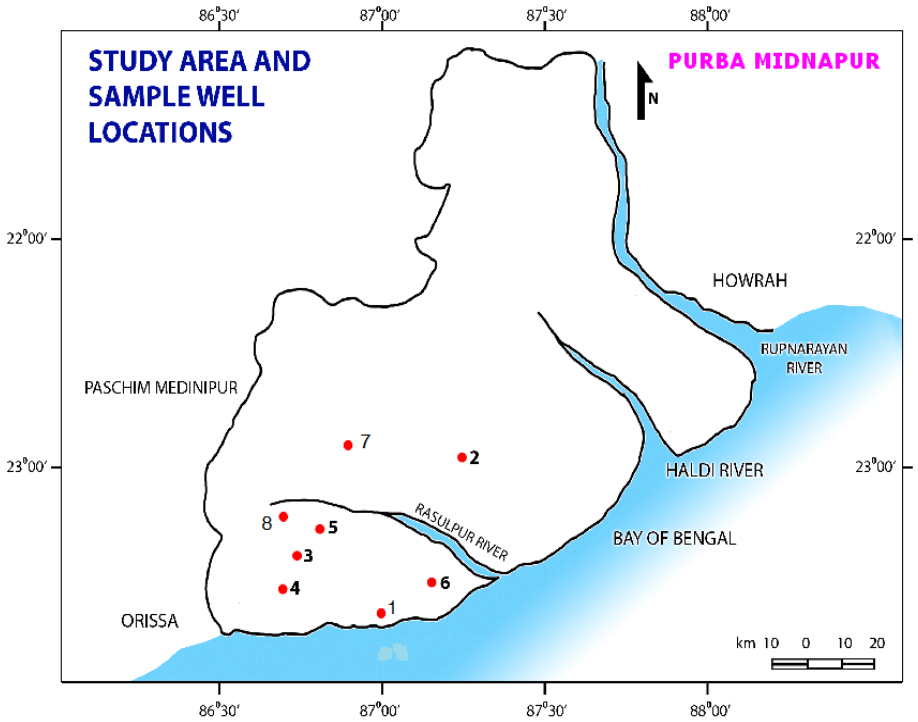

Fig. 8.6: Location map of eight groundwater monitoring wells.

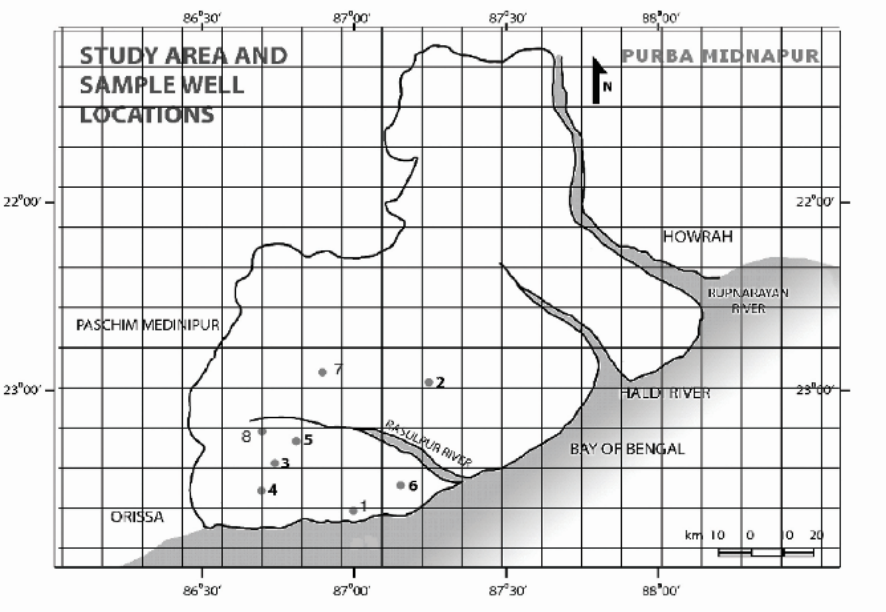

Fig. 8.7: Proposed coverage of study area in modelled grid form.

The entire study area is uniformly graded except eight numbers of groundwater monitoring well locations site is finely graded as shown in Figure 8.7. The parameters applied for calibration is given in Table 8.1. The data of discharge values for the year 2002 are given as input for simulation for the year 2012 where the hydraulic heads come as output, so the time period of simulation is taken as 10 years or 3650 days.

Table 8.2 shows the pumping rate of eight numbers of locations in study area. The values of pumping well discharge data were put in as input like SW 1 (-2362 m^3/day) and so likewise. The negative sign was given to the discharge values for extracting water from the wells into the ground layers. The hydraulic conductivity values were given as input as shown in Table 8.1. The three different layers looked like Figure 8.8 which is highlighted in blue.

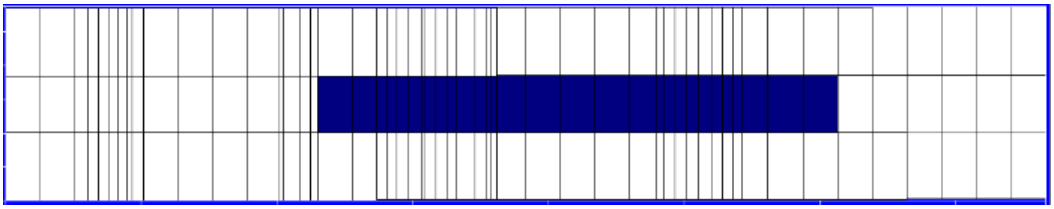

Fig. 8.8: Three layer discretisation showing upper unconfined aquifer, middle aquitard and lower aquifer.

The aquitard region was created from north-west corner of the study area to south-east corner of study area. The blue region of the middle aquitard region indicates further calibration was necessary so that three layers were looked like uniform. After proper calibration, the three layers of the study area were looked like Figure 8.9 as given below.

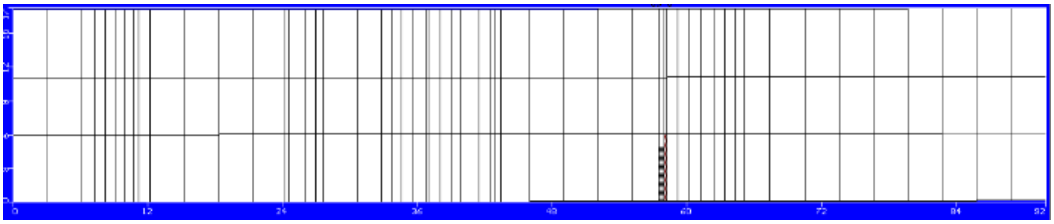

Fig. 8.9: Calibrated three model layers of study area.

The recharge rate for the site location was taken as input of 12% of average precipitation (Waterloo, 2006) which is 180 mm/year was taken. The well discharge data for the year 2012 were given as input to simulate the water level data for the year of 2017. The input data for the year 2012 are shown in Table 8.3.

The site locations map of thirty wells in the study area for the year 2012 is shown in Figure 8.10. The well discharge data of the study area for the year 2012 are used as an input then the area surrounding the wells were discredited using fine grading technique apart from that rest of the area were discredited using uniform grading technique with 30 rows × 30 columns × 3 layers. In addition the groundwater levels of different locations in the study area collected in 2002 are shown in Table 8.4.

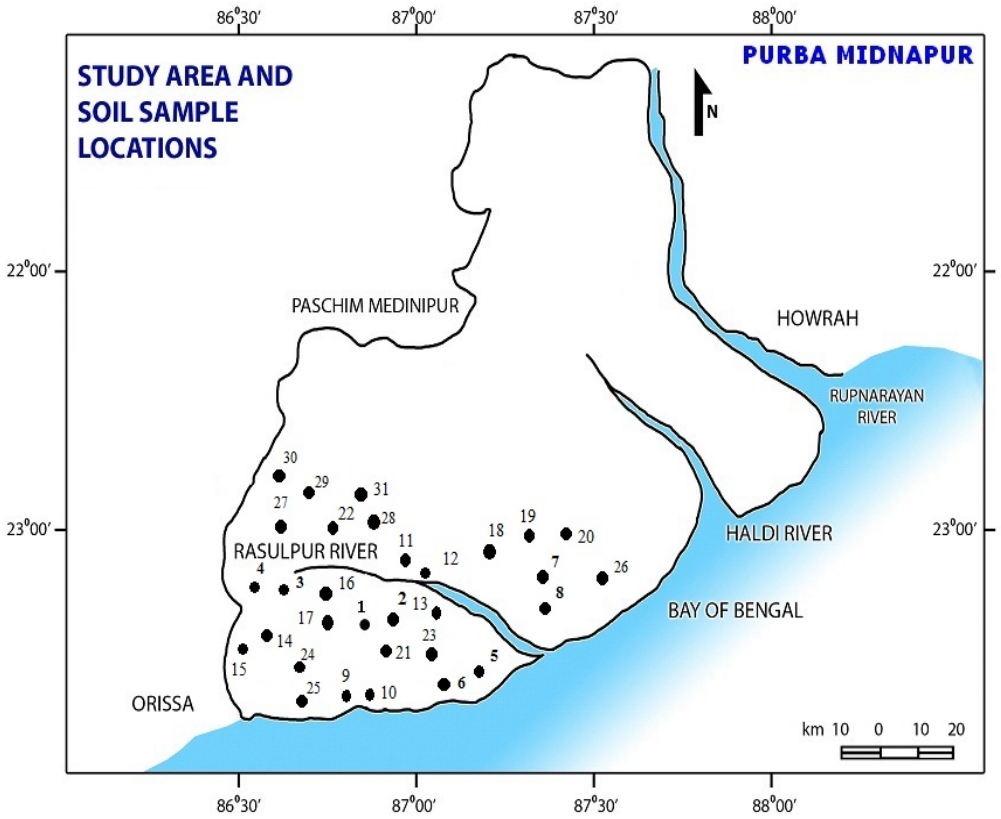

Fig. 8.10: Site location map of 30 tubewells in study area in 2012.

Table 8.3: Pumping well discharges from different locations of Purba Midnapur in 2012.

Sl. no.	Name and location of well	Pumping well discharge rate (m^3/day)
1	Talda WS Scheme	1353
2	Talda WS Well Scheme (2)	1590
3	Bhajachauli	1000
4	Bhajachauli WS (2^{nd} TW site)	1080
5	Haripur WS	1770
6	Haripur WS (2^{nd} TW site	1930
7	Chandiveti WS	1590
8	Chandiveti WS(2^{nd} TW site)	2225
9	Sankarpur WS	908
10	Sankarpur WS (2^{nd} TW site)	1080
11	Sapai WS	808
12	Sapai WS (2^{nd} TW site)	1045
13	Anurai WS	1108
14	Jumbani WS	2362
15	Jumbani WS (2^{nd} TW site)	2889

16	Durmuth WS	1285
17	Durmuth WS (2nd TW site)	1444
18	Paschim Kumarda WS	754
19	Paschim Batya WS	930
20	Paschim Batya WS (2nd TW site)	1030
21	Contai Saline area Zone-II	1590
22	Dakshin Charikhia (2nd TW site	1770
23	Bankipur WS	940
24	Bagmari WS	2090
25	Barchunfuli WS	705
26	Barasubarnanagar WS	1362
27	Dhanghora WS	1590
28	Amtalia WS (2nd TW site)	818
29	Kumirda WS(2nd TW site)	1930
30	Kumirda WS	1363

Table 8.4: Groundwater level data at eight monitoring wells in 2002.

Sl no.	Area	Static water table (m) from ground surface
1	Kalindi water supply (SW1)	4.85
2	Sherkhan chawk (SW2)	9.45
3	Ratanpur (SW3)	5.45
4	Pichabani (SW4)	3.66
5	Majha (SW5)	8.70
6	Basantia high school(SW6)	6.0
7	Mukutshila (SW7)	12.4
8	Majha 2 (SW8)	9.9

8.8 Simulated GWLs for 2012

The discharge data of eight wells for the year 2002 are displayed in Table 8.2. These data were given as input and then groundwater levels were simulated for any locations of the Purba Midnapur district for the year 2012. The output results are shown in Figure 8.11. The simulated groundwater level data and actual field data of the year 2012 are then compared.

In the digitized map given in Figure 8.11, the south direction shows southern part of Purba Midnapur which is near the Bay of Bengal and north direction of map shows northern part of Purba Midnapur that is inland locations. The simulated water levels for the year 2012 for the study area are tabulated in Table 8.5.

Groundwater always flows from higher level (elevation) to lower level. So the groundwater flow moves from the area of higher groundwater level to the area where groundwater level is low. As shown in the Table 8.5, the south direction of Purba

Midnapur near the Bay of Bengal, the groundwater levels at Station 5 - Haripur WS was 11.61 m, Station 6 - Haripur WS (2nd TW Site) was 11.49 m, Station 9 - Sankarpur WS was 11.61 m, Station10 - Sankarpur WS (2nd TW Site) was 11.60 m whereas in the north direction i.e. at the inland locations, the groundwater levels at Station 11 - Sapai WS was 12.81 m, Station 12 - Sapai WS (2nd TW Site) was 12.50 m, Station 18 - Paschim Kumarda WS 13.21 m, Station 19 - Paschim Batya WS was 13.42 m.

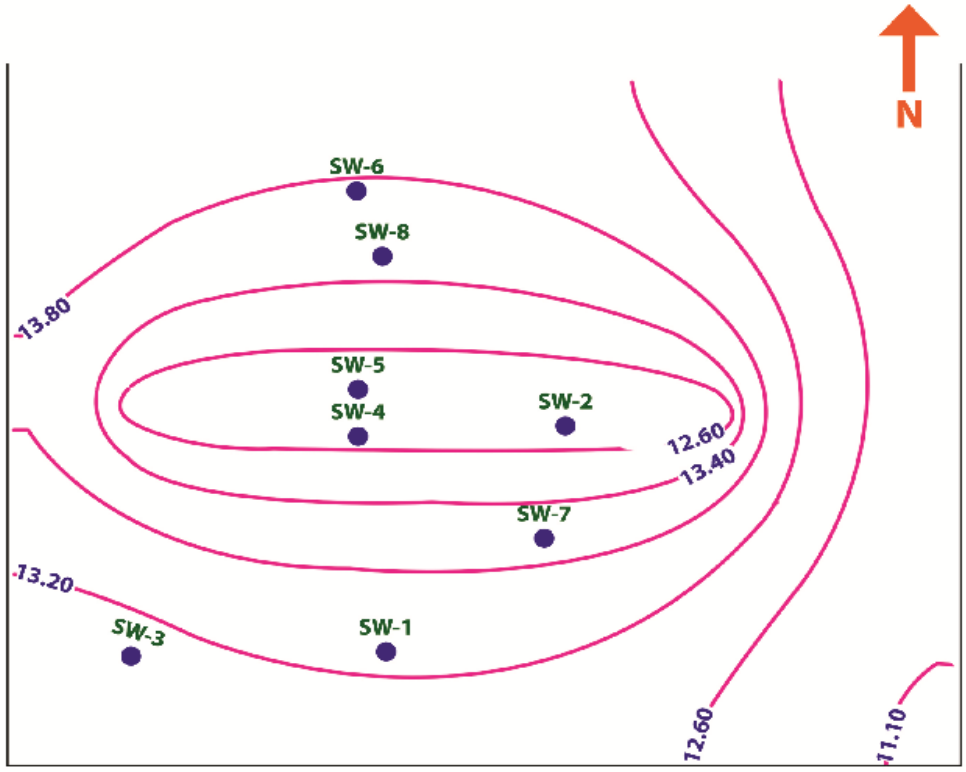

Fig. 8.11: Digitized output of GWL contours of study area in 2012.

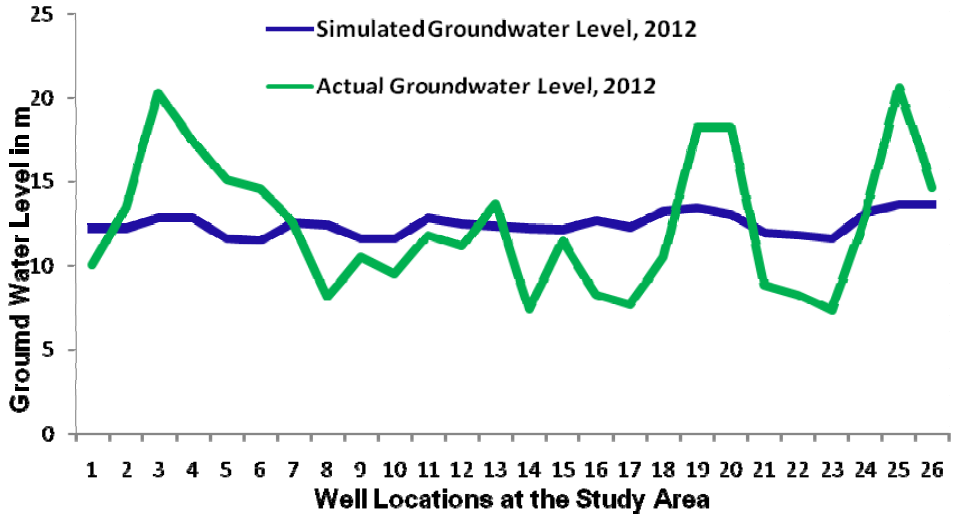

Fig. 8.12: Actual versus simulated GWLs for the year 2012.

So the overall trend of groundwater levels in the southern part of Purba Midnapur is higher than groundwater levels in northern part of Purba Midnapur.

In Purba Midenapur, saline water intrusion takes place from the Bay of Bengal from the direction of south to north of Purba Midnapur. Therefore based on the saline water intrusion impact the worst affected areas are a Jumbani WS where groundwater level was 12.24 m and Station 15 - Jumbani WS (2nd tubewell Site) where groundwater level was 12.13 m.

Table 8.5: Simulated GWLs for the study area in 2012 based on 2002 data.

Sl. No. (Station)	Name of location	Simulated water table (m)
1	Talda WS Scheme	12.24
2	Talda WS Well Scheme (2)	12.24
3	Bhajachauli	12.84
4	Bhajachauli WS	12.84
5	Haripur WS	11.61
6	Haripur WS (2nd TW site)	11.49
7	Chandiveti WS	12.52
8	Chandiveti WS (2nd TW site)	12.43
9	Sankarpur WS	11.61
10	Sankarpur WS (2nd TW site)	11.60
11	Sapai WS	12.81
12	Sapai WS (2nd TW site)	12.50
13	Anurai WS	12.36
14	Jumbani WS	12.24
15	Jumbani WS (2nd TW site)	12.13
16	Durmuth WS	12.70
17	Durmuth WS 2nd TW	12.30
18	Paschim Kumarda WS	13.21
19	Paschim Batya WS	13.42
20	Paschim Batya WS (2nd TW site)	13.03
21	Contai Saline area Zone-II	11.93
22	Bankipur WS	11.83
23	Barchunfuli WS	11.61
24	Barasubarnanagar WS	13.12
25	Dhanghora WS	13.60
26	Kumirda WS (2nd TW site)	13.58

WS : Water Supply

8.9 Comparison between Simulated and Actual GWLs for 2012

Table 8.6: Simulated and actual GWLs of study area for 2012.

Sl. no.	Name of location	Simulated groundwater level (m)	Actual groundwater level (m)
1	Talda WS Scheme	12.24	10.05
2	Talda WS Well Scheme (2)	12.24	13.43
3	Bhajachauli	12.84	20.35
4	Bhajachauli WS	12.84	17.38
5	Haripur WS	11.61	15.06
6	Haripur WS (2nd TW site)	11.49	14.58
7	Chandiveti WS	12.52	12.58
8	Chandiveti WS (2nd TW site)	12.43	8.10
9	Sankarpur WS	11.61	10.50
10	Sankarpur WS (2nd TW site)	11.60	09.50
11	Sapai WS	12.81	11.81
12	Sapai WS (2nd TW site)	12.50	11.15
13	Anurai WS	12.36	13.70
14	Jumbani WS	12.24	07.34
15	Jumbani WS (2nd TW site)	12.13	11.48
16	Durmuth WS	12.70	08.20
17	Durmuth WS 2nd TW	12.30	07.60
18	Paschim Kumarda WS	13.21	10.49
19	Paschim Batya WS	13.42	18.30
20	Paschim Batya WS (2nd TW site)	13.03	18.30
21	Contai Saline area Zone-II	11.93	08.84
22	Bankipur WS	11.83	08.23
23	Barchunfuli WS	11.61	07.30
24	Barasubarnanagar WS	13.12	13.12
25	Dhanghora WS	13.60	20.67
26	Kumirda WS (2nd TW site)	13.58	14.63

8.9.1 Correlation Coefficient

The simulated groundwater level of Purba Midnapur for the year 2012 is compared with the actual water levels for the same area and same year and is put in Table 8.6. Equation (8.2) illustrates the formula for determining the correlation coefficient (*r*).

$$r = \frac{n\left(\sum xy - \sum x \sum y\right)}{\sqrt{\left[n\sum x^2 - \left(\sum x\right)^2\right]\left[n\sum y^2 - \left(\sum y\right)^2\right]}} \quad (8.2)$$

where r =correlation coefficient
x=values of one variable which is to be correlated with another variable
y= values of another variable which is to be correlated with x variable

Now, taking the values of simulated groundwater levels for study area for the year 2012 as (x) and field data of groundwater level in study area in the year 2012 as (y) the value of correlation coefficient is obtained 0.56.

The magnitude of correlation coefficient shows that the simulated groundwater levels moderately matches with actual groundwater levels for the study area for the year 2012. Also the graphical representation of actual versus simulated GWLs for the year 2012 is shown in Figure 8.12. The correlation coefficient value also confirms that the model calibration is moderate. Since the simulated values matches reasonably well based on this correlation coefficient, therefore it validates the model.

8.10 Simulated GWLs for 2019-2023 based on 2002 Data

The well discharge data for the year 2002 are provided as input and it is simulated (time period of simulation=17, 18, 19, 20 and 21 days) for the years 2019 to 2023. The digitized outputs are given in Figures 8.13 to 8.17. The outcomes show future groundwater levels at different locations of the study area for the years 2019 to 2023. The outcomes are also listed in Table 8.7.

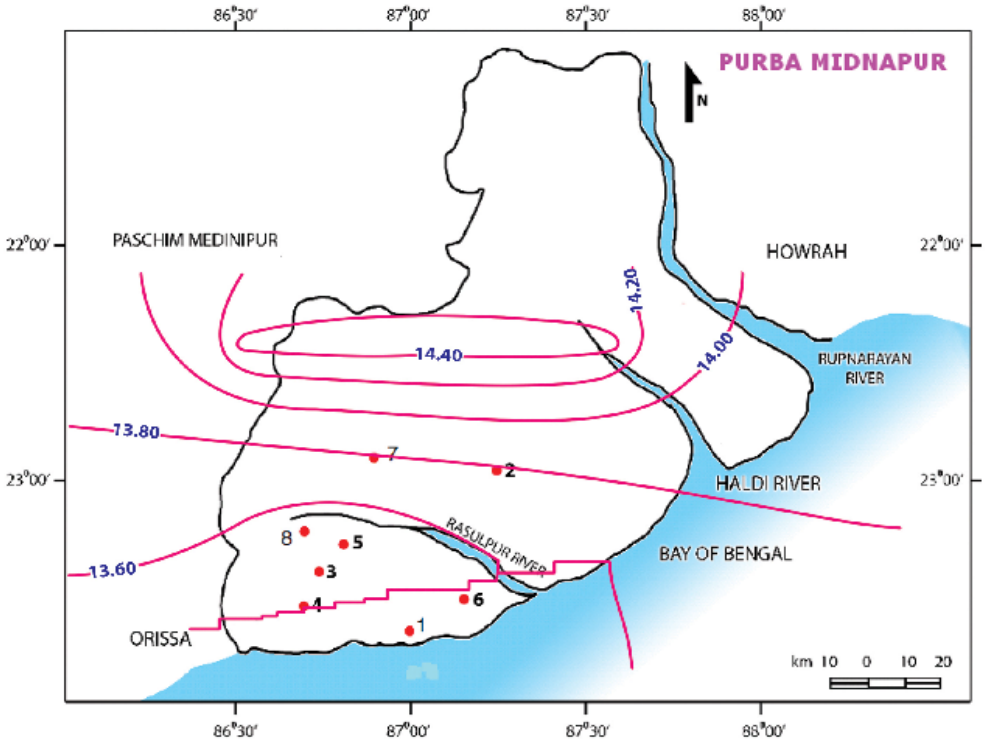

Fig. 8.13: Contour map showing simulated groundwater levels of the study area for 2019 based on 2002 data.

Table 8.7: Simulated groundwater levels for the year 2019 to 2023 based on the well discharge data observed in 2002.

Sl. no.	Name of location	Simulated GWL for 2019 (m)	Simulated GWL for 2020 (m)	Simulated GWL for 2021 (m)	Simulated GWL for 2022 (m)	Simulated GWL for 2023 (m)
1	Talda WS Scheme	13.5	14.0	14.5	14.9	15.0
2	Talda WS Well Scheme (2)	13.5	14.0	14.5	14.9	15.0
3	Bhajachauli	13.6	13.9	14.5	14.8	14.9
4	Bhajachauli WS (2nd TW Site)	13.6	13.7	14.5	14.8	15.0
5	Haripur WS	13.5	13.9	14.5	14.8	14.8
6	Haripur WS (2nd TW Site	13.5	14.1	14.5	14.7	14.8
7	Chandiveti WS	13.6	14.0	14.5	14.9	15.1
8	Chandiveti WS (2nd TW Site)	13.6	13.9	14.5	14.9	15.0
9	Sankarpur WS	13.5	13.9	14.5	14.7	14.8
10	Sankarpur WS (2nd TW Site)	13.5	13.9	14.5	14.7	14.9
11	Sapai WS	13.6	14.1	14.6	14.8	15.0
12	Sapai WS (2nd TW site)	13.6	14.1	14.5	14.8	15.0
13	Anurai WS	13.6	14	14.5	14.9	15.0
14	Jumbani WS	13.6	13.7	14.6	14.9	15.0
15	Junbani WS (2nd TW site	13.6	13.7	14.5	14.9	15.0
16	Durmuth WS	13.5	13.9	14.5	14.8	14.9
17	Durmuth WS (2nd TW site)	13.5	13.9	14.5	14.9	15.0
18	Paschim Kumarda WS	13.7	14.1	14.6	14.9	15.1
19	Paschim Batya WS	13.7	14.2	14.7	15.0	15.2
20	Paschim Batya WS (2nd TW site)	13.8	14.2	14.7	15.0	15.2
21	Contai Saline area Zone-II	13.6	14.0	14.6	14.8	14.9
22	Dakshin Charikhia (2nd TW site)	13.7	14.1	14.6	14.9	15.1
23	Bankipur WS	13.6	14.0	14.6	14.8	14.9
24	Bagmari WS	13.6	13.8	14.6	14.7	14.9
25	Barchunfuli WS	13.5	13.9	14.5	14.7	14.9
26	Barasubarnanagar WS	13.7	14.0	14.6	15.0	15.1
27	Dhanghora WS	13.7	14.0	14.6	14.9	15.0
28	Amtalia WS (2nd TW site)	13.7	14.2	14.6	15.0	15.1
29	Kumirda WS (2nd TW site)	13.8	14.3	14.7	15.2	15.2
30	Kumirda WS	13.9	14.3	14.8	15.2	15.3

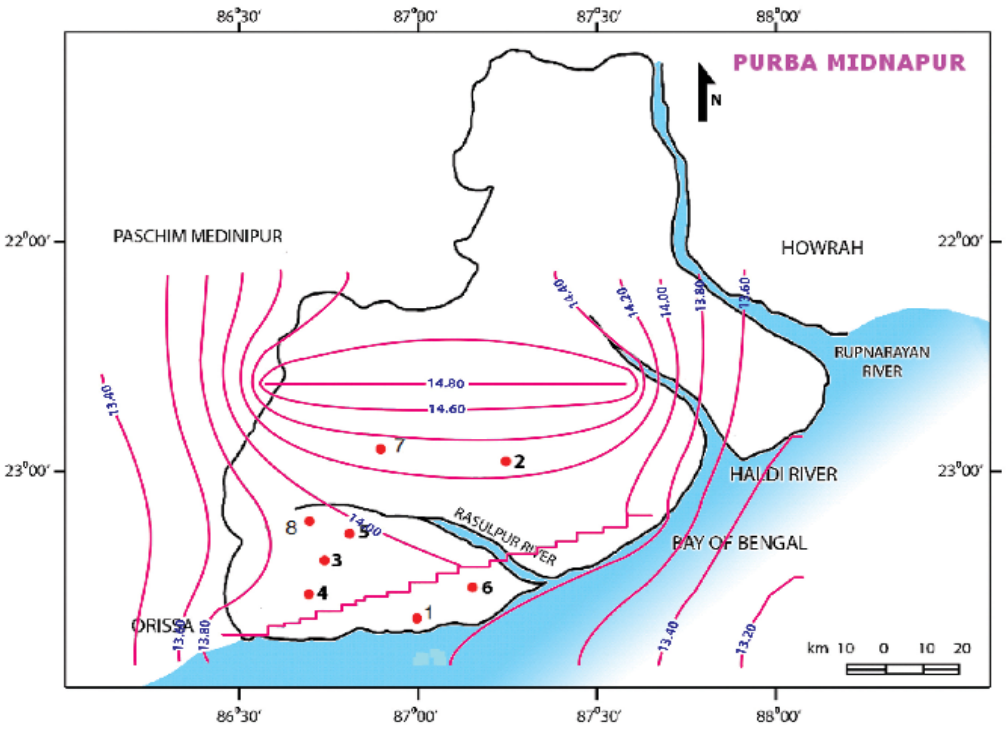

Fig. 8.14: Contour map showing simulated groundwater levels of study area for 2020 based on 2002 data.

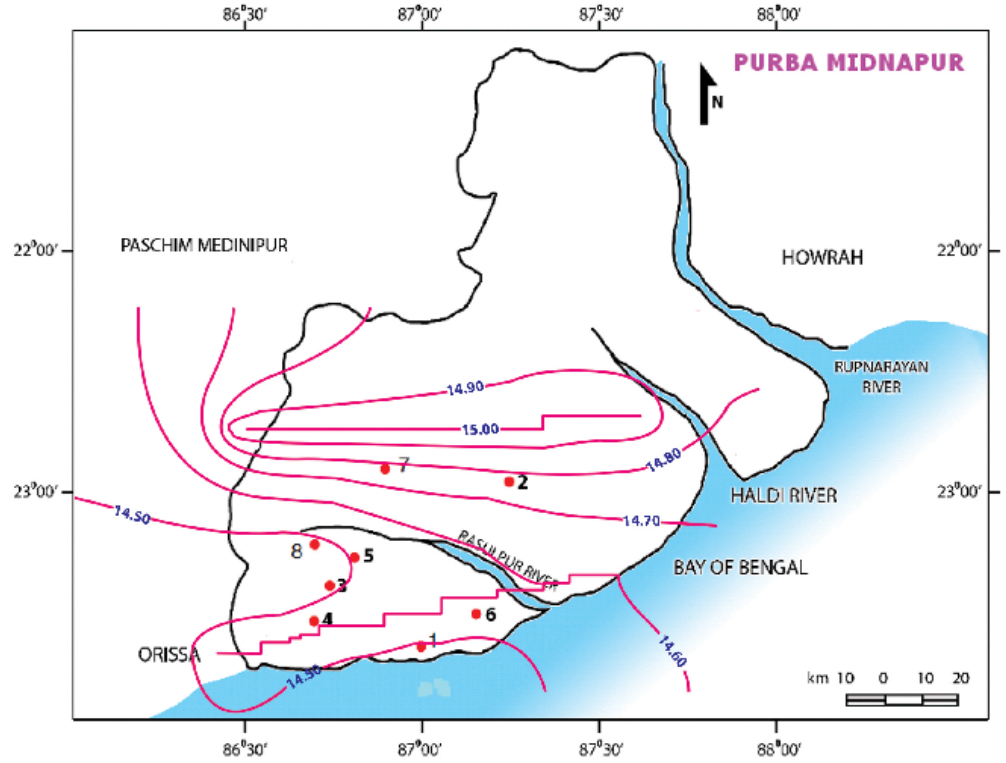

Fig. 8.15: Contour map showing simulated groundwater levels of study area for 2021 based on 2002 data.

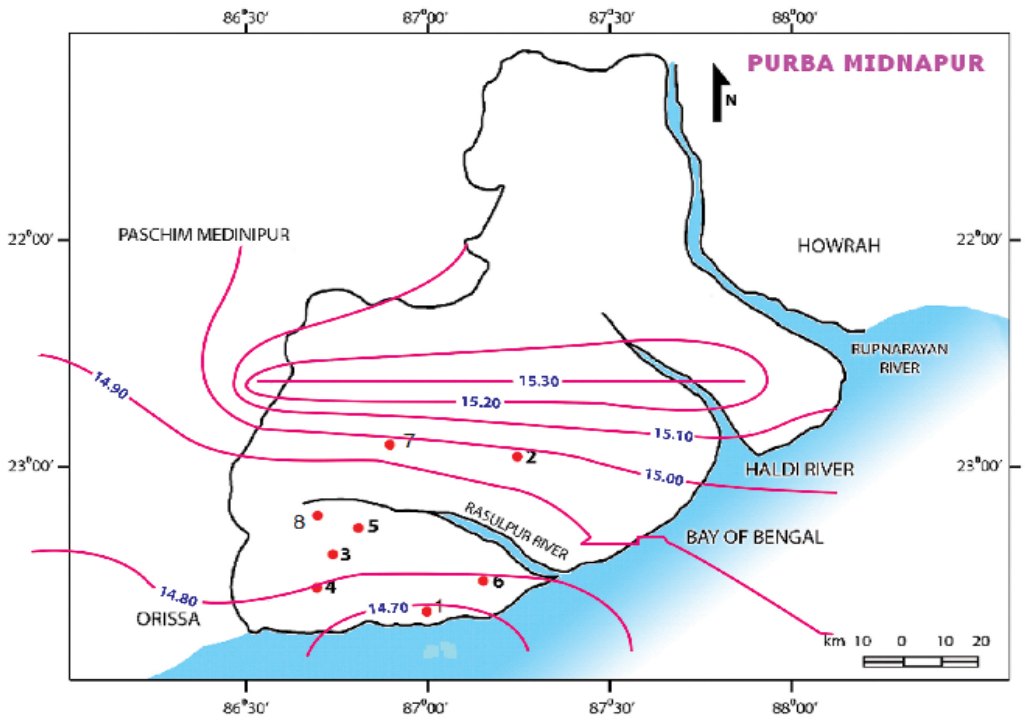

Fig. 8.16: Contour map showing simulated groundwater levels of study area for 2022 based on 2002 data.

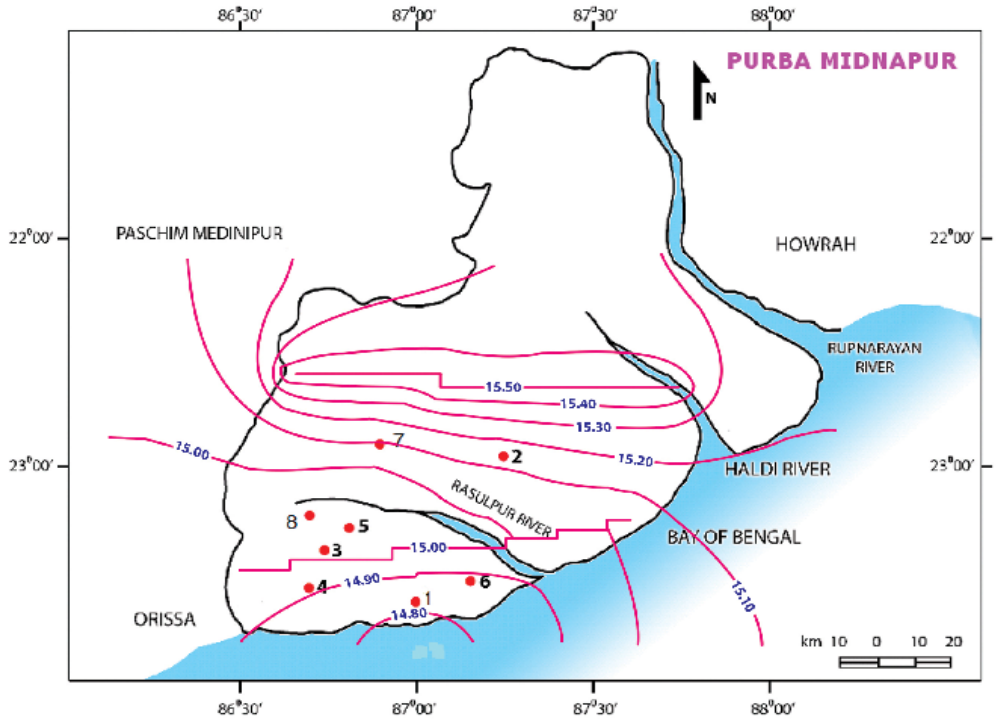

Fig. 8.17: Contour map showing simulated groundwater levels of study area for 2023 based on 2002 data.

8.11 Simulated GWLs for 2019-2023 based on 2012 Data

Thirty numbers of well discharge data measured in 2012 at different site locations of Purba Midnapur were given as input and simulated water table for the thirty locations of Purba Midnapur for the year 2019 to 2023 have been determined.

The simulated values of groundwater levels for the years 2019 to 2023 of these thirty locations of Purba Midnapur are depicted in Table 8.10.

The procedure of simulation is same as mentioned in previous section. Only in this case, fine grading in MODFLOW window map for thirty well locations has been done and discharge of thirty wells has been provided. The grading map of the study area is given in Figure 8.18.

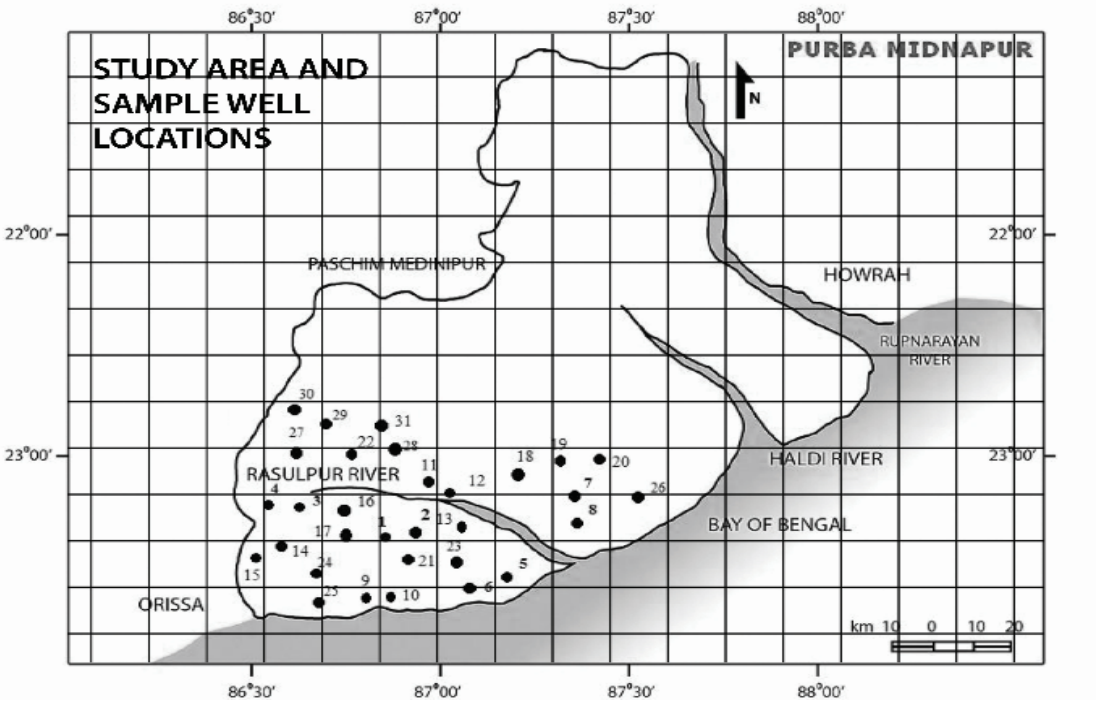

Fig. 8.18: Fine grading of thirty well locations of Purba Midnapur for 2012.

When the software was run in preconditioned conjugate gradient (PCG) solver then the output is obtained as groundwater level contours as given in Figures 8.19 to 8.23.

Here the bottom part of the map indicates the southern area of Purba Midnapur which is located near Bay of Bengal and upper part of map indicates the northern area of Purba Midnapur. From the digitized map it is also seen that groundwater levels are low in southern area compared to the northern area as displayed in Tables 8.8 and 8.9.

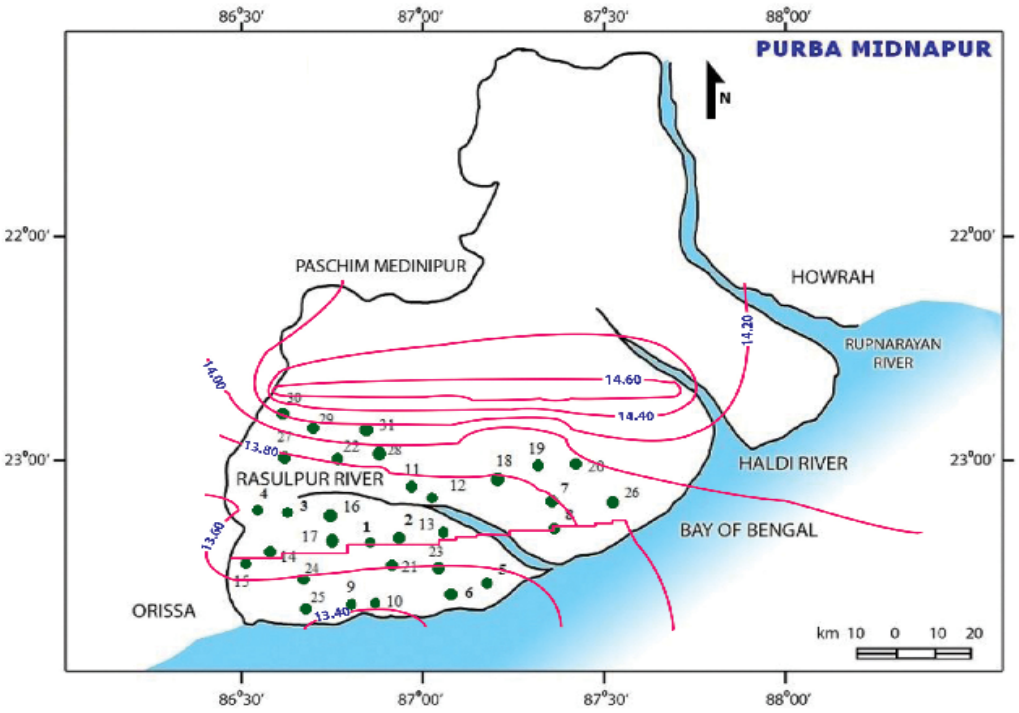

Fig. 8.19: Contour map showing simulated groundwater levels for the year of 2019 based on observed well discharge data gauged in 2012.

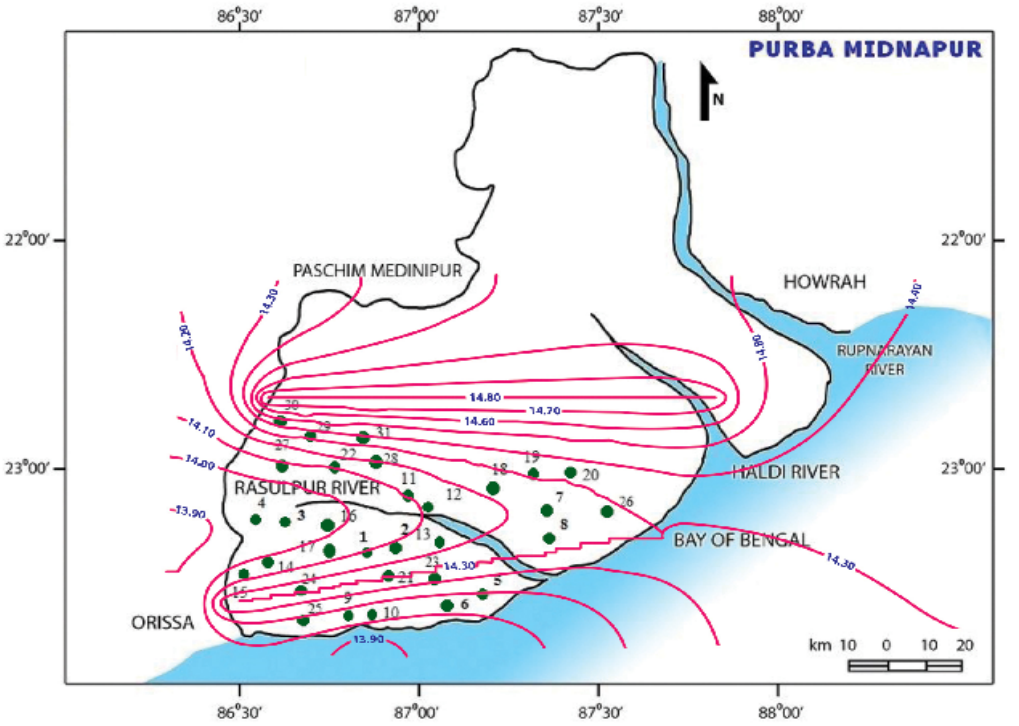

Fig. 8.20: Contour map showing simulated groundwater levels for the year of 2020 based on observed well discharge data gauged in 2012.

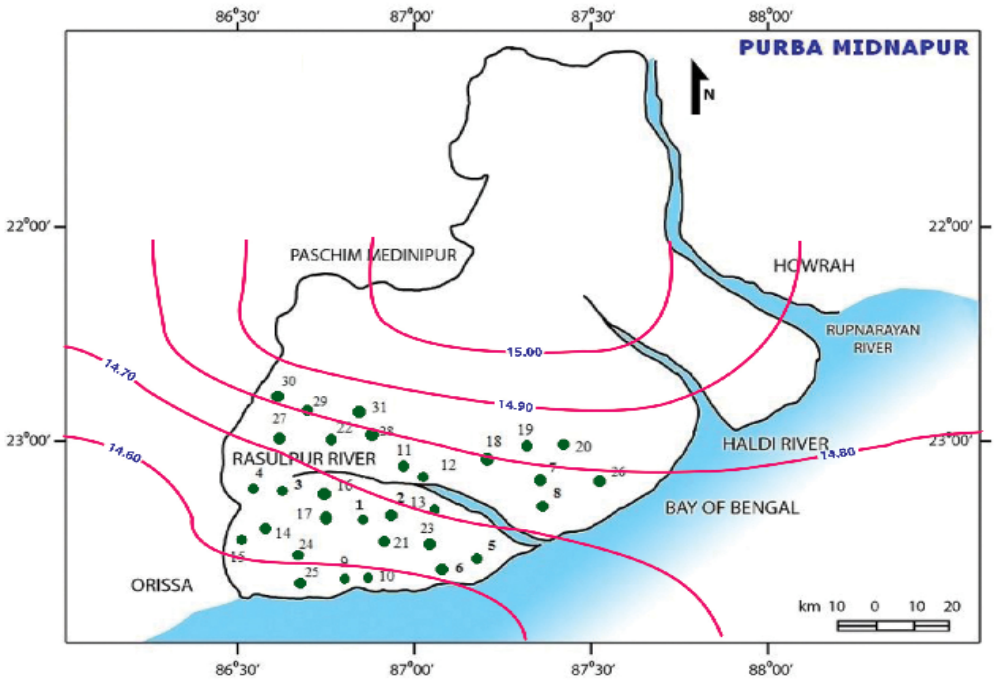

Fig. 8.21: Contour map showing simulated groundwater levels for the year of 2021 based on observed well discharge data gauged in 2012.

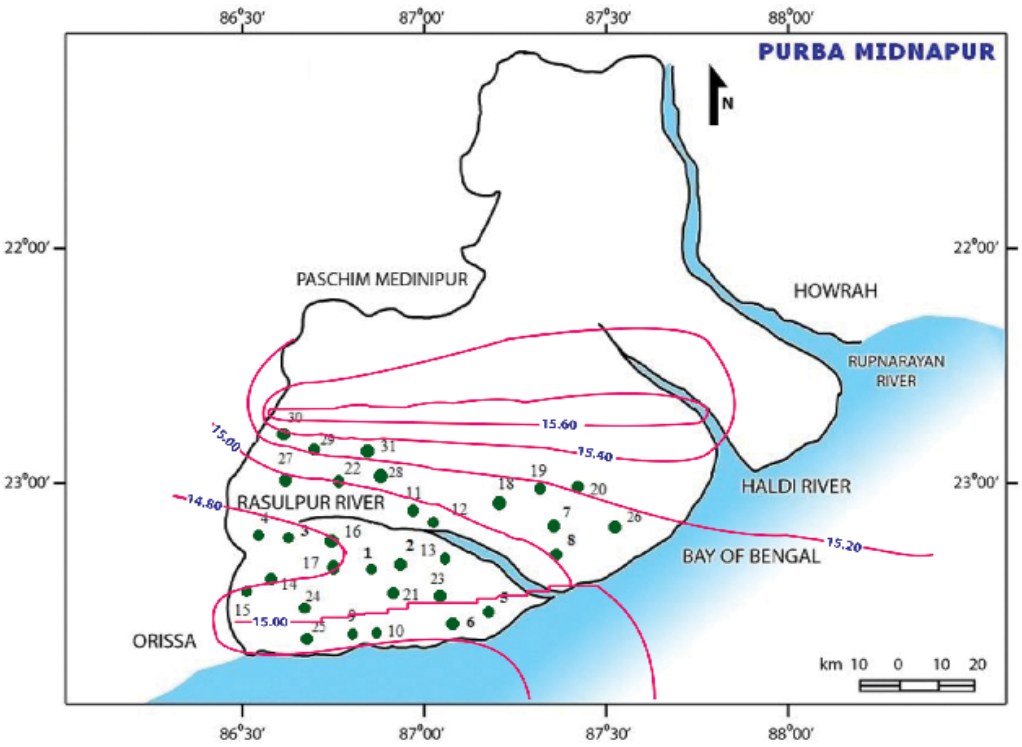

Fig. 8.22: Contour map showing simulated groundwater levels for the year of 2022 based on observed well discharge data gauged in 2012.

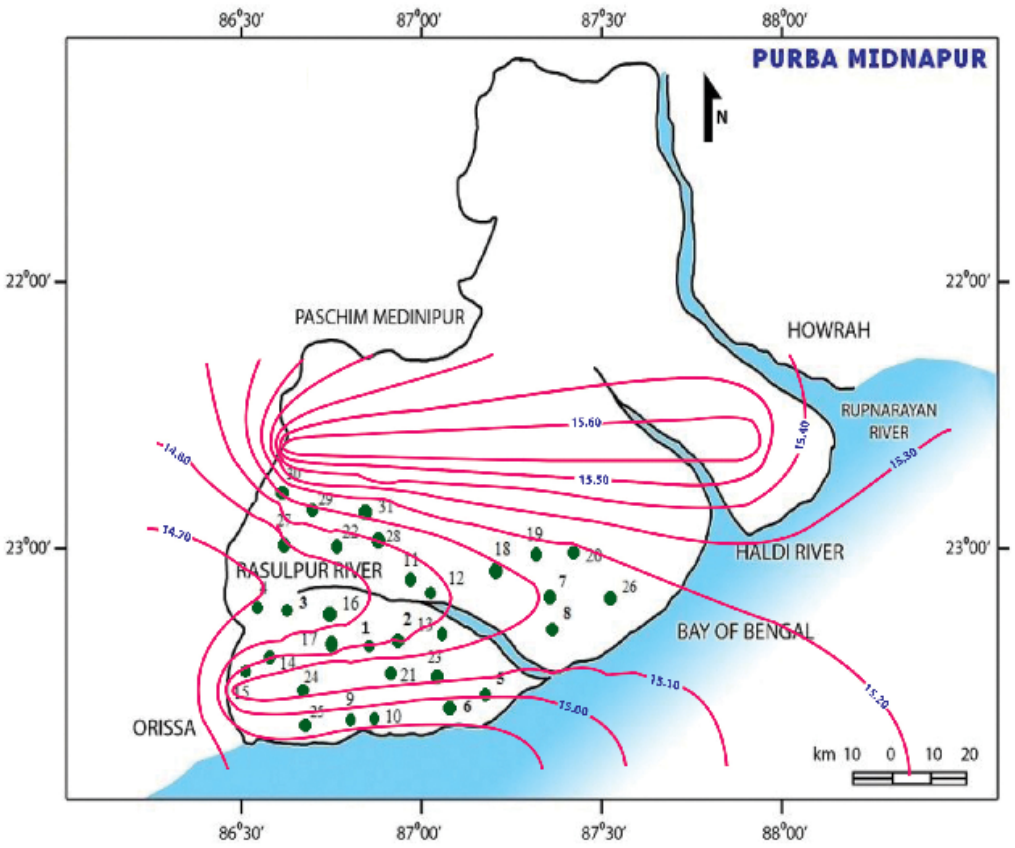

Fig. 8.23: Contour map showing simulated groundwater levels for the year of 2023 based on observed well discharge data gauged in 2012.

Table 8.8: Simulated groundwater levels for 2019 to 2023 based on 2002 data.

Sl. no.	Southside locations of Purba Midnapur	Simulated GWLs for the years 2019, 2020, 2021, 2022, 2023 (m)	North side locations of Purba Midnapur	Simulated GWLs for the years 2019, 2020, 2021, 2022, 2023 (m)
01	Haripur WS	13.5,13.9,14.5, 14.8, 14.8	Dhanghora WS	13.7, 14.0, 14.6, 14.9, 15.0
02	Haripur WS (2nd TW site)	13.5,14.1,14.5, 14.9, 14.8	Kumirda WS (2nd TW site)	13.8, 14.3, 14.7, 15.2, 15.2
03	Sankarpur WS	13.5,13.9,14.5, 14.7, 14.8	Kumirda WS	13.9, 14.3, 14.8, 15.2, 15.3
04	Sankarpur WS (2nd TW site)	13.5,13.9,14.5, 14.7, 14.9	Amtalia WS (2nd TW site)	13.7, 14.2, 14.6, 15.0, 15.1
05	Barchunfuli WS	13.5,13.9, 14.5, 14.7, 14.9	Sapai WS	13.6, 14.1, 14.6, 14.8, 15.0

Table 8.9: Simulated groundwater levels for 2019 to 2023 based on 2012 data.

Sl. no.	Southside locations of Purba Midnapur	Simulated GWLs for the years 2019, 2020, 2021, 2022, 2023 (m)	North side locations of Purba Midnapur	Simulated GWLs for the years 2019, 2020, 2021, 2022, 2023 (m)
01	Haripur WS	13.6, 13.9, 14.5, 14.9, 15.0	Dhanghora WS	13.8,14.1, 14.6, 15.1, 15.0
02	Haripur WS (2nd TW site)	13.5, 14.1, 14.5, 14.9, 15.0	Kumirda WS (2nd TW site)	14.3, 14.4, 14.7, 15.6, 15.7
03	Sankarpur WS	13.4, 13.9, 14.5, 14.7, 14.8	Kumirda WS	14.4, 14.5, 14.8, 15.6, 15.7
04	Sankarpur WS (2nd TW site)	13.5, 14, 14.5, 14.7, 14.8	Amtalia WS (2nd TW site)	13.9, 14.2, 14.6, 15.2, 15.3
05	Barchunfuli WS	13.4, 14, 14.5, 14.7, 14.9	Sapai WS	13.5,14.1, 14.6, 15.0, 15.1

It was evident from the discussion that groundwater is flowing from south direction to north direction. It means the groundwater is moving from the side of Bay of Bengal towards north direction of Purba Midnapur. The results are shown in Tables 8.8 and 8.9.

Two simulation processes has been carried out. In first simulation, the well discharge data of study area for the year 2002 has been taken as input and groundwater levels for the years 2019 to 2023 have been simulated. In second simulation, well discharge data for the year 2012 has been taken in place of the data observed in 2002 and it has been simulated to obtain groundwater levels for the years of 2019 to 2023. This way an attempt has been made to find out the relationship between the simulated results and checked how strong the simulated values match with each other. Tables 8.11 and 8.12 show the simulated groundwater levels for the years 2019 to 2023 based on well discharge input data observed in the year 2002 and 2012.

8.12 Correlation Coefficient

For the study area, the simulated values of groundwater levels for the years 2019 to 2023 based on pumping well discharge data observed in 2002 is taken as x and simulated values of groundwater levels for the years 2019 to 2023 based on pumping well discharge data observed in 2012 is taken as y. These values are used to determine the correlation coefficient using Equation (8.2) as elaborated previously. The correlation coefficients for the years 2019 to 2023 are found out as 0.83, 0.82, 0.84, 0.82 and 0.81, respectively. The range of these correlation coefficients indicate the simulated groundwater levels at study area for the years of 2019 to 2023 based on well discharge data in the year of 2002 and 2012 match closely. It confirms both the simulations put forward almost the same value of groundwater levels at different locations of study area.

Table 8.10: Simulated GWLs for 2019 to 2023 based on data observed in 2012.

Sl. no.	Name of location	Simulated GWL based on data observed in 2012 for				
		2019 (m)	2020 (m)	2021 (m)	2022 (m)	2023 (m)
1	Talda WS Scheme	13.8	14.1	14.6	14.8	15.0
2	Talda WS Well Scheme (2)	13.7	14.1	14.6	14.8	15.0
3	Bhajachauli	13.6	13.9	14.5	14.8	14.9
4	Bhajachauli WS (2nd TW site)	13.6	13.9	14.5	14.8	14.9
5	Haripur WS	13.6	13.9	14.5	14.9	15.0
6	Haripur WS (2nd TW site	13.5	14.1	14.5	14.9	15.0
7	Chandiveti WS	13.8	14.1	14.5	15.0	15.1
8	Chandiveti WS (2nd TW site)	13.8	14.1	14.5	15.0	15.1
9	Sankarpur WS	13.4	13.9	14.5	14.7	14.8
10	Sankarpur WS (2nd TW site)	13.5	14.0	14.5	14.7	14.9
11	Sapai WS	13.5	14.1	14.6	15	15.1
12	Sapai WS (2nd TW site)	13.7	14.1	14.5	14.8	15.0
13	Anurai WS	13.7	14.0	14.6	14.8	15.1
14	Jumbani WS	13.7	14.0	14.6	14.8	15.0
15	Junbani WS (2nd TW site	13.8	14.0	14.6	14.8	15.1
16	Durmuth WS	13.7	14.0	14.5	14.8	14.9
17	Durmuth WS (2nd TW site)	13.7	13.9	14.6	14.8	15
18	Paschim Kumarda WS	13.8	14.2	14.6	15.1	15.3
19	Paschim Batya WS	13.9	14.3	14.7	15.2	15.3
20	Paschim Batya WS (2nd TW site)	14.0	14.4	14.6	15.3	15.3
21	Contai Saline area Zone-II	13.6	14.2	14.6	15.0	15.1
22	Dakshin Charikhia (2nd TW site)	13.8	14.2	14.6	15.0	15.1
23	Bankipur WS	13.7	14.0	14.6	14.8	15.1
24	Bagmari WS	13.6	13.9	14.6	15.0	15.1
25	Barchunfuli WS	13.4	14.0	14.5	14.7	14.9
26	Barasubarnanagar WS	13.8	14.3	14.6	15.1	15.2
27	Dhanghora WS	13.8	14.1	14.6	15.1	15.0
28	Amtalia WS (2nd TW site)	13.9	14.2	14.6	15.2	15.3
29	Kumirda WS (2nd TW site)	14.3	14.4	14.7	15.6	15.7
30	Kumirda WS	14.4	14.5	14.8	15.6	15.7

Table 8.11: Simulated groundwater levels for the years 2019 and 2020 based on well discharge data observed in 2002 and 2012.

Sl. no.	Name of location	Simulated GWL (m) for 2019 based on well discharge value for		Simulated GWL (m) for 2020 based on well discharge value for	
		2002	2012	2002	2012
1	Talda WS Scheme	13.5	13.8	14.0	14.1
2	Talda WS Well Scheme (2)	13.5	13.7	14.0	14.1
3	Bhajachauli	13.6	13.6	13.9	13.9
4	Bhajachauli WS (2nd TW site)	13.6	13.6	13.7	13.9
5	Haripur WS	13.5	13.6	13.9	13.9
6	Haripur WS (2nd TW Site	13.5	13.5	14.1	14.1
7	Chandiveti WS	13.6	13.8	14.0	14.1
8	Chandiveti WS (2nd TW site)	13.6	13.8	13.9	14.1
9	Sankarpur WS	13.5	13.4	13.9	13.9
10	Sankarpur WS (2nd TW site)	13.5	13.5	13.9	14.0
11	Sapai WS	13.6	13.5	14.1	14.1
12	Sapai WS (2nd TW site)	13.6	13.7	14.1	14.1
13	Anurai WS	13.6	13.7	14	14.0
14	Jumbani WS	13.6	13.7	13.7	14.0
15	Junbani WS (2nd TW site	13.6	13.8	13.7	14.0
16	Durmuth WS	13.5	13.7	13.9	14.0
17	Durmuth WS (2nd TW site)	13.5	13.7	13.9	13.9
18	Paschim Kumarda WS	13.7	13.8	14.1	14.2
19	Paschim Batya WS	13.7	13.9	14.2	14.3
20	Paschim Batya WS (2nd TW site)	13.8	14.0	14.2	14.4
21	Contai Saline area Zone-II	13.6	13.6	14.0	14.2
22	Dakshin Charikhia (2nd TW site)	13.7	13.8	14.1	14.2
23	Bankipur WS	13.6	13.7	14.0	14.0
24	Bagmari WS	13.6	13.6	13.8	13.9
25	Barchunfuli WS	13.5	13.4	13.9	14.0
26	Barasubarnanagar WS	13.7	13.8	14.0	14.3
27	Dhanghora WS	13.7	13.8	14.0	14.1
28	Amtalia WS (2nd TW site)	13.7	13.9	14.2	14.2
29	Kumirda WS (2nd TW site)	13.8	14.3	14.3	14.4
30	Kumirda WS	13.9	14.4	14.3	14.5

Table 8.12: Simulated groundwater levels for the years 2021, 2022 and 2023 based on well discharge data observed in 2002 and 2012.

Sl. no.	Name of location	Simulated GWLs (m) for					
		2021		2022		2023	
		based on well discharge value for					
		2002	2012	2002	2012	2002	2012
1	Talda WS Scheme	14.5	14.6	14.9	14.8	15.0	15.0
2	Talda WS Well Scheme (2)	14.5	14.6	14.9	14.8	15.0	15.0
3	Bhajachauli	14.5	14.5	14.8	14.8	14.9	14.9
4	Bhajachauli WS (2nd TW site)	14.5	14.5	14.8	14.8	15.0	14.9
5	Haripur WS	14.5	14.5	14.8	14.9	14.8	15.0
6	Haripur WS (2nd TW site	14.5	14.5	14.7	14.9	14.8	15.0
7	Chandiveti WS	14.5	14.5	14.9	15.0	15.1	15.1
8	Chandiveti WS (2nd TW site)	14.5	14.5	14.9	15.0	15.0	15.1
9	Sankarpur WS	14.5	14.5	14.7	14.7	14.8	14.8
10	Sankarpur WS (2nd TW site)	14.5	14.5	14.7	14.7	14.9	14.9
11	Sapai WS	14.6	14.6	14.8	15.0	15.0	15.1
12	Sapai WS (2nd TW site)	14.5	14.5	14.8	14.8	15.0	15
13	Anurai WS	14.5	14.6	14.9	14.8	15.0	15.1
14	Jumbani WS	14.6	14.6	14.9	14.8	15.0	15
15	Junbani WS (2nd TW site	14.5	14.6	14.9	14.8	15.0	15.1
16	Durmuth WS	14.5	14.5	14.8	14.8	14.9	14.9
17	Durmuth WS (2nd TW site)	14.5	14.6	14.9	14.8	15.0	15
18	Paschim Kumarda WS	14.6	14.6	14.9	15.1	15.1	15.3
19	Paschim Batya WS	14.7	14.7	15.0	15.2	15.2	15.3
20	Paschim Batya WS (2nd TW site)	14.7	14.6	15.0	15.3	15.2	15.3
21	Contai Saline area Zone-II	14.6	14.6	14.8	15.0	14.9	15.1
22	Dakshin Charikhia (2nd TW site)	14.6	14.6	14.9	15.0	15.1	15.1
23	Bankipur WS	14.6	14.6	14.8	14.8	14.9	15.1
24	Bagmari WS	14.6	14.6	14.7	15.0	14.9	15.1
25	Barchunfuli WS	14.5	14.5	14.7	14.7	14.9	14.9
26	Barasubarnanagar WS	14.6	14.6	15.0	15.1	15.1	15.2
27	Dhanghora WS	14.6	14.6	14.9	15.1	15.0	15.0
28	Amtalia WS (2nd TW site)	14.6	14.6	15.0	15.2	15.1	15.3
29	Kumirda WS (2nd TW site)	14.7	14.7	15.2	15.6	15.2	15.7
30	Kumirda WS	14.8	14.8	15.2	15.6	15.3	15.7

8.13 Simulated GWLs for 2019-2023 based on 2002 and 2012 Data

The pumping well discharge data for thirty locations measured in 2012 and for eight locations measured in 2002 are shown in Table 8.13. Figure 8.24 shows the locations of these 38 pumping wells. First 2002 data were simulated for the years 2012 for eight numbers of locations. Then the final simulation has been performed taking these eight numbers of simulated data and 30 numbers of measured data for the year 2012 to find out groundwater levels for the period 2019 to 2023 as shown in Table 8.14. The contour maps of simulated such data for period 2019 to 2023 are illustrated in Figures 8.25-8.29.

Table 8.13: Input data of pumping discharges from 38 deep tubewells in 2012 and 2002.

Pumping discharges rate of 30 wells measured in 2012					
Sl. No.	Name and location of well	Pumping discharge rate (m^3/day)	Sl. No.	Name and location of well	Pumping discharge rate (m^3/day)
1	Talda WS Scheme	1353	16	Durmuth WS	1285
2	Talda WS Scheme (2)	1590	17	Durmuth WS (2^{nd} TW site)	1444
3	Bhajachauli	1000	18	Paschim Kumarda WS	754
4	Bhajachauli WS (2^{nd} TW site)	1080	19	Paschim Batya WS	930
5	Haripur WS	1770	20	Paschim Batya WS (2^{nd} TW site)	1030
6	Haripur WS (2^{nd} TW site)	1930	21	Contai Saline area Zone-II	1590
7	Chandiveti WS	1590	22	Dakshin Charikhia (2^{nd} TW site)	1770
8	Chandiveti WS (2^{nd} TW site)	2225	23	Bankipur WS	940
9	Sankarpur WS	908	24	Bagmari WS	2090
10	Sankarpur WS (2^{nd} TW site)	1080	25	Barchunfuli WS	705
11	Sapai WS	808	26	Barasubarnanagar WS	1362
12	Sapai WS (2^{nd} TW site)	1045	27	Dhanghora WS	1590
13	Anurai WS	1108	28	Amtalia WS (2^{nd} TW site)	818
14	Jumbani WS	2362	29	Kumirda WS (2^{nd} TW site)	1930
15	Jumbani WS (2^{nd} TW site)	2889	30	Kumirda WS	1363
Pumping discharges rate of 8 wells measured in 2002					
31	Kalindi water supply (SW1)	2362	35	Majha (SW5)	2671
32	Sherkhanchawk (SW2)	2671	36	Basantia High School (SW6)	3157
33	Ratanpur (SW3)	2226	37	Mukutshila (SW7)	2998
34	Pichabani (SW4)	3725	38	Majha 2 (SW8)	1417

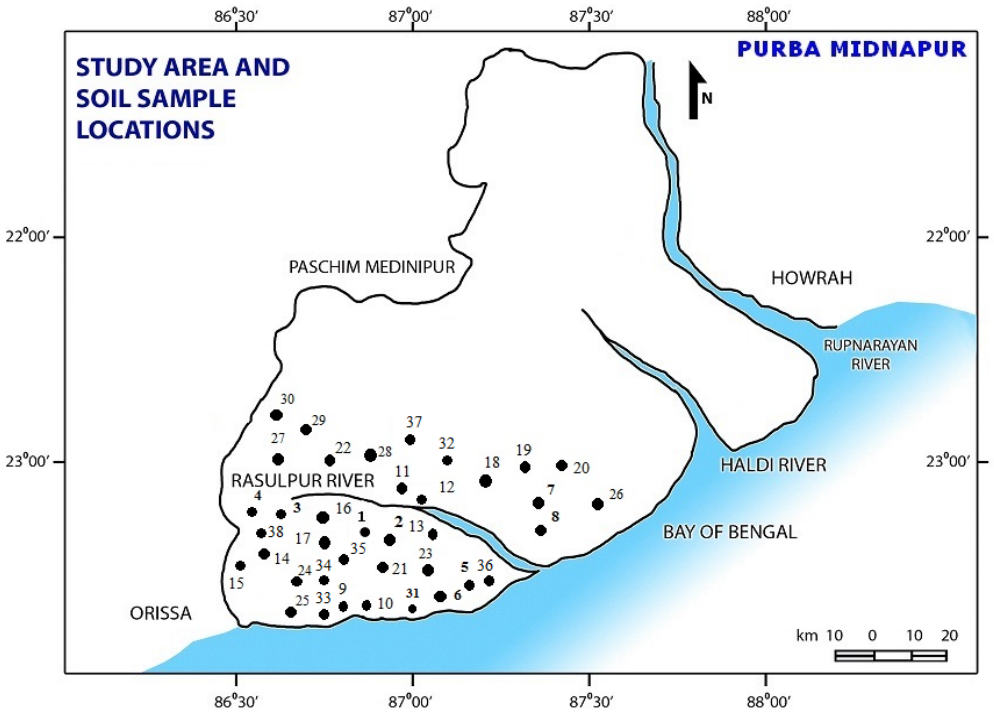

Fig. 8.24: Site location map of 30 pumping wells from where data collected in 2012 and eight pumping wells from where data collected in 2002.

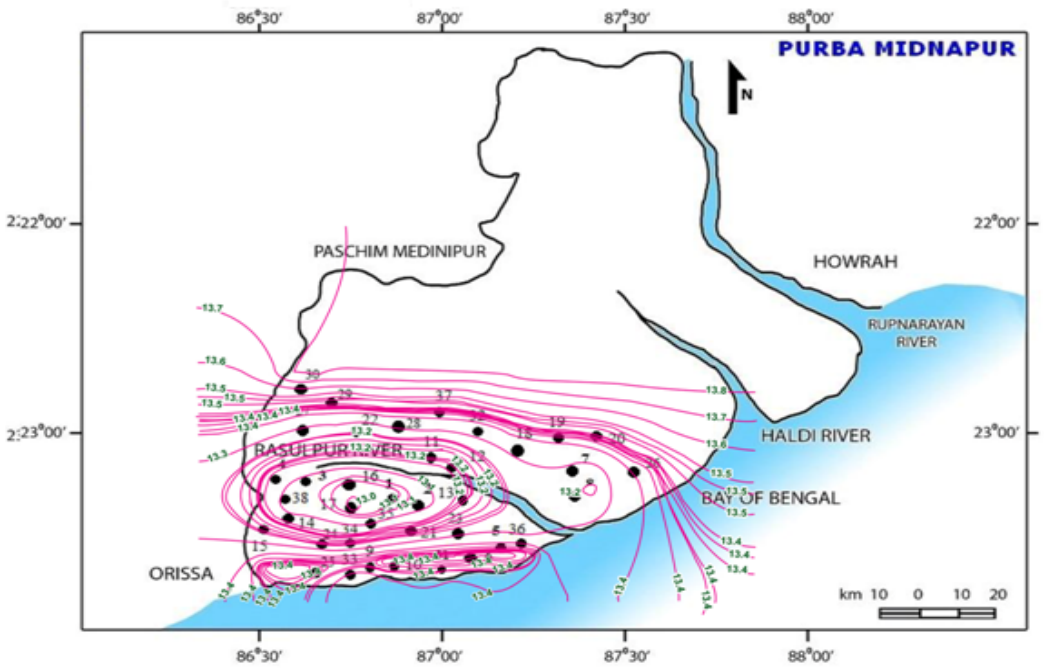

Fig. 8.25: Contour map showing simulated groundwater levels for the year of 2019 based on observed well discharge data gauged in 2002 and 2012.

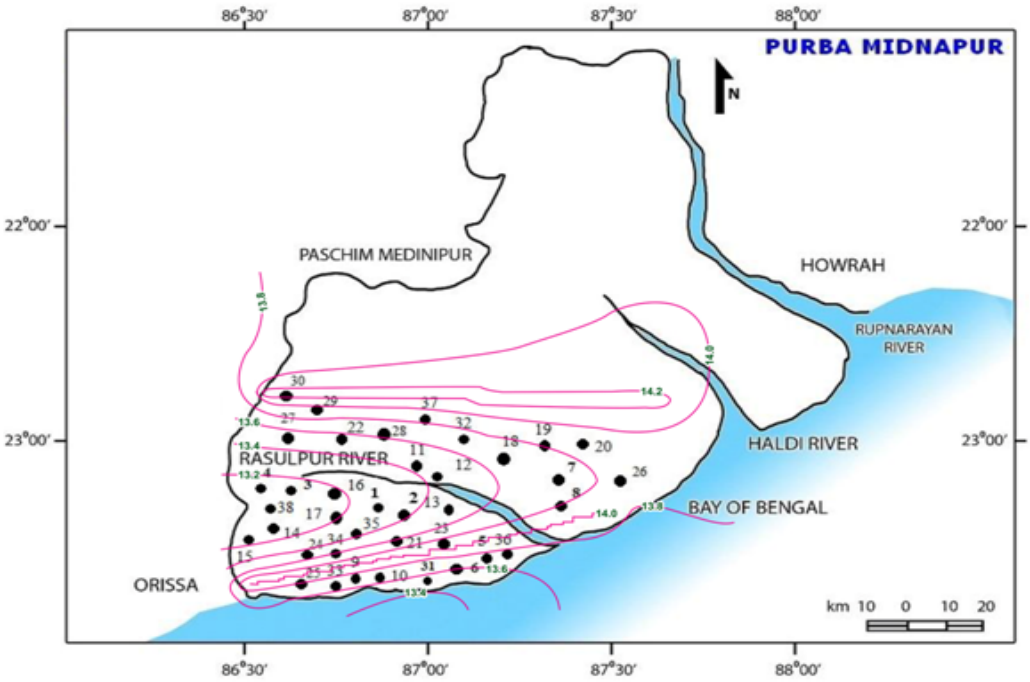

Fig. 8.26: Contour map showing simulated groundwater levels for the year of 2020 based on observed well discharge data gauged in 2002 and 2012.

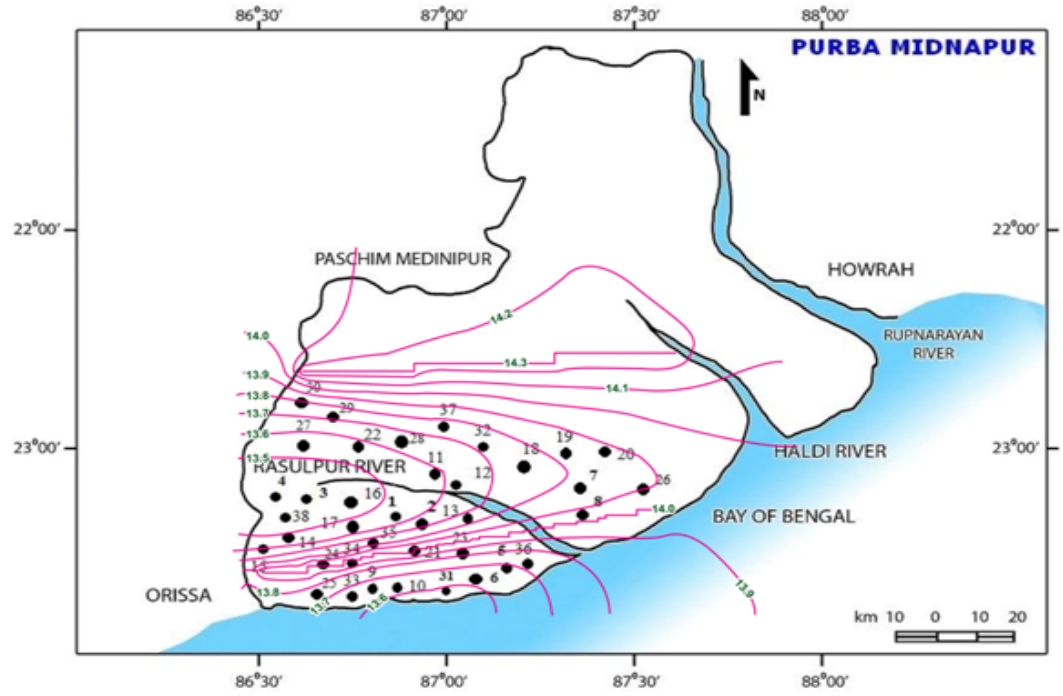

Fig. 8.27: Contour map showing simulated groundwater levels for the year of 2021 based on observed well discharge data gauged in 2002 and 2012.

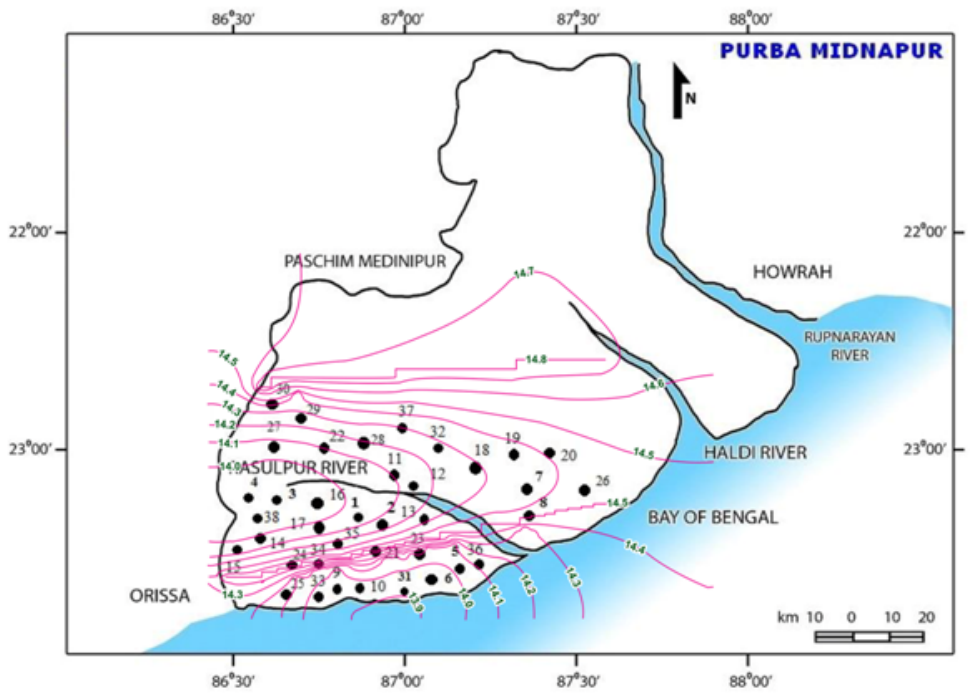

Fig. 8.28: Contour map showing simulated groundwater levels for the year of 2022 based on observed well discharge data gauged in 2002 and 2012.

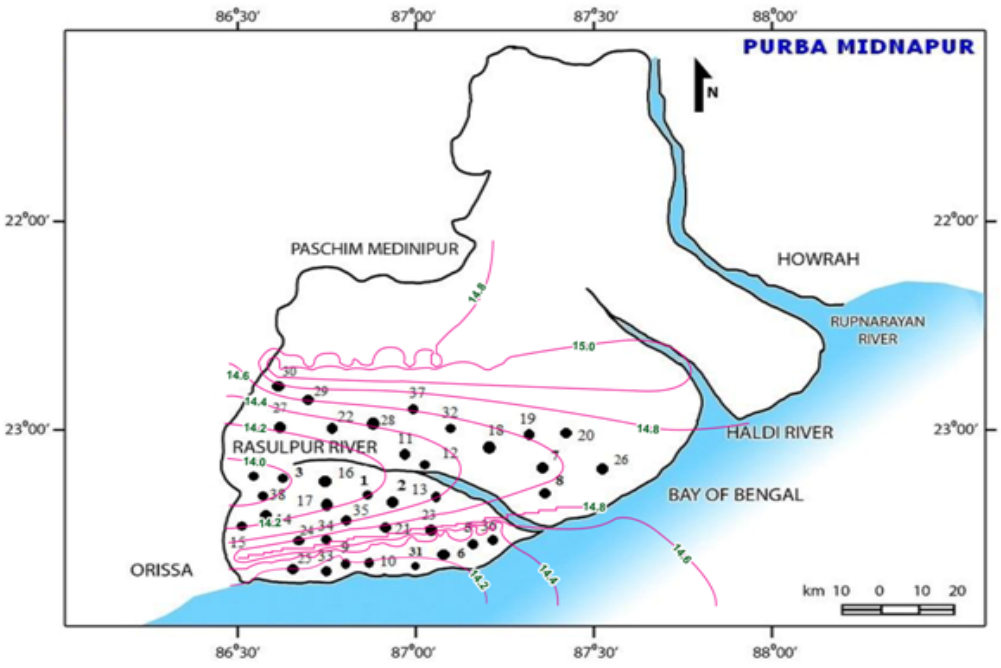

Fig. 8.29: Contour map showing simulated groundwater levels for the year of 2023 based on observed well discharge data gauged in 2002 and 2012.

Table 8.14: Simulated groundwater levels for the years 2019 to 2023 based on combined well discharge data observed in 2002 and 2012.

Sl. No.	Name of the well	Simulated groundwater levels for the year				
		2019	2020	2021	2022	2023
01	Talda WS Scheme	13.1	13.2	13.5	14.0	14.2
02	Talda WS Scheme (2)	13.1	13.4	13.6	14.1	14.3
03	Bhajachauli	13.1	13.2	13.4	13.9	14.0
04	Bhajachauli WS (2nd TW Site)	13.2	13.2	13.4	13.9	14.0
05	Haripur WS	13.4	13.8	13.9	14.0	14.3
06	Haripur WS (2nd TW Site)	13.4	13.6	13.7	13.9	14.2
07	Chandiveti WS	13.4	13.7	13.8	14.3	14.6
08	Chandiveti WS (2nd TW Site)	13.2	13.8	13.9	14.5	14.6
09	Sankarpur WS	13.4	13.6	13.7	13.9	14.2
10	Sankarpur WS (2nd TW Site)	13.4	13.6	13.7	13.9	14.2
11	Sapai WS	13.2	13.4	13.6	14.1	14.3
12	Sapai WS (2nd TW Site)	13.2	13.4	13.6	14.1	14.3
13	Anurai WS	13.2	13.4	13.8	14.2	14.4
14	Jumbani WS	13.1	13.5	13.6	14.0	14.1
15	Jumbani WS (2nd TW Site)	13.2	13.4	13.5	14.0	14.2
16	Durmuth WS	13.1	13.4	13.5	14.0	14.1
17	Durmuth WS (2nd TW Site)	13.0	13.2	13.5	14.0	14.1
18	Paschim Kumarda WS	13.4	13.5	13.8	14.3	14.6
19	Paschim Batya WS	13.5	13.7	13.9	14.4	14.6
20	Paschim Batya WS (2nd TW Site)	13.5	13.8	13.9	14.0	14.6
21	Contai Saline area Zone II	13.2	13.4	13.9	14.0	14.6
22	Dakshin Charikhia (2nd TW Site)	13.3	13.4	13.6	14.1	14.4
23	Bankipur WS	13.3	13.9	14.0	14.1	14.3
24	Baghmari WS	13.2	13.4	13.8	14.0	14.2
25	Barchubnfuli WS	13.4	13.6	13.7	14.2	14.3
26	Barsubarnanagar WS	13.4	13.8	13.9	14.2	14.6
27	Dhanghora WS	13.3	13.4	13.6	14.1	14.2
28	Kumirda WS (2nd TW Site)	13.4	13.6	13.7	14.2	14.4
29	Kumirda WS	13.5	13.8	13.9	14.2	14.6
30	Dhanghora WS 2nd TW Site)	13.7	14.0	14.1	14.4	15.0

8.13.1 Correlation Coefficient

For the study area, the simulated values of groundwater levels for the years 2019 to 2023 based on pumping well discharge data measured in 2002 (case 1) and 2012 (case 2) are taken as *x* and simulated values of groundwater levels for the years 2019 to 2023 based on combined pumping well discharge data measured in 2002 and 2012 is taken as *y*.

These values are used to determine the correlation coefficients using Equation (8.2) as elaborated previously. The correlation coefficients for the years 2019 to 2023 are depicted in Table 8.15. The range of these correlation coefficients indicate the simulated groundwater levels at study area for the years of 2019 to 2023 based on well discharge data in the year of between 2002 data and 2002 & 2012 for case 1 and between 2012 data and 2002 & 2012 for case 2 match moderately.

The magnitude of correlation coefficient shows that the simulated groundwater levels moderately match; the correlation coefficient values also confirm that the model calibration is moderate. Since the simulated values match reasonably well based on these correlation coefficients, therefore these data validate the model.

Table 8.15: Correlation coefficients.

Case	Correlation coefficients based on	Data simulated for the year				
		2019	2020	2021	2022	2023
1	2002 data and 2002-2012 combined data	0.550	0.536	0.370	0.491	0.519
2	2012 data and 2002-2012 combined data	0.653	0.545	0.279	0.644	0.705

8.14 Prediction of Groundwater Flow Path

The simulated groundwater levels at the coastal part of Purba Midnapur for the year 2012 based on the pumping well discharge data measured in 2002 are displayed in Table 8.5 and simulated groundwater levels for the years 2019 to 2023 based on the pumping well discharge data measured in 2002 and 2012 are illustrated in Tables 8.11-8.12.

The simulated groundwater levels for the years 2019 to 2023 based on the pumping well discharge combined data of 2002 and 2012 are displayed in Tables 8.14.

It is observed that the groundwater levels in south direction are lower compared to the groundwater levels observed in the north direction. Groundwater always flows from higher level (elevation) to lower level. It is evident from the discussion that water is flowing from south direction to north direction that is from Bay of Bengal side saline water intrusion is taking place into the aquifers towards inland direction.

In the real field situation saline water encroachments have substantial effect and cover up to 50 km of location from Kalindi (near sea) to Nandakumar (inland location). Saline water also enters the aquifer through the highly porous coastal deposits near Contai and Digha.

The Table 8.16 is showing the blocks of Purba Midnapur which are affected by saline water intrusion.

Table 8.16: The blocks affected and unaffected by saline water intrusion.

District	Affected blocks		Unaffected blocks
Purba Midnapur	1.Ramnagar-I	10.Nandigram-III	1. Pataspur-I
	2.Ramnagar-II	11.Sutahata-I	2. Pataspur-II
	3.Contai-I	12.Sutahata-II	3. Bhagwanpur-I
	4.Contai-II	13.Mahisadal-I	4. Bhagwanpur-II
	5.Contai-III	14.Mahisadal-II	5. Moyna
	6.Khejuri-I	15.Tamluk-I	6. Panskura-I
	7.Khejuri-II	16.Tamluk-II	
	8.Nandigram-I	17. Egra-I	
	9.Nandigram-II	18 Egra-II	

8.15 Significant Remarks

From the entire investigation, the following significant remarks are drawn:

- In the present research work, future groundwater levels or piezometric surface have been predicted using numerical simulation technique. The digitized map of the entire coastal areas of Purba Midnapur district has been taken as base map. Groundwater level conditions at different time period has been estimated. Temporal interrelationships between these estimated groundwater levels are found out too.
- During calibration and validation phases, the data of well discharges and other data for the year 2002 have been simulated for estimating groundwater levels for the year 2012. Then these estimated values have been compared with the actual field data of groundwater measured in 2012. The correlation coefficient between the estimated and observed groundwater levels for the year 2012 is calculated 0.56. It shows a moderate calibration as the results were highly dependent on only eight numbers of pumping well discharge data measured in 2002.
- The comparison between simulated groundwater levels for the years 2019 to 2023 for the pumping well discharge data observed in the year of 2002 and in the year of 2012 has been made. The correlation coefficient between these two values is found 0.83, 0.82, 0.84, 0.82 and 0.81 for the years 2019 to 2023, respectively. It indicates predicted of groundwater levels for the years 2019 to 2023 for both the cases closely match and provide almost correct predictions. So the groundwater levels for the years 2019 to 2023 at different locations of the study area have been found out without actually measuring it.
- The comparison between simulated groundwater levels for the years 2019 to 2023 for the pumping well discharge data observed in the year of 2002 and combined data of 2002 and 2012 have been made. And another comparison, the simulated groundwater levels for the years 2019 to 2023 between 2012 data and combined data of 2002 and 2012 has been estimated. The correlation coefficients are

determined for both the cases which show that the simulated groundwater levels moderately match; the correlation coefficient values also confirm that the model calibration is moderate.

- Since sufficient numbers (30 locations) of pumping well discharge data for the year 2012 are available and simulation of predicted groundwater levels for the study area for the years 2019 to 2023 are highly dependent on these thirty numbers of pumping well discharge data for the year 2012, hence it can be concluded that the future prediction of groundwater levels in this scenario are very much realistic.
- From the years 2019 to 2023, the groundwater level has been decreased as estimated by simulation process with an average magnitude 13.4 m of groundwater level in southern part of Purba Midnapur to an average 15.7 m in northern part of Purba Midnapur. So the groundwater levels in coastal areas of Purba Midnapur are decreasing. It may happen that few places of the study area become water scarce during pre-monsoon period. The groundwater levels in the southern part of Purba Midnapur are high compared to the groundwater levels in the northern part of Purba Midnapur. It confirms that the seawater intrusion is taking place towards inland areas of Purba Midnapur from the side of Bay of Bengal which is in the south direction of Purba Midnapur. Thereby this salt water intrusion is making the groundwater and soil saline.

8.16 References

Al-Salamah, I.S., Ghazaw, Y.M. and Ghumman, A.R. (2011). Groundwater modelling of Saq Aquifer Buraydah Al Qassim for better water management strategies. *Environmental Monitoring and Assessment*, Vol. 173, No. 1, pp. 851-860.

Das, S., Nayek, M., Das, S. Dutta, P. and Mazumdar, A. (2014). Impact on Water Quality in Piyali River, Sundarbans, India due to Saline Water Intrusion. *Indian Journal of Environmental Protection*, Vol. 34, No. 12, pp. 1010-1019.

Dhar, S., Das, S. and Mazumdar, A. (2009*a*). Salinity Intrusion Impact on the Piyali River of the Sundarbans, International Conference on Emerging Technologies in Environmental Science and Engineering, Aligarh, Uttar Pradesh, pp. 383-391, 26 - 28 October, 2009.

Dhar, S., Das, S., Ray, S.S. and Mazumdar, A. (2009*b*). Environmental Monitoring of the Salt Water Intrusion Phenomenon of the Piyali River, Proceedings of National Conference on Advances in Environmental Engineering (AEE-09), Department of Civil Engineering, NIT Rourkela, Orissa, pp. 377-382, 14-15 November, 2009.

Dhar, S., Das, S., Ray, S.S., Debbarma, J. and Mazumdar, A. (2009*c*). First Investigation of the Status of potable water availability of the Piyali River, National Seminar on Good Governance in Water Supply & Sanitation Management in Context to Millennium Development Goal, pp. 121- 126.

Dhar, S., Das, S., Ray, S.S., Debbarma, J. and Mazumdar, A. (2009*d*). Effects of Climate Change on the Crop Productivity in the Saline Soils of the Piyali River, 5th Asian

Regional Conference of International Commission on Irrigation and Drainage (ICID), New Delhi, India, pp. 300, 9-11 December 2009.

Dhar, S., Das, S., Debbarma, J. and Mazumdar, A. (2009*e*). First Investigation of the Climate Change Impact on the Crop Productivity of the Piyali River Region, 60th International Executive Council Meeting & 5th Asian Regional Conference, New Delhi, India, 6-11 December 2009.

Dhar, S., Das, S. and Mazumdar, A. (2010). Salt Water Intrusion into the Piyali River Aquifer of the Sundarbans, West Bengal, Proceedings of the National Conference on Groundwater Resource Development and Management in Hard Rocks – supported by DST, GoI, University of Pune, pp. 35-36, February, 2010.

Freeze, R.A. (1971). Three-dimensional, Transient, Saturated-Unsaturated Flow in a Groundwater Basin. *Water Resources Research*, Vol. 7, No. 2, pp. 347-366.

Freeze, R.A. and Witherspoon, P.A. (1966). Theoretical Analysis of Regional Groundwater Flow: 1. Analytical and Numerical Solutions to the Mathematical Model. *Water Resources Research*, Vol. 2, No. 4, pp. 641-656.

Gao, H. (2011). Groundwater Modelling for Flow Systems with Complex Geological and Hydrogeological Conditions. *Procedia Earth and Planetary Science*, Vol. 3, pp. 23-28.

Ismail, W.M.Z., Yusoff, I and Rahim, B.E.A. (2013) Simulation_of horizontal well performance using Visual MODFLOW. *Environmental Earth Science*, Vol. 68, No. 4, pp. 1119-1126.

Jin-sheng, J., Jing-jie, Y. and Chang-ming, L. (2002). Groundwater regime and calculation of yield response in North China Plain: a case study of Luancheng County in Hebei Province. *Journal of Geographical Sciences*, Vol. 12, No. 2, pp. 217-225.

Korkmaz, S., Pekkan, E. and Guney, Y. (2016). Transient Analysis with MODFLOW for Developing Water-Diversion Function. *Journal of Hydrologic Engineering*, Vol. 21, Iss. 6, pp. 05016009.

Lakshmi P.C. and Narayanan R.M. (2015). Study on Groundwater Modeling of Aquifers Using Visual Modflow. *International Research Journal of Engineering and Technology*, Vol. 2, Iss. 2, pp. 23-26.

Lasya, C.R. and Inayathulla, M. (2015). Groundwater flow analysis using Visual Modflow. *IOSR Journal of Mechanical and Civil Engineering*, Vol. 12, Iss. 2, pp. 5-9.

Malik, V.S., Singh, S.K. and Singh, R.K. (2012). Application of "Processing MODFLOW for Windows (PMWIN)" For Sustainable Ground Water Resources Study for Gurgaon District, Haryana, India. *International Journal of Engineering Science and Technology*, Vol. 4, No. 9, pp. 3988-4002.

McDonald, M.G. and Harbaugh, A.W. (1988). A Modular Three-dimensional Finite-difference Ground-water Flow Model. Open-File Report 83–875, U.S. Geological Survey, Colorado, USA.

Singh, R.M. and Shukla, P. (2016). Groundwater System Simulation and Management Using Visual MODFLOW and Arc-SWAT. *Journal of Water Resource and Hydraulic Engineering*, Vol. 5, Iss. 1, pp. 29-35.

Sun, R.J. and Johnston, R.H. (1994). Regional Aquifer System Analysis Program of the U.S. Geological Survey, 1978–1992. U.S. Geological Survey, Circular 1099, United States Government Printing Office, Washington, USA.

Takounjou, F.A., Rao, V.V.S.G., Ngoupayou, N., Nkamdjou, L.S. and Ekodeck, G.E. (2009). Groundwater flow modeling in the upper Anga' river watershed, Yaounde, Cameroon. *African Journal of Environmental Science and Technology*, Vol. 3, No. 10, pp. 341-352.

Toth, J. (1963). A Theoretical Analysis of Groundwater Flow in Small Drainage Basins. *Journal of Geophysical Research*, Vol. 68, Iss. 16, pp. 4795-4812.

Trescott, P.C. (1975). *Documentation of a Finite Difference Model for Simulation of Three Dimensional Ground-Water Flow*. Open-File Report 75-438, U.S. Geological Survey, Virginia, USA.

USGS (2000). MODFLOW-2000, The U.S. Geological Survey Modular Ground-Water Model—User Guide to Modularization Concepts and The Ground-Water Flow Process. U.S. Geological Survey, Open-File Report 00-92, Virginia, USA.

Varalakshmi,V., Rao, B.V. Surinaidu, L. and Tejaswini, M. (2014). Groundwater Flow Modelling of a Hard Rock Aquifer: Case Study. *Journal of Hydrologic Engineering*, Vol. 19, Iss. 5, pp. 877-886.

Waterloo (2006). Visual MODFLOW v.4.2 User's Manual. Waterloo Hydrogeologic Inc, USA.

CHAPTER - 9

(Field Investigation-II: Groundwater Quality Assessment)

- Field Investigation for groundwater Sampling
- Water Quality Analysis
- Interpretation from Groundwater Quality Analysis
- Water Use for Drinking Purpose
- Photography View of Different Wells and Sites
- References

9.1 Field Survey for Groundwater Sampling

The coastal region of Purba Midnapur district nearby the Bay of Bengal is getting influenced by saline water ingression through aquifers and canals. Because of effect of salinity in soil the crop yields are decreasing day by day, which gives a caution to the future economy of the concerned zone.

From geological investigation, it is seen that since long years prior the coastal area of Purba Midnapur was located near Bay of Bengal at lower region of Rajmahal and Singbhum. In actual fact the coastal areas of West Bengal were constructed by stratified layers which are framed through the deposition of sediment and stones in years after years carrying by rivers Ganga, Bhagirathi and others. Because of normal disaster, numerous lives and trees are covered under soil layers formation since long consequential, the normal of soil is acidic. Generally stratified soil has more permeability in the horizontal direction entrance of saline water from ocean (Bay of Bengal). Therefore it is quite obvious that the soil in the coastal area is highly saline.

The fertility of soil of the coastal zone of Purba Midnapur may be improved if the following measures are taken by (i) adopting proper drainage and (ii) decreasing or removing salinity from soil and water. Mainly four types of soil are found in the coastal areas which are (i) saline soil, (ii) saline alkali soil, (iii) non saline alkali soil and (iv) degraded saline soil. The soil structures of the coastal area are immature and electrical conductivity is not suitable for seeding. The following measures are taken for better development of saline affected area.

- The different blocks contain different types of saline soil with sodium, potassium and chloride within permissible limit.
- Good result is obtained if the saline canals are properly lined.
- After ploughing, freshwater is allowed to flow over the land and saline water is controlled after seeding.
- Rabi and boro crops are not possible due to shortage of freshwater.
- Kharip and Rabi crops may be possible only if the ground level of the land is high.
- Canals, ponds and reservoirs are cleaned, discharged silt water from reservoir and stored freshwater which are used for irrigation and other works.

In rainy season there is no effect of salinity on the crops because all crops are mainly grown up by rain fed water. However, in summer season all crops are affected due to salinity. Some salt tolerant crops may grow successfully in summer season like sunflower, chilli, cotton, etc.

In 2002, the Midnapur district was divided into Purba Midnapur and Paschim Midnapur districts. The Purba Midnapur district has five sub-divisions naming Tamluk, Contai, Panskura, Egra and Haldia. The township Haldia is a noteworthy seaport in Purba Midnapur district. It is located around 150 kilometres southwest of Kolkata close to the mouth of the Hooghly River, one of the mouths of the Ganges. Haldia is becoming as a noteworthy exchange port for Kolkata, expected basically for mass cargoes. The township has a fertilizer factory, petrochemical complex and refinery, in addition to various light industries.

Table 9.1: Location of saline canals in coastal region of Purba Midnapur.

Sl. No.	Blocks	Source of saline water
01	Khejuri-I	Canal
02	Khejuri-II	Sea and canal
03	Contai-I	Sea and canal
04	Contai-II	Sea and canal
05	Contai-III	Canal
06	Ramnagar-I	Sea and canal
07	Ramnagar-II	Sea and canal
08	Bhagbanpur-II	Canal

In the brackish zone of Contai area of Purba Midnapur district, big Rural Water Supply Scheme (WSS) covering populations of 1,10,000 in 207 habitations has been successfully commissioned with technical assistance obtained from Bhaba Atomic Research Centre (BARC) for locating sustainable sources. The coastal belt of Purba Midnapur district is 150 km long and average width is 8 to 20 km towards inland. Agriculture, fishing and industrial trading are the chief sources of earning of the common people in this district. Three streams, Haldi and Rupnarayan towards the north and Rasulpur towards the south, are considered as responsible for saline water intrusion. Saline water also enters the aquifer through the highly porous coastal deposits near Contai and Digha. The locations of saline canals in coastal region of Purba Midnapur are displayed in Table 9.1. Tables 9.2(a) and 9.2(b) represent the affected and unaffected blocks of Purba Midnapur due to seawater intrusion. As shown in Figure 9.1, Purba Midnapur district is divided into blocks which are the smallest units for administrative purposes. Groundwater takes an essential part in human life and advancement. A comprehension of the synthetic nature of groundwater is fundamental in deciding its convenience for domestic, industrial and farming purposes. Good quality of water, for agriculture purpose, can possibly cause better product yields under great soil and water management practices.

The appropriateness of irrigation water relies on numerous variables including the nature of water, soil compose, salt resistance qualities of plants, atmosphere and seepage features of soil.

Groundwater dependably contains little measures of solvent salts. The kind and nature of these salts rely on the sources for recharge of the groundwater and the strata through which it streams. An abundance of dissolvable salts can be destructive for some harvests. Henceforth, a comprehension of the science of groundwater is basic to appropriately assess groundwater quality for drinking, enterprises and irrigation purposes. The present examination has been attempted with the goal of (a) chemical characterisation of groundwater of the study area and (b) assessment of the reasonableness of groundwater in the investigation zone for drinking businesses and irrigation purposes. The district is drained by the Haldi, Rupnarayan and Rasulpur rivers and their many tributaries and distributaries, which form a network of rivers and tidal creeks.

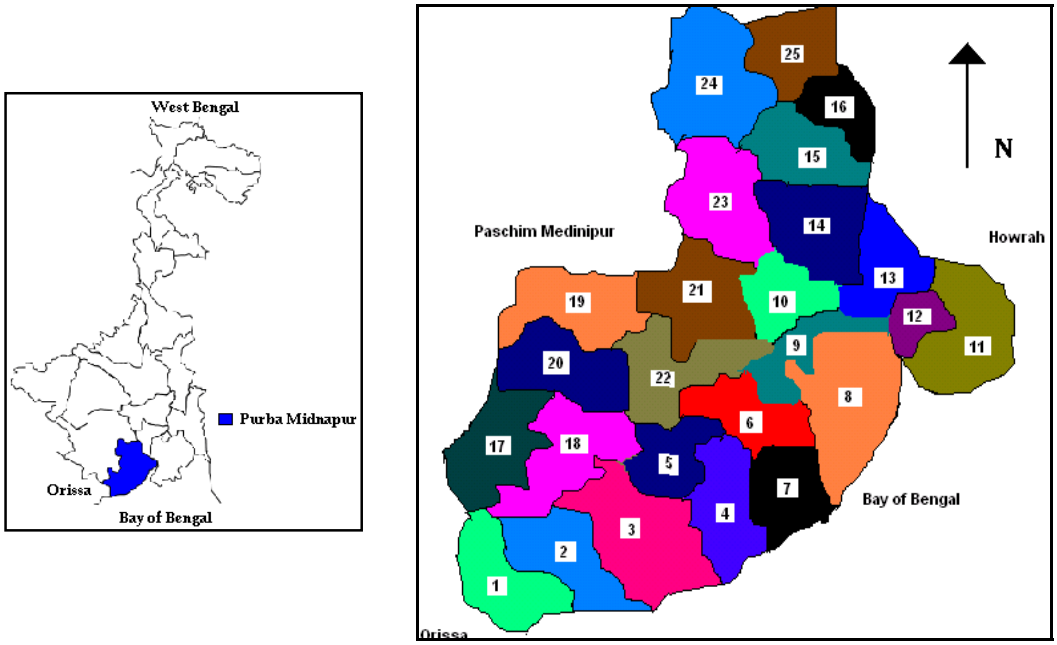

Fig. 9.1: Different blocks of Purba Midnapur district.

Table 9.2 (a): The blocks affected by saline water intrusion.

District	Block	Block	Block
Purba Midnapur	1.Ramnagar-I	7. Khejuri-II	13. Mahishadal-I
	2. Ramnagar-II	8. Nandigram-I	14. Mahishadal-II
	3. Contai-I	9. Nandigram-II	15. Tamluk-I
	4. Contai-II	10. Nandigram-III	16. Tamluk-II
	5. Contai-III	11. Sutahata-I	17. Egra-I
	6. Khejuri-I	12. Sutahata-II	18. Egra-II

Table 9.2 (b): The unaffected blocks of Purba Midnapur.

District	Block	Block	Block
Purba Midnapur	19. Pataspur-I	21. Bhagwanpur-I	23. Moyna
	20. Pataspur-II	22. Bhagwanpur-II	24. Panskura-I

9.1.1 Phase wise Water Sample Collection

Groundwater samples have been collected from various profound tubewells, under Public Health Department of Government of West Bengal, in coastal areas of Purba Midnapur on phase I, phase II, phase III and phase IV basis. In the phase I to phase IV, groundwater samples have been collected from the tube wells/bore wells and examined at the Chemical Laboratory of State Water Investigation Directorate under Government of West Bengal at Saltlake for checking different chemical parameters. Figure 9.2 shows the geographical location of the sampling points in the study area. The parameters monitored based on the collected water samples - include pH, electrical conductivity, total dissolved solids (TDS) and anions such as carbonates, bicarbonates and chlorides [Table 9.3].

Phase I: Total eight samples have been collected from eight tubewells located at Nijkashba, Serkhan Chak well-I, Serkhan Chak well-II, Mukutsila-I, Mukutsila-II, Kharipukhuria, Kalindi and one from seawater. These tubewells cover the blocks of Contai-I, Contai-II, Khajuri-I and Nandigram-I.

Phase II: Total twelve samples have been collected from the tubewells located at Ramnagar, Well-I, Basantia High School, Majna, well-II, Katchlageria,well, Charaichia, well-II, Panichiari, well-I, Mukutsila (zone-I) well-II, Khejuri, well-II, Shilaberia, well No.-I, Kamarda, well-II, Digha central zone, well-II, Digha western zone, well-I and Mandar, well-I covering the blocks of Ramnagar-I, Ramnagar-II and Khejuri-II.

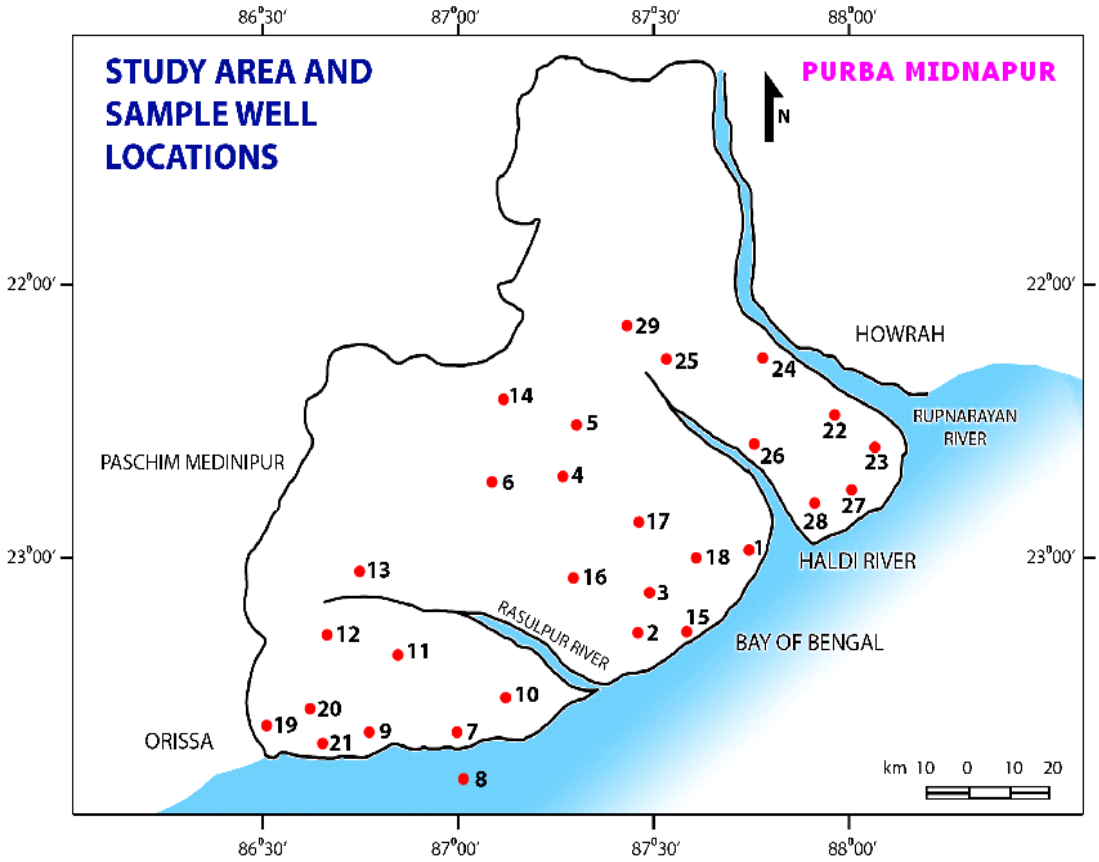

Fig. 9.2: Groundwater sampling locations at the study area.

Phase III: The tubewells such as Betkundu-Water Supply-Scheme P.H.No-1, Dhekua-Water Supply-Scheme P.H.No-2, Natsal Water Supply Scheme P.H.No-1, Zone-2, Gopalpur-Water Supply-Scheme P.H.No-1, Laksha-Supply Scheme P.H.No-1, Chaitanyapur Supply Scheme-P.H.No-1, Zone-1, Chaitanyapur Supply Scheme-P.H.No-1, Zone-2 and Nandakumar Supply Scheme P.H.No-1 total eight samples have been collected under phase III covering different blocks Sutahata-I, Sutahata-II, Mahishadal-I, Mahishadal-II and Nandakumar. The results of chemical analysis done for Phase I, II and III are given in Table 9.3.

Phase IV: The water samples were collected from 20 number shallow tube wells located in Contai Municipality area. The results of chemical analysis done for Phase IV are given in Table 9.3.

9.1.2 Procedure for water samples collection

At first a jar ken of capacity 1.5 litres was used to wash with distilled water. After that collected deep tube well water sample was poured in this jar ken and tightened with inward top and external top for anticipation of air passing.

9.1.3 Physico-Chemical Properties of Water Samples

Chemical analysis of groundwater samples, collected from deep tube wells located at different blocks of Purba Midnapur, have been conducted at the laboratory of State Water Investigation Directorate in Saltlake. The water samples have been collected from an average depth of around 200 m below ground level.

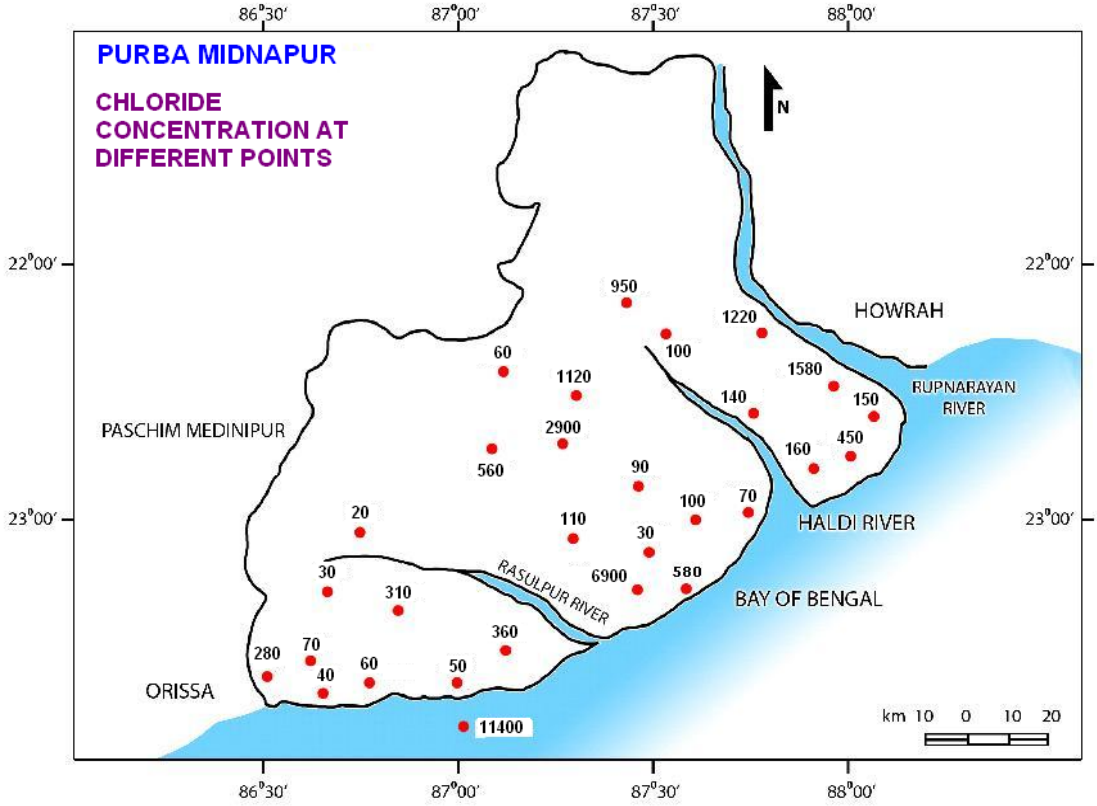

Fig. 9.3: Variation of groundwater chloride concentration (ppm) at study area.

From the physico-chemical examination as shown in Table 9.3, the information obtained for chloride concentration (ppm) has been plotted in Figure 9.3 for the investigation area and applicable contour shapes have been built as shown in Figure 9.4. The specific gravity of tubewell water samples collected from different locations is illustrated in Table 9.4.

Table 9.3: Physico-chemical properties of groundwater samples and seawater sample.

Sl. No.	Area/Blocks	pH	Specific conduc-tivity ($\mu\Omega^{-1}$/cm) at 25^0C	Carbo-nate CO_3^{2-} (ppm)	Bicar-bonate HCO_3^- (ppm)	Chlori-de (Cl^-) (ppm)	Total Hard-ness $CaCO_3$ (ppm)	Iron (ppm)	TDS (ppm)	Cl / (HCO_3 + CO_3) (---)
1	Nijkashba	8.61	1040	40	280	70	250	0.25	666	0.219
2	Serkhan Chak Well-I	7.29	16000	Nil	570	6900	2480	14.39	10240	12.105
3	Serkhan Chak Well-II	8.14	1190	Nil	450	30	280	0.14	762	0.053
4	Mukutsila-I	7.72	6700	Nil	100	2900	1500	20.44	4288	29.00
5	Mukutsila-II	7.63	3300	Nil	210	1120	660	0.23	2112	5.330
6	Kharipukuria	7.77	1900	Nil	240	580	400	5.30	1216	2.416
7	Kalindi Well	8.50	470	40	250	50	120	0.17	301	0.173
8	Seawater	7.80	26000	Nil	180	11400	3570	0.72	16640	63.330
9	Ramnagar, Well-I	7.38	550	Nil	420	60	200	0.20	352	0.1428
10	Basantia-High School	7.86	1350	Nil	240	360	410	0.38	864	1.500
11	Majna, Well-II	7.36	1380	Nil	310	310	490	1.20	883	1.00
12	Katchlageria, Well	7.68	490	Nil	490	30	250	0.38	314	0.061
13	Charaichia, WelI-II	7.76	450	Nil	330	20	110	0.18	288	0.061
14	Panichiari, Well-I	7.38	1900	Nil	340	560	550	0.11	1216	1.647
15	Mukutsila (Zone-I) Well-II	8.19	580	Nil	280	60	210	0.18	371	0.214
16	Khejuri, Well-II	7.75	810	Nil	330	110	180	0.26	518	0.333
17	Shilaberia, Well	7.84	810	Nil	410	90	260	0.19	518	0.219
18	Kamarda, Well-II	7.18	850	Nil	360	100	230	0.09	544	0.220
19	Digha Central Zone, Well-II	7.67	1230	Nil	310	280	270	0.12	787	0.903
20	Digha-Western Zone, Well-I	7.17	560	Nil	250	70	150	0.13	358	0.280
21	Mandar, Well-I	7.47	480	Nil	270	40	290	0.12	307	0.148
22	Betkundu WSS	7.55	4700	Nil	250	1580	660	0.3	3008	6.320
23	Dhekua WSS P.H.No-2	7.71	910	Nil	280	150	100	0.2	582	0.535
24	Natsal WSS P.H.No-1, Zone-2	7.67	3900	Nil	200	1220	560	2.0	2496	6.100
25	Gopalpur WSS	7.71	920	Nil	230	100	40	2.0	589	0.434
26	Laksha-SS P.H.No 1	7.65	970	Nil	250	140	50	0.2	621	0.560
27	Chaitanyapur SS-P.H.No-1, Zone-1	8.64	1590	60	140	450	240	Nil	1018	2.250
28	Chaitanyapur SS-P.H.No-1, Zone-2	7.54	1010	Nil	200	160	440	Nil	646	0.800
29	Nandakumar SS P.H.No-1	7.31	3100	Nil	100	950	560	0.2	1984	9.500

Table 9.4: Specific gravity of tubewell water samples collected from different locations.

Sl. No.	Area/Blocks	Density of fluid (kg/m^3)	Sl. No.	Area/Blocks	Density of fluid (kg/m^3)
1	Nijkashba	993	16	Khejuri, Well-II	1001
2	Serkhan Chak, Well-I	991	17	Shilaberia, Well-I	989
3	Serkhan Chak, Wel- II	1010	18	Kamarda, Well-II	992
4	Mukutsila I	990	19	Digha Central Zone, Well-II	993
5	Mukutsila II	1000	20	Digha Western Zone, Well-I	993
6	Kharipukhuria	998	21	Mandar, Well-I	995
7	Kalindi Well	994	22	Betkundu WSS P.H.No-1	990
8	Seawater	1012	23	Dhekua WSS P.H.No-2	993
9	Ramnagar,Well-I	997	24	Natsal WSS P.H.No-1, Zone-2	992
10	Basantia High School	996	25	Gopalpur WSS P.H.No-1	991
11	Majna, Well-II	995	26	Laksha SS P.H.No-1	998
12	Katchlageria, Well	996	27	Chaitanyapur SS, P.H.No-1, Zone-1	994
13	Charaichia, Well-II	1012	28	Chaitanyapur SS, P.H.No-1, Zone-2	997
14	Panichiari, Well-I	992	29	Nandakumar SS P.H.No-1	996
15	Mukutsila (Zone-I) Well-II	998			

WSS : Water Supply Scheme
SS: Supply Scheme P.H. : Pump House

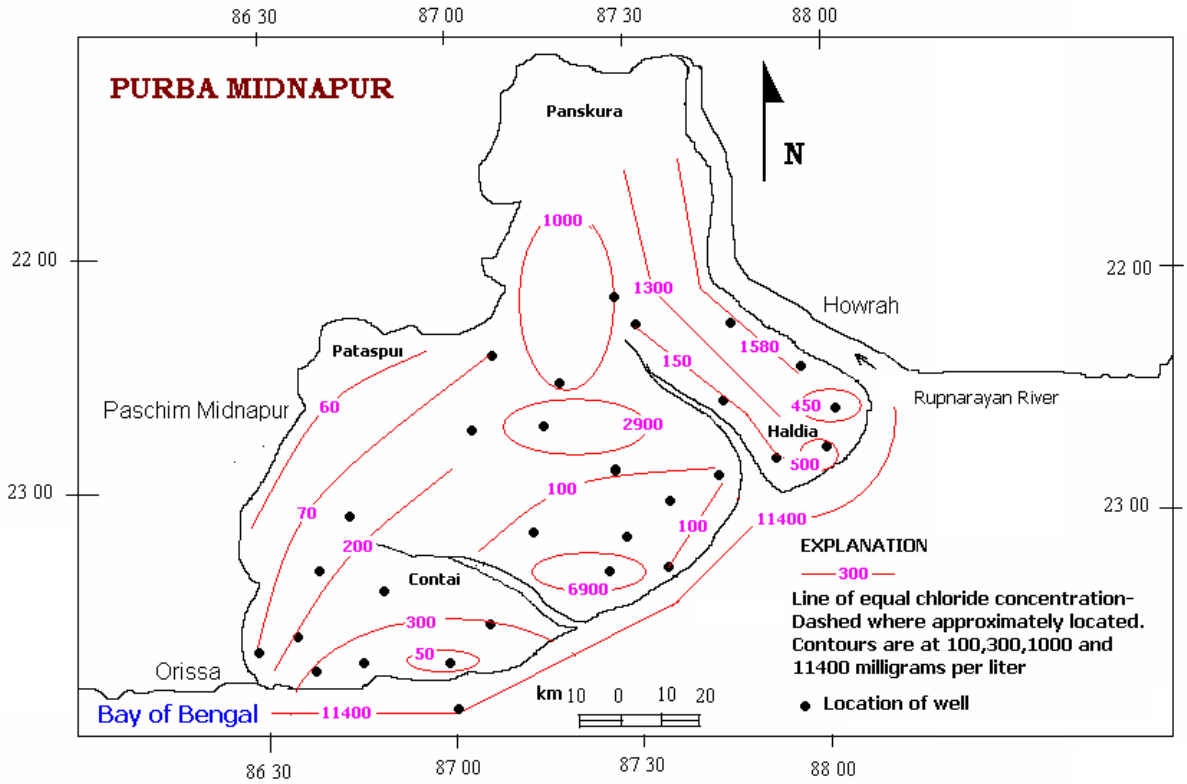

Fig. 9.4: Contours showing the change of chloride concentration (ppm) at study area.

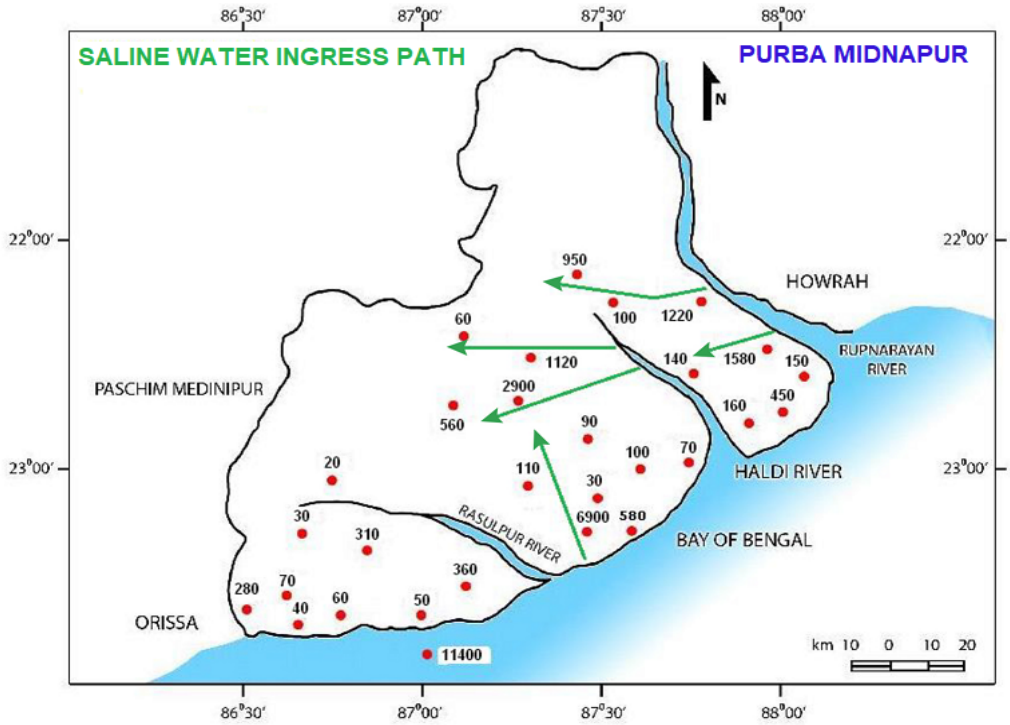

Fig. 9.5: Probable path of saline water ingress towards the study area.

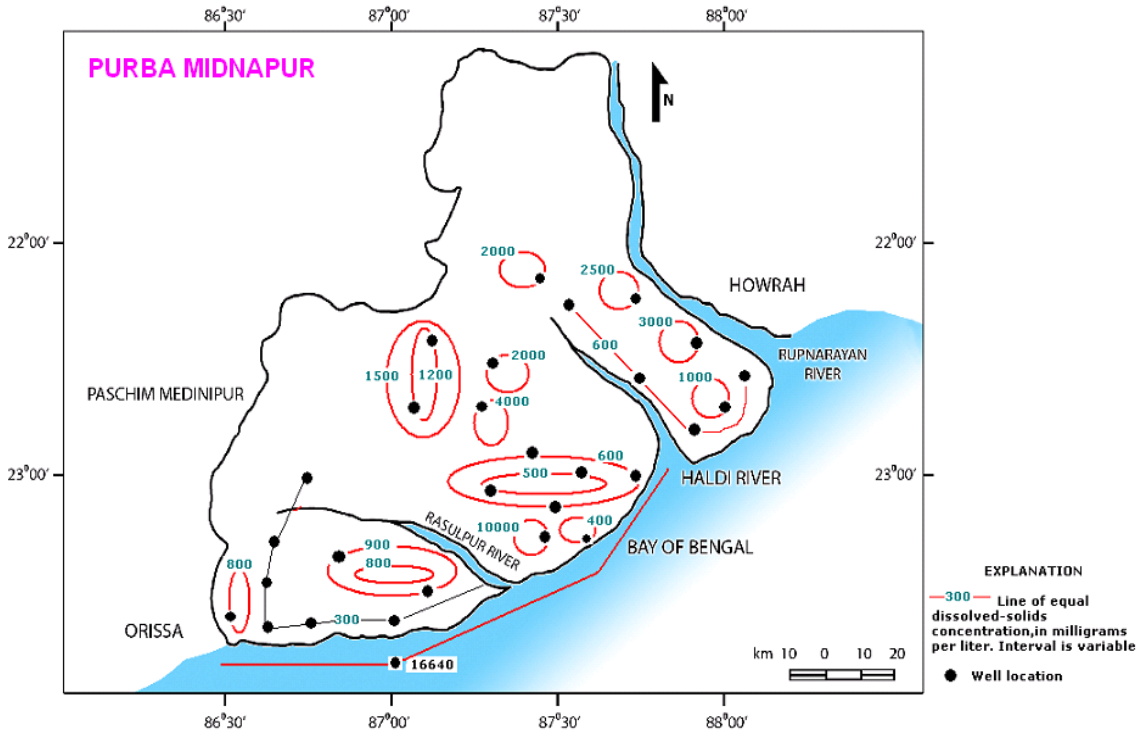

Fig. 9.6: Contours showing the variation of TDS concentration (ppm) at coastal areas.

As observed, the chloride concentration differs from as high as 11400 ppm along the ocean shore line to as low as 20 ppm at Khejuri. The examples of diversity of the chloride concentration in the aquifer at the profundity taken have been observed to be

very unpredictable. At a few areas, the chloride concentration is very high, for example, at Serkhan Chak (6900 ppm) and Mukutsila I (2900 ppm). Along the Rupnarayan stream bank chloride concentration is 1500 ppm. Then again, at couple of areas, the chloride concentration is essentially low like Charaichia (20 ppm), Kalindi (50 ppm), Pataspur (60 ppm), Nandigram (100 ppm) and Henria (200 ppm) and so forth. This heterogeneity in the aquifer media of the investigation region has ascribed to this inconsistency of the contours for chloride concentration.

The specific conductivity of water in micromhos/cm ($\mu\Omega^{-1}$/cm) is multiplied by 0.65 so as to obtain the dissolved salt content in ppm. The specific conductivity is expressed as follows:

$$\text{Specific conductivity} = \text{Dissolved salt} / 0.65 \qquad (9.1)$$

The specific conductivity is otherwise called salinity of groundwater table. From the chemical examination information, the specific conductivity in $\mu\Omega^{-1}$/cm has been plotted for the investigating zone and significant contours have been developed as shown in Figure 9.7.

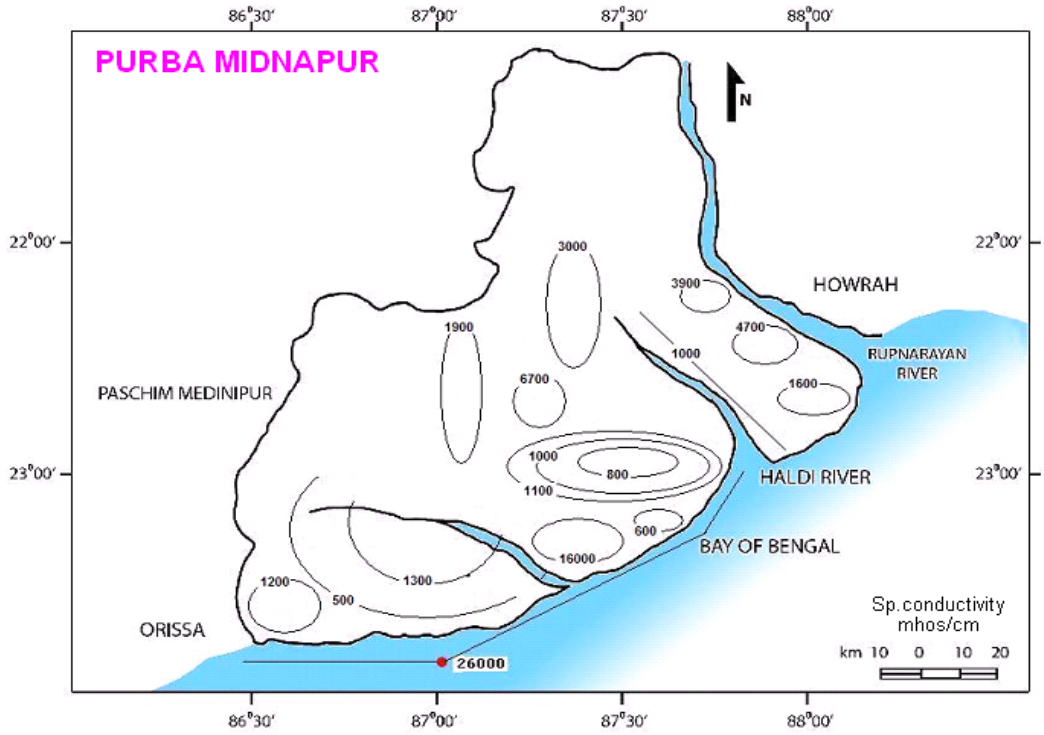

Fig. 9.7: Variation of salinity (specific conductivity) in $\mu\Omega^{-1}$/cm at 25^0C.

The specific conductivity fluctuates from as high as 26000 $\mu\Omega^{-1}$/cm along the ocean shore line from Digha to Haldia and as low as 450 $\mu\Omega^{-1}$/cm at Charaichia. The diversity of the specific conductivity in the aquifer at the profundity taken was observed to be reasonably uneven pattern. At some areas the specific conductivity concentration is very high, for example, at Serkhan Chak (16000 $\mu\Omega^{-1}$/cm) and Betkundu (4700 $\mu\Omega^{-1}$/cm). Along the Rupnarayan waterway bank specific conductivity is 4000 $\mu\Omega^{-1}$/cm. Then again, at couple of areas, the specific conductivity is essentially low like Katchlageria, (490 $\mu\Omega^{-1}$/cm) and Chandpur (550 $\mu\Omega^{-1}$/cm) and so on.

The water samples so collected from profound tube wells in the study area were chemically tested. The iron concentration in ppm has been plotted and the significant contours have been developed as shown in Figure 9.8. Out in the public water supply the permissible limit reaches of iron is 0.3 ppm according to IS-10500: 2012. As observed, the iron concentration fluctuates from as high as 0.72 ppm along the ocean shore line from Digha to Haldia to as low as 0.1 ppm at Panichiari. In some areas the iron concentration is very high, for example at Serkhan Chak (14.39 ppm) and Mukutsila (20.44 ppm). Along the Rupnarayan waterway bank iron concentration is in between of 0.2 ppm to 0.3 ppm. In any case, at couple of areas, the iron is considerably low like Digha-western zone (0.13 ppm), Kamarda (0.09 ppm) and Nijkashba at Nandigram (0.25 ppm) etc. High iron concentration makes the water turbid. Therefore iron should be removed by filtration or other process before using groundwater from different sectors.

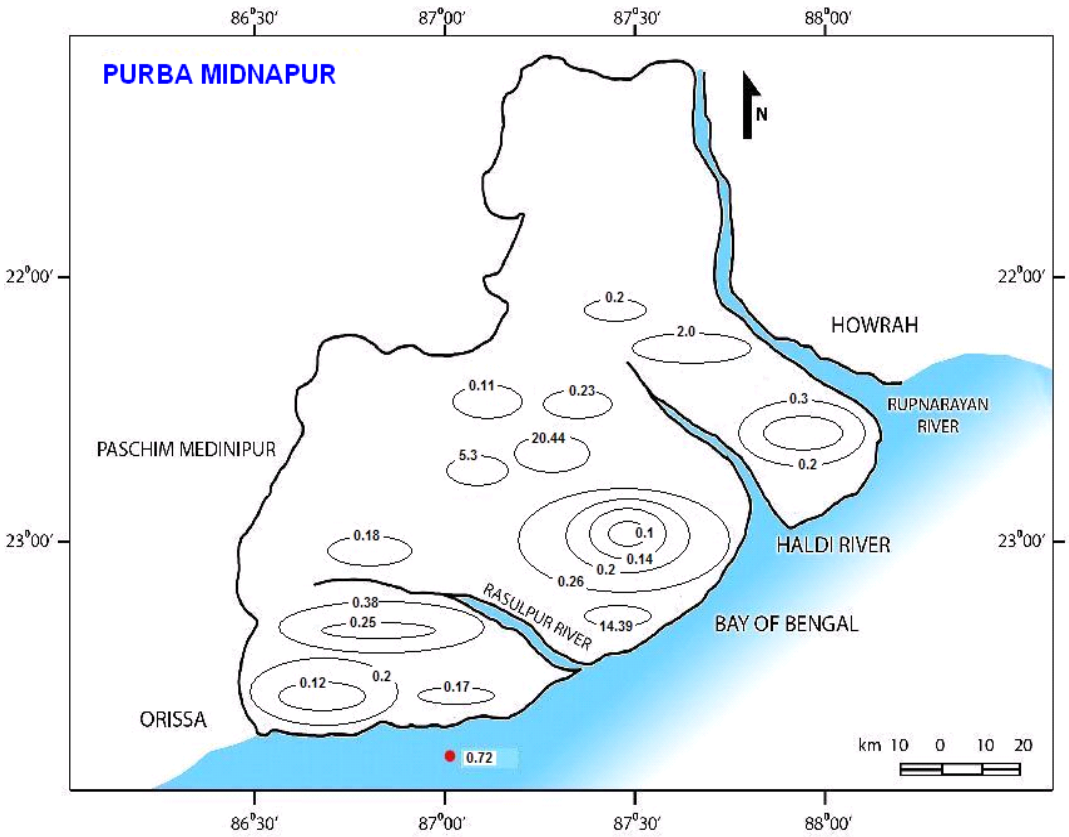

Fig. 9.8: Contour lines showing the change iron concentration at coastal areas.

9.1.4 Variation of Physico-chemical parameters in Contai

Contai municipality town [Figures 9.9-9.10] is the head quarter of Contai sub-division in the district of Purba Midnapur. The total area of this town is 14.30 sq. km. The town is very near to the coast of Bay of Bengal and the sea resort town of Digha is only 32 km away from Contai town. Population of the town as per 2011 census is 92,226 and projected population in 2029 is 1,16,122 [Table 9.5]. The zone wise population, according to census, are shown in Table 9.6.

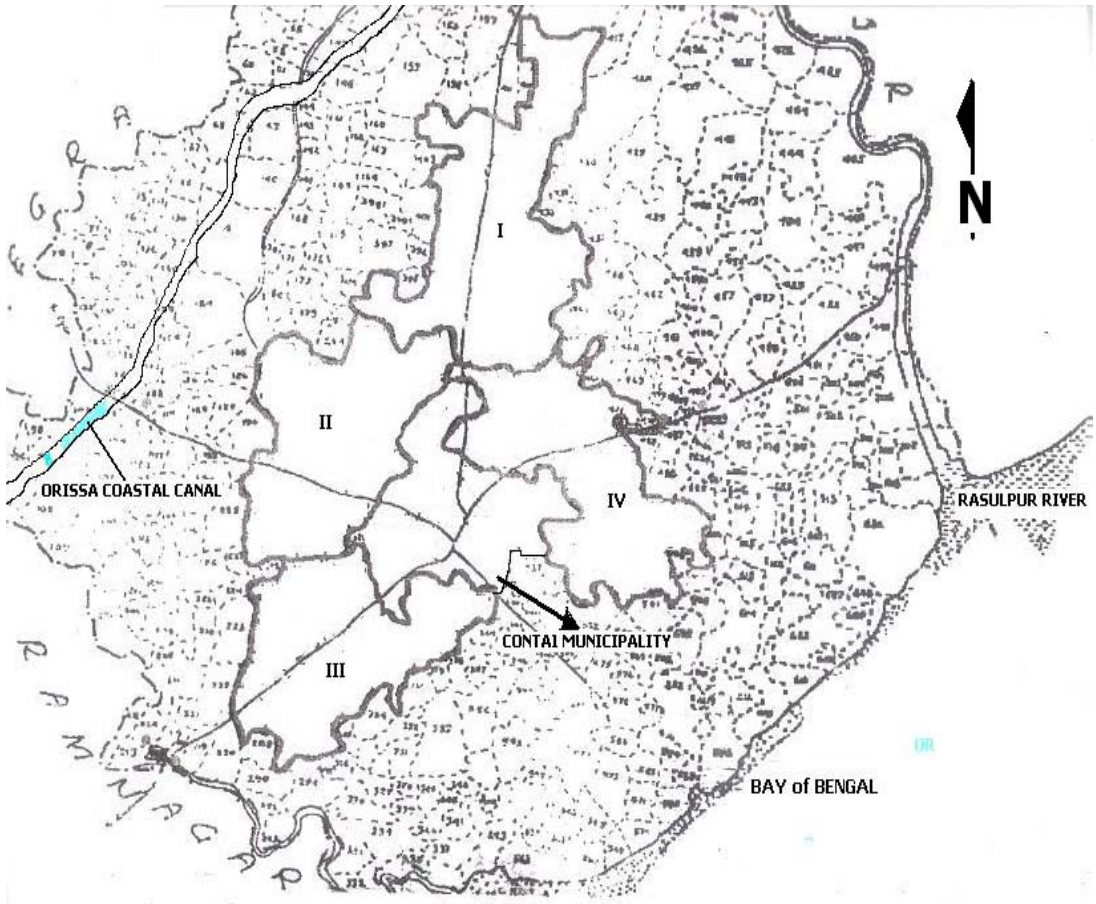

Fig. 9.9: Map showing four zones of Contai municipality town in Purba Midnapur.

Table 9.5: Population in different wards of Contai municipality town.

Ward no.	Population in 2011	Projected population in 2029	Ward no.	Population in 2011	Projected population in 2029
I	5067	6381	X	6844	8617
II	4389	5527	XI	4541	5718
III	7625	9600	XII	4379	5514
IV	2966	3734	XIII	6646	8369
V	3369	3242	XIV	4044	5092
VI	4796	6039	XV	4972	6260
VII	7953	10014	XVI	3574	4500
VIII	5383	6777	XVII	7040	8865
IX	5229	6584	XVIII	3408	4291
			Total	92226	116122

Table: 9.6: Population in different zones of Contai municipality town.

Zone-I	Ward no.	Population in 2011	Projected population in 2029
	I	5067	6381
	XIII	6646	8369
	XV	4972	6260
	XVI	3574	4500
	XVII	7040	8865
	XVIII	3408	4291
	Total	30707	38665
Zone-II			
	II	4389	5527
	VIII	5383	6777
	IX	5229	6584
	X	6844	8617
	XI	4541	5718
	XIV	4044	5092
	Total	30430	43828
Zone-III			
	III	7625	9600
	IV	2966	3734
	V	3369	3242
	VI	4796	6039
	VII	7953	10014
	XII	4379	5514
	Total	31088	38143

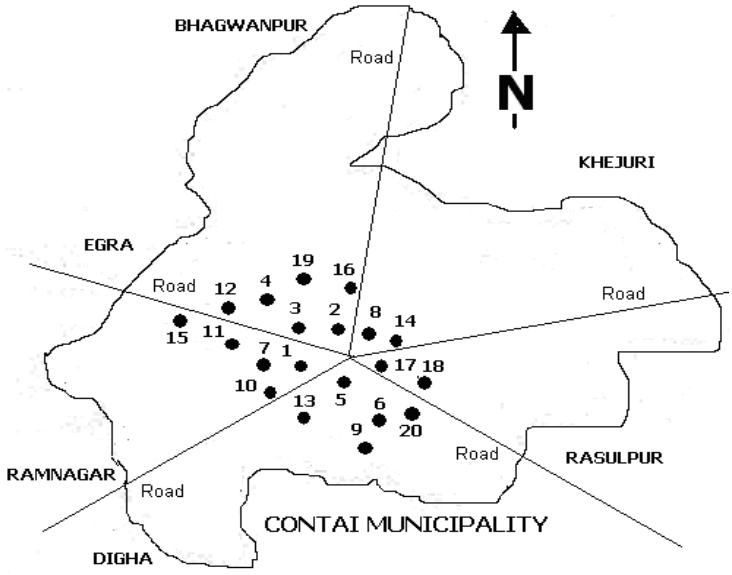

Fig. 9.10: Key locations of Contai municipality town.

Table 9.7: Test results of water samples collected from shallow tube wells within the area of Contai municipality.

Sl. No.	Location of tubewell	pH	Turbi-dity (mg/l)	Total hardness (mg/l)	Chloride (mg/l)	Nitrate (mg/l)	Iron (mg/l)	TDS (mg/l)	EC (mg/l)
01	Contai-Housing Complex	6.73	0.48	216	159.0	-	0.04	1210	2440
02	Contai-Central-Bus Stand	6.56	2.5	232	84.8	-	0.27	1100	2220
03	Contai Police Station	6.85	0.71	340	254.4	-	0.18	1920	3830
04	Athilagori-Near-Kali Mandir	7.21	0.98	90	300.5	<0.9	0.34	910	890
05	Krishnakanta Pukurpar	6.98	2.67	310	231.0	<0.9	0.42	750	1170
06	Contai PHE Office	7.54	3.87	350	240.5	<0.9	1.47	710	1200
07	Contai SDO Office	7.32	3.00	300	222.0	30.1	0.57	659	1300
08	Canalpar-near Bhabatarini Mandir	7.61	4.87	320	220.5	33.1	0.27	650	1400
09	Contai S.D. Hospital	6.98	0.76	320	220.5	33.1	0.27	610	1890
10	Digha Bypass	8.21	0.87	980	1141.0	1.0	1.24	2130	1908
11	Contai P.K. College	6.81	5.00	110	35.0	16.7	0.03	201	1400
12	Kshetra Mohan High School	6.45	5.01	420	326.5	<0.9	0.89	910	1600
13	Contai High School	6.94	4.01	230	130.0	44.1	0.06	330	1700
14	Karkuli-near- Dr. G.K. Ghosh Chamber	7.01	3.78	330	691.0	<0.9	1.58	1800	1800
15	Kharagpur Bypass	7.30	3.67	570	339.0	<0.9	0.82	930	1980
16	Mechada Bypass	7.21	3.87	210	174.0	<0.9	0.48	630	2100
17	Susanta Sarani near Kali Mandir	8.43	3.89	160	212.0	39.6	0.18	630	2300
18	Padmapukuria near Dr. B. Roy Chamber	6.86	4.89	170	57.5	<0.9	0.30	150	2400
19	Kishore Nagar High School	7.83	4.86	180	100.0	<0.9	0.56	210	2010
20	Municipality Dormitory	7.32	3.87	100	38.0	7.2	0.85	129	1890

Note: EC denotes electrical conductivity

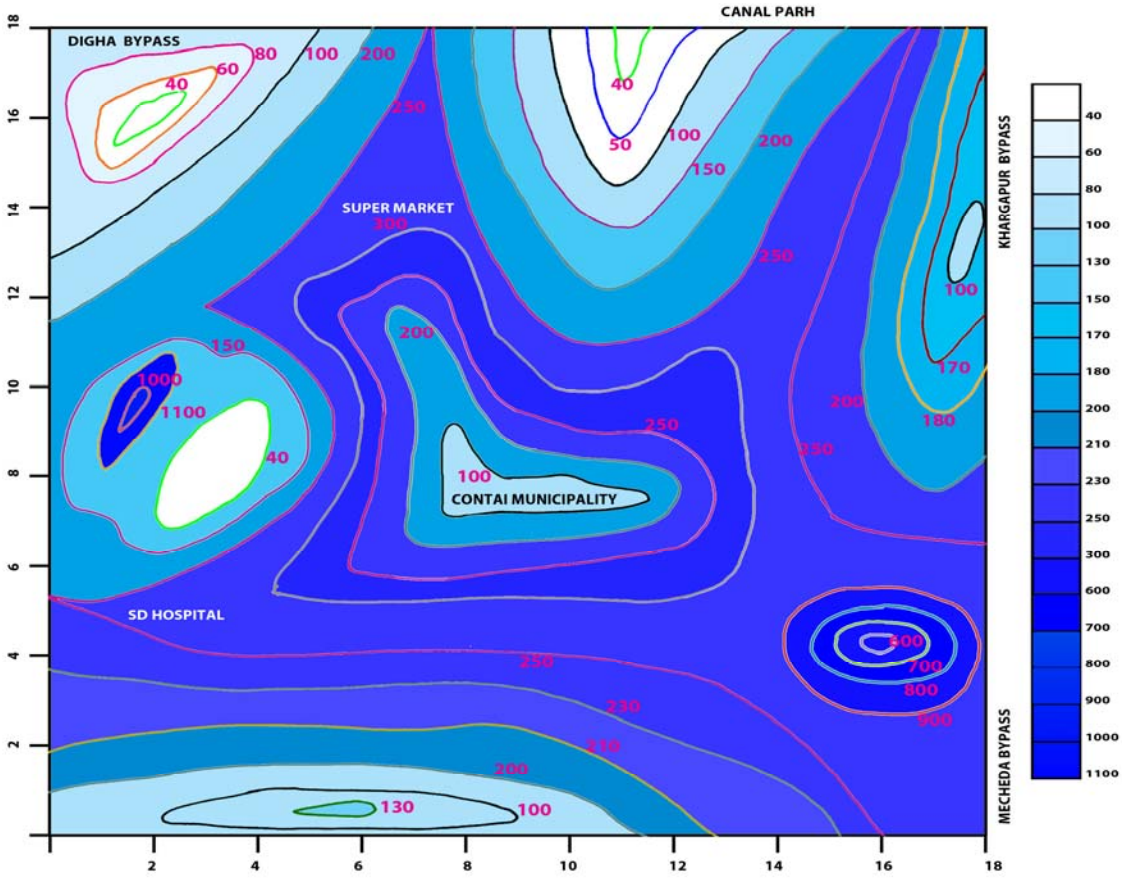

Fig. 9.11: Map showing contours of chloride concentration (ppm) in Contai.

The water samples have been collected from different shallow tube wells from Contai Municipality zone. In light of chemical examination conducted, as shown in Table 9.7, the test results obtained for chloride concentration (ppm) has been plotted for the entire Contai Municipality zone and significant contours have been drawn as shown in Figure 9.11. As observed, the chloride concentration varies from as high as 1100 ppm at Darua to as low as 20 ppm at canal bank and Digha bypass. The diversity of the chloride concentration in the aquifer at the profundity taken was observed to be reasonably unequal pattern. At a few areas the chloride concentration is very high, for example, at Monoharchak (1000 ppm) and Mechada bypass (900 ppm). Then again, at couple of areas, the chloride concentration is essentially low like Hatabari (20 ppm), Athelaguri (50 ppm) and Kumarpur (60 ppm) and so on. Inside the Contai municipality zone wide variations in salinity concentration is observed which can be, in any event in part credited to the high level of spatial heterogeneity of the aquifer fundamental the area.

9.1.4.1 Water Management Scenario

The proposed site will associate with 8 km from Contai town where there are hand tube wells discharging sweet water inside a separation from the municipality in the south-eastern side. In this way, it is proposed to sink the tube wells for groundwater with in the

Contai subdivision zone. Orissa coastal canal and Rasulpur River which are streaming from north-west to north – east conveys saline water. No seized non saline water is accessible any place close to the region. It has been discovered that the Contai town with its encompassing rural regions of around 116.55 sq. km frames a saline zone. The present water supply system for the area under Contai municipality has got two numbers of deep tube wells. Recently two tubewells became defunct which are located outside this saline zone at Mukundapur. These deep tube wells have been working acceptable for almost 10 years. Eight numbers of deep tube wells were became defunct in the year 1978 at Rautora and Kapasda in the west, Nachinda in the north and Mukundapur in the east. These tubewells were immense source of water supply for the zones encompassing the Contai municipality. Out of these eight tube wells, four tube wells are not functioning because of chock age of strainers by fine sand. These chocked tube wells were situated in the west side that is at Rautora and Kapasda regions. While the correct reason for breakdown of tube wells within a short time is not known, chloride content in the groundwater samples of some of the tube wells are known to have increased considerably before their failure [Figures 9.12-13].

Fig. 9.12: The abandoned tubewell at Contai under Rautora water supply scheme due to saline water intrusion.

This offers ascends to the apprehension of a conceivable saline water ingression in the aquifer deep tube wells sunk in the north at Nachinda, 14 km dependably from Contai town are as yet working adequately. Sinking of tube wells for the present water supply expansion design conspire for Contai municipality at Nachinda is considered yet must be disposed of thinking about the excessive cost of 14 km length of rising primary. Two tube wells of the current Municipal plan and other two tube wells of the rural scheme have been sunk at Mukundapur in the north-east direction beyond the saline region, at a distance of 8 km. from the current raised supply, in Contai town. Since the tube wells are running effectively here further the number of tube wells required - is additionally proposed to be sunk here for zone-II as illustrated in Figure 9.9. It is proposed to sink the

tube wells required for zone-I around Majna on Contai Depal Street. Larger diameter tube well sunk around there for Majna village water supply scheme is working agreeably. The tube wells for zone-III at mouja Dauki along from Contai to Junput, should keep a protected separation from the saline zone limit. Before sinking of tube wells, a point by point investigation of the well field ought to be embraced by thorough preliminary exhausting around there. A decent water bearing strata of thickness of 30 m is normal here at a profundity of 180 m beneath ground level.

Fig. 9.13: The tubewell under Kapasda water supply scheme P.H.No-1 in Contai abandoned due to saline water intrusion.

Fig. 9.14: Testing of collected groundwater samples.

9.2 Water Quality Analysis

Water Samples have been collected from 28 deep tubewells at different blocks of Purba Midnapur district and chemical analysis has been conducted. The water quality analysis laboratory of State Water Investigation Directorate where the collected groundwater samples were tested, are shown in Figure 9.14. Table 9.3 shows the physicochemical properties consisting of pH, specific conductivity, total dissolved solids (TDS), hardness, carbonate, bicarbonate, chloride and iron which have been determined from chemical analysis tests. The results obtained from these tests and discussions are presented in this section.

Hydrogen Ion Concentration (pH)

The pH value of water indicates the acidity or alkalinity of water. The pH value 7 means the water sample is neutral. If the pH of water is more than 7, it will be alkaline, and if it is less than 7, it will be acidic. The permissible values of pH for public water supplies may range between 6.5 and 8.5. The average pH values for 28 groundwater samples collected from tubewells was 7.719 and for one seawater sample it was 7.8. So it is within permissible limit.

Specific Conductivity

Total amount of dissolved salt can be determined by measuring the specific conductivity of water. The specific conductivity of water in micro-mhos per cm ($\mu\Omega^{-1}$/cm) at 25ºC is multiplied by a coefficient generally 0.65 so as to directly obtain the dissolved salt content in ppm. The specific conductance of groundwater varies widely, from a few tens of micro-mhos (in chemically inert rocks where there are abundant precipitation) to over 100,000 $\mu\Omega^{-1}$/cm (in some desert brines). The specific conductance of ocean water is of the order of 50,000 $\mu\Omega^{-1}$/cm.

Carbonate and Bicarbonate

The principle source of carbonate and bicarbonate ions in groundwater is the dissolved carbon dioxide in rain. The pH of the water indicates the form in which carbon dioxide is present. For bicarbonate, pH range is 4.5 to 8.2 and for carbonate, pH is over 8.2. Under usual conditions the bicarbonate concentration in groundwater ranges mainly from 100 to 800 ppm.

Chloride

Chlorides are normally present in water in the form of sodium chloride (NaCl). Their concentration above 250 mg/l produces a noticeable salt taste in drinking water. For sample numbers 2, 4, 5, 6, 8 (seawater), 10, 11, 14, 19, 22, 24, 27, 29 - the chloride values in ppm are 6900, 2900, 1120, 580, 11400 (seawater), 360, 310, 560, 280, 1580, 1220, 450 and 950, respectively. So for seawater sample, maximum chloride value is 11400 ppm. High Chloride content indicates that the seawater intrusion takes places in that location.

Total Hardness as $CaCO_3$

Hardness is caused by the presence of certain salt of calcium and magnesium, dissolved in water.

Temporary Hardness

If bicarbonates of calcium and magnesium are present in water, this hardness can be removed by simple boiling or by adding lime to the water. Such hardness is known as temporary hardness or carbonate hardness.

Permanent Hardness

If sulphate, chloride and nitrates of calcium or magnesium are present in water, such hardness is known as permanent hardness. The permissible value of hardness of water as $CaCO_3$ in ppm is 300. For sample numbers 2, 4, 5, 6, 8, 10, 11, 14, 22, 24, 28, 29 - the hardness in ppm are 480, 1500, 660, 400, 3570, 410, 490, 550, 660, 560, 440 and 560, respectively. It is obvious that seawater intrusion takes place in this area.

Iron (+++)

Both physico-chemical and microbiological factors control the concentration of the iron in natural water. In groundwater iron generally occurs in two oxidation states i.e., ferrous and ferric. The presence of Iron is within the tolerance limit as the upper limit setup by World Health Organization (WHO) is 1.00 mg/l. According to the Indian Council of Medical Research, the maximum desirable limit of iron is 0.1 mg/l (ICMR, 1975). Iron in irrigation water should not exceed 20 mg/l in neutral or alkaline soils and 5 mg/l in acidic soil. For Sample numbers 2, 4, 6, 11, 24 and 25 the iron concentrations are 14.39, 20.44, 5.3, 1.2, 2.0 and 2.0 ppm, respectively.

Total Dissolved Solids (TDS)

The permissible limit of total dissolved solids in drinking water in ppm is 500 ppm. The maps of contours showing the variation of total dissolved solids concentration at the study are illustrated in Figure 9.6. The amount of TDS in sample numbers 1, 2, 3, 4, 5, 6, 8, 9, 10, 11, 12, 14, 15, 16, 17, 18, 19, 20, 22, 23, 24, 25, 26, 27, 28 and 29 are 666, 10240, 762, 4288, 2112, 1216, 16640, 352, 864, 883, 314, 1216, 371, 518, 518, 544, 787, 358, 3008, 582, 2496, 589, 621, 1018, 646 and 1984 ppm, respectively. The total dissolved solids concentration varies from as high as 16640 ppm along the sea shore line from Digha to Haldia to as low as 300 ppm at Charaichia. At some locations, the total dissolved solids concentration is quite high such as at Serkhanchak -I (10240 ppm) and Mukutshila I (4288 ppm). Along the Rupnarayan River bank, the total dissolved solids concentration is 2500 ppm. Conversely, at few locations, the chloride concentration is significantly low like at Charaichia (288 ppm) and Mander (307 ppm) etc. From the above results, it is obvious that the increase of TDS is due to the salt-water intrusion in the coastal side. Based on the total dissolved solids present, the water samples have been categorized as saline, brackish and freshwater.

9.3 Interpretation from Groundwater Quality Analysis

Almost all the theories developed for saline water intrusion have been for homogenous, isotropic aquifers, a condition not found in Purba Midnapur district, which is characterized by special heterogeneity of the aquifer. Soil of low hydraulic conductivity is mixed with soil of high hydraulic conductivity in a relatively irregular way. As a result, filaments of high hydraulic conductivity protrude deep inland from the sea causing ingress of seawater inland through this preferential path [Figure 9.5]. The orientation of these filaments inland is often curvilinear with sharp bends and changes in directions occurring sometimes. In view of the great heterogeneity of the aquifer, it is very difficult, if not impossible to apply the saline water ingress theories for a homogenous aquifer to the coastal aquifer of Purba Midnapur. The importance of collection of water samples and their chemical analyses arises in this context. Sodium chloride is a relatively stable compound, which does not chemically react with most aquifer minerals. Subsequently concentration of sodium chloride is mainly governed by interaction and the balance between freshwater and saline water, in other words, knowing the saline concentration of seawater, any other saline concentration can be interspersed as the result of mixing seawater and freshwater in a certain ratio. Ideally, water samples should be taken at average depths 200 m and at different locations in coastal area of Purba Midnapur to obtain the salinity at different points in the aquifer underneath there. However, for doing these drilling of boreholes is required, which is expensive and time-consuming. To expedite the process of characterization of salinity of the aquifer, it is chosen to utilize the deep tube wells installed by the PHED to obtain water samples that are subsequently analysed chemically.

From the chemical analyses of the water samples, the chloride concentration of each of the samples can be ascertained. Since, the depth of the deep tube wells is the same as all of them have been made following the same design, by plotting the chloride concentrations at different points and then plotting the chloride concentrations for different tube wells the pattern of salinity concentration at the depth under concentration can be easily visualized [Figure 9.3].

9.3.1 Mixing Zone between Seawater and Freshwater

Because freshwater mixes with saline water a mixing zone exists between the freshwater and saline water. If an aquifer is idealized as homogeneous and isotropic, the mixing is amenable to theoretical analysis. However, if the aquifer is highly heterogeneous as in the case of Purba Midnapur, it is extremely difficult, if not impossible, to analyse the mixing zone in the absence of hydro-geo-chemical data on chloride concentration. Mixing zones may have a length of tens of kms where the hydraulic conductivity is high.

Penetration of saline water into coastal aquifers through zones of hydraulic conductivity may result in mixing zones over large areas. In reasons of low or very low hydraulic conductivity, mixing zones are much smaller. A picture of the mixing zones present in Purba Midnapur can be obtained from the saline water intrusion map of Purba Midnapur.

9.3.2 Change of Salinity with Distance from Shoreline

The variation of saline concentration with distance from shoreline for Purba Midnapur is observed. It is seen that in Purba Midnapur, owing to great heterogeneity of the aquifer, the variation of saline concentration with distance for shoreline is highly irregular. Whereas, in some places relatively close to the sea, the hydraulic conductivity or saline concentration is found to be very low, in some other places several kilometres inland the saline concentration is fairly high. This spatial irregularity in saline concentration is due to the heterogeneity in the soil deposits [Figure 9.4].

The coastal areas of Purba Midnapur are a complex mixture of marine and alluvial deposits belonging to the quaternary era, the primary difference between marine and alluvial deposits is that marine deposits are characterized by soil grains, which are more rounded than soil grains of alluvial origin. The rounding is caused by attrition and rolling of the grains against each other due to wave action. The progression and recession of the shoreline due to a long-term climatic change causes soils of marine origin to be deposited on shorelines during periods of lowering of the mean sea level. Two mechanisms of saline water ingress into coastal aquifers have been identified. Firstly, there is a direct lateral entry of seawater from the sea. Secondly, the seawater infiltrates vertically into the sea floor, which is usually highly porous due to the constant shifting and rolling of the sound caused by tidal action and the consequent rounding of the sand grains and subsequently moves horizontally towards the land. This occurrence is likewise called submarine groundwater recharge (SGR). It is presently trusted that the SGR assumes vital part in saline water ingression into mainland landmasses. The quantum of submarine groundwater recharge is extremely hard to measure as it is extremely very difficult to form reliable estimates of the amount of seawater infiltrating into the sea floor and even more difficult to accurately evaluate what portion of the undersea groundwater moves towards to land. Civil engineers, geologists, oceanographers and others have conducted very few studies in this area.

The general geographical feature of Purba Midnapur is very flat terrain with the ground heights at most places very slightly higher than the sea. Two rivers, Haldi to the north and Rasulpur to the south, allow for saline water ingress. Saline water also enters the aquifer through the highly porous coastal deposits near Digha. The aquifer is heterogeneous to the point of being almost randomly distributed. In this context, the ingress of seawater is most closely understood from a geochemical analysis. This analysis has been carried out through a collection of water from tube wells of depth of approximately 200 m from the coastal areas and subjecting the water to a chemical analysis. The results from the chemical analysis, displayed in Tables 9.3 and 9.7, show that the chloride (Cl^-) concentration in the area is highly variable. Given that the only source of Cl^- is the sea (due to the absence of Cl^- bearing rocks in the area); the Cl^- concentration may be attributed to a balance between the freshwater and the intruded seawater locally.

From Figure 9.2 and Figure 9.3, the Cl^- concentrations at 28 locations, beside the sea, are well observed and the following conclusions may be drawn:

- The Rasulpur waterway goes about as a course for saline water ingression and generally permeable aquifer in the region as the village Heria causes a salinisation of the groundwater here. As a result of which the Cl^- concentration in that area are high in spite of much lower Cl^- concentration near the coast except for one site which appears to be due to a local high hydraulic conductivity area.
- Contai town is in a saline inclined territory and the likely pathway of entrance of saline water into Contai is appeared in saline water intrusion map of Purba Midnapur [Figure 9.5].
- Digha, on the seacoast, witnesses direct salinity intrusion because of low water hydraulic conductivity of the aquifer of the region and this is reflected in the Cl^- concentrations of two destinations more deep inland whose low salinity reinforces the appreciative that the hydraulic conductivity (efficient horizontal hydraulic conductivity) is low on the area. Improved Cl^- concentration is of sporadic apprehension in various parts of Purba Midnapur. It has been accounted for that various deep tube wells have turned out of order due to an upgraded level of Cl^- concentrations.

9.4 Water Use for Drinking Purpose

Water use in domestic purpose should be free from colour, turbidity, odour and micro-organisms. However, these do not fall in the realm of chemical quality. Chemically, the water should preferably be soft, low in dissolved solids, and free from poisonous constituents. Some chemical quality Standards in use are given in Table 9.8.

9.4.1 Use of Irrigation Water for Agriculture

A chemical constituent which affects the suitability of water for irrigation purpose are given below.

- The concentration of boron
- The relative proportion of sodium to calcium and magnesium
- The relative proportion of bicarbonate to calcium and magnesium
- The total concentration of soluble salt (which is broadly related to the specific
- conductance of water

The TDS content, measured in terms of specific electrical conductance, gives the salinity hazard of irrigation waters. Besides the salinity hazard, excessive sodium contents in water renders it unsuitable for soils containing exchangeable Ca^{++} and Mg^{++} ions. If the percentage of Na^{++} to $Ca^{++} + Mg^{++} + Na^{++}$ is considerably above 50 in irrigation waters, soils containing exchangeable calcium and magnesium take up sodium in exchange for calcium and magnesium causing deflocculating and impairment of the plant growth and permeability of soils.

Table 9.8: Standards for physical and chemical quality of drinking water.

Quality Physical	WHO IS:1971		IS-10500:2012	
	Highest desirable	Maximum permissible	Highest desirable	Maximum permissible
Turbidity (JTU units)	5	25	10	25
Colour, Hazen-units (on platinum cobalt scale)	5	50	5	50
Taste and odour , Chemical	Unobjection-able	-	-	Unobjection-able
pH	7.0-8.5	6.5-9.2	6.5-8.5	6.5-9.2
TDS (mg/l)	500	1500	500	1500
Total hardness $CaCO_3$ (mg/l)	100	500	300	600
Total hardness as Calcium (mg/l)	75	200	75	200
Total hardness as Magnesium (mg/l)	<30 if SO_4 is 250 mg/l, upto 150 if SO_4<250 mg/l	150	30	100
Iron (as Fe) (mg/l)	0.05	1.5	0.3	1.0
Manganese (Mn) (mg/l)	0.1	1.0	0.1	0.5
Copper (as Cu) (mg/l)	0.05	1.5	0.05	1.5
Zinc (as Zn) (mg/l)	5.0	15.0	5.0	15.0
Chloride (mg/l)	**200**	**600**	**250**	**1000**
Sulphate (mg/l)	200	400	150	Upto 400 if Mg ≤ 30 mg/l
Phenolic substances (as phenol) (mg/l)	0.001	0.002	0.001	0.002
Fluorides (mg/l)	0.6-0.9	0.8-1.78	0.6-1.2	1.5
Nitrates (mg/l)	-	45	45	No relaxation
Toxic Constituents	-	-	-	-
Arsenic (mg/l)	-	0.05	0.05	-do-
Mercury (mg/l)	-	0.001	0.001	-do-
Cadmium (mg/l)	-	0.01	0.01	-do-
Chromium (Hexavalent) (mg/l)	-	-	0.05	-do-
Cyanide (as CN) (mg/l)	-	0.05	0.05	-do-
Lead (mg/l)	-	0.1	0.1	-do-
Selenium (mg/l)		0.01	0.01	-do-
Radioactivity				
Gross Alfa-emitters	-	3	-	-do-
Gross Alfa-emitters	-	30	-	-

Note: IS indicates International Standards

The sodium hazard in irrigation water is determining the sodium adsorption ratio (SAR) by the relation given in Eq. 9.2 in which the concentration is expressed in milliequivalent (mEq) per litre.

$$SAR = \frac{Na}{\sqrt{\left(\frac{Ca^{++} + Na^{++}}{2}\right)}} \tag{9.2}$$

The classification of irrigation water with respect to salinity and sodium hazards (Figure 9.15 and Figure 9.16) are as follows (Richards, 1954 and Wilcox, 1955):

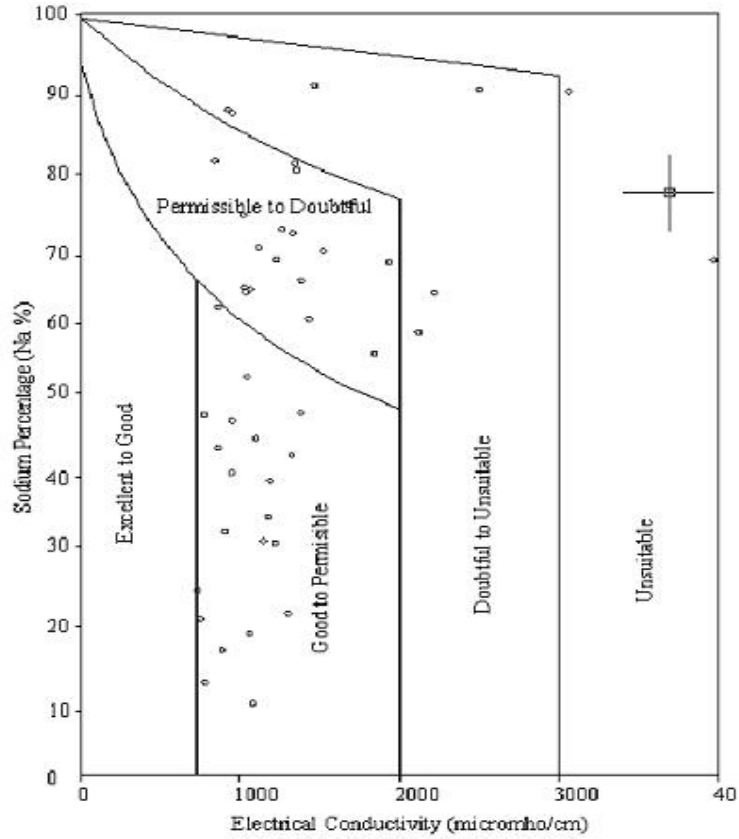

Fig. 9.15: Diagram for classification of irrigation water (after Richards, 1954).

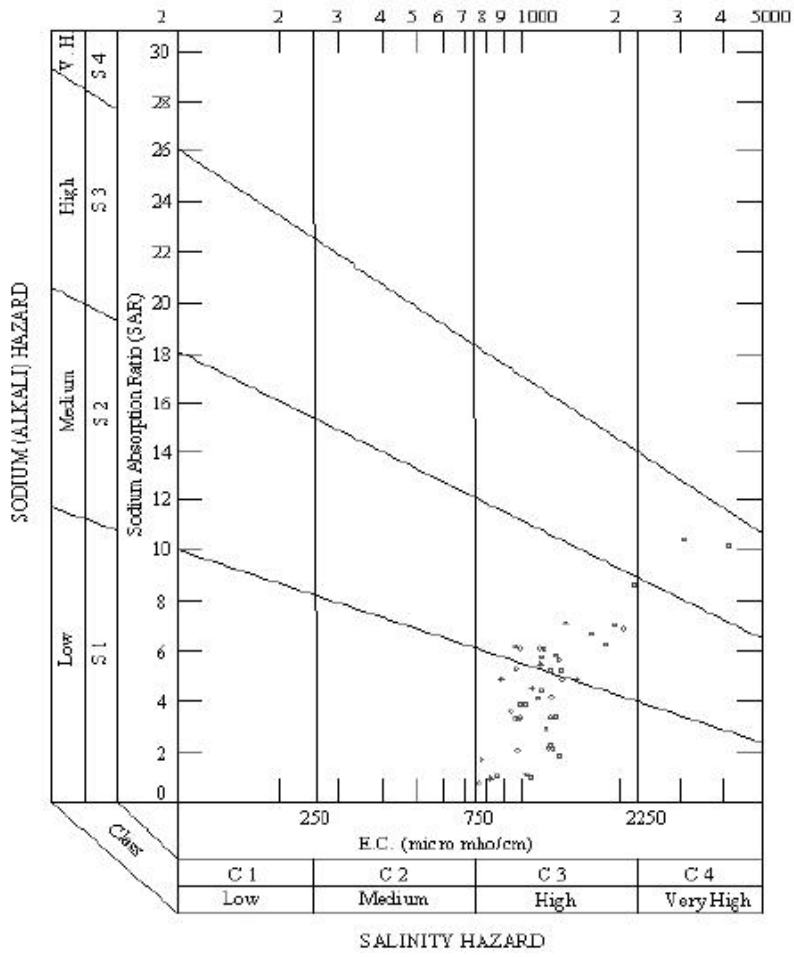

Fig. 9.16: Diagram for classification of irrigation water (after Wilcox, 1955).

9.5 Photographic View of Different Wells and Sites

A few of the photographic view of the different sites of the study area of Purba Midnapur where water samples are collected are displayed in Figure 9.17 to Figure 9.21.

Fig. 9.17: The water supply scheme (pump house) of Pichaboni, Contai.

Fig. 9.18: The Kalindi water supply scheme tubewell No-1 at Contai.

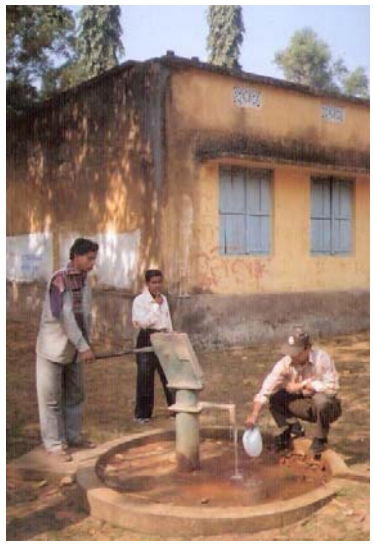

Fig. 9.19: The hand tube well at Digha bus stand.

Fig. 9.20: Direct rotary drilling method conducted at Ratanpur, Digha Water Supply Scheme.

Fig. 9.21: The Katchlageria water supply scheme at Contai.

9.6 References

ICMR (1975). Indian Council of Medical Research (ICMR). Manual of Standards of Quality for Drinking Water Supplies.

Richards, L.A. (1954). Diagnosis and Improvement of Saline Alkali Soils. *Handbook U.S. Department of Agriculture*, No. 60, pp. 69-82.

Wilcox, L.V. (1955). Classification and use of irrigation water. U*.S. Department of Agriculture, Technical Bulletin*, No. 969.

CHAPTER - 10

(Management and Control of Saline Water Intrusion)

- Background
- Existing Method for Controlling Saline Water Intrusion
- Review of Literatures
- A New Approach to Control of Saline Water Intrusion
- Typical Case Study with Quantification
- Appropriate Engineering Design
- Aquifers Improvement Plan
- Using alternative freshwater Sources
- References

10.1 Background

Whenever there is any withdrawal of groundwater from a coastal aquifer, there is an advancement of saltwater-freshwater interface from a shore line towards to the point of withdrawal. This continues till the withdrawal is compensated by an equivalent artificial recharge, one of the popular recharge techniques adopted worldwide is rainwater harvesting. Though there are several conventional methodologies to control and reduce the problems connected with groundwater extraction followed by saline water intrusion, this field study proposes a suitable and effective analytical model for groundwater management in the coastal zones to control saltwater ingression. The technique consists of coastal freshwater withdrawals by using qanat well structures connected with artificial recharge through rainwater harvesting supported with percolation ponds and recharge wells, the study is found to be cost-effective and useful.

The cost effective model is appropriate particularly for urbanised coastal areas with considerable annual rainfall, good yield of the aquifer materials and a shallow depth of groundwater table. The cost effective model, as a field study is implemented to a coastal zone of district of Purba Midnapur in West Bengal. The efficiency of the methodology with sufficient quantification is incorporated and significant conclusions are drawn from its field application of the model.

In addition, a newly improved cost-effective qanat-well structure is suggested in two ways (i) aquifers Improvement Plan and (ii) using alternative freshwater sources to overcome threat of saline water intrusion as follows.

10.2 Existing Methods for Controlling Saline Water Intrusion

There is a great threat to freshwater resources in major Indian cities lying near coastal area due to over-use of groundwater triggered by saltwater ingression. It is required to adopt sustainable methods to reduce the rate of saline water intrusion in order to save the freshwater resources from damage. The intricacy of hydro-geological structural stratification of the concerned area calls for scientific management techniques to be implemented in the groundwater development. It is required to properly understand the hydrogeology of the area concerned, appreciate the possible outcome of over or under developments and coordination among the planners, hydro-geologists, social scientists and hydraulic engineers in the field.

The over extraction of freshwater from coastal area will front to lowering of groundwater table with coupled hazards reminiscent of putting the well out of commission, depiction the abstraction running at a loss of augmented lift. The groundwater development consequently lowering the water table below sea level runs danger of saline water encroachment, constant for confined coastal aquifers.

The objective of any control method of salt water intrusion should be to prevent further encroachment and if possible to reduce the area already intruded. Out of available methods, the followings techniques are popular (Karanth, 1987; Raghunath, 1987; Todd, 1995):

● Creation of Hydraulic Barriers, ● Canal Irrigation, ● Desalination and Reverse Osmosis, ● Rainwater Harvesting Technology and ● Artificial Recharging Methods.

10.2.1 Hydraulic Barriers

The hydraulic barriers are four types (i) keeping basin water level high, (ii) creating a freshwater ridge near the sea and, (iii) creating a pumping trough or extraction barrier trough, (iv) development of a semi pervious barrier. These methods are described below:

(i) Although it is clear that reduction in pumping draft would tend to effect a rise in groundwater levels, additional comment is warranted regarding effects of arrangement of pumping pattern. In the event that the area of most important withdrawals is shifted from the coastal portion of a basin to a zone encourage inland, the landward hydraulic gradient in land form the trough would be expanded. Such a condition would have a tendency to moderate or stop the inflow of saline water. Groundwater levels in the overdrawn aquifers can be raised and kept up above ocean level by artificial recharge using surface spreading, injection wells or both.

(ii) The method would require the continuous maintenance of a freshwater ridge in the principal water bearing deposits along the coast, through the application of water by surface spreading or injection wells or both would depend on whether free groundwater or pressure condition exists, as determined by geologic and engineering investigations. In basins where pressure conditions exist and injection wells are utilized. The total injection rates along the recharge line must be equal to the sum of the freshwater to the sea, necessary to maintain the position of seawater wedge and the overdraft to the basin originally being satisfied by landward flow of the seawater.

(iii) Development of an extraction barrier would require maintaining a continuous pumping trough adjacent to the ocean. A pumping trough can be created and be developed by means of a line of pumping wells, properly spaced along the seacoast. The wells would produce a mixture of saline and freshwater and could result in the waste of considerable quantities of freshwater. It has been concluded that intrusion of saline water can be intercepted by establishment of a pumping trough created by a line of pumping wells parallel to the coast.

(iv) This method involves the establishment of a semi pervious barrier to reduce the permeability of the water bearing deposits sufficiently to prevent the inflow of saline water into freshwater strata. This barriers are formed by the subsurface injection of nutrient solutions/or other material into the freshwater portions of the aquifer. The average hydraulic conductivity in the vicinity of the barrier has been reduced from 2.1×10^{-2} to 1.3×10^{-4} cm/sec, a 99.4% decrease. Implementation of this method would require knowledge of location, extent, thickness, depth and other physical characteristics of the water bearing deposits.

10.2.2 Canal Irrigation

Canal irrigation system is one of the vital techniques utilized for enhancing the development of the crop. After wells and deep tube wells, canal irrigation system is the second most imperative water system source in Purba Midnapur area. Canals can be both perennial as well as non-perennial aside from these canals; there are a few stream channels that are taken off from the Haldi, Rasulpur and Rupnarayan streams without the constructing of the barrages. Steady attempts have been made to restore the immersed canals by the perennial one. In mitigating the agonies and affliction of the farmers, canal irrigation system works have gone long way. Canals are man-made channels for water. Irrigation is heavily dependent on groundwater; the water in canal network should be used in irrigation throughout the watershed. Canal irrigation can eliminate the uncontrolled use of deep tube wells for irrigation. Canal seeps freshwater which in turn back saline water intrusion as a result upconing is controlled.

10.2.3 Desalination and Reverse Osmosis

The movement of salt water into freshwater aquifers is severely affecting the quality of industrial and domestic water supplies and overtaxing treatment facilities. In solving freshwater shortage, there are numerous arrangements including control of water utilization, protection, enhanced conveyance and capacity, recovery refinement and reuse, tapping of new sources, and so forth. Desalination is viewed as just when the various potential outcomes have been managed out of for different reasons.

There are also many methods for desalination such as distillation, vapour compression, solar distillation, freezing, electro-dialysis, and reverse osmosis (RO). However, among the methods for desalination, RO is receiving increasing attention because of high purity effluent water, ranging from 1 to 500 parts per million total dissolved solids. This process will allow the removal of particles as small as ions from a solution. There are also many advantages of RO such as: simple system, low installation cost, low maintenance, non-metallic materials in construction, high organic and inorganic contaminant removal and minimal use of chemicals. Desalination gives water to residential purposes, industrial preparing, parks and agricultural irrigation, power plant applications, and recharge of groundwater supplies.

10.2.4 Rainwater Harvesting Technology

Water is the basic parameter for development in any sector. The country needs a huge quantity of water for sustaining its pace of development. In coming years the requirement of water is likely to exceed the total available utilizable potential. The need demands sustainable water development. Water harvesting and artificial recharge have been important for sustainable development. Rainwater harvesting (RWH) and conservation involve direct collection of rain water. The rain water so collected can be stored in the surface or in the subsurface for future use.

The main aim is to minimize the surface run off through drains and drainage channels to the rivers and sea without a single use. The rain water harvesting and conservation may lead to optimum utilization of the natural resources.

Rainwater harvesting serve the following purposes:

- In coastal areas, it provides good quality water as well as helps in maintaining balance between the fresh saline water aquifers.
- Reduce saline water ingress in coastal aquifer.

10.2.5 Artificial Recharging Methods

Artificial groundwater recharge is a procedure by which the groundwater reservoir is enlarged at a rate surpassing the increase rate under usual environment of replacement. In a few sections of India, due to over-extraction of groundwater, decrease in groundwater levels bringing about lack of supply of water, and ingression of saline water in coastal regions have been watched. In such territories, there is requirement for artificial recharge of groundwater by increasing the natural infiltration of precipitation or surface-water into underground developments by strategies for different artificial recharge methods. The decision of a specific technique is represented by nearby land, geographical and soil conditions; the amount and nature of water accessible for energize; and the scientific-economical feasibility and social suitability of such schemes.

The various methods of artificial recharge are as follows (i) Spreading method: (Spreading within channel, Spreading of stream water through a network of ditches and furrows, Ponding over large area, Along stream channel viz. Check Dams/ Nala Bunds, Vast open terrain of a drainage basin viz. Percolation Tanks, Modification of village tanks as recharge structures), (ii) Recharge Shafts: (Vertical Shafts, Lateral Shafts), (iii) Injection Wells, (iv) Induced Recharge, (v) Improved Land and Watershed Management: (Contour Bunding, Contour Trenching, Bench Terracing and Gully Plugging).

Injection Well: Injection wells are design like a tube well yet with the motivation behind enlarging the groundwater stockpiling of a confined aquifer by “pumping in" treated surface-water under pressure. Artificial recharge of aquifers by injection wells is likewise done in coastal areas to capture the entrance of seawater in zones where confined aquifers are delightful pumped. It is hereby mentioned that the performance of a recharge well may be progressively deteriorated due to the following factors: microbial growth in the well, iron precipitation, chemical biochemical ionic reactions between recharge water and groundwater etc (O’Hare *et al.*, 1986).

Gravity-Head Recharge Well: In adding together to specifically calculated injection wells, common bore wells and dug wells utilized for pumping may likewise be on the other hand utilized as recharge wells, at whatever point source water ends up accessible. In specific circumstances, such wells may likewise be built for affecting recharge by gravity inflow. In zones where water levels are presently declining due to over-improvement,

utilizing accessible structures for suggest recharge might be the instantly accessible financial alternative.

Percolation Tank: In zones where uncultivated land is accessible in and around the stream-channel area, and adequately high hydraulic conductivity exists for sub-surface percolation, little tanks are made by making stop dams of low height over the stream. The tanks can likewise be found nearby the stream by excavation and involving them to the stream through conveyance channels. These tanks are called "percolation tanks" and are in this way artificially made surface-water bodies submerging an exceedingly porous land zone so the surface run-off is made to seep into and recharge the groundwater storage. It should to be found downstream of a run-off zone, ideally towards the edge of a piedmont zone or in the upper piece of a transition zone (land slope between 3 to 5 rate percentage points). There must to be satisfactory region appropriate for irrigation almost a percolation tank.

10.2.5.1 Planning of Artificial Recharge Scheme

Sarkar (2007) recommended a scheme for rainwater harvesting with gravity head recharge well for TCS building at Salt Lake in West Bengal. The coordinate of the location is $22^{\circ}34'20.5''$ N; $88^{\circ}26'22.3''$ E. The roof area of the main building was approximately 1840 m^2 and the roof area under the scheme was considered 460 m^2.

Rainfall Pattern in the Region

- Average annual rainfall – 1600 mm
- Average annual monsoon rainfall – 1200 mm
- Maximum and minimum rainfall – Maximum in July and minimum in December.
- Present groundwater level fluctuation – 11 m bgl in closing phase of monsoon and 15 m bgl in the pre-monsoon.

Roof Top Rain Water Harvesting Potential of the Main Building

- Area of the roof catchment – 1840 m^2
- Annual average monsoon rainfall – 1200 mm
- Rain water endowment of the roof in monsoon – 1840×1.2 m^3 i.e. 2208 m^3.
- Runoff coefficient of the roof surface – 0.85 (considered)
- Coefficient for different losses like first flush, evaporation, spilling etc – 0.80 (considered)
- Quantity of harvestable roof top rain water during monsoon – $2208 \times 0.8 \times 0.80$ m^3 i.e. 1501.44 m^3, say, 1500 m^3
- Size of the pilot scheme – 25%
- Harvestable quantity for pilot scheme – 25% of 1500 m^3 i.e. 375 m^3 say, 3.80×10^5 liters

The pilot scheme is aimed at finding the efficiency of roof top rain water harvesting and conservation for different uses. So, 50% of the harvested water is to be conserved for direct uses and the rest 50% is to be utilized for artificial recharge of groundwater.

Quantity for direct uses per year: 50% of 3.80×10^5 litres i.e. 1.9×10^5 litres

Quantity for artificial recharge per year: 1.9×10^5 litres

Total quantity of conservation: 3.6×10^5 liters

The salient features of this scheme are: design of RWH structures with cast iron down water pipes, design of fire fighting underground tanks, first flushing provision through diversion line with valve, catch basin, and underground rainwater transmission line.

Design of structure for artificial recharge of groundwater involves: first flushing provisions, diversion line to carry harvested rain water to the system, filtration unit, recharge chamber, and gravity head recharge well.

Recharge Chamber: In this chamber, filtered rain water is received for recharge. The outlet of the filter unit is the inlet for this chamber. In this chamber, filter materials is provided. Pebbles of 20 to 40 mm size are effective for this purpose. This filter bed together with the coir filter of the filtration unit forms an inverted filtering arrangements slowing down the flow rate and thereby helping settling of carried materials, if any. Capacity of this chamber with the filter unit is kept to store 20% of the daily average rainfall considering steady recharge through the gravity head recharge well [Figure 10.1].

Fig. 10.1: Recharge chamber with recharge well (after Sarkar, 2007).

Capacity of the filter unit = 1.6 m × 1.0 m × 0.75 m = 1.2 m^3

Total required capacity = 20% of 8 m^3 = 1.6 m^3

So, the required capacity of the recharge chamber = 1.6 m^3 – 1.2 m^3 = 0.4 m^3

The inner size of the chamber is kept at 1.0 m × 1.0 m × 1.2 m = 1.2 m^3

The void in the pebble bed is 40%

So the effective space = 0.4 × 1.2 m^3 = 0.48 m^3

Therefore the size of 1 m × 1 m ×1.2 m is sufficient.

A free board of 0.6 m is dept for overflow in case of heavy rains which may occur in 3 to 4 occasions in a monsoon.

Gravity Head Recharge Well: Considering the hydro-geological and geophysical information of the subsurface, the size of the well is designed as follows [Figure 10.2]:

Diameter of the well	100 mm
Strainer diameter in the aquifer	100 mm
Length of strainer	12 m
Diameter of inlet strainer placed in recharge chamber	150 mm
Length of 150 mm strainer	800 mm

The rate of recharge through such well would be more than 30 m^3/day.

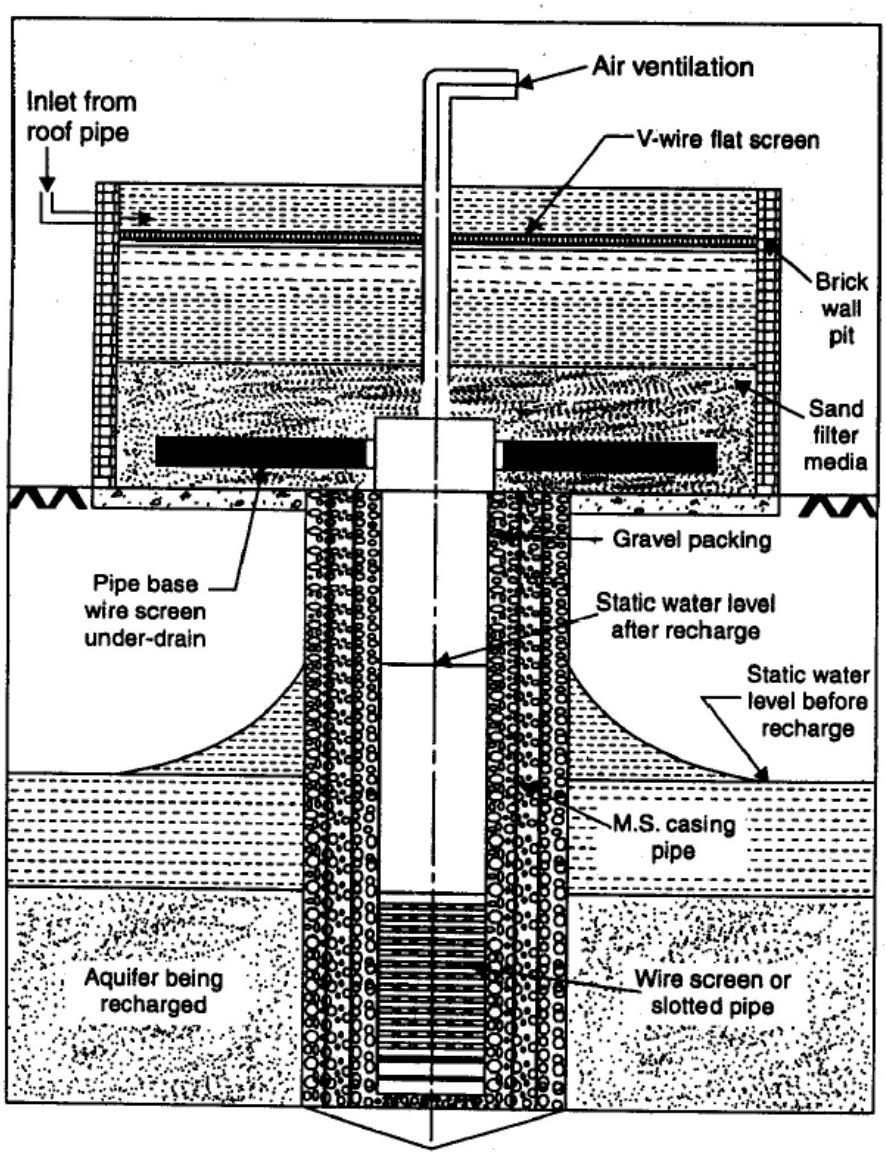

Fig. 10.2: Section of a recharge well (after Sarkar, 2007).

10.3 Review of Literatures

The significant contributions on available models for coastal groundwater management:

Muskat (1937) estimated the rise of the interface is small and it acts as a streamline or an impervious boundary. It was further assumed that no flow occurs beneath the interface. The analytical model was used to estimate the critical pumping rate from well using site specific parameters. However, the critical pumping rate was found to be relatively insensitive to changes in values of well radius. The author suggested further development of numerical solutions for an aquifer overlain by a leaky confining bed using the sharp-interface and the density dependent solute transport approaches.

Hantush and Papadapulos (1962) developed basic standard drawdown formulas; it is most likely the extensively used for predicting the yield of radial collector wells.

Bennett *et al.* (1968) extended the analysis of Muskat and Wyckoff (1935) to the skimming well problem, using an analog model for a radial flow to obtain the required head distributions in the freshwater zone. This model was made up of a network of electric resistances, equipped with a system of switches, by means of which the lower portion of the network of resistors could be adjusted by trial and error to obtain a lower boundary. It would simulate the freshwater and saline water interface for a given set of conditions. The results provided an evaluation of skimming well operation following the attainment of a stable interface, under a variety of conditions relating to original fresh and saline groundwater and well penetration.

Dasgupta and Gaikwad (1987) developed a simplified mathematical model to predict the equilibrium location of upconed interface due to horizontal well in unconfined coastal aquifers of finite thickness. The model was based on Dupit assumption and Ghyben-Herzberg approximation with modified boundary conditions along the shore line. Under the natural flow condition, the computed interface profile by the model was found to be in good agreement with the results of available analytical solutions and by conducting experiments for different well locations and withdrawal rates. The comparison indicated that the proposed model underestimated the interface depth below MSL because of the simplified assumptions of horizontal flow and hydrostatic pressure distribution. But presumably the model provided an acceptable prediction. At low withdrawal rate of water, the interface was observed moving upward from its position in natural flow condition without any upconing effect along its length.

Motz (1992) developed an analytical model to study the upconing of saline water beneath a well pumping freshwater from an aquifer over-lain by a leaky confining bed. The drawdown was calculated along and then, the Ghyben-Herzberg relation was used to calculate rise in the interface. The interface rise and the critical pumping rate were determined in terms of aquifer and confining bed properties and the degree of penetration of the pumping well into the freshwater zone.

Raghubabu *et al.* (2004) conducted field study at the coastal area of Srikakulam, Guntur and Nellore districts of Andhra Pradesh and Pulicat Lake in the north to Cape Comarine in the south of Tamil Nadu, identified as coastal sandy soils. In most of these coastal sandy soils, there exists a shallow depth of good quality water with the freshwater floating at a depth of 0.5 - 3.0 m below ground level and thickness of 3.0 - 4.0 m over

saline water/clay layers. These waters cannot be extracted in high qualities by conventional tube well due to saline water underlying the area. He suggested that the skimming well with horizontal collector system was a viable solution for preventing saline water intrusion into the inland freshwater aquifer. The author has shown that this technology had been accepted and adopted in coastal sandy soils of Andhra Pradesh, Tamil Nadu, Orissa and West Bengal.

Yasin *et al.* (2004) conducted in classifying different groundwater quality zones by GIS method, helped in selecting fifteen villages of saline zones that had hydro-geological potential for installing and operating skimming wells. In these selected villages, preliminary survey was carried out to get information on the farmers' willingness to use skimming well technology. Based on the GIS analysis and preliminary survey, different sites in six villages were selected to carry out the Diagnostic Analysis (DA) for investigating the hydro-salinity and hydro-geological conditions of the aquifer. Based on the DA results, four villages for the Participatory Rural Appraisal (PRA) to assess farmers' practices and perceptions in opting for skimming well technologies was implemented.

Chandra (2005) conducted field study on surface geophysical data and borehole logging had been carried out in the coastal tracts of India with varied objective. Electrical resistivity measurements surface as well as bore hole had been the most widely used techniques. The groundwater quality interface and the spatial disposition of freshwater aquifer upto 300m depth had been successfully identified. The case study from coastal tracts manifests the applications and limitations of the resistivity techniques and the essentiality of techniques of integrating other geophysical to remove ambiguities had been conducted. The interpretation of geophysical data being contextual, a variety of problems related to exploration, development and conservation of groundwater could be geophysically addressed and solutions achieved economically. The useful mathematical models for withdrawal of freshwater by means of horizontal wells,

Abd-Elhamid and Javadi (2011) proposed a cost effective methodology to control the saltwater intrusion into the coastal aquifer based on Abstraction, Desalination and Recharge (ADR). A coupled transient density-dependent finite element model was developed to simulate fluid flow, solute transport and seawater intrusion. The optimum depths, locations and abstraction/ recharge rate were determined to minimize the total cost. It was observed that the proposed area system performs significantly better than separate use of abstraction and recharge well in terms of cost effectiveness and reduction of saline concentration in the aquifer.

Javadi *et al.* (2013) presented a new method for optimal control of seawater intrusion. The proposed method was based on a combination of abstraction of saline water near shoreline and recharge of aquifer using surface ponds. The source of water for the surface pond could be treated waste water or excess of desalinated brackish water (if any), etc. The variable density flow and solute transport model, SUTRA (Saturated-Unsaturated TRAansport), was integrated with a Genetic Algorithm optimization tool in order to investigate the efficacy of different scenarios of the seawater intrusion control in an unconfined costal aquifer. The locations of the pond and the abstraction well in relation to the shoreline, depth of abstraction well and the rates of abstraction and

recharge was considered as the main decision variables of the optimization model, which aims to minimize the costs of construction and operation of the abstraction wells and recharge ponds as well as the salt concentrations in the aquifer. Comparison was made between the results of the proposed method and other methods of seawater intrusion control. The results indicate that the proposed method was efficient in controlling seawater intrusion. This proposed strategy could be considered as a powerful tool for cost-effective management of seawater intrusion in coastal aquifers.

Venkataramana (2016) investigated the management of groundwater with covering area Bapatla, Karlapalem, Pittalavanipalem, Nizampatnam, Cherukupally and Repallemandals, coastal sands was being utilized through shallow open wells known as Doruvus. The Water table was influenced by canal irrigation system and Krishna western delta and Precipitation. Freshwater in the coastal sands was floating above the saline groundwater which occurs in the underlying clay layers. Thickness of sand aquifer was very limited in the area and varies from 2.5 to 5.0 m. Occurrence of sand aquifer was not uniform and hence these coastal sandy areas with shallow freshwater in saline groundwater region need better management technologies of Skimming and recharging to maintain environmental balance and sustainable irrigation.

It is evident that significant research and development has already been carried out by various scientists, engineers and researchers at different parts of the world in the field of analysis and control of saline water intrusion into coastal aquifers and other relevant areas. Amongst the important works, the most significant contributions are briefly reviewed. As observed, the different types of theoretical works, Laboratory-based experimental works and field-based studies i.e. Muskat (1937), Hantush and Papadapulos (1962), Bennett *et al.* (1968), Dasgupta and Gaikwad (1987), Motz (1992), Yasin *et al.* (2004), Abd-Elhamid and Javadi (2011), Raghu Babu *et al.* (2004), Chandra (2005), Javadi *et al.* (2013) and Venkataramana (2016). However various researchers suggested that the skimming well with horizontal collector system was a viable solution for preventing saline water intrusion into the inland freshwater aquifer. However, the prescribed model is only withdrawal of groundwater; no artificial recharge through rainwater harvesting to compensate the withdrawal was estimated for controlling saline water intrusion is yet to be carried out.

An innovative cost-effective model has developed to control salt water intrusion into coastal aquifers; the technique includes withdrawal of coastal freshwater by means of qanat-well structures associated with artificial recharge through rainwater harvesting aided with percolation pond and recharge well. A case study on a selected location of the coastal zone of Purba Midnapur has been carried out. Adequate quantification of the effectiveness of this new methodology has been incorporated and relevant conclusions are drawn there from.

10.4 A New Approach to Control Seawater Intrusion

The model so developed for coastal zones freshwater management is suitable and simply appropriate at a specific site, provided the magnitude of in-situ parameters are properly

assessed and used. The water demand in the particular population under consideration, the model qanat well structures to withdrawal freshwater is proposed while shallow wells are inappropriate for low yields and the implementation of deep tube wells initiates the problem of upconing. An extraction of freshwater in coastal zones is well recognized, as evidenced from the existing literature, the design of such qanat-well structures has no specific methodology. The existing discharge correlation for a horizontal well, by principle of superposition and the upconing phenomena, an attempt for the design methodology has been established in this work, which is quite obvious for coastal zones. The encroachment interface in the coastal area at the point of extraction, induced by such freshwater extraction by qanat-well structure, the rainwater harvesting method associated with recharge well and recharge ponds is proposed.

From the existing literature survey, the correlation for the recharge structure is used to design methodology in the model which is appropriate for management of groundwater in a particular community in a coastal zone and its application depends upon effectively selected field parameters. Though, the design methodology is merely appropriate for coastal zones that have considerable annual precipitation, good hydraulic conductivity of the aquifer soil, with a shallow depth of groundwater table and are not excessively urbanised.

10.4.1 Adoption of Qanat-Well Structure

A qanat is a horizontal well (termed 'leg') connected together at their ends with a vertical riser, constructed in sandy coastal zones for groundwater withdrawal. Due to the negative effect of over extraction of groundwater by way of irresponsible pumping the inland aquifers are badly affected and the offshore aquifers are susceptible to the threat of saline water ingression and saline water upconing [Figure 10.1]. Due to seawater intrusion, deep tube-well is not recommended because of the upconing problems. As the discharge of shallow well is very low, it is duly established (Ball and Herbert, 1992; Raghubabu *et al.*, 2004; Sawyer and Lieuallen-Dalam, 1998) that implementation of qanats structures under such environment yields greater discharge along with significant lower upconing problems.

Some compensation of qanat-well structures in excess of usual vertical wells, specifically for shallow highly permeable coastal aquifers, has been highlighted in the past (Ball and Herbert, 1992; Haitjema *et al.*, 2010; Sawyer and Lieuallen-Dalam, 1998) Horizontal wells are more efficient than conventional vertical wells for environmental remediation of groundwater for a number of reasons such as:

- Greater zone of influence and more efficient for producing yields.
- Horizontal wells can therefore be favourably oriented to take advantage of plume geometry and flow direction.
- The horizontal well is more advantageous to great contact for geometry of groundwater that a chain of vertical wells.
- Horizontal wells to achieve greater efficiency of delivery or recovery than vertical wells in many hydro-geologic settings.

Beljin and Losonsky (1992) and Joshi (1986) obtained a solution of horizontal wells and the effect of upconning by the classical analysis of Dagan and Bear (1968) theory, combining the both analytical model structures for predicting maximum yield of the qanat well which is evident in a coastal environment. In 1992, Beljin and Losonsky presented a comprehensive solution, considering analysis of Joshi (1986), for estimating steady-state discharge for extraction of freshwater from an aquifer by horizontal well. The solution provided was given by:

$$Q = \frac{2\pi K_h h_s}{\ln\left[\left(\frac{\sqrt{1+\sqrt{1+64R_1^4/L^4}}+\sqrt{-1+\sqrt{1+64R_1^4/L^4}}}{\sqrt{2}}\right)\left(\frac{\frac{\beta H^2}{2}+2\beta\delta^2}{Hr_w}\right)^{\frac{\beta H}{L}}\right]} \quad (10.1)$$

where Q is the steady state discharge, s is the drawdown, L is the length of the horizontal well, r_w is the well radius, K_h is the horizontal hydraulic conductivity, H is aquifer thickness; $\beta = (K_h/K_v)^{0.5}$, K_v is the vertical hydraulic conductivity, δ is the well eccentricity and R_1 is the radius of influence of the equivalent vertical well in the same aquifer for the same drawdown, which can be convincingly calculated using the available correlations (e.g. Sichardt's formulae).

By the method of superimposition, the Equation (10.1) has been modified, to reasonably estimate the steady-state discharge by means of a qanat structures. The final equation has been obtained as below in Equations (10.2-3):

$$Q_q = \frac{2\pi K_h h_s}{\ln\left[\left(\frac{\sqrt{1+\sqrt{1+4R_1^4/L_q^4}}+\sqrt{-1+\sqrt{1+4R_1^4/L_q^4}}}{\sqrt{2}}\right)\left(\frac{\frac{\beta H^2}{2}+2\beta\delta^2}{Hr_q}\right)^{\frac{2\beta H}{L_q}}\right]} \quad (10.2)$$

where, Q_q is the flow rate from the qanat-well, L_q is the qanat leg length [see Figure 10.3] and r_q is the qanat legs inner radius. By putting the $s = d - 2r_q$ in the Equation (10.2) for utmost yields from the qanat well structures in full flow condition, neglecting the wall thickness of the qanat legs, as Equation (10.3) is obtained.

$$Q_q(\max) = \frac{2\pi K_h H(d-2r_q)}{\ln\left[\left(\frac{\sqrt{1+\sqrt{1+4R_1^4/L_q^4}}+\sqrt{-1+\sqrt{1+4R_1^4/L_q^4}}}{\sqrt{2}}\right)\left(\frac{\frac{\beta H^2}{2}+2\beta\delta^2}{Hr_q}\right)^{\frac{2\beta H}{L_q}}\right]} \quad (10.3)$$

where, Q_q (max) is the maximum possible discharge from the qanat and d is the depth of the bottom surface of the qanat legs below the undisturbed water table.

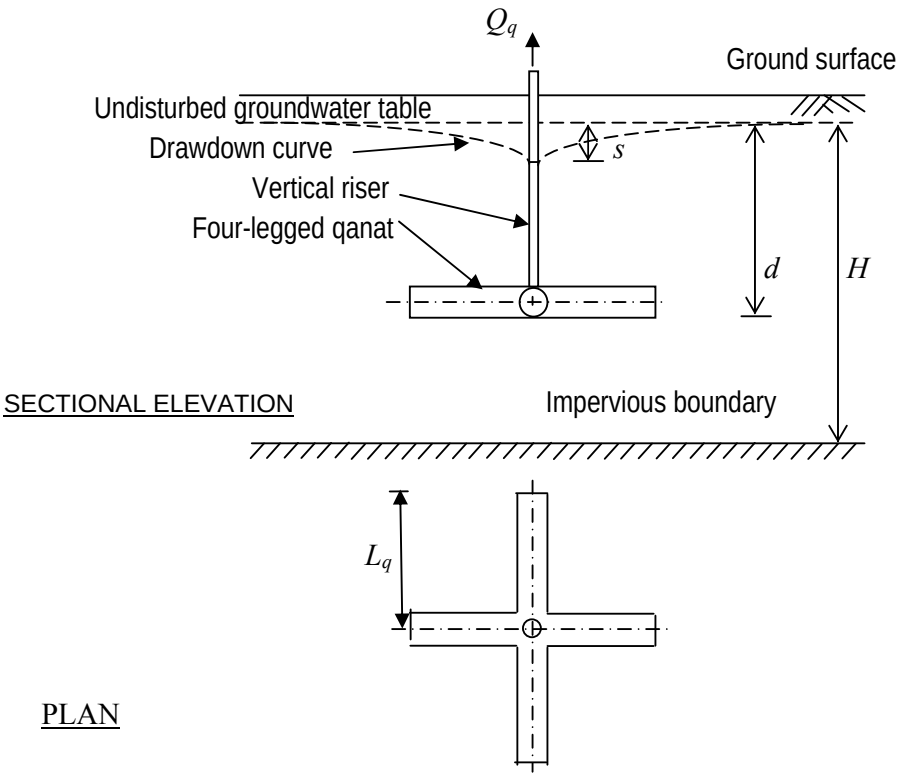

Fig. 10.3: A typical four legged qanat.

Using Sichardt's formulae, $R_1 = 3000(d\text{-}2r_q)\sqrt{K_h}$ in Equation(10.3), where all terms should essentially be in SI units and h_f is the depth of freshwater from interface to undisturbed water table. Then Equation (10.3) can be written as given in Equation (10.4):

$$Q_q(\max) = \frac{2\pi K_h h_f (d - 2r_q)}{ln\left[\xi\left(\frac{\frac{BH^2}{2} + 2\beta\delta^2}{h_f\ r_q}\right)^{\frac{2\beta h_f}{L_q}}\right]} \tag{10.4}$$

where $\xi = \dfrac{\sqrt{1+\sqrt{1+4\left[3000\left(d-r_q\right)\sqrt{K_h}\right]^4 / L_q}} + \sqrt{-1+\sqrt{1+4\left[3000\left(d-r_q\right)\sqrt{K_q}\right]^4 / L_q}}}{\sqrt{2}}$

In the situation of upconing of qanat structures is apparently not practical specifically when the saltwater –freshwater interface is situated at a significant depth below the bottom of the structures, the upconing problem may be catastrophic for shallow depth of interface in the regions near the sea. Therefore, the present analysis is extended considering upconing as well [Figure 10.4].

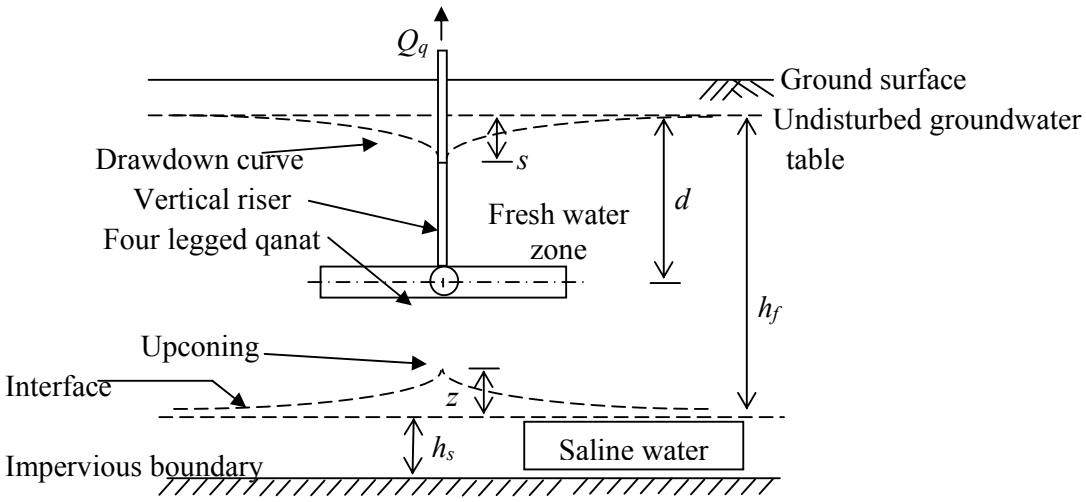

Fig. 10.4: Withdrawal of groundwater by qanat in salinity affected aquifer.

Dagan and Bear (1968) gave a mathematical expression for determining the height of the cone "Z_t" below the well. The formula is as follows:

$$Z_\alpha = \frac{Q_q}{2\pi\left(\frac{\rho_s}{\rho_f}-1\right)K_h\left(h_f - d\right)} \tag{10.5}$$

where, ρ_s is the density of saline water, ρ_f is the density of freshwater, h_f is the elevation of the phreatic level above sea level, K_h is the horizontal hydraulic conductivity of the aquifer soil, t (time since start of pumping) =∞, the equilibrium height Z_∞ of the cone is obtained from Equation (10.5). The value of Q attains the maximum value when putting $Z_\infty = H_f – d$ in above expression, from which the following equation can be written as:

$$Q_q\left(\max\right) = 2\pi K_h\left(\frac{\rho_s}{\rho_f}-1\right)\left(h_f - d\right) \tag{10.6}$$

The optimum values of Q_q (max) shall be the least of the two values obtained from the Equations (10.4-10.6). From the above expression, the design values of qanat-well are estimated as reasonably high. To meet water demand for any particular community, the number of qanat-well should be realistically increased as necessary.

10.4.2 Groundwater Recharge by Rainwater Harvesting

The interface of saline water and freshwater is gradually encroach in off-shore coastal area if freshwater is withdrawal regularly unless the extraction is reasonable remunerated by appropriate groundwater recharge techniques. The recharge to the aquifers of rainwater harvesting by through recharge wells and recharge ponds combines the best of both methods, the recharge ponds would acquire a vast of superfluous area while providing only wells would necessitate pressure injection into the aquifers.

10.4.2 (a) Recharge Area

Aquifers are replenished with water from the surface through a process called "recharge." This occurs as a part of the hydrologic cycle when water from rainfall percolates into underlying aquifers. The rate of recharge can be influenced by different factors, such as soil, plant cover, water content of surface materials, and rainfall intensity. Groundwater recharge may also occur from surface water bodies in arid areas. For any particular community the total area A_t is calculated as below:

$$A_t = A_{roof} + A_{road} + A_p + A_l \tag{10.7}$$

where, A_t = Total area of the community.
A_{roof} = Total roof cover area for all building in the community.
A_{road} = Total road area in the community.
A_p = Total pond area of the community.
A_l = Total area of vacant land in the community.

10.4.2 (b) Factor of Safety for Rainfall Recharge

The volume of freshwater extraction in a specific period of time should not exceed the volume of recharge available for that period in a coastal region for a particular community under consideration. With this concept, the corresponding factor of safety F the particular community has been formulated for the volumetric constancy. It is mentioned here that the other sources such as irrigation recycle, canals, nearby streams channels possible recharge assessment shall be taken into account, the factor of safety F is estimated as

$$F = \frac{\text{Volume of water annually available for recharge}}{\text{Volume of water annually extracted}} = \frac{\left[\left(A_t - A_{roof}\right)\eta + \alpha A_{roof}\right]P}{365WP_c} \tag{10.8}$$

where W is water consumption of people in the community (litre per capita per day), P_c is population of the *community*, P is designed annual rainfall (mm), η is recharge coefficient, and α is fraction of rainwater collected on roofs that is directed towards the recharge well. When the factor of safety is little beat higher than unity then the proposed technique becomes most effective. The extremely greater F value may be needed for sufficient drainage provision in the regions under concern to prevent adverse situation such as flooding and water logging. Conversely, while the value of the F is less than one, the condition can be compensated for by either reducing the extraction of freshwater or increasing the catchments area for rainfall recharge. In that circumstances F is excessively high for a given locality, the total surplus volume of water may be designed using expression as:

$$V_C = \left[\left(A_t - A_{roof}\right)\eta + \alpha A_{roof}\right]P + V_O - F_D\left(365WP_c\right) \tag{10.9}$$

where, V_o is the volume of water available annually from other sources such as, nearby stream/canal, irrigation recycle, etc, V_c is the volume of excess water annually and F_D is the design factor of safety (slightly greater than unity). An adequate drainage facility should be constructed to mitigate this volume of excess water.

10.4.2 (c) Percolation Pond

A percolation pond is a small water storage structure constructed across a water body to harvest the runoff from the catchment and impound for a longer time thereby recharging groundwater storage in the zone of influence of pond. The greater precipitation depends on the longer design return period of precipitation.

The design precipitation specifically for the particular design structures depends on the design return period of the precipitation. The harvested rainwater collected from roofs of the structures in the community under consideration is partly seeped into through recharge well and other parts are stored for future use. The area of design pond may be estimated reasonably taking into consideration the effective volume of water to be accumulated in the design pond during the monsoon period. Therefore,

$$A_p = \frac{\left[\left(A_t - A_{roof} - A_{road}\right)\eta_1 + A_{road}\right]P_m}{1000H_p - \left(1-\eta_1\right)P_m} \tag{10.10}$$

where A_p = area of the pond;

P_m = monsoon rainfall in mm;

η_1 = runoff coefficient relevant to the area; and

H_p = depth of pond to be excavated.

10.4.2 (d) Recharge Chamber with Recharge Well

Sarkar (2007) designed a RWH scheme for a building at Salt Lake. Following his recommendations, the recharge chambers connected with 100 mm diameter recharge well dimension for the particular community under consideration may be determined by:

$$\frac{V_w N_w}{V_{ws} N_{ws}} = \frac{\alpha P A_{roof}}{\alpha_s P_s A_{roof\ s}} \tag{10.11}$$

where V_w is the recharge chamber volume, N_w is the number of recharge chambers fitted with 100 diameter recharge well adopted in the community, The suffix '*s*' denotes the corresponding parameter for the relevant to Sarkar (2007).

10.5 A Typical Case Study with Quantification

The proposed methodology as described above has been utilized for carrying out an intensive study with adequate quantification in the Contai Polytechnic College Campus situated at Contai in Purba Midnapur.

10.5.1 Geographical Description

Contai (also known as Kanthi) is the head quarter of Contai subdivision in Purba Medinipur district. Its geographical location is 21°46'40" N latitude and 87°44'50" E longitude. It is 10 km away from beach and having an elevation of 6 m above the mean sea level.

10.5.2 Site Characteristics

Contai falls on the south side of Purba Midnapur district and on borders of West Bengal and Orissa [Figure 10.5]. The geological formation is of tertiary sediments and of Pleistocene lower age. The litho-stratigraphic unit is of Lalgarh formation consisting of residual soil and is composed of sand, silt and clay (soft sediments). Geomorphologically the area is a flat terrain (flood plain). The unconsolidated recent sediments are essentially a sequence of clay, sand and gravel exhibiting wide variation in grade and colour. Usually these sediments are characterized by shades of grey, brown and yellow colour. The sand is of quartz feldspathic material often associated with gravel, calcareous shelly material. The unconsolidated sediments are very thick (300 m) close to the coast.

The Contai polytechnic college is situated in the village of Raghurampur which is 7 km away from Contai town. From the available hydro-geological data, the average groundwater table and the interface are situated at depths of about 2-3 m and 5-60 m below the ground surface, respectively.

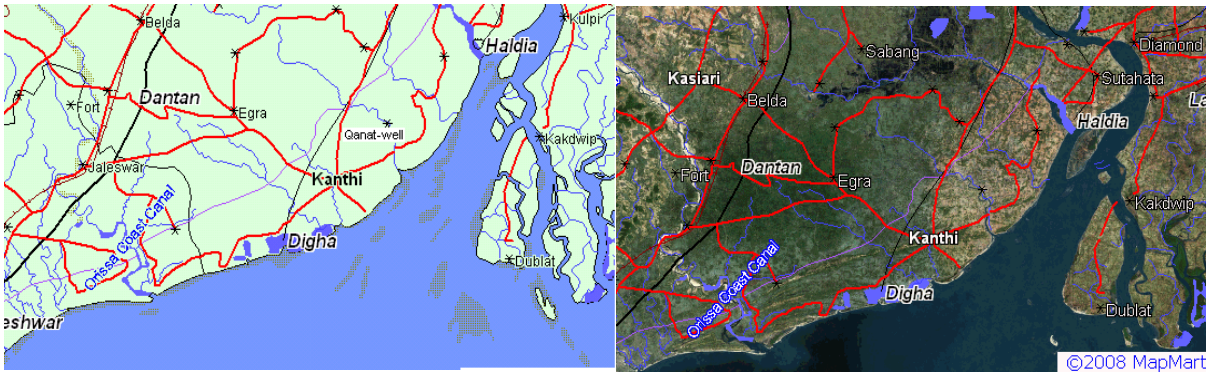

Fig. 10.5: Satellite imagery of Contai (Kanthi).

A plan view of the college, showing salient features, is presented in Figure 10.6 (a-b). Hydro-geologically the area is a moderate zone for groundwater development. The water table lies between 1 m to 4 m below ground level in the unconsolidated sandy sediments of recent alluvium. Due close proximity with sea, salt water intrusion is evident. After studying the geological and geophysical properties of the borehole and interpreting the logging data's through various self potential and resistivity graphs the findings are 200 m drilled depth, 195 m electro-logged depth and the sand aquifer zones are saline in nature

10.5.3 Subsurface Survey

Self potential (SP) measurement: Also known as spontaneous potential which is the potential difference caused by variations in potential of the downhole electrode. The difference between salinity of the formation water in the permeable beds and the salinity of the mud in the borehole causes the difference in potential which is recorded in SP log. The value is represented in mili-Volt. The SP can be positive and negative. The SP log is recorded on the left hand side.

Resistivity Measurement: The current always takes the path of least resistance. Therefore the resistivity of a formation depends on the lithology as well as the moisture content and above all the pre-fluid present in the interstices, cracks and crevasses of the formation. The relevant field data obtained are given in Table 10.1. From the field examination, SP reading is seen to move towards negative side demonstrating nearness of sand aquifer underneath.

Table 10.1: Lithology of the study area.

Stratum	Depth (m)	Resistivity (Ωm)	Nature of formation
1	0 - 9	30-60	Fine sand yellow grey
2	9 - 15	30-50	Fine sand greyish
3	15 - 24	30-50	Fine to medium sand
4	24 - 27	35-45	Clay with sand greyish
5	27 - 36	20-50	Medium sand orange
6	36 - 51	20-40	Fine sand yellow
7	51 - 54	25-45	Clay yellow grey
8	54 - 57	50-60	Medium sand yellow
9	57 - 60	60-90	Coarse sand grey white
10	60 - 72	20-30	Fine sand grey white
11	72 - 75	25-40	Clay yellow
12	75 - 78	25-35	Clay black
13	78 - 81	50-60	Medium sand orange
14	81 - 93	25-37	Clay grey
15	93 - 96	20-30	Fine sand grey
16	96 - 105	27-34	Clay yellow black
17	105 - 111	20-30	Fine sand grey white
18	111 - 120	60-90	Coarse sand yellow
19	120 - 135	20-30	Fine sand grey white
20	135 - 144	25-35	Very fine sand grey white
21	144 - 150	25-45	Clay grey white
22	150 - 198	25-70	Fine sand grey

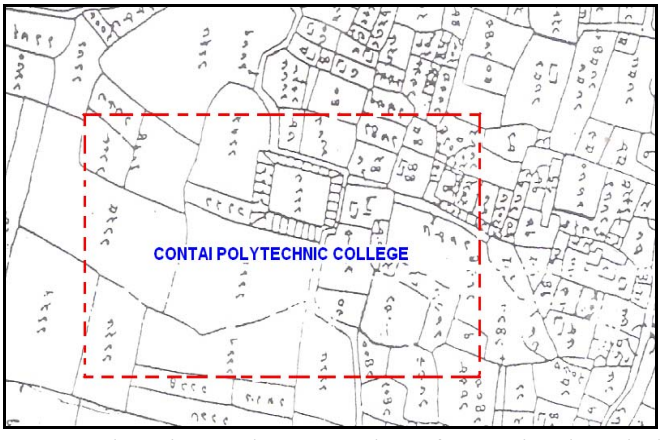

Fig. 10.6 (a): Key location and Mouza plan of Contai polytechnic college.

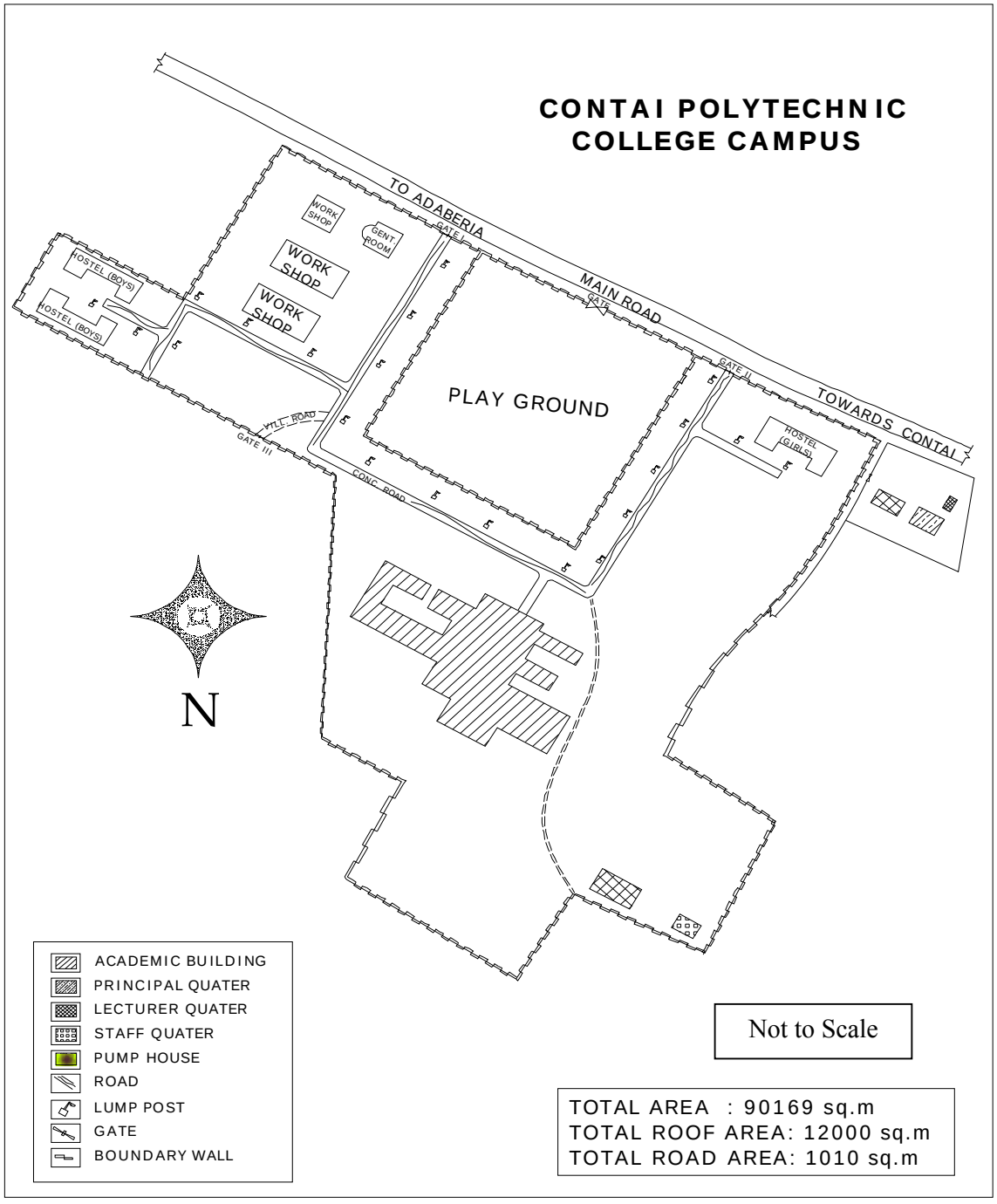

Fig. 10.6 (b): Plan of the Contai polytechnic college showing salient features.

As seen from Figure 10.7, the average depth freshwater-saltwater interface is located at a depth of around 40 m beneath the ground surface. It is prudent not to go for 'deep tubewell' development; qanat-well structures are best in this circumstance.

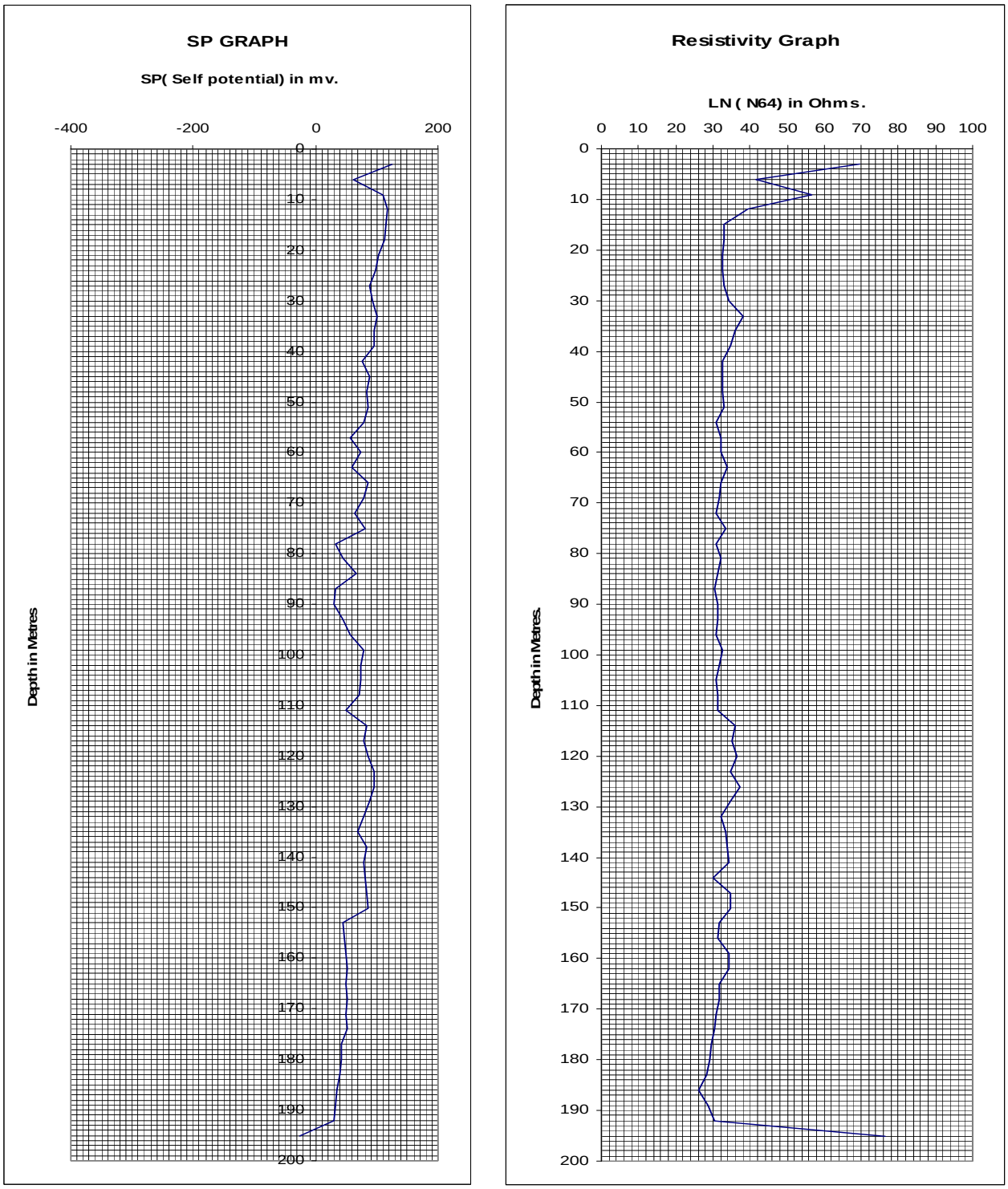

Fig. 10.7.: SP and resistivity graph of electro-logging test for the bore well at Contai polytechnic college.

10.5.4 Rainfall Data

From available literatures, the yearly variation of total annual precipitation is given in Table 10.2.

Table 10.2: Monthly Rainfall in the district of Purba Midnapur.

Month	Normal (mm)	Actual (mm)				
	2014	2010	2011	2012	2013	2014
January	11	-	3	56	2	0
February	27	16	10	9	5	72
March	40	1	13	1	1	10
April	52	1	76	47	31	6
May	128	94	112	43	191	187
June	273	178	309	116	290	236
July	312	266	272	310	292	354
August	359	295	384	249	436	464
September	296	246	335	368	365	298
October	124	125	24	79	465	102
November	36	5	-	25	-	0
December	8	17	-	39	-	0
Total	1666	1244	1538	1342	2078	1729

Source : Agricultural Meteorologist, Directorate of Agriculture, Govt. of W.B.

Table 10.3: Average monsoonal and kharif rainfall, in mm, in Purba Midnapur.

Districts/ regions	May 15^{th} - 31^{st}	June	July	August	Sept.	Oct. 1^{st} -15^{th}	June-Sept. monsoon
Purba Midnapur	74.9	280.3	315.6	367.1	303.3	84.9	1266.3 (74.4%)
Paschim Midnapur	65.1	258.5	319.6	334.5	263.5	67.9	1176.1 (76.4%)

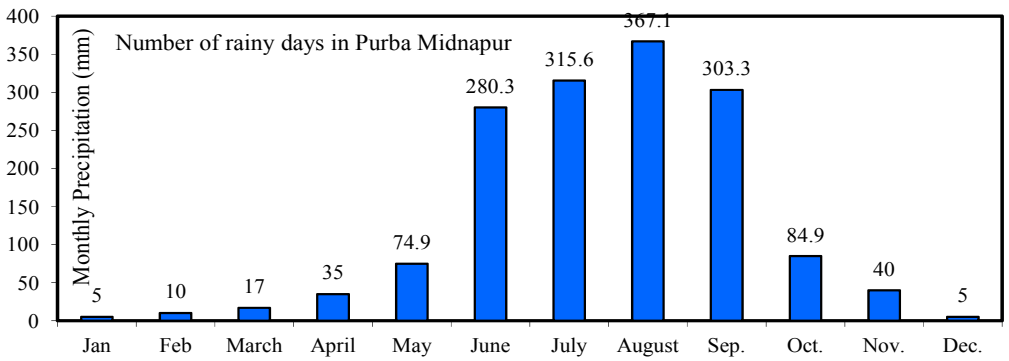

Fig. 10.8: Average monthly precipitation from 2005-2010 (after Patra, 2010).

The monthly variation for the district of Purba Midnapur is given in Table 10.3 and Figure 10.8. In Purba Midnapur district, during the monsoon period i.e. from June to September the average rainfall occurs around 1800 mm. The area generally experiences

three seasons annually, namely, summer, monsoon and winter. Winter starts from the end of November and continues to early past of March. December and January are the coldest months with temperature of temperature of around 10°C. The lowest temperature recorded is 5°C. The winter is followed by summer and continues upto May-June, until monsoon comes. During summer, day temperature increases upto about 45°C, though the highest recorded so far has been around 48°C. The input parameters necessary for design in the locality under consideration are summarised in Table 10.4.

Table 10.4: Values of variables determined from hydro-geological investigation.

Input parameter	Values
Maximum design discharge, Q_q (max)	Calculated using Equations 10.4 and 10.6
Aquifer thickness, H	40 m
Horizontal hydraulic conductivity, K_h	3.512×10^{-4} m/s, [from laboratory test]
Vertical hydraulic conductivity, K_v	3.614×10^{-4} m/s, [from laboratory test]
Conductivity contrast, $\beta = \sqrt{K_h / K_v}$	0.9857
Well eccentricity, δ	0
Population in Contai polytechnic college, P_c	300
Total area of the college campus, A_t	90169 m^2
Total roof area including student hostels, A_{roof}	12000 m^2
Total road area, A_{road}	1010 m^2
Total area of pond, A_p	1204 m^2
Area of vacant land, A_l	75955 m^2
Design annual precipitation, P	Taken various values
Design monsoonal precipitation, P_m	Taken various values
Per capita water consumption, W	140 litres/capita/day
Recharge coefficient, η	Chosen from available literature
Runoff coefficient, η_l	- do -

10.5.5 Design of Qanat-Well Structure

The aquifer is unconfined having an average hydraulic conductivity of $K_h = 3.512\times10^{-4}$ m/s and $K_v = 3.614\times10^{-4}$ m/s (from laboratory tests). From the existing data (UNDP Report, 2006; WHO, 2010), the value of W (water demand) was selected as 140 litre/capita/day. The average population (P_c) in the Institute campus is 250. Considering a 20% increase, the value of P_c is taken as 300. On the basis of water daily water in the Institute with hourly pumping operation per day (t) chosen as 2, 3, 4, 5, the various parameters of the qanat well structures (e.g. L_q, r_q and d) have been estimated using the Equation (10. 4). The value of Q_q(max) was determined as

$$Q_q(\max) = \frac{WP_c}{3600\times10^3\times t} \tag{10.12}$$

where, t is the hourly pumping rate in the college campus per day.

Table 10.5: Depth of qanat d (m) for qanat-well design (t= 2 hours/day).

Qanat radius r_q (mm)	100	125	150	200	250	300
Qanat length L_q (m)						
1.5	7.981	7.693	7.469	7.131	6.869	6.698
2.0	6.085	5.886	5.726	5.498	5.334	5.223
2.5	4.932	4.774	4.662	4.498	4.397	4.331
3.0	4.164	4.042	3.954	3.886	3.759	3.746
3.5	3.618	3.519	3.447	3.358	3.310	3.291
4.0	3.192	3.119	3.064	3.001	2.972	2.964

Table 10.6: Depth of qanat d (m) for qanat-well design (t= 3 hours/day).

Qanat radius r_q (mm)	100	125	150	200	250	300
Qanat length L_q (m)						
1.5	5.378	5.181	5.064	4.870	4.743	4.658
2.0	4.090	3.981	3.894	3.781	3.712	3.663
2.5	3.341	3.250	3.189	3.115	3.072	3.094
3.0	2.826	2.763	2.721	2.675	2.639	2.624
3.5	2.456	2.411	2.385	2.362	2.357	2.354
4.0	2.184	2.147	2.116	2.107	2.102	2.099

Table 10.7: Depth of qanat d (m) for qanat-well design (t= 4 hours/day).

Qanat radius r_q (mm)	100	125	150	200	250	300
Qanat length L_q (m)						
1.5	4.079	3.953	3.866	3.749	3.678	3.629
2.0	3.121	3.044	2.991	2.926	2.890	2.881
2.5	2.547	2.498	2.464	2.432	2.424	2.422
3.0	2.165	2.132	2.112	2.099	2.098	2.097
3.5	1.892	1.869	1.855	1.853	1.853	1.852
4.0	1.682	1.669	1.667	1.6665	1.666	1.6655

Table 10.8: Depth of qanat d (m) for qanat-well design (t= 5 hours/day).

Qanat radius r_q (mm)	100	125	150	200	250	300
Qanat length L_q (m)						
1.5	3.303	3.214	3.153	3.076	3.047	3.031
2.0	2.537	2.468	2.449	2.419	2.413	2.411
2.5	2.078	2.048	2.034	2.022	2.020	2.017
3.0	1.769	1.751	1.745	1.744	1.742	1.741
3.5	1.551	1.543	1.5415	1.541	1.5405	1.540
4.0	1.386	1.384	1.383	1.382	1.381	1.3805

Using Equation (10.4), the values of the depth of the qanat base for the chosen value of L_q and r_q are calculated and put into in Tables 10.5 to 10.8.

The qanat-well structure depth (d) has been determined by using Equation (10.4) and is substituted in Equation (10.6) to check for upconing. If the discharge determined from Equation (10.6) exceeds the design discharge as estimated previously, upconing will not take place. Or else the depth d may be estimated taking into consideration upconing with using Equation (10.6). But it is mentioned here that upconing does not happen at the study area. The depth d for different values of the length (L_q) and radius of the qanat leg (r_q) are plotted in Figure 10.9.

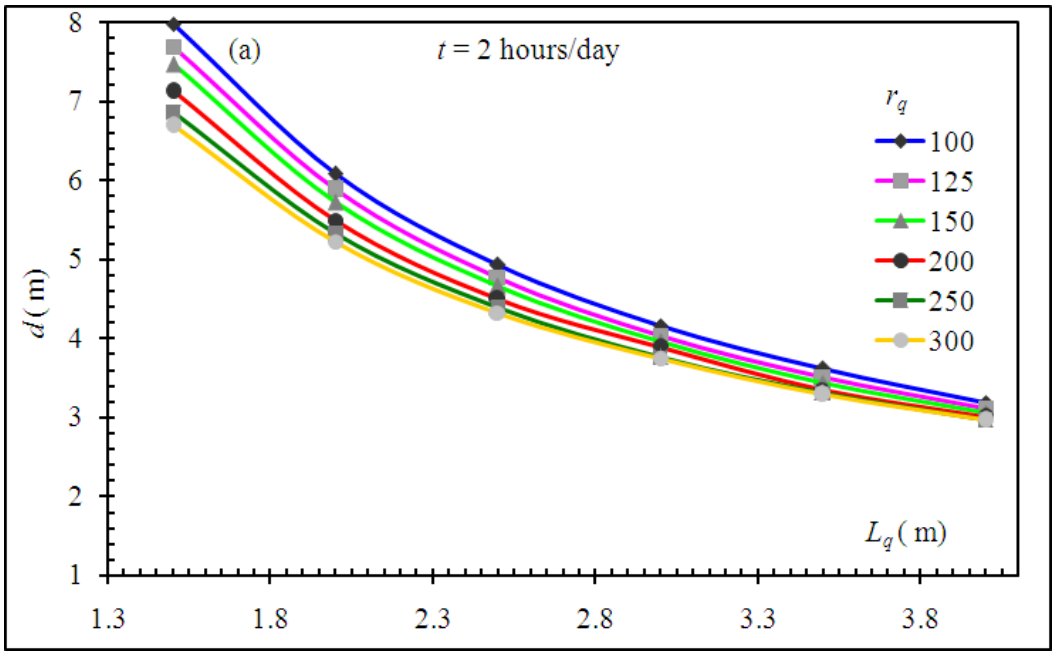

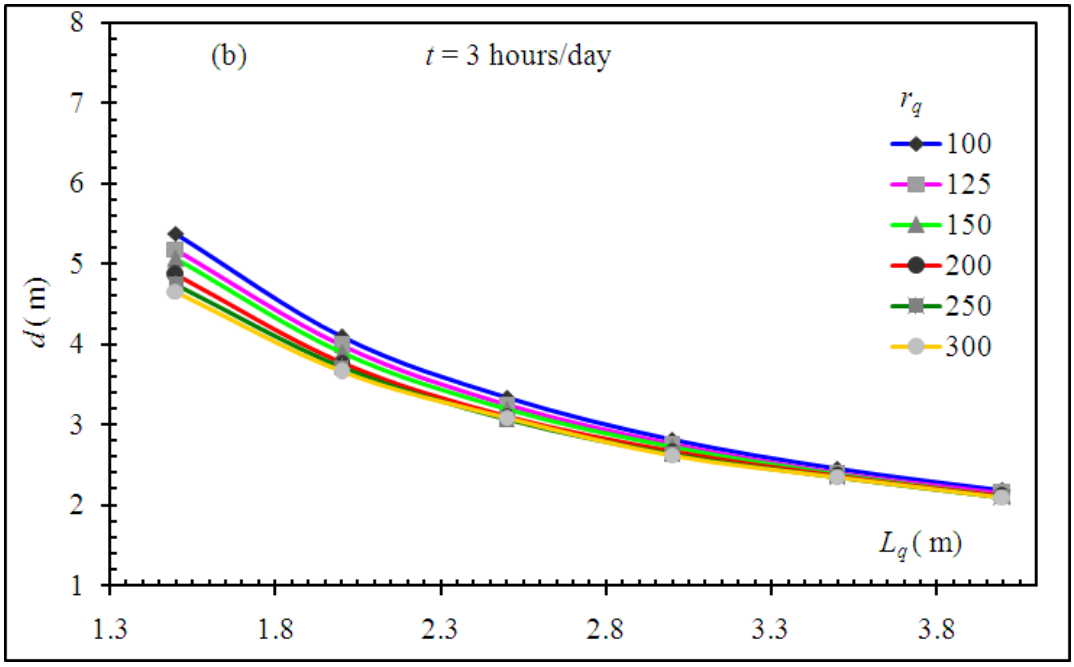

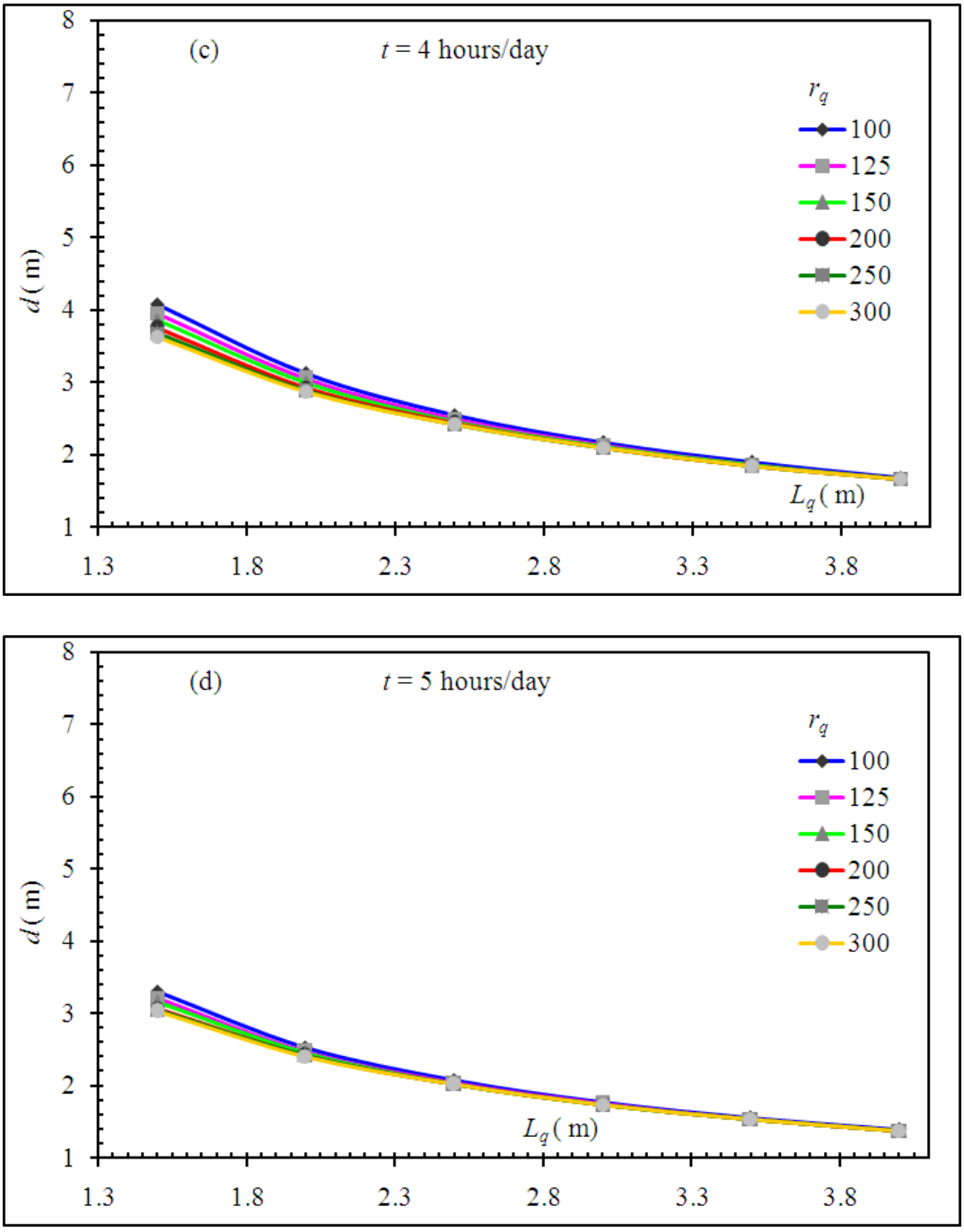

Fig. 10.9: Variation of depth of qanat at different length of qanat leg for pumping duration of (a) 2 hours / day, (b) 3 hours / day, (c) 4 hours / day, (d) 5 hours /day.

Parameter d decreases following a curvilinear pattern with the length of leg L_q. The length of qanat-well variation is reasonable sharp in the range 1m $\leq$ L_q $\leq$3m and assumes a linear pattern for L_q > 3 m. The variation of depth of qanat at base, length of qanat leg for pumping duration i.e. the curves in Figure 10.9 would be useful to implement appropriate values of the qanat parameters (r_q, L_q, d and t) considering other design aspects such as maximum depth of water table, feasibility of construction, etc.

10.5.6 Recharge Structures

10.5.6.1 Rainfall Recharge

The methodology for design features of the recharge structures was implemented in the proposed site, is explained above. The degree of compaction, arrangement of soil particles, porosity, hydraulic conductivity of soil and estimation of precipitation and infiltration, these characteristics which greatly influences successful implementation of the proposed model, but also on other factors such as vegetative cover, climatic conditions, soil moisture condition, the porous medium extension from the natural ground surface, etc. (Linsley *et al.*, 1982). The determination of the recharge volume may be assessed by field investigation tests data and existing literature available from the site under contemplation and engineering judgement. It is mentioned here that the total precipitation in Purba Midnapur district for the time period of 2010-2014 varied from 1244 to 2078 mm as mention in Table 10.2. In the design consideration connected with artificial recharge through recharge chambers for the annual precipitation and in the design connection with the percolation ponds for the monsoon precipitation is considered as 1296 to 2256 mm. and 200 to 700 mm. respectively. The factor of safety for recharge and extraction volume of water available for the given community may be calculated using Equation (10.8) considering $A_t = 90169$ m^2 and $A_{roof} = 12000$ m^2.

The Water Resources Department under government of India carried out extensive survey and data acquisition on studies in different water balance project at various locations of the India and values of recharge coefficient based on soil characteristics and other environmental conditions (MoWR, 2009). The values of coefficient relevant to MoWR (2009) were considered for this study area to estimate the factor of safety.

Chaturvedi (1973) studied the hydro-geological investigation at Ganga-Yamuna Doab the segment of the Indo-Gangetic plain in western and south-western part of Uttar Pradesh state in India. He computed a rainfall-infiltration correlation formula based on the field study.

Wu and Zhang (1994) computed the infiltration recharge process to groundwater and its relationship with rainfall by in-situ lysimeter experiments, statistical methods, and numerical simulations. The infiltration-recharge could be predicted directly from rainfall events through a statistical correlation. The advantage to use the statistical correlation for estimating the recharge was a minimal requirement of input data and computation effort, compared with numerical simulations. The recharge data were collected from the lysimeter installed in the field at an irrigation experiment station in Hebei province of the northern China. A linear relation of the effective rainfall data (P) and the recharge data (R) was formulated. Even though the model is on the field condition appropriate to China, it was specifically applied for current site location due to its adaptability.

Kumar and Seethapathi (2002) estimated the forecast of groundwater recharge and capacity of aquifer was essential issues in effective groundwater resource, made modified the Chaturvedi (1973) formula, the recharge and precipitation formula was developed. The location near the current study area, the rainfall recharge and precipitation were incorporated for the present case study. The recharge coefficients were

determined from the available literatures of Chaturvedi (1973); Wu and Zhang (1994); Kumar and Seethapathi (2002); and MoWR (2009) as revealed in Table 10.9.

Wu and Zhang (1994) estimated correlation between annual precipitation P and the total amount of recharge R produced as given in Equation (10.13) which is applicable for Hebei province of the northern China.

$$R = 0.87(P - 5.25) \tag{10.13}$$

where R is the infiltration recharge in mm and P is the effective rainfall in mm.

Chaturvedi (1973) derived an empirical relationship for recharge as an annual precipitation in Ganga-Yamuna doab basin the segment of the Indo-Gangetic plain in western and south-western part of Uttar Pradesh in India, as given in Equation (10.14).

$$R = 6.807(P - 355.6)^{0.5} \tag{10.14}$$

where R is the net recharge due to precipitation during the year (in mm) and P is an annual precipitation (in mm).

The formula of Chaturvedi (1973) was later modified further by Kumar and Seethapathi (2002) to yield the relation given in Equation (10.15).

$$R = 3.175(P - 388.1)^{0.76} \tag{10.15}$$

The Water Resources Department under Government of India recommended (MoWR, 2009) the formula given in Equation (10.16).

$$R = \eta P \tag{10.16}$$

where η is the recharge coefficient as given in Table 10.9.

MoWR (2009) redefined realistic values of recharge coefficients based on soil characteristics and other environmental conditions. The value of η may be realistically calculated as 0.160 for alluvial area of the coastal zones of east India. Variation of the factor of safety for rainfall recharge with annual precipitation was studied and revealed in Figure 10.10. The factor of safety (F) is estimated as per Equation (10.8), the F increases linearly with an increase in annual precipitation (P). The values (magnitude and gradient) of factor of safety (F) relevant to the formula of Wu and Zhang (1994) are appreciably higher ($6 < F < 11$) than the range ($1.25 < F < 3$) for the work of Chaturvedi (1973), Kumar and Seethapathi (2002) and MoWR (2009). By using the correlation, relevant to MoWR (2009), for factor of safety of rainfall recharge and annual precipitation results are found normally consistent for Indian environment condition. The values of factor of safety at varying rainfall and subsequent fraction of rainwater collected on roofs are presented in Table 10.10.

Table 10.9: The values of recharge coefficient.

Mean annual rainfall (P) (mm)	Recharge coefficient η			
	Chaturvedi (1973)	Wu and Zhang (1994)	Kumar and Seethapathi (2002)	MoWR (2009)
1296	0.161	0.866	0.187	0.160
1525	0.153	0.867	0.189	0.160
1750	0.145	0.868	0.188	0.160
1975	0.139	0.869	0.188	0.160
2259	0.131	0.870	0.186	0.160

Table 10.10: Values of factor of safety at varying rainfall and subsequent fraction of rainwater collected on roofs.

Fraction of rainwater collected on roofs	Chaturvedi (1973)		Wu and Zhang (1994)		Kumar and Seethapathi (2002)	
α	P (mm)	F	P (mm)	F	P (mm)	F
0.25	1296	1.333	1296	5.881	1296	1.312
	1525	1.477	1525	6.941	1525	1.478
	1750	1.608	1750	7.984	1750	1.630
	1975	1.732	1975	9.026	1975	1.773
	2259	1.818	2259	10.341	2259	1.945
0.50	1296	1.586	1296	6.135	1296	1.565
	1525	1.775	1525	7.239	1525	1.776
	1750	1.951	1750	8.326	1750	1.973
	1975	2.118	1975	9.412	1975	2.159
	2259	2.321	2259	10.783	2259	2.387
0.75	1296	1.840	1296	6.388	1296	1.819
	1525	2.074	1525	7.538	1525	2.074
	1750	2.293	1750	8.669	1750	2.315
	1975	2.504	1975	9.799	1975	2.505
	2259	2.762	2259	11.225	2259	2.829

10.5.6.2 Percolation Pond

The water harvesting potential of a site could be estimated using the formula given as:

Water harvesting potential = Rainfall × Area of catchment × Runoff coefficient

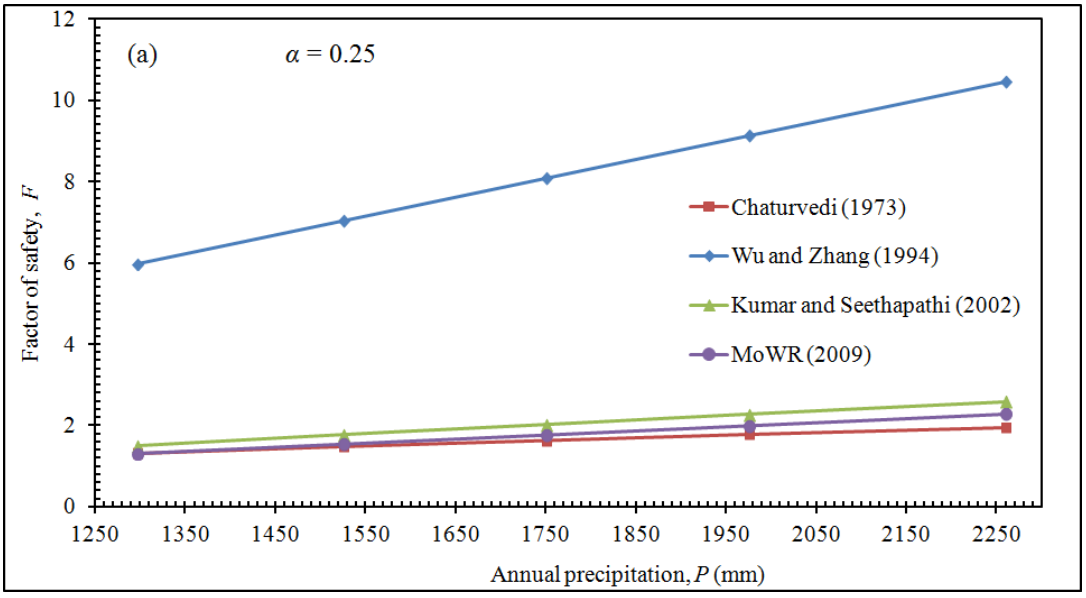

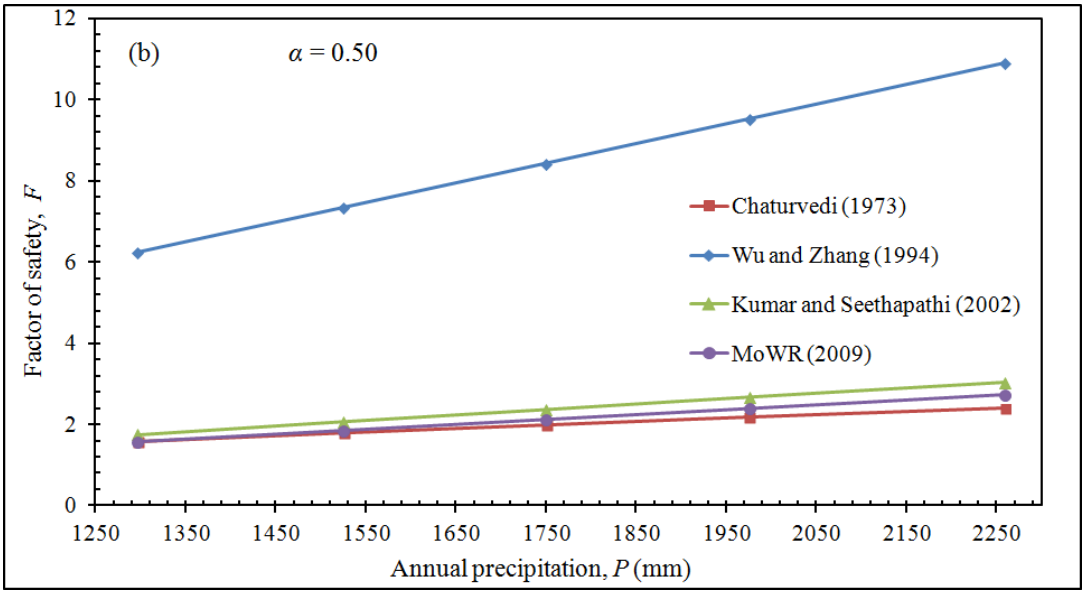

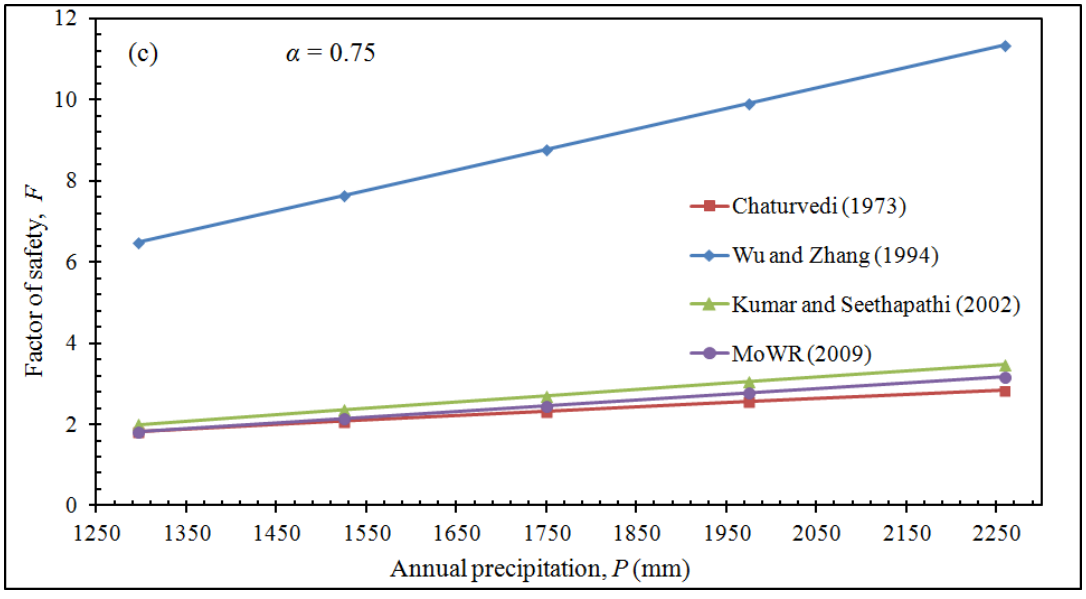

Fig. 10.10: Variation of the factor of safety F with annual precipitation P for: (a) α = 0.25, (b) α = 0.50 and (c) α = 0.75.

Runoff coefficient plays an important role in assessing the runoff availability and depends upon the catchment characteristics. The runoff coefficients are given in the Table 10.11. These values have been used in the present analysis relevant to the formula of Patra (2010) for West Bengal. By using the Equation (10.10) and the data estimated from hydro-geological investigation in the study area in the Table 10.4 and reasonable assume the depth of pond H_p, the required depth of pond is determined A_p and put into in Table 10.12. The depth of pond H_p, area of pond A_p for various values runoff coefficients for various catchment surfaces with different monsoon precipitation is plotted in Figure 10.11.

Table 10.11: Values of runoff coefficient η_1 (after Patra, 2010).

Type of catchments	Runoff coefficient
Roof top catchments	
• Tiles	0.8-0.9
• Corrugated metal sheets	0.7-0.9
Ground surface coverings	
• Concrete	0.6-0.8
• Brick pavement	0.5-0.6
Untreated ground catchments	
• Soil on slopes less than 10%	0.0-0.3
• Rocky natural catchments	0.2-0.5
• Green area	0.05-0.10

Table 10.12: Depth and area of pond for different monsoonal precipitations P_m.

η_1	P_m = 200 mm		P_m = 350 mm		P_m = 500 mm		P_m = 750 mm	
	H_p (m)	A_p (m^2)	H_p (m)	A_p (m^2)	H_p (m)	A_p (m^2)	H_p (m)	A_p (m^2)
0.05	2.0	538	2.0	1021	2.0	1596	2.0	2835
	3.0	346	3.0	639	3.0	964	3.0	1596
	4.0	255	4.0	464	4.0	690	4.0	1110
	5.0	202	5.0	365	5.0	538	5.0	851
	6.0	167	6.0	300	6.0	440	6.0	690
0.1	2.0	959	2.0	1812	2.0	2814	2.0	4938
	3.0	619	3.0	1137	3.0	1711	3.0	2814
	4.0	457	4.0	829	4.0	1229	4.0	1968
	5.0	362	5.0	652	5.0	959	5.0	1513
	6.0	300	6.0	537	6.0	786	6.0	1229
0.2	2.0	1787	2.0	3345	2.0	5137	2.0	8806
	3.0	1158	3.0	2115	3.0	3161	3.0	5137
	4.0	856	4.0	1547	4.0	2283	4.0	3626
	5.0	679	5.0	1219	5.0	1787	5.0	2802
	6.0	563	6.0	1006	6.0	1468	6.0	2283
0.3	2.0	2597	2.0	4817	2.0	7319	2.0	12281
	3.0	1689	3.0	3069	3.0	4557	3.0	7320
	4.0	1252	4.0	2251	4.0	3309	4.0	5213
	5.0	994	5.0	1778	5.0	2597	5.0	4048
	6.0	824	6.0	1469	6.0	2138	6.0	3309
0.4	2.0	3390	2.0	6231	2.0	9373	2.0	15420
	3.0	2213	3.0	3998	3.0	5902	3.0	9373
	4.0	1643	4.0	2943	4.0	4307	4.0	6733
	5.0	1306	5.0	2329	5.0	3391	5.0	5253
	6.0	1084	6.0	1927	6.0	2796	6.0	4307

As observed in Figure 10.11, the required area of recharge pond decreases in a hyperbolic maner with the depth of pond to be excavated, which is well in agrement with Equation (10.10).

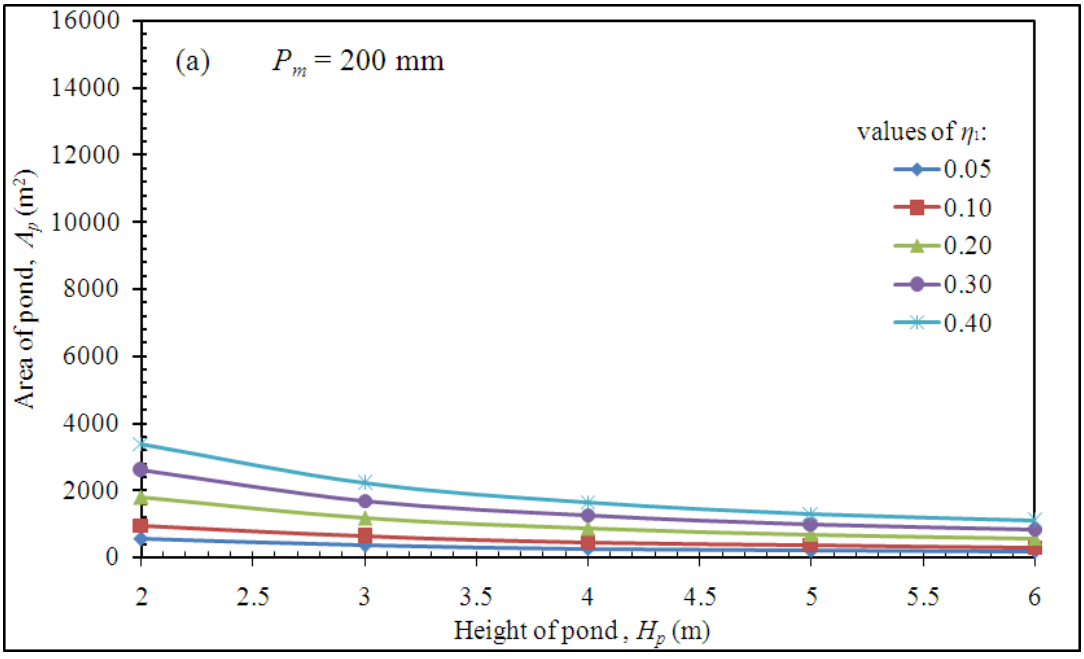

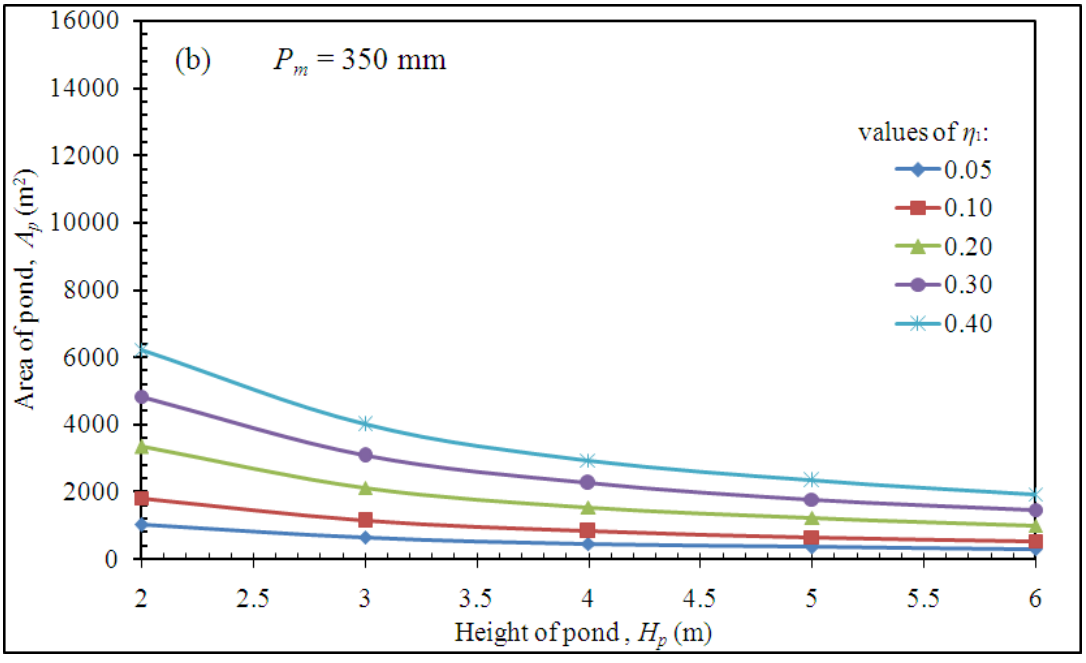

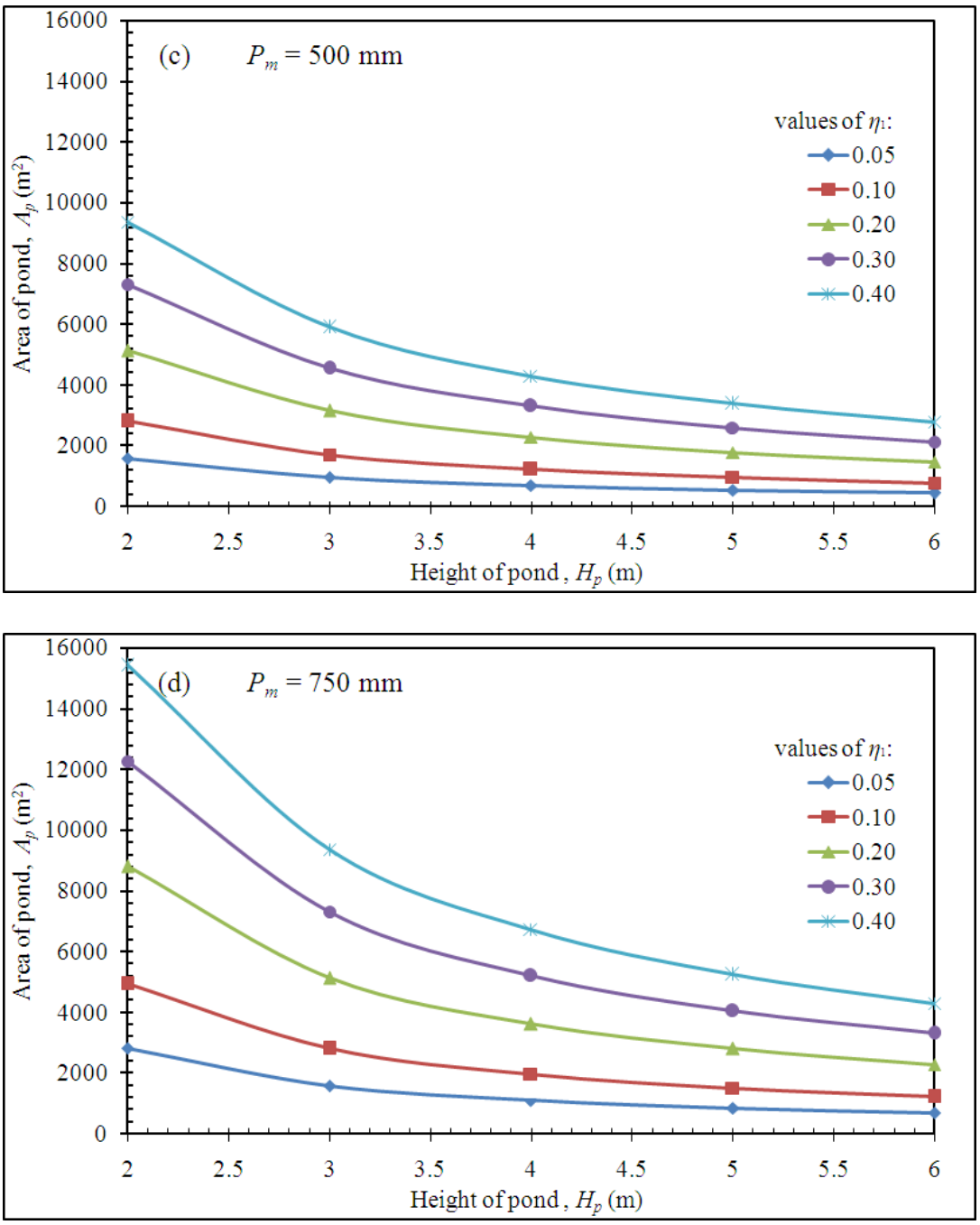

Fig. 10.11: Variation of recharge pond area at different depth of recharge pond for precipitation of (a) 200, (b) 350, (c) 500 and (d) 750 mm.

10.5.6.3 Recharge Chamber with Recharge Well

The dimensions of recharge chamber length (L), breadth (B), height (H), volume (V) and number of recharge chamber (N_w) coupled with 100 mm diameter recharge well for various values of roof rainwater collection factor α may be reasonable estimated using Equation (10.11). The number of recharge chambers N_w and the volume of recharge chambers V_w for various values of annual precipitation (P) and roof rainwater collection

factor α is plotted in Figure 10.12. The number of recharge chamber (N_w) is decreased with increased volume of recharge chamber (V_w) for $V_w < 5$, beyond which a stabilising tendency is noted. The relevant dimensions for recharge chamber with recharge well are described in Tables 10.13 to 10.15.

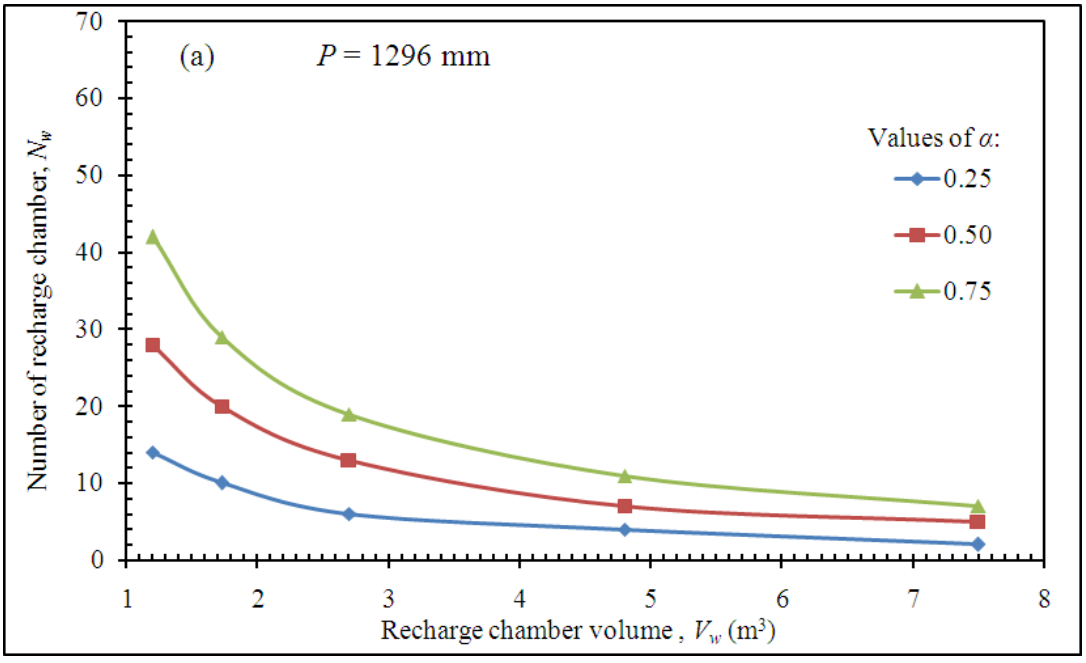

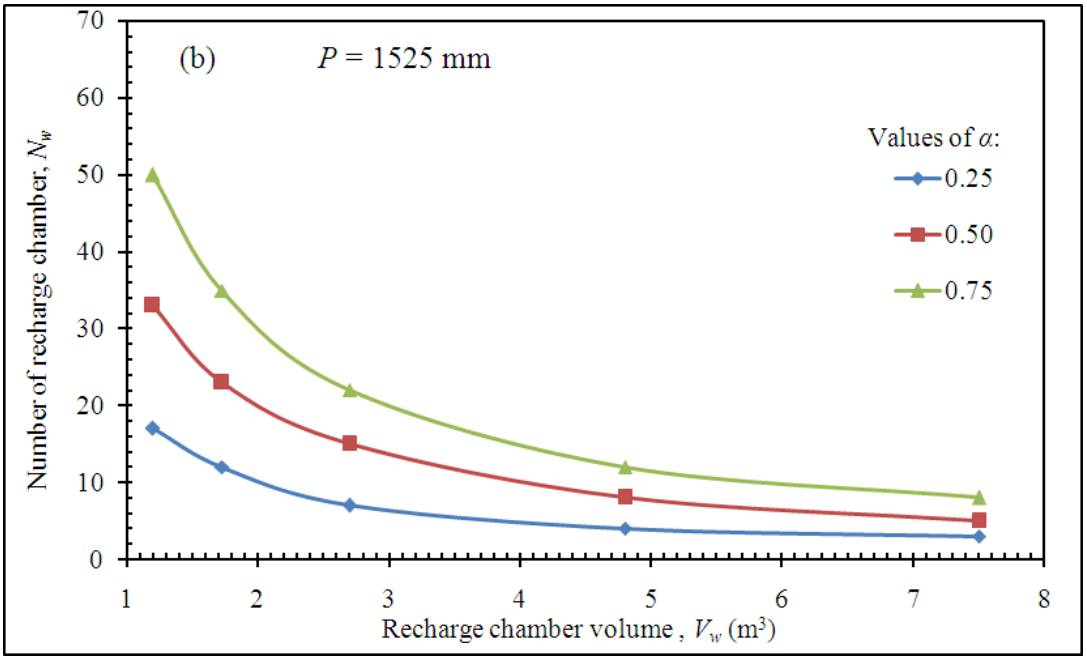

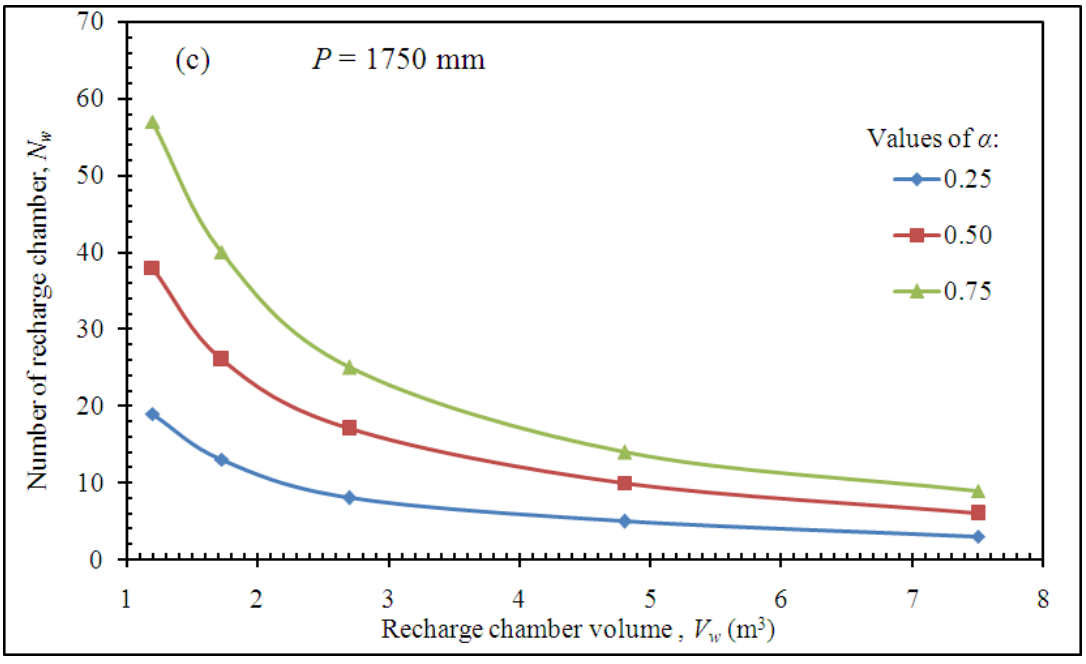

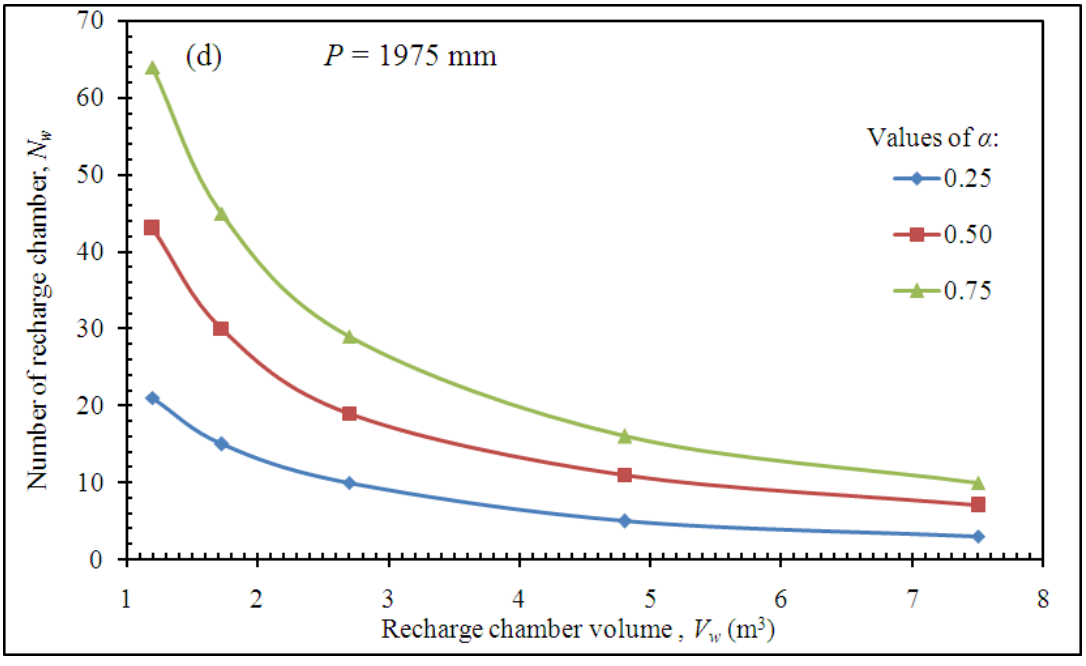

As observed from Figure 10.12, the number of recharge chambers N_w decreases fairly exponentially with the volume V_w of the recharge chambers. The rate of decrease is pronounced in the range of V_w<5, beyond which a stabilizing tendency is noted.

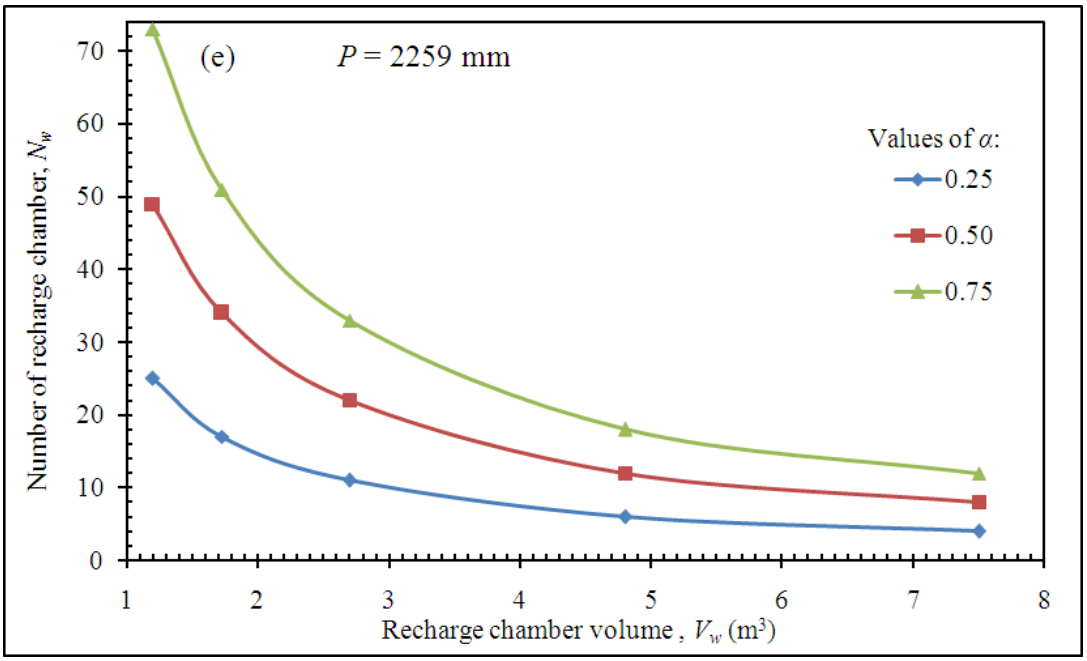

Fig. 10.12: Variation of recharge chamber volume with number of recharge chambers for annual precipitation of (a) 1296, (b) 1525, (c) 1750, (d) 1975, and (e) 2259 mm.

Table 10.13: Recharge chamber dimensions for precipitations P = 1296 and 1525 mm.

α	P = 1296 mm					P = 1525 mm				
	Recharge chamber dimensions				N_w	Recharge chamber dimensions				N_w
	L (m)	B (m)	H (m)	V (m^3)		L (m)	B (m)	H (m)	V (m^3)	
0.25	1.0	1.0	1.2	1.20	14	1.0	1.0	1.2	1.20	17
	1.2	1.2	1.2	1.728	10	1.2	1.2	1.2	1.728	12
	1.5	1.5	1.2	2.70	6	1.5	1.5	1.2	2.70	7
	2.0	2.0	1.2	4.80	4	2.0	2.0	1.2	4.80	4
	2.5	2.5	1.2	7.50	2	2.5	2.5	1.2	7.50	3
0.50	1.0	1.0	1.2	1.20	28	1.0	1.0	1.2	1.20	33
	1.2	1.2	1.2	1.728	20	1.2	1.2	1.2	1.728	23
	1.5	1.5	1.2	2.70	13	1.5	1.5	1.2	2.70	15
	2.0	2.0	1.2	4.80	7	2.0	2.0	1.2	4.80	8
	2.5	2.5	1.2	7.50	5	2.5	2.5	1.2	7.50	5
0.75	1.0	1.0	1.2	1.20	42	1.0	1.0	1.2	1.20	50
	1.2	1.2	1.2	1.728	29	1.2	1.2	1.2	1.728	35
	1.5	1.5	1.2	2.70	19	1.5	1.5	1.2	2.70	22
	2.0	2.0	1.2	4.80	11	2.0	2.0	1.2	4.80	12
	2.5	2.5	1.2	7.50	7	2.5	2.5	1.2	7.50	8

Table 10.14: Recharge chamber dimensions for precipitations P = 1750 and 1975 mm.

α	P = 1750 mm					P = 1975 mm				
	Recharge chamber dimensions				N_w	Recharge chamber dimensions				N_w
	L (m)	B (m)	H (m)	V (m^3)		L (m)	B (m)	H (m)	V (m^3)	
0.25	1.0	1.0	1.2	1.20	19	1.0	1.0	1.2	1.20	21
	1.2	1.2	1.2	1.728	13	1.2	1.2	1.2	1.728	15
	1.5	1.5	1.2	2.70	8	1.5	1.5	1.2	2.70	10
	2.0	2.0	1.2	4.80	5	2.0	2.0	1.2	4.80	5
	2.5	2.5	1.2	7.50	3	2.5	2.5	1.2	7.50	3
0.50	1.0	1.0	1.2	1.20	38	1.0	1.0	1.2	1.20	43
	1.2	1.2	1.2	1.728	26	1.2	1.2	1.2	1.728	30
	1.5	1.5	1.2	2.70	17	1.5	1.5	1.2	2.70	19
	2.0	2.0	1.2	4.80	10	2.0	2.0	1.2	4.80	11
	2.5	2.5	1.2	7.50	6	2.5	2.5	1.2	7.50	7
0.75	1.0	1.0	1.2	1.20	57	1.0	1.0	1.2	1.20	64
	1.2	1.2	1.2	1.728	40	1.2	1.2	1.2	1.728	45
	1.5	1.5	1.2	2.70	25	1.5	1.5	1.2	2.70	29
	2.0	2.0	1.2	4.80	14	2.0	2.0	1.2	4.80	16
	2.5	2.5	1.2	7.50	9	2.5	2.5	1.2	7.50	10

Table 10.15: Recharge chamber dimensions for precipitation P = 2259 mm.

α	Recharge chamber dimensions				N_w
	L (m)	B (m)	H (m)	V (m^3)	
0.25	1.0	1.0	1.2	1.20	25
	1.2	1.2	1.2	1.728	17
	1.5	1.5	1.2	2.70	11
	2.0	2.0	1.2	4.80	6
	2.5	2.5	1.2	7.50	4
0.50	1.0	1.0	1.2	1.20	49
	1.2	1.2	1.2	1.728	34
	1.5	1.5	1.2	2.70	22
	2.0	2.0	1.2	4.80	12
	2.5	2.5	1.2	7.50	8
0.75	1.0	1.0	1.2	1.20	73
	1.2	1.2	1.2	1.728	51
	1.5	1.5	1.2	2.70	33
	2.0	2.0	1.2	4.80	18
	2.5	2.5	1.2	7.50	12

10.6 Appropriate Engineering Design

10.6.1 Qanat-well Structure

The recommended values of length, depth of qanat for different values of diameter of qanat at different time period of operation of pumping was estimated by Equation (10.12) and from Figure 10.9, the schedule of pumping operation and diminutions of qanat structures is implemented as follows: t= 3 h, r_q = 125 mm, L_q = 2.5 m, and d = 3.25 m. For future safety provision, two qanat-well structures are recommended for alternative use.

The depth of the qanat below natural ground surface
= depth of qanat from undisturbed groundwater table plus maximum depth of water table from ground surface
= (3.25 + 3) m = 6.25 m

10.6.2 Factor of Safety

The maximum and minimum values of the factor of safety of rainfall recharge versus annual precipitation P for α = 0.25, 0.50 and 0.75 were determined from Figure 10.10 and are presented in Table 10.16.

Table 10.16: Designed safety factors for maximum and minimum rainfall for α= 0.5.

Rainfall	Factor of Safety F	Proposed by
Minimum	1.33	Chaturvedi (1973)
	5.88	Wu and Zhang (1994)
	1.49	Kumar and Seethapathi (2002)
	1.27	MoWR (2009)
Maximum	2.76	Chaturvedi (1973)
	11.23	Wu and Zhang (1994)
	3.47	Kumar and Seethapathi (2002)
	3.17	MoWR (2009)

The suggested value as per Kumar and Seethapathi (2002) is mostly appropriate for Indian situation. The value of factor of safety F under minimum precipitation since previous period of 10 years should not fall below 1.0, consequently acceptable in stipulations of realistic compensation of withdrawal of groundwater. In addition for maximum precipitation since previous 10 years period, the value of factor of safety F exceed 2.0, consequently it is mentioned here that the interface of saline water would push back towards the sea shore. Meanwhile for extreme high value of factor of safety F, sufficient drainage should provided at the site towards nearby watercourse channel.

10.6.3 Area and depth of Percolation Pond

The monsoon precipitation was selected as P_m = 367.1 mm from the Figure 10.11 for the proposed site. The depth of percolation pond is selected as H_p = 3 m. Consequently by means of data from Figure 10.11 the required area of pond A_p is estimated by interpolation. Therefore in the Contai polytechnic college campus four ponds each having 301 m^2 area and 3.0 m depth are constructed for implementation.

10.6.4 Dimensions of Recharge Chamber coupled with Recharge Well

From Figure 10.12, the recharge chamber volume with number of recharge chamber with annual precipitation P= 2259 mm, the maximum precipitation in last ten years, total roof area in the site 12000 m^2, α = 0.5 were designed for application of the classical model. With having dimensions of the recharge chamber as 2 m length, 2 m width and 1.2 m height, total twelve numbers of recharge chambers (N_w =12) coupled with recharge well were designed at the site. As per recommendations of Sarkar (2007), the dimension of installed recharge well like the inner diameter is 100 mm, strainer diameter in the aquifer is 100 mm, strainer length is 12 m, and length of 150 mm strainer is 800 mm. The application the model scheme is enumerated in Figure 10.13 and recharge well is shown in Figure 10.14.

10.7 Aquifer Improvement Plan

Spontaneous and uncontrolled groundwater extraction has brought about bringing down the water levels and thus saline water intrusion in country and urban territories in most pieces of coastal regions of Purba Midnapur. With the expanding populace, the water request in agribusiness, industrial and urban sectors has enlarged manifold in the past decade. Groundwater, which is once thought as the steady source of water, is now no more a reliable source due to faster lowering in water table. The result of which is notable as water shortage. So water preservation and in this manner rainwater harvesting gives an answer for the present emergency. Quick industrialization combined with aimless tapping of groundwater has prompted a consistent decrease in the groundwater table by 10 m here, threatening to transform the zone into a saline-inclined zone within a couple of years if the subsidence of the groundwater level proceeds.

An improvement design of the aquifers of Purba Midnapur area has been prepared [Figure 10.15] in light of depth of the aquifers, status of piezometric surface and characteristics soil nature. In light of these parameters, the study area has been separated into six zones and the proposals for groundwater improvement in every one of these zones are recorded in Table 10.17.

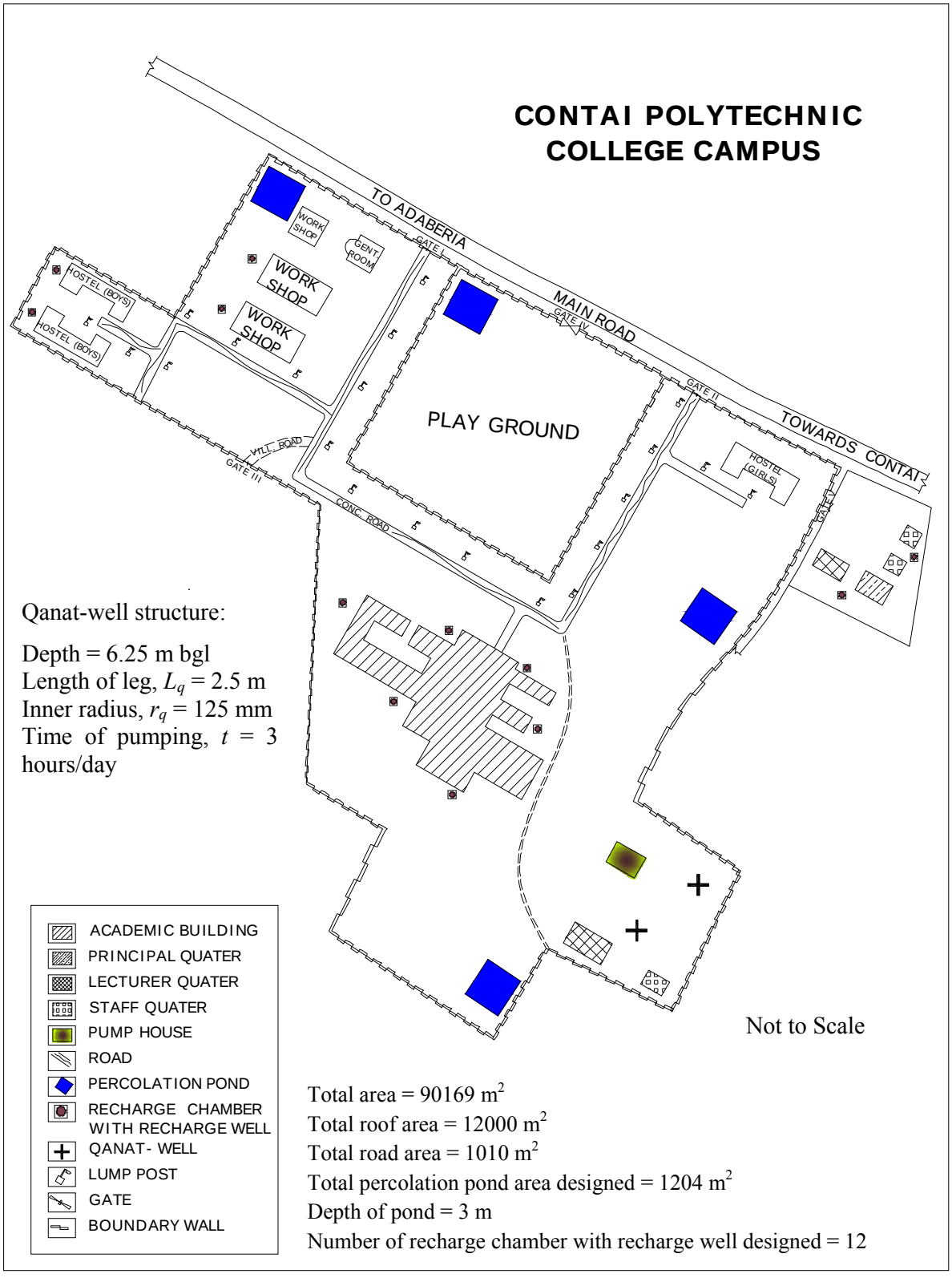

Fig. 10.13: Contai polytechnic college campus area showing location of qanat-well structures, percolation ponds and recharge chambers with recharge well

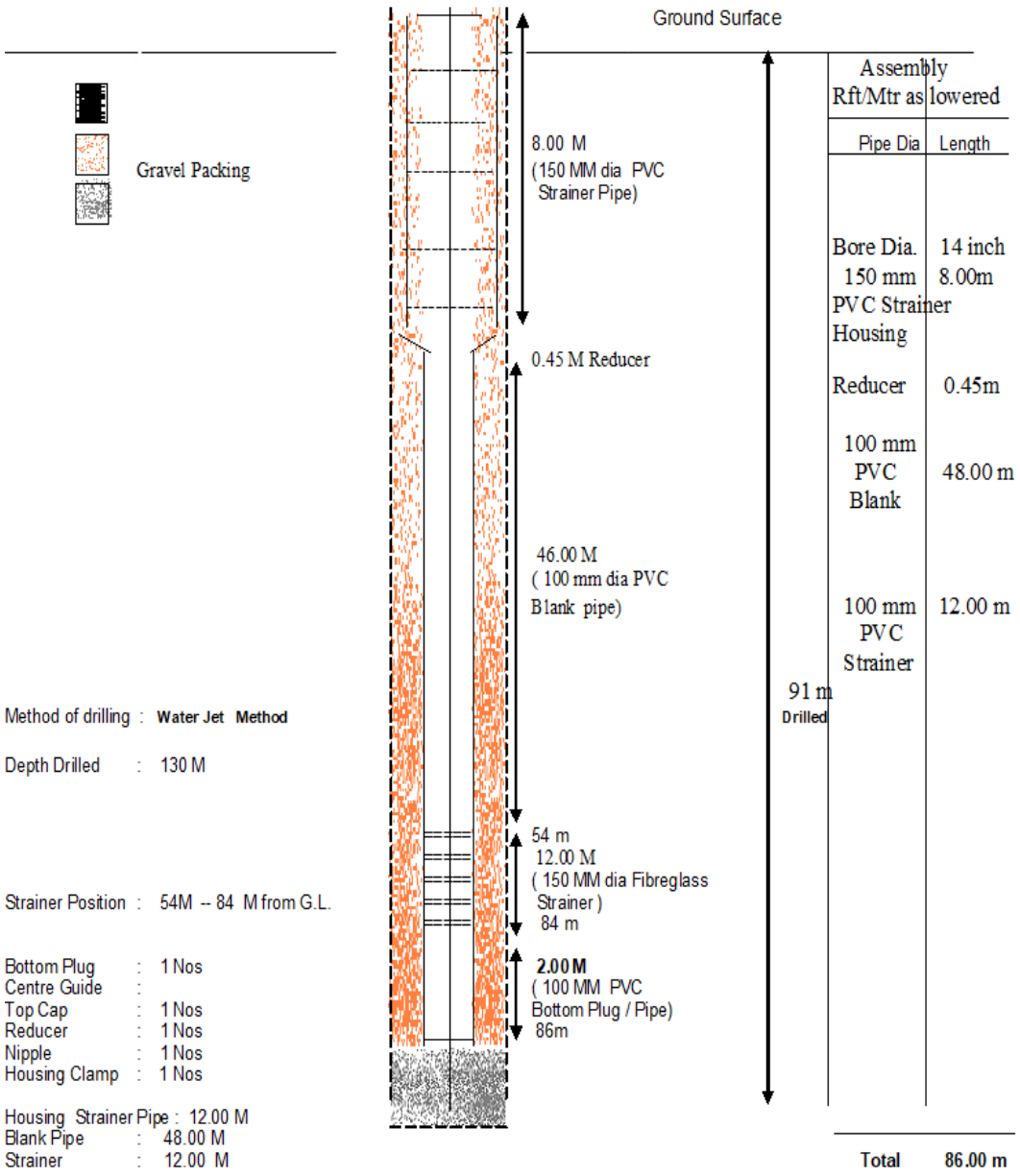

Fig. 10.14: Cross section of recharge well adopted.

Table 10.17: Aquifer improvement plan.

Zone	Depth of aquifer (m)	Status of interface between saline water and freshwater	Predominant soil type	Improvement plan
1	90 – 120	The interface of freshwater and saline water is close to 90 m below ground level (bgl).	Sandy clay to clayey sand	No groundwater extraction, surface water supply system may be used from waterway.
2	100 – 150	The interface of freshwater and saline water is in the vicinity of 87 m bgl.	Sand, medium to coarse, white	No groundwater extraction.
3	160 - 183	Saline water and freshwater interface is near 138 m bgl. Zone upto 90 m contain high salinity content, groundwater while zone upto 138 m contain reasonably less saline water.	very coarse sand	No groundwater extraction in the saline zone [Figure 10.18]. Deep tube well might be introduced outside the saline zone.
4	161 – 185	The granular zone above 60 m contains inferior quality of groundwater.	Medium sand, greyish	No groundwater extraction, it is to be synchronized by reducing tubewell functioning time.
5	205 - 252	Groundwater restricted upto 123 m bgl is inferior in nature and best portion accessible for tapping lies in between 216-249 m bgl and hence.	Fine to medium sand, greyish	Extra tube wells might be introduced for future groundwater extraction.
6	110 – 170	The interface of freshwater and saline water is near 85 m bgl.	Sandy clay to clayey sand	Extra tube wells might be introduced for future groundwater extraction..

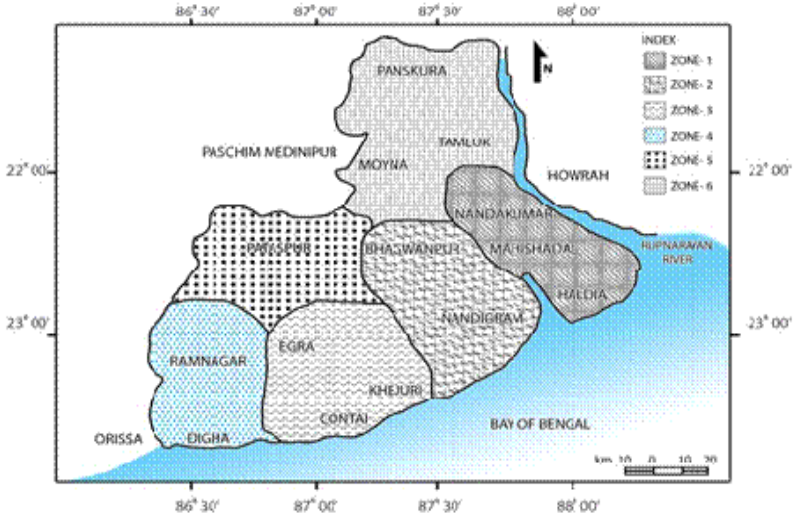

Fig. 10.15: Aquifer improvement plan.

10.8 Using Alternative Freshwater Sources

10.8.1 Background

The coastal groundwater basin in Purba Midnapur is under a genuine threat in respect to groundwater quantity (volume) and quality because of seawater intrusion from Bay of Bengal. In the southern part of Purba Midnapur at Contai sub division there is an acute scarcity of drinking water which are already identified as saline area under Contai-I, Contai-II and Contai-III. The overhead reservoirs for drinking water supply scheme were installed in 1982-1983 in three different places by the Public Health Engineering Department under Government of West Bengal. But it appears from present situation that these projects are now not in position to fulfill the demand of the drinking water for the areas concerned. These schemes are running almost inactively in these areas. As the commanding area of the projects are entirely not based on tubewells in nature, therefore the total safe drinking water is required to be provided in these areas to meet up the acute need of the drinking water for the people of these areas as well as in the various educational institutions, post office, block development office, banks, Integrated Child Development Services, Shishu Shiksha Kendra, Madhyamik Shiksha Kendra, hostels, restaurants, lodge, police stations, industrial factories etc. For better management and supply of sufficient drinking water for the people of the saline zones in contain, *new water supply scheme* should be proposed on very urgent basis at present scenario as an essential purpose.

10.8.2 Proposal for New Water Supply Scheme

A) Contai Saline Zone-III

Contai saline areas under Zone-III of water supply scheme under Contai-I block cover a number of mouzas since the existing scheme was established or constructed in the year of 1982, more than 40 years ago and most of the deep tube wells were out of order due to saline water ingression. Therefore new deep tube wells or new schemes are essential for acute need of the area as an urgent basis for drinking water supply. The followings are the reasons as mentioned below:

- More than 80% people in this area are suffering from inadequate drinking water.
- The area is fully saline and there is no alternative source of water supply.
- More than 60,000 people are dependent on this new water supply (WS) scheme.

The scheme will cover Sabajput and adjoining areas. Underground sources will be available at Gopalpur and Samudrapur near sea dyke under Sabajput Gram Panchayat. Six numbers wells and deep tube wells are required be installed for each zone.

B) Contai Saline Zone-II

Contai saline areas under Zone-II of water supply scheme under Contai-I and Contai -III blocks cover a number of mouzas since the existing scheme was established or constructed in the year of 1982, more than 40 years ago. Most of the deep tube wells are out of order due to saline water ingression and new deep tube wells or new schemes are essential for acute need of the areas as an urgent basis for drinking water supply. The followings are the reasons as mentioned below:

- More than 80% people are suffering from inadequate drinking water.
- The area is fully saline and there is no alternative source of water supply.
- More than 42,000 people are dependent on this new WS scheme.

The scheme will cover Purba Fatepur and adjoining areas. Underground sources are required to be available at Rampur at Nilpur and overhead reservoir will be constructed at Purba Fatepur where eight kilometre long pipeline will be required. Four numbers of deep tube wells will be required for both the zones.

C) Contai Saline Zone-I

Contai saline areas under zone-I of water supply scheme under Contai -III block covers a number of mouzas since the existing scheme was established or constructed in the year 1982. Most of the deep tube wells are out of order due to saline water ingression. Therefore new deep tube wells or schemes are essential for acute need of the areas as an urgent basis for drinking water supply.

The Contai Saline Zone-I covers large area compared to other zones. Therefore two new water supply schemes are essential to meet up the drinking water resources, the construction of overhead reservoir area of the scheme are at Marishada and Daisai as discussed below:

This new scheme should cover Marishda and adjoining areas. Underground sources will be available at Panichiary and an overhead reservoir is needed to be constructed at Marishda where eight kilometre long pipeline will be required. Around four deep tube wells will also be required for this zone.

The scheme will cover Daisai and adjoining area, underground source will be available at Kukraowl and an overhead reservoir is needed to be constructed at Daisai where eight kilometre long pipeline will be required. Around four deep tube wells will also be required for this zone.

10.8.3 Alternative New Source of Water Supply

The drinking water scarcity due to saline water ingression is observed in non-tubewell areas like Sabajput G.P., Raipur G.P., Nayaput G.P. under Contai-I block; Kusumpur G.P., Durmut G.P, Marisda G.P., Kanaidighi G.P. under Contai-III block and Sarda G.P., Chalti G.P., Deshapran G.P. under Contai –II block of Purba Midnapur district. About

158 mouzas are non tube-well zones within three blocks Contai-I, Contai-II and Contai-III including Contai Municipality. There is no source of groundwater supply that is potable water is not available in the saline prone aquifer areas. People of these areas are suffering from acute problems of drinking water since last 25 years. The existing water supply scheme in the saline area of Contai was failed in the year of 1982. Tube-wells have sunk repeatedly and failed due to saline water intrusion.

Groundwater pumping is the primary cause of saltwater intrusion from the coastal sides. It creates hydraulic stresses that reduce freshwater flow in coastal aquifers. The natural flow, small stream channels of the area and river water may be used after proper treatment which eventually will minimise groundwater extraction. Consequently in the aquifers of the areas concern, saline water intrusion will be reduced.

Therefore a new water supply scheme is proposed and is very much essential to meet up the demand of water in the area concern.

The Subarnarekha River basin map is shown in Figure 10.16. Subarnarekha River passes through Dantan –I block in Paschim Midnapur. The intake well point may be selected at Dantan nearby National Highway No. 60. After implementation of the proposed scheme, near about three lakhs people will be benefitted.

The width of Subarnarekha River at Dantan intake Point and proposed line plan of drinking water supply scheme and treatment project have been given in Figures 10.17 and 10.18, respectively. It may solve the drinking water problem of the area concern.

Fig. 10.16: Subarnarekha River basin.

Fig. 10.17: Subarnarerkha River width at Dantan intake point in Paschim Midnapur.

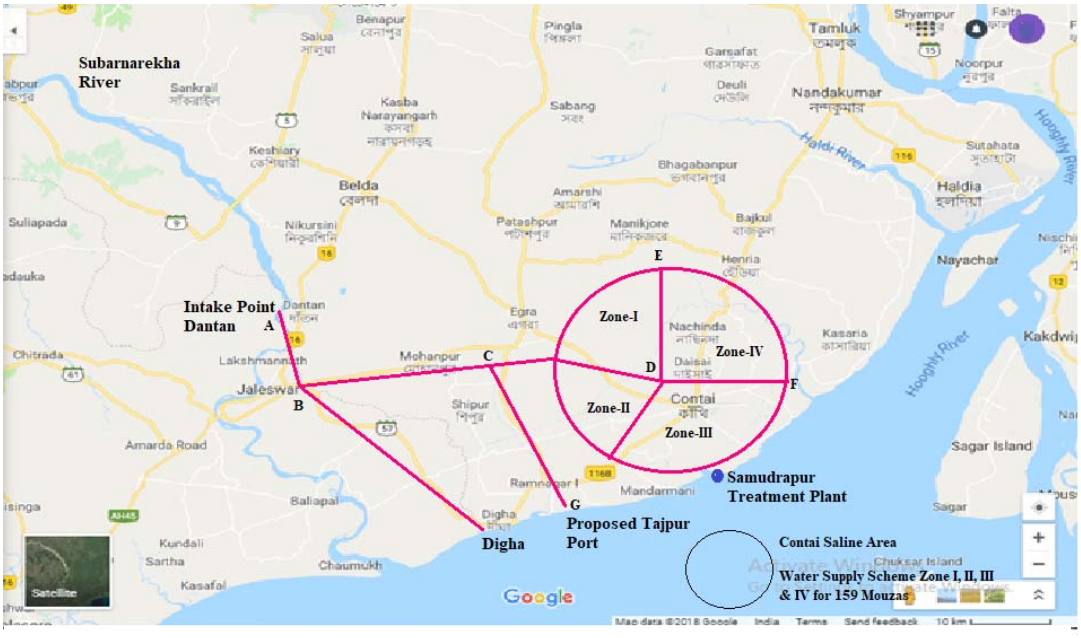

Proposed length of water line: AB- 12 km, BC-14 km, CD-27 km, DE-10 km, DF-10 km and CG-40 km

Fig. 10.18: Proposed water treatment scheme and drinking water supply for southern part of Purba Midnapur.

10.9 References

Abd-Elhamid, H.F. and Javidi, A.A. (2011). A cost-effective method to control seawater intrusion in coastal aquifers. *Water Resource Management*, Vol. 25, Iss. 11, pp. 2755–2780.

Ball, D.F. and Herbert, R. (1992). The use and performance of collector wells within the regolith aquifer of Sri Lanka. *Groundwater*, Vol. 30, No. 5, pp. 683–688.

Beljin, M.S. and Losonsky, G. (1992). HWELL: A horizontal well model. In Solving Groundwater Problems with Models. International Groundwater Modeling Center and the Association of Groundwater Scientists and Engineers, Colorado, USA, pp. 45–54.

Bennett, G.D., Mundorff, M.J., and Hussain, S.A. (1968). Electric Analog Studies of Brine Coning beneath Fresh water Wells in the Punjab Region, West Pakistan. *Geological Survey Water Supply Paper,* 1608-J, Vol. 1, pp. 121-126.

Chandra, P.C. (2005). Geophysical Investigation for Groundwater in Coastal Tracts. *Jalvigyan Sameeksha,* Vol. 20, pp. 1–14.

Chaturvedi, R.S. (1973). A Note on the Investigation of Groundwater Resources in Western Districts of Uttar Pradesh. Annual Report, U.P. Irrigation Research Institute, Uttar Pradesh, India, pp. 86–122.

Dagan, G. and Bear, J. (1968). Solving the problem of local interface upconing in a coastal aquifer by the method of small perturbations. *Journal of Hydraulic Research*, Vol. 6, Iss. 1, pp. 15–44.

Dasgupta, A. and Gaikwad V.P. (1987). Interface Upconing Due to a Horizontal Well in unconfined Aquifer. *Groundwater,* Vol. 25, No. 4, pp. 466-474.

Haitjema, H., Kuzin, S., Kelson, V. and Abrams, D. (2010). Modeling flow into horizontal wells in a Dupuit–Forchheimer model. *Groundwater*, Vol. 48, No. 6, pp. 878–883.

Hantush, M.S. and Papadapulos, I.S. (1962). Flow of ground water to collector wells. *Journal of the Hydraulics Division*, Vol. 88, Iss. 5, pp. 221–244.

Javadi, A.A., Hussain, M.S. and Sherif, M.M. (2013). Optimal control of seawater intrusion in coastal aquifers. International Conference on Computational Mechanics (CM13), 25-27 March 2013, Durham, UK, India.

Joshi, S.D. (1986). Augmentation of well productivity using slant and horizontal wells. Proceedings of 61st Annual Technical Conference and Exhibition Society of Petroleum Engineers, New Orleans, LA, USA, Paper SPE 15375.

Karanth, K.R. (1987). Groundwater Assessment Development and Management. Tata McGraw-Hill, New Delhi, India.

Kumar, C.P. and Seethapathi, P.V. (2002). Assessment of natural ground water recharge in Upper Ganga Canal command area. *Journal of Applied Hydrology*, Vol. 15, No. 4, pp. 13–20.

Linsley, R.K., Kohler, M.A. and Paulhus, J.L.H. (1982). Hydrology for Engineers. McGraw-Hill, New York, USA.

Motz, L.H. (1992). Salt water Upconing in an Aquifer Overlain by a Leaky Confining Bed. *Groundwater,* Vol. 30, No. 2, pp. 192-198.

MoWR (2009). Ground Water Resource Estimation Methodology. Report of the Ground Water Resource Estimation Committee. Ministry of Water Resources, New Delhi, India.

Muskat, M. and Wyckoff, R.D. (1935). An Approximate Theory of Water Coning in Oil Production. *Transactions of the AIME*, Vol. 114, Iss. 1, pp. 144-163.

Muskat, M. (1937). Flow of Homogeneous Fluids Through Porous Media. University of Michigan, McGraw-Hill, New York, USA.

O'Hare, M.P., Fairchild, D.M., Hajali, P.A., Canter, L.W. (1986). Artificial Recharge of Groundwater: Status and Potential in the Contiguous United States. Environmental and Groundwater Institute, University of Oklahoma, Lewis Publishers, Chelsea, MI, United Kingdom.

Patra, M.N. (2010). Localised and Generalised Subsidence and Swelling of the Ground Surface due to Change in Groundwater Piezometric Level with a Special Reference to Calcutta. PhD Thesis, Bengal Engineering and Science University, Howrah, India.

Raghubabu, M., Prasad, B.R. and Srikanth, I. (2004). Subsurface Skimming Techniques for Coastal Sandy Soils. AICRP Saline Water Scheme. Bapatla, Andhra Pradesh, India, Bulletin 1/04.

Raghunath, H.M. (1987). Ground Water. 2nd Edition, New Age International, New Delhi, India.

Sarkar, A.K. (2007). Project Report on the Design of Rainwater Harvesting Scheme for Water Conservation for Fire Fighting and Others and Artificial Recharge to Groundwater at TCS Main Building Campus, Salt Lake, Kolkata. Water Harvesting Solutions, Kolkata, India.

Sawyer, C.S. and Lieuallen-Dulam, K.K. (1998). Productivity comparison of horizontal and vertical ground water remediation well scenarios. *Groundwater*, Vol. 36, No. 1, pp. 98-103.

Todd, D.K. (1995). Groundwater Hydrology. Second Edition, Wiley, New York, USA.

UNDP Report (2006). United Nations Human Development Report. Beyond Scarcity: Power, Poverty and Global Water Crisis. United Nations Development Programme, New York, USA.

Venkataramana, R. (2016). Identify the Feasible Shallow Aquifer Zones in Coastal Sands in Part of Krishna Western Delta Region of A.P.. *International Journal of Applied Environmental Sciences*, Vol. 11, No. 2, pp. 535-540.

WHO (2010). World Health Organization. Progress on Sanitation and Drinking Water – 2010 Update. WHO/ UNICEF Joint Monitoring Programme for Water Supply and Sanitation, Geneva, Switzerland.

Wu, J. and Zhang, R. (1994). Analysis of rainfall infiltration recharge to groundwater. Proceedings of 14th Annual American Geophysical Union: Hydrology Days, CO, USA, pp. 420–430.

Yasin, M., Asghar, M.N., Alam, M.M., Akbar, G. and Khan, Z. (2004). Methodology for site selection to introduce skimming well source pressurized irrigation systems. In Asghar, M.N., Yasin, M., Alam, M.M. and Qureshi, A.S. (Eds.). Root zone salinity management using fractional skimming wells with pressurized Irrigation: Proceedings of the Project-End Workshop 2003. Lahore, Pakistan: IWMI. pp. 1-13.

CHAPTER - 11

(Summary and Conclusions)

- Summary
- Conclusions
- Limitations and Future Scopes`
- References

11.1 Summary

Saline water intrusion into fresh groundwater aquifers takes place in the vicinity of coastal regions whenever seawater displaces or mixes with freshwater. This circumstance happens in coastal areas having hydraulic connection with the ocean. Seawater intrusion into freshwater coastal aquifers is likely to cause serious problems if only such aquifer is tapped for domestic water supply or for irrigation. In order to increase the protectiveness of sustainable freshwater from coastal salinity, the proper mechanism regarding generation of salinity should be understood thoroughly.

The coastal area of Purba Midnapur district in West Bengal is influenced by saline water ingression. Arsenic is absent in the coastal tracts. Saline water intrusion in the coastal aquifers is intense and causing problems, particularly at those areas which are very fertile and there is intensive cultivation as well. For these reasons an extensive study and research on meteorology, geomorphology and geology of the coastal areas of Purba Midnapur district has been conducted.

Previous literatures were reviewed on a global basis and due emphasis was given to Indian publications. The significant contributions have been recapitulated as theoretical contribution, laboratory-based experimental works and field-based studies. Some analyses in light of the interrelations of two miscible liquids in permeable media have been directed both hypothetically and under field conditions. Amongst significant contributions in the relevant area of investigation, the works of Wang (1965), Bennett *et al.* (1968), Li and Yeh (1968), Goswami (1968), Pinder and Cooper (1970), Fetter (1972), Mughal and Awan (1977), Gupta and Gaikwad (1987), Reilly and Goodman (1987), Fand *et al.* (1987), Schincariol and Schwartz (1990), Motz (1992), Kececioglu and Jiang (1994), Xue *et al.* (1995), Mahesha (2001), Barlow (2003), Raghubabu *et al.* (2004), Chandra (2005), Chachadi (2005), Papadopoulou *et al.* (2005), Mohan and Pramada (2005), Gallardo and Marui (2007), Abd-Elhamid and Javadi (2008), Mahesha (2009), Werner and Simmons (2009), Olufemi *et al.* (2010), Bianchi *et al.* (2011), Sherif *et al.* (2012), Ayolabi *et al.* (2013), Das *et al.* (2014), Sahu (2014), Adedotun *et al.* (2015), Grundmann *et al.* (2016), Toste *et al.* (2017) and Alfarrah and Walraevens (2018) have been found to be worthy of note.

Several methods of controlling saline water intrusion and managing groundwater exploitation in the coastal areas have been suggested in this research. These proposed methods equally suggest the need of further studies and researches that can lead to sustainable use and management of groundwater resources in coastal areas.

A few studies on saline water ingression and hydrogeology had been done on the Indian coasts and a few different areas. These studies are based on the hypothetical and realistic assumptions. These assumptions have been utilized for investigating the collecting information from boreholes located in the coastal areas of Purba Midnapur.

Horizontal infiltration galleries called qanat coupled with vertical risers are presented in this thesis as a viable solution to the problem of upconing below deep vertical wells. As the analysis and design presented in this thesis has shown, vertical

wells may not be attainable in a few circumstances and qanat combined with vertical risers can be effectively utilized as a part of such cases.

The laboratory work is aimed towards conducting a thorough experimental and theoretical analysis regarding linear and non-linear flow of sodium chloride solution through granular porous medium, preferably well graded sand. Firstly, variation of specific gravity and viscosity of sodium chloride solution with saline concentration at different temperatures are found out by standard laboratory tests. The experiments regarding variation of kinematic viscosity of sodium chloride solutions for different saline concentration at different temperatures and variation of density for the same saline concentration have been conducted and the relevant curves have been plotted. It is observed from the graph that the viscosity decreases with the temperature and increases with saline concentration. Similarly the density increases with the increase in saline concentration.

Experimental results showing the variation of hydraulic conductivity with the percentage of saturated salinity concentration indicates that hydraulic conductivity decreases sharply with the increase in percentage of saturated salinity concentration upto 50%, afterwards it approaches stabilization. Variation of hydraulic conductivity with time confirms that hydraulic conductivity decreases as the period of submergence in different concentration of sodium chloride solution increases, but the rate of decrease of hydraulic conductivity is quite slow for the samples, which were submerged in sodium chloride solutions for more than three days.

The phreatic lines of saline water intrusion and the interfaces of freshwater recharge are observed to be of irregular pattern. In case of saline water intrusion, the phreatic line at any time instance slopes down from the inlet end with a sudden change in slope at a normalized distance of 0.3 m to 0.5 m. With the advent of time, the phreatic line translates gradually further towards the downstream. For freshwater recharge, the interface gradually slopes towards the downstream end in advent of time. The time variation of normalized *y*-coordinates of the interface at different locations, although of irregular pattern, the slopes are observed to be sufficiently small.

From model tests, the friction factor and Reynolds number for Darcy's and Forchheimer's flow have been studied, the Reynolds number increases with the decrease of the friction factor. And also from the plotted curves for modified Reynolds number versus modified friction factor, it can be said that, modified friction factor and modified Reynolds number change inversely proportional way.

The three tier aquifer system down to the depth of about 300 m has been observed in Purba Midnapur coastal belt. The aquifer at depth below 100 m occurs under phreatic condition and middle aquifer at depth below 155 m and deeper aquifer at depth above 165 m are in semi-confined/confined conditions with increasing depth. Away from the coast but within the saline tract Marisda, Contai, Nilpur, Chandipur and Nandigram saline groundwater is observed mainly as isolated pockets at different depths. It is observed that the upper soil horizon of Purba Midnapur is of quaternary foundation and comprises of rotating stores of clay and sand of marine starting point. Likewise with every marine deposit, rounded grains and high porosity are predominant attributes. The northern part of the area comprises of a mixture of alluvial and marine deposits. In

addition, there is a great spatial heterogeneity in the aquifer, which makes any predictive method for estimating the depth of saline water ingression futile.

For the year 2014 and 2015, the pre-monsoon piezometric surface contours confirm the occurring of drawdown close to Ramnagar, Bhagbanpur and Sutahata. In the predominant climatic situation in this region, the pre- monsoon condition is far more significant compared to the post-monsoon condition. Accordingly, assessment of the potential for salinisation is completed considering the pre-monsoon position. It is evident that the Ramnagar zone which incorporates the tourist resort of Digha and the town of Contai, is profoundly inclined to saline water ingression just like the Sutahata territory which incorporates the modern town of Haldia. Prompt and imperative measures are expected to push back saline water intrusion in these areas.

The Visual MODFLOW software has been utilized to analyze the groundwater level changes in Purba Midnapur. The data of pumping well discharge was collected for two different years 2002 and 2012 from Public Health Engineering Directorate under Government of West Bengal. The simulated data for the year 2012 based on the measured data in 2002, 2012 and combined data of 2002 & 2012 have been compared and subsequent correlation coefficients are found out to signify data validity. Also simulated groundwater level data for the period 2019 to 2023 based on well discharge data of 2002 and 2012 have been correlated for its justification. The groundwater flow occurs from south to north direction of Purba Midnapur as the saline water intrusion from the Bay of Bengal takes place into the aquifers towards inland direction. The simulated groundwater level data for future are in good agreement with this proclamation. In the real field situation saline water encroachments have affected the aquifers and it has covered up to 50 km of location from Kalindi (near sea shore) to Nandakumar (inland) location. This work focuses the future groundwater levels prediction in potential groundwater management scenarios in the region concern.

The results of the chemical analysis show that the chloride (Cl^-) concentration in this area is highly erratic. Given that, the only source of chloride is the sea (due to the absence of chloride bearing rocks in the area); the chloride concentration may be attributed to a balance between the freshwater and the intruded seawater locally. The physico-chemical studies involve pH value, specific conductivity, total hardness, anions (HCO_3^- , Cl^-, $CO_3^=$) and iron. The test results of these properties have been compared with the drinking water standards set up by the World Health Organisation.

A new technique for controlling saltwater ingression into the coastal aquifers has been proposed. This new strategy comprises of withdrawal by qanat well structures with realistic compensation by rain water harvesting by methods for recharging ponds and recharging well. A remarkable highlight of this strategy is depicted by considering an outline case presented at the Contai Polytechnic Institute Campus in Purba Midnapur district.

Aquifer improvement plan of Purba Midnapur has been demarcated by indicating six zones based on aquifer soil characteristics and significance of piezometric surface and imposing certain restriction of abstraction of groundwater by deep tubewells in the

zones concern. It will help in recharging the aquifer, defeating the danger of saline water intrusion and enhancing the nature of groundwater quality.

Other arrangement to mitigate future freshwater demand in this zone by utilizing elective freshwater sources will be empowered. From the existing small rivers of Rupnarayan, River Subarnarekha in Purba Midnapur water can be collected and circulated for the different purposes after appropriate treatment.

11.2 Conclusions

From the entire investigation, the following significant conclusions are drawn:

- Concerning to the formulations developed for safe yield of vertical well considering upconing in coastal regions, it may be concluded that the well discharge initially increases with freshwater head above mean sea level following a fairly parabolic pattern. Also, at zero discharge, the variation of the depth of well with the freshwater head above mean sea level follows parabolic pattern.

- From the observations made based on the results obtained from the laboratory experiments with falling head permeameter, in case of flow of sodium chloride solution through sand, it may be concluded that the hydraulic conductivity decreases with saline concentration as well as with period of submergence. The time rate of decrease of hydraulic conductivity is sharp when the saline concentration lies in the range of 0-40% and gradually stabilises thereafter. Also, this rate of reduction is high enough when the period of submergence lies in the range of 0-4 days with a gradual stabilisation thereafter.

- The phreatic lines of saline water intrusion and the interfaces in freshwater recharge are observed to be of irregular pattern. In case of saline water intrusion, the phreatic line at any time instance slopes down from the inlet end with a sudden change in slope at a normalized distance of 0.3 m to 0.5 m. With the advent of time, the phreatic line shifts gradually further towards the downstream. The time variation of normalized *y*-coordinates of the interface at different locations, although of irregular pattern, the slopes are observed to be sufficiently small. More importantly, significant diffusion between fluids of two different densities is observed to take place indicating absence of any sharp interface at mixing zone.

- The depth to piezometric surface is within 8 m below ground level. Due to large scale withdrawal of groundwater in Sutahata, Mahishadal and Haldia sectors - drawdown of piezometric head in the tune of 1.6 m over the last ten years has been noted. In the southwest part of Contai town, the groundwater table is found interfering with the sand dunes overlying the upper clay blanket. Underlying this fresh unconfined groundwater is saline down to 235 m depth with chloride concentration upto 17,000 ppm.

- The coastal zone of Purba Midnapur by its own particular prudence has high geologic heterogeneity. The soil of low hydraulic conductivity is interspersed with soil of high hydraulic conductivity in an almost random manner. The pattern of variation of salinity concentration is heterogeneous in three dimensional spaces. Some inland areas, for example, Sharkhanchak, Kalindi and Betkundu are found as more prominent saline prone areas than comparing seaside regions because of entrance of saline water through the preferential path. The investigation finds that the interface of saline water ingression is dynamically moving inwards towards the zones of Nachinda, Contai, Mukutshila and Haldia.

- During calibration and validation phases, the data of pumping well discharge and other data measured in the year 2002 have been simulated for groundwater level in the year 2012 and it has been compared with the actual field data measured in 2012. The correlation coefficients between these two groundwater levels are found 0.56. It shows a moderate calibration.

- A comparison have been made between simulated groundwater levels for the years 2019 and 2023 based on the pumping well discharge data obtained for the years 2002 and 2012. The correlation coefficients between the observed and simulated groundwater levels are found in the range of 0.81-0.84. It indicates that the predicted groundwater levels for the years 2019 to 2023 for both the cases are closely matching with good accuracy. So the groundwater levels at different locations of study area for the years 2019 to 2023 have been predicted accurately without actually measuring them.

- The comparison between simulated groundwater levels for the years 2019 to 2023 for the pumping well discharge data observed in the year of 2002 and combined data of 2002 and 2012 have been made. And in another comparison, the simulated groundwater levels for the years 2019 to 2023 using pumping well discharge data measured in 2012 and combined data of 2002 & 2012 has been estimated. The correlation coefficients are determined for both the cases which show that the simulated groundwater levels moderately match; the correlation coefficient values also confirm that the model calibration is moderate.

- Since the measured well discharge data in the year 2012 were sufficient and simulation of groundwater level of study area in the year 2019 to 2023 are based on the pumping well discharge data of the year 2012, hence it can be concluded that the future prediction of groundwater level in this scenario is more realistic.

- The groundwater levels are found decreasing using simulation technique for the years 2019 to 2023 with an average groundwater level of 13.4 m in southern part of Purba Midnapur to 15.7 m in northern part of Purba Midnapur. Therefore the groundwater levels in coastal part of Purba Midnapur are actually decreasing. It was observed so as few places of study area are becoming water scarce during pre-monsoon period.

The average groundwater level in southern part of Purba Midnapur is high compared to the average groundwater level in northern part of Purba Midnapur. So seawater intrusion is taking place towards inland of Purba Midnapur from Bay of Bengal which is from the south direction of Purba Midnapur. So it is making the groundwater saline day-by-day.

- The investigation demonstrates that the artificial recharge by rainwater harvesting through percolation pond, injection well and improvement of pumping area will likewise help in diminishing the saline water ingression in the zone of Heria, Bajkul, Tamluk, Sutahata and Mahishadal.

- A new technique has been introduced for coastal zone groundwater management which includes withdrawal of groundwater by qanat well structures related with identical counterfeit recharge by rainwater harvesting through percolation pond and recharge well. In the event that sufficiently connected and plan the proposed system is relied upon to be very helpful and advantageous, for unconfined state of the coastal aquifers.

- As the proposed strategy has been implemented at coastal site situated in Purba Midnapur distrcit to examine the different quantitative aspects of the technique, it was observed that depth of qanat d decreases following a curvilinear pattern with the length of the qanat leg L_q. The variation of qanat leg length is quite sharp and is in the range of 1-3 m. It also follows a linear pattern when the length of the qanat leg is more than 3 m.

- The factor of safety for rainwater recharge in the chosen area increases directly with increase in annual precipitation. The curves relevant to the formulae of Chaturvedi (1973), Kumar and Seethapathi (2002) and MoWR (2009) almost coincide. Both the magnitudes and slopes of the curves following Wu and Zhang (1994) are significantly higher. For Indian conditions, the results obtained using the correlation of MoWR (2009) are most reliable. The proposed method is best suitable when the estimation of the factor of safety is marginally higher than unity.

- The required area of recharge pond diminishes in a hyperbolic way with the depth of pond to be excavated.

- The number of recharge chambers (N_w) decreases almost exponentially with the volume of the recharge chambers (V_w). The rate of decrease N_w is pronounced in the range of $V_w < 5$, beyond which a stabilizing tendency is noted.

- It is hereby mentioned that the suggested model is site specific. Effective application of this type of technique will be feasible when the design parameters are satisfactorily decided for the specific site under consideration.

- Aquifer improvement plan, thus, will help in recharging the aquifer, conquering the risk of saline water intrusion and enhancing the nature of groundwater quality. The examination additionally reveals that only in limited confined areas of Purba Midnapur, groundwater might be securely extracted. Therefore, to ensure steady water supply for the growing population in a sustainable manner, the regional water supply authority should look for alternative resources.

- The periodical increment in limit to the surface water (Rupnarayan, Rasulpur and Haldi Rivers) supply framework; aquifer artificial recharge, rainwater harvesting, in the monsoon season aggregated water from the current waterways of Purba Midnapur are gathered and circulated to the different sectors after legitimate treatment.

- The change in task and shielding of the water supply framework and decrease in wastage of water through spillage and unlawful tapping, desalination plant and underground storage reservoirs are the permanent and unique solutions for the concerned coastal area.

11.3 Limitations and Future Scopes

The present research has been carried out largely keeping in view of the situation like seawater intrusion in Purba Midnapur district of West Bengal. Some of the limitations and scopes for further investigations in future are briefly narrated below:

- Field conditions in the study are actually heterogeneous but saline water intrusion modelling has been done with the simplified idealization of homogeneous aquifer. Better results are expected if heterogeneity is considered in modeling.

- Sharp interface between saline water and freshwater has been assumed during the mathematical analysis in this research. In actual practice there exists a brackish water zone. More accurate results may be obtained in future by taking into account of the mixing zone between saline water and freshwater more precisely during the mathematical analysis.

- Due to *limitation of funding*, digging of bore holes for research purpose in the study area was unfeasible. Therefore the secondary groundwater levels from the boreholes of the deep tubewells monitored by the Public Heath Engineering Directorate under Government of West Bengal were rendered for this study.

- More investigation is needed for detailed analytical or numerical study on the performance on the qanat well structure in coastal environment followed by experimental validation.

- A detailed analysis on the freshwater recharge into coastal aquifer is expected to improve the control methodology as suggested in this thesis.

- The software Visual MODFLOW can be used for predicting groundwater levels, flow and flow directions. Using this software the relationship between the inflow and outflow can also be determined in such a way so that how much inflow can affect outflow. By using this software, groundwater management strategies may also be taken care off. MODPATH software is also incorporated in Visual MODFLOW software which may help to identify flow path of groundwater in Purba Midnapur and also in other areas. Three-dimensional method-of-characteristics groundwater flow and transport model integrated with MODFLOW (MOC3D) may also be incorporated to determine the solute concentration in groundwater in future.

11.4 References

Abd-Elhamid, H.F. and Javadi, A.A. (2008). Mathematical Model to Control Saltwater Intrusion in Coastal aquifers. Proceeding of Geo-Congress, New Orleans, Louisiana, USA.

Adedotun, I.A., Gregory, O.O. and A.A. Obasanmi (2015). Hydrochemical Investigation of Saline Water Intrusion into Aquifers in Part of Eastern Dahomey Basin, Southwestern Nigeria. *Journal of Environment and Earth Science*, Vol. 5, No.11, pp. 138-153.

Ayolabi, E.A., Folorunso, A.F., Odukoya, A.M. and Adeniran, A.E. (2013). Mapping saline water intrusion into the coastal aquifer with geophysical and geochemical techniques: The University of Lagos campus case (Nigeria). *SpringerPlus*, Vol. 2, No. 433, pp. 1-14.

Alfarrah, N. and WalraevensI K. (2018). Groundwater Overexploitation and Seawater Intrusion in Coastal Areas of Arid and Semi-Arid Regions. *Water*, Vol. 10, No. 2, pp. 1-24.

Barlow, P.M. (2003). Ground Water in Freshwater-Saltwater Environments of the Atlantic Coast. Circular 1262, U.S. Geological Survey, Reston, Virginia, USA.

Bennett, G.D., Mundorff, M.J. and Hussain, S.A. (1968). Electric Analog Studies of Brine Coning Beneath Fresh water Wells in the Punjab Region, West Pakistan. *Geological Survey Water Supply*, Paper 1608-J, Vol.1, pp 121-126.

Bianchi, S., Nocchi, M. and Salleolini, M. (2011). Hydrogeological investigations in southern Tuscany (Italy) for coastal aquifer management. *AQUA mundi*, Am03028: pp. 53 –70.

Chachadi, A.G. (2005). Seawater Intrusion Mapping Using Modified GALDIT Indicator Model-a Case Study in Goa. *Jalvigyan Sameeksha*, Vol. 20, pp. 1-14.

Chandra, P.C. (2005). Geophysical Investigation for Groundwater in Coastal Tracts. *Jalvigyan Sameeksha*, Vol. 20, pp. 1-14.

Chaturvedi, R.S. (1973). A Note on the Investigation of Groundwater Resources in Western Districts of Uttar Pradesh. U.P. Irrigation Research Institute, Uttar Pradesh, India, pp. 86–122.

Gupta, A.D. and Gaikwad V.P. (1987). Interface Upconing Due to a Horizontal Well in Unconfined Aquifer. *Groundwater*, Vol. 25, No. 4, pp. 466-474.

Das, S., Nayek, M., Das, S., Dutta, P. and Mazumdar, A. (2014). Impact on Water Quality in Piyali River, Sundarbans, India due to Saline Water Intrusion. *Indian Journal of Environmental Protection*, Vol. 34, No. 12, pp. 1010-1019.

Fand, R.M., Kim, B.Y.K., Lam, A.C.C. and Phan, R.T. (1987). Resistance to the Flow of Fluids through Simple and Complex Porous Media Whose Matrices are Composed of Randomly Packed Spheres. *Journal of Fluids Engineering*, Vol. 109, No. 3, pp. 268-273.

Fetter, C.W.Jr. (1972). Position of Saline Interface Beneath Oceanic Islands. *Water Resources Research*, Vol. 8, Iss. 5, pp. 1307-1315.

Gallardo, A.H. and Marui, A. (2007). Modeling the Dynamics of the Freshwater-Saltwater Interface in Response to Construction Activities at a Coastal Site. *International Journal of Environmental Science & Technology*, Vol. 4, Iss. 3, pp. 285-294.

Grundmann, J., Al-Khatri, A. and Schütze, N. (2016). Managing saltwater intrusion in coastal arid regions and its societal implications for agriculture. Proceedings of the International Association of Hydrological Sciences, Vol. 373, pp. 31–35.

Goswami, A.B. (1968). A Study of Salt Water Encroachment in the Coastal Aquifer at Digha, Midnapore District, West Bengal, India. *Bulletin, International Association of Scientific Hydrology*, Vol. 13, No. 3, pp. 77-87.

Kececioglu, I. and Jiang, Y. (1994). Flow through Porous Media of Packed Spheres Saturated With Water. *Journal of Fluids Engineering*, Vol. 116, No. 1, pp. 164-170.

Kumar, C.P. and Seethapathi, P.V. (2002). Assessment of natural ground water recharge in Upper Ganga Canal command area. *Journal of Applied Hydrology*, Vol. 15, No. 4, pp. 13–20.

Li, W.H. and Yeh, G.T. (1968). Dispersion at the Interface of Miscible Liquids in a Soil. *Journal of Water Resources Research*, Vol. 4, No. 2, pp. 369-377.

Mahesha. A. (2001). Effect of Strip Recharge on Sea Water Intrusion into Aquifers. *Hydrological Sciences Journal*, Vol. 46, No. 2, pp.199-210.

Mahesha, A. (2009). Conceptual Model for the Safe Withdrawal of Freshwater from Coastal Aquifers. *Journal of Environmental Engineering*, Vol. 135, No. 10, pp. 980–988.

Mohan, S. and Pramada, S.K. (2005). Management of South Chennai Coastal Aquifer System-A Multi Objective Approach. *Jalvigyan Sameeksha*, Vol. 20, pp. 1-14.

Motz, L.H. (1992). Salt-Water Upconing in an Aquifer Overlain by a Leaky Confining Bed. *Groundwater*, Vol. 30, No. 2, pp. 192-198.

MoWR (2009). Ground Water Resource Estimation Methodology. Report of the Ground Water Resource Estimation Committee. Ministry of Water Resources, New Delhi, India.

Mughal, I. and Awan, N.M. (1977). Upconing of Salt Fresh water Interface Beneath Wells in Fresh Water Zones. CEWRE Publication, 005.

Olufemi, A.G., Utieyin, O.O. and Adebayo, O.M. (2010). Assessment of groundwater quality and saline intrusions in coastal aquifers of Lagos Metropolis, Nigeria. *Journal of Water Resource and Protection*, Vol. 2, No. 10, pp. 849-853.

Papadopoulou, M.P., Karatzas, G.P., Koukadaki, M. A. and Trichakis, Y. (2005). Modeling the Saltwater Intrusion Phenomenon in Coastal Aquifers - A Case Study in the Industrial Zone of Herakleio in Crete. *Global Nest Journal*, Vol. 7, No. 2, pp. 197-203.

Pinder, G.F. and Cooper, H.H. (1970). A Numerical Technique for calculating the Transient Position of Salt Water Front. *Water Resources Research*, Vol. 6, Iss. 3, pp. 875-882.

Raghubabu M., Prasad, B.R. and Srikanth, I. (2004). Subsurface Skimming Techniques for Coastal Sandy Soils. Bulletin No. 1/04, AICRP Saline Water Scheme, Bapatla, AP, India, p. 18.

Reilly, T.E. and Goodman, A.E. (1987). Analysis of saltwater upconing beneath a pumping well. *Journal of Hydrology*, Vol. 89, Iss. 3-4, pp. 169-204.

Sahu, A. (2014). Status of Soil in Purba Medinipur District, West Bengal– A *Review*. *Indian Journal of Geography and Environment*, Vol. 13, pp. 121-126.

Schincariol, R.A. and Schwartz, F.W. (1990). An Experimental Investigation of Variable Density Flow and Mixing in Homogeneous and Heterogeneous Media. *Water Resources Research*, Vol.26, Iss. 10, pp. 2317-2329.

Sherif, M., Kacimov, A., Javadi, A. and Ebraheem, A.A. (2012). Modeling Groundwater Flow and Seawater Intrusion in the Coastal Aquifer of Wadi Ham, UAE. *Water Resources Management*, Vol. 26, Iss. 3, pp. 751–774.

Toste. R., Rosman, P.C.C. and Freitas, D.A.V. (2017). Saline Intrusion Response to Sea Level Rise and Its Implications on Water and Coastal Management: A Case Study in Brazil. *Journal of Water Resource and Protection*, Vol. 9, No. 5, pp. 510-522.

Werner, A.D. and Simmons C.T. (2009). Impact of Sea-Level Rise on Sea Water Intrusion in Coastal Aquifers. *Groundwater*, Vol. 47, No. 2, pp. 197-204.

Wang, F.C., (1965). Approximate Theory for Skimming Well Formulation in the Indus Plain of West Pakistan. *Journal of Geophysical Research*, Vol. 70, No. 20, pp. 5055-5063.

Wu, J. and Zhang, R. (1994). Analysis of rainfall infiltration recharge to groundwater. Proceedings of 14th Annual American Geophysical Union: Hydrology Days, CO, USA, pp. 420–430.

Xue, Y., Xie, C. and Wu, J. (1995). A Three Dimensional Miscible Transport Model for Seawater Intrusion in China. *Journal of Water Resources Research*, Vol. 31, No. 4, pp. 903-912.

.

Programme-1

```
/*programme to find the value of q*/
#include<stdio.h>
#include<math.h>
#include<conio.h>
void main( )
{
clrscr( );
int n,i,j;
float hf,dw,q,m;
float kx=25;
printf("enter the group");
scanf("%d",&n);
for(i=0;i<n;i++)
{
printf("enter the value of dw");
scanf("%f",&dw);
for(j=0;j<12;j++)
{
printf("enter the values of hf");
scanf("%f",&hf);
m=(41*hf-dw);
q=0.157*kx*pow(m,2);
printf("the value of q=%f\n",q);
}
getch( );
}
}
```

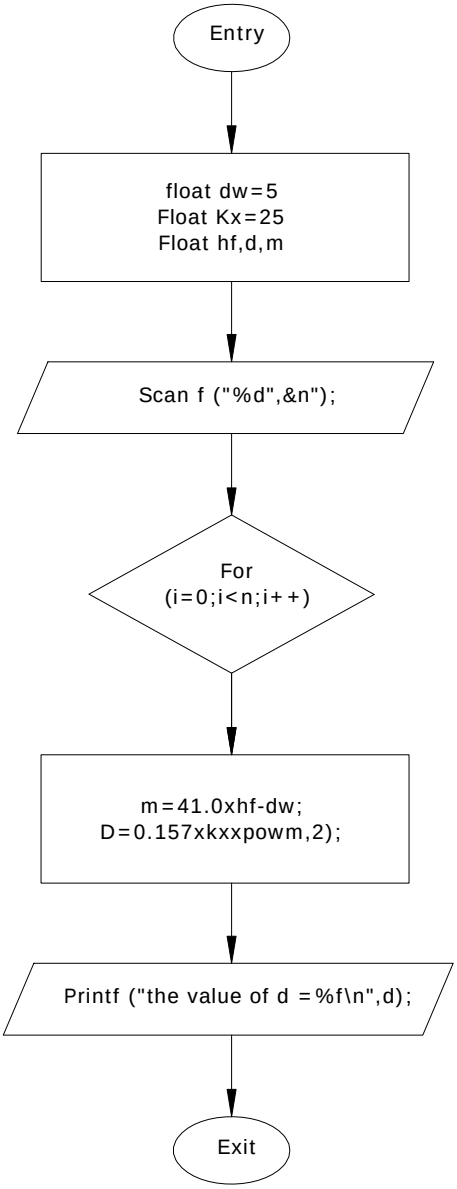

Flow Chart: Programme-1

Programme-2

```
/*program to find the value of q*/
#include<stdio.h>
#include<math.h>
#include<conio.h>
#include<stdlib.h>
void main( )
{
clrscr( );
int n,i;
float dw=5;
float kx=25;
float hf,q,m;
printf("enter the value of n\n");
scanf("%d",&n);
printf("enter the value of hf\n");
for(i=0;i<n;i++)
{
scanf("%f",&hf);
m=41.0*hf-dw;
q=0.157*kx*pow(m,2);
printf("the value of q=%f\n",q);
}
getch( );
}
```

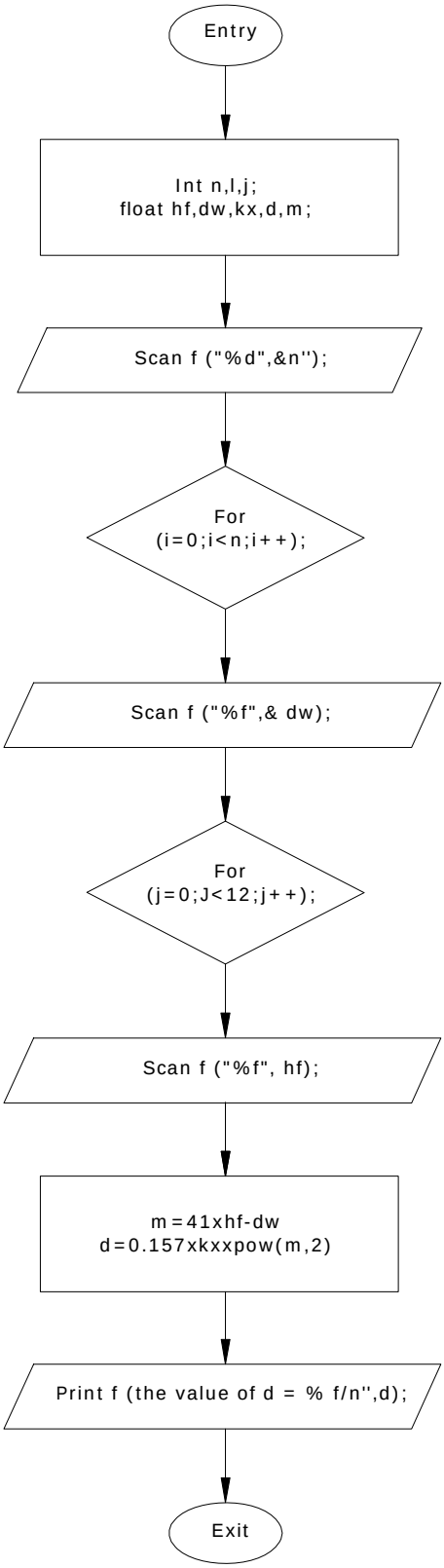

Flow Chart: Programme-2

Program-3

```
/*programme to find the value of q*/
#include<stdio.h>
#include<conio.h>
#include<math.h>
void main( )
{
float q,h,H,k,cdr,cp,l;
int i,j,n;
clrscr( );
h=0.8;
k=25.0;
cdr=0.75;
cp=1.2;
printf("\n enter the value of n: ");
scanf("%d",&n);
{
printf("enter the value of H:\n");
for(i=0;i<n;i++)
{
scanf("%f",&H);
printf("enter the value of l:\n");
for(j=0;j<n;j++)
{
scanf("%f",&l);
q=(8*cdr*cp*k*(pow(H,2)-pow(h,2)))/l;
printf("\n the value of q is:%f",q);
}
getch( );
}
}
}
```

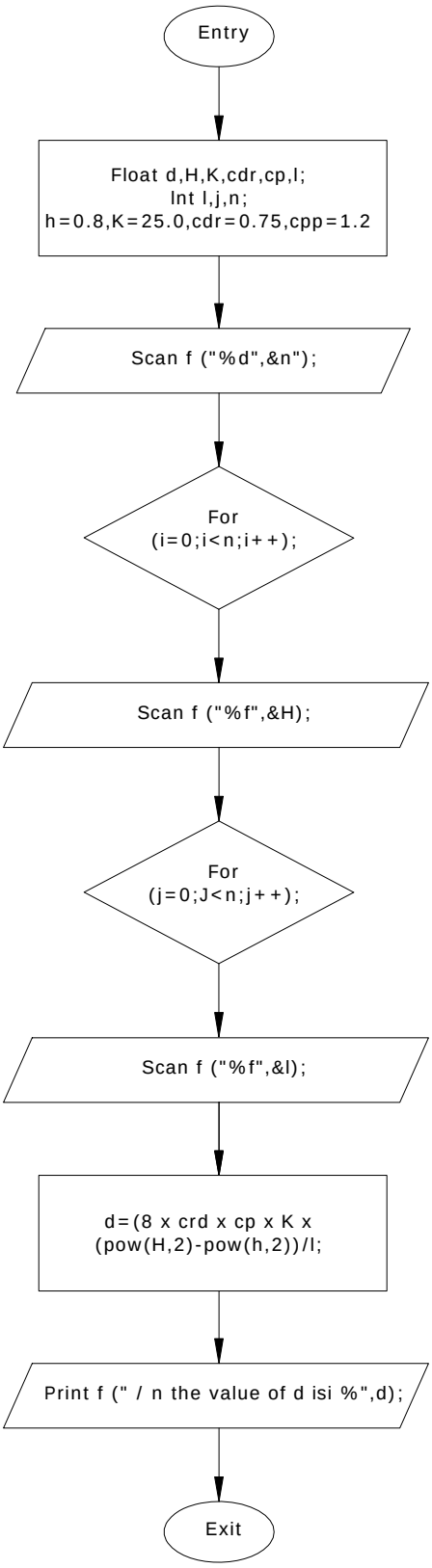

Flow Chart: Programme-3

PRABIR KUMAR MAITY
Ph.D. Scholar
School of Water Resources Engineering
Jadavpur University